

EFFECTS OF DIABETES MELLITUS ON THE BIOMECHANICAL PROPERTIES AND
PHARMACOLOGICAL FUNCTION OF THE FEMALE RAT URETHRA *EX-VIVO*

by

Rachelle Lynn Prantil

BS, Syracuse University, 2000

Submitted to the Graduate Faculty of
School of Engineering in partial fulfillment
of the requirements for the degree of
Master of Science in Bioengineering

University of Pittsburgh

2004

UNIVERSITY OF PITTSBURGH

SCHOOL OF ENGINEERING

This thesis was presented

by

Rachelle Lynn Prantil

It was defended on

April 6th, 2004

and approved by

Harvey S. Borovetz, Ph.D., Professor, Department of Bioengineering

Richard E. Debski, Ph.D., Assistant Professor, Department of Bioengineering and Orthopedic
Surgery

William C. de Groat, Ph.D., Professor, Department of Pharmacology

Thesis Advisor: David A. Vorp, Ph.D., Associate Professor, Departments of Surgery and
Bioengineering

Copyright by Rachelle Lynn Prantil
2004

EFFECTS OF DIABETES MELLITUS ON THE BIOMECHANICAL PROPERTIES AND PHARMACOLOGICAL FUNCTION OF THE FEMALE RAT URETHRA *EX-VIVO*

Rachelle Lynn Prantil, MS

University of Pittsburgh, 2004

Diabetic cystopathy results in a grossly distended, hypomotile bladder due to inefficient voiding. While the bladder has been extensively studied, little effort has been made towards the understanding of the urethra and the effects of this devastating disease. The current study is aimed to evaluate the effects of diabetes mellitus (DM) on the biomechanical properties and the pharmacological function of the female rat urethra *ex vivo*.

DM was induced in female rats by injection of streptozotocin. At 3, 5, and 10 weeks, the urethras were excised and mounted into an *ex-vivo* system at *in vivo* length. For mechanical testing, urethras were subjected to stepwise increases of static, intraurethral pressure from 0 to 20 mmHg in both a baseline and passive state. Continuous outer diameter measurements were made using a laser micrometer at proximal, middle, and distal portions of the urethra. Compliance and beta stiffness were calculated from measured data. Pharmacological experiments involved assessments of mid urethral outer diameter response to $\text{N}\omega$ Nitro-L-arginine, phenylephrine, and EDTA. Age matched normal urethras served as controls. Statistical comparisons were made via ANOVA. Tissue was then processed for immuno- and histochemical quantification of smooth muscle, collagen, and elastin.

For baseline healthy tissue, results showed a proximal to distal compliance gradient (proximal most compliant and distal least compliant), and the passive state enhanced the observation. Baseline beta stiffness values showed an increased stiffness in proximal and middle urethral portions by 5 and 10 weeks, and baseline compliance values showed at low pressures showed an increase in proximal compliance at 3 weeks and a decrease in proximal compliance at 5 weeks at high pressures. Passive beta stiffness and compliance values indicated proximal urethral stiffening by 10 weeks DM. Pharmacological studies revealed that DM abolishes

endogenous nitric oxide release and increases the time to reach maximal relaxation. In cases of severe DM, alpha 1 adrenergic contraction was minimized. Little or no differences were found in the amount collagen, smooth muscle, and elastin.

From these findings, it can be concluded that DM causes urethral stiffening and impaired contractile and relaxation urethral mechanism. Damaged urethral properties and function have serious implications for outlet resistance; thus, contributing to diabetic cystopathy.

TABLE OF CONTENTS

1.0 INTRODUCTION	1
1.1 TYPES AND CLINICAL SIGNIFICANCE OF DIABETES MELLITUS (DM).....	1
1.2 LOWER URINARY TRACT ANATOMY AND FUNCTION.....	2
1.3 EFFECTS OF DM ON THE LOWER URINARY TRACT	3
1.3.1 Effects of DM on the Bladder	6
1.3.2 Effects of DM on the Urethra	6
1.4 COMPARISON OF EXPERIMENTAL MODELS FOR URETHRAL BIOMECHANICS	7
1.4.1 Importance of Studying Urethral Biomechanics.....	8
1.4.2 In Vivo Studies On Urethral Biomechanics.....	8
1.4.2.1 In Vivo Stress Relaxation Tests.....	8
1.4.2.2 In Vivo Animal Model.....	9
1.4.2.3 Limitations of These Studies	10
1.4.3 Ex Vivo Assessment of the Urethra Using Whole Mount Urethral Models.....	10
1.4.4 Ideal Biomechanical Studies for the Urethra	11
1.5 ANIMAL MODELS FOR DM INDUCTION AND URETHRAL BIOMECHANICS	12
1.5.1 Comparisons of the Rat Lower Urinary Tract vs. Human Lower Urinary Tract.....	13

1.5.2. Female versus Male: Anatomical Considerations.....	13
A.6 SCIENTIFIC OBJECTIVES AND HYPOTHESES	16
2.0 METHODS	18
2.1 DM INDUCTION AND URETHRAL HARVEST	18
2.2 EX VIVO URETHRAL TESTING SYSTEM	18
2.2.1 Static Pressure Measurements.....	19
2.2.2 Measurement of Outer Diameter	19
2.2.3 Components of the Ex Vivo Perfusion System.....	20
2.3 BIOMECHANICAL TESTING	23
2.3.1 Parameters for Biomechanical Studies	23
2.3.2 Baseline Biomechanical Studies	26
2.3.3 Passive Biomechanical Studies.....	28
2.4 PHARMACOLOGICAL ASSESSMENT OF URETHRAL SMOOTH MUSCLE FUNCTION	28
2.5 MICROSTRUCTURAL ANALYSIS	29
2.5.1 Identification of Smooth Muscle	30
2.5.2 Identification of the Connective Tissue	31
2.5.3 Quantification of Tissue Constituents.....	31
2.6 STASTICAL ANALYSIS	32
3.0 RESULTS	34
3.1 THE DIABETIC RAT MODEL.....	34
3.2 BIOMECHANICAL STUDIES.....	34
3.2.1 Baseline Biomechanics	34

3.2.2 Passive Biomechanics.....	45
3.3 PHARMACOLOGICAL ASSESSMENT.....	55
3.4 HISTOLOGICAL RESULTS.....	59
3.4.1 Smooth Muscle Quantification.....	59
3.4.2 Collagen Quantification.....	61
3.4.3 Elastin Quantification.....	63
4.0 DISCUSSION.....	66
4.1 BIOMECHANICAL RESULTS.....	66
4.2 PHARMACOLOGICAL FUNCTION OF SMOOTH MUSCLE.....	70
4.3 EXPERIMENTAL LIMITATIONS.....	77
4.3.1 Limitations to the Ex-Vivo Experiments.....	77
4.3.2 Limitations to Microstructural Analysis.....	80
4.3.3 Limitations of the Diabetic Rat Model.....	81
5.0 CONCLUSIONS AND FUTURE WORK.....	82
APPENDIX A. INDIVIDUAL DATA.....	85
A.1 CONTROL DATA.....	85
A.1.1 Baseline State.....	85
A.1.2 Passive State.....	94
A.1.3 Pharmacological Data for Control Urethras.....	103
A. 2 3-WEEK DM DATA.....	108
A.2.1 Baseline Data.....	108
A.2.2 3-week DM Passive Data.....	114
A.3 5-WEEK DM DATA.....	120

A.3.1 Baseline State.....	120
A.3.2 Passive State.....	127
A.3.3 Pharmacological Data for 5-week DM Urethras.....	132
A.4 10-WEEK DM DATA	136
A.4.1 Baseline Data	136
A.4.2 Passive Data	143
A.4.3 Pharmacological Data	149
APPENDIX B. PROPOGATION OF ERROR ANALYSIS.....	154
BIBLIOGRAPHY.....	158

LIST OF TABLES

Table 4.1: Beta stiffness values for the proximal urethra in the baseline and passive states compared to values calculated for arterial tissues in past literature. Note: the error values represent standard error of the mean.....	78
Table 4.2: Compliance values for low (0-6 mmHg), middle (6-12 mmHg), and high (12-20 mmHg) pressure compliance for the proximal urethra compared to that calculated in past literature for passive porcine coronary arteries.....	78

LIST OF FIGURES

Figure 1.1: A) A basic schematic of the female lower urinary tract; B) A cross section of the female urethra. Both panels adapted from www.beresford.hsc.wvu.edu	4
Figure 1.2: Depiction of the lower urinary tract of a male muriform rodent. The female muriform rodent lower urinary tract is more comparable to that of the female human. Adapted from www.uscd.edu/jpathology	15
Figure 2.1: A schematic of the modified ex vivo urethral testing system	21
Figure 2.2: A photograph of the entire testing system (top), and a female rat urethra mounted onto the attachment/infusion tees (bottom). The urethras tested had an average length of approximately 20mm.	22
Figure 2.3 : The above picture represents the results of the preconditioning regimen of the middle region for a female rat urethra in the baseline state. The dotted line indicates the diameter of the urethra after the first cycle’s pressure step, illustrating the change in peak diameter over from the first cycle to the tenth. Note that by the sixth or seventh cycle the cycles begin to appear repeatable.	24
Figure 2.4: Top: The pressure profile for a static pressure experiment holding each increment of pressure for 5 minutes. Bottom: The resulting outer diameter measurement for the proximal portion of a female rat urethra.	25
Figure 2.5: Schematic depicting the identification of the three positions used for measurement along the length of the urethra. L was taken as 3mm less than the measured in vivo length.neck, the value of ‘L’ used here was 3mm less than the in actual measured vivo length. L was actually considered to be the length of the urethra.....	26
Figure 3.1: Blood glucose levels of DM rats compared to healthy controls.....	35
Figure 3.2: The average pressure-diameter data for 11 healthy urethras in the baseline condition. Note the proximal to distal stiffening effect as indicated by the leftward shift of the curves.	36

Figure 3.3: Average pressure-diameter response of proximal (top), middle (middle) and distal (bottom) portions of DM urethras and controls in the baseline state.....	37
Figure 3.4: Low pressure incremental compliance (0 to 6 mmHg) values for DM (A) and three time points of DM (B) in comparison to control values in the baseline state. Error bars represent standard error of the mean.....	39
Figure 3.5: Middle-pressure incremental compliance (6 to 12 mmHg) values for DM (A) and three time points of DM (B) both in comparison to control values in the baseline state. Error bars represent standard.....	41
Figure 3.6: High-pressure incremental compliance (12 to 20 mmHg) values for DM (A) and three time points of DM (B) both in comparison to control values in the baseline state. Error bars represent standard error of the mean.	42
Figure 3.7: Beta Stiffness values for DM (A) and three time points of DM (B) both in comparison to control values in the baseline state. Error bars represent standard error of the mean.....	44
Figure 3.8: Pressure-diameter curves for the three different positions along the length of the urethra. With a proximal-to-distal shift to left, this data suggests that the proximal portion is more compliant than both the mid and distal portions.....	45
Figure 3.9: The average and normalized pressure-diameter response of proximal (top), middle (middle) and distal (bottom) portions of 3, 5, and 10-week DM urethras and controls in the passive state.	47
Figure 3.10: Low pressure incremental compliance (0 to 6 mmHg) values for combined DM (A) and three time points of DM (B) compared to control values in the passive state. Error bars represent standard error of the mean.....	49
Figure 3.11: Middle pressure incremental compliance (6 to 12 mmHg) values for combined DM (A) and three time points of DM (B) compared to control values in the passive state. Error bars represent standard error of the mean.	51
Figure 3.12: High-pressure incremental compliance (12 to 20 mmHg) values for combined DM (A) and three time points of DM (B) compared to control values in the passive state. Error bars represent standard error of the mean.	52
Figure 3.13: Beta Stiffness values for combined DM (A) and three time points of DM (B) compared to control values in the passive state. Error bars represent standard error of the mean.....	54

Figure 3.14: Urethral response to N ω -nitro-L-arginine, phenylephrine and EDTA. The error bars represent SEM.....	55
Figure 3.15: Urethral response to nitric oxide inhibitor (N ω -nitro-L-arginine), contractile (PE) and relaxation agents (EDTA). The error bars represent SEM.....	56
Figure 3.16: Urethral response to contractile (PE) and relaxation agents (EDTA). The error bars represent SEM.....	57
Figure 3.17: The time to reach maximal response to PE and EDTA for each group. No differences were seen for PE, but DM increased the time for relaxation in response to EDTA.....	59
Figure 3.18: (Left) Smooth muscle alpha actin antibody staining of a proximal urethra (red) with the background of Hoescht (blue) at 5x using a Nikon fluorescent microscope. (Right) A closer view at (20x).....	60
Figure 3.19: The amount of smooth muscle alpha actin in the proximal, middle, and distal portions of control and DM urethra. Error bars represent standard error. No significant differences were noted in any comparisons.....	61
Figure 3.20: (Left) Masson's trichrome histological stain of a proximal urethra, collagen (blue) with muscle (red/brown) at 5x using a light microscope. (Right) A closer view of the region within the green box of the figure to the left (20x).....	62
Figure 3.21: The amount of collagen in the proximal, middle, and distal portions of control and DM urethra. Error bars represent standard error. No significant differences were noted in any comparisons.....	63
Figure 3.22: (Left) Weigert's Recorsin Fuschin histological stain of a proximal urethra, elastic fibers, dark purple/ black at 5x using a light microscope (Right) A closer view (20x) Note: no background stain was performed.....	64
Figure 3.23: The amount of elastin in the proximal, middle, and distal portions of the urethra and the effects from DM. Error bars represent standard error.....	65
Figure 4.1: Typical proximal pressure-diameter responses which are sigmoidal for baseline tissue (A) and exponential for passive tissue (B).....	68
Figure 4.2: Depiction of the pathway of nitric oxide in urethral smooth muscle or the bladder neck (From Mumtaz et al, 2000 [65]).....	72
Figure 4.3: The STZ injected animals were grouped into high (less than 400 mg/dl) blood glucose (n=7) and low (greater than 400 mg/dl) blood glucose (n=7) in order to assess whether the absence of NO were due to DM or STZ. (*p<0.05).....	73

Figure 4.4: A schematic representing the mechanism behind the activation of alpha 1-adrenoceptor smooth muscle contraction. Note: this mechanism is dependent upon both intra- and extra-cellular calcium levels (From Ruffolo et al. 1991 [78]).	76
Figure A.1: Pressure-diameter data for proximal, middle, and distal portions of control urethras in the baseline state	85
Figure A.2: Pressure-diameter data for proximal, middle, and distal portions of control urethras in the baseline state.	86
Figure A.3: Pressure-diameter data for proximal, middle, and distal portions of control urethras in the baseline state	87
Figure A.4: Low, middle, and high pressure compliance data for proximal, middle, and distal portions of control urethras in the baseline state	88
Figure A.5: Low, middle, and high pressure compliance data for proximal, middle, and distal portions of control urethras in the baseline state	89
Figure A.6: Low, middle, and high pressure compliance data for proximal, middle, and distal portions of control urethras in the baseline state	90
Figure A.7: Beta stiffness data for proximal, middle, and distal portions of control urethras in the baseline state	91
Figure A.8: Beta stiffness data for proximal, middle, and distal portions of control urethras in the baseline state	92
Figure A.9: Beta stiffness data for proximal, middle, and distal portions of control urethras in the baseline state	93
Figure A.10: Pressure-diameter data for proximal, middle, and distal portions of control urethras in the passive state	94
Figure A.11: Pressure-diameter data for proximal, middle, and distal portions of control urethras in the passive state	95
Figure A.12: Pressure-diameter data for proximal, middle, and distal portions of control urethras in the passive state	96
Figure A.13: Low, middle, and high pressure compliance data for proximal, middle, and distal portions of control urethras in the passive state	97

Figure A.14: Low, middle, and high pressure compliance data for proximal, middle, and distal portions of control urethras in the passive state.....	98
Figure A.15: Low, middle, and high pressure compliance data for proximal, middle, and distal portions of control urethras in the passive state.....	99
Figure A.16: Beta stiffness data for proximal, middle, and distal portions of control urethras in the passive state.....	100
Figure A.17: Beta stiffness data for proximal, middle, and distal portions of control urethras in the passive state.....	101
Figure A.18: Beta stiffness data for proximal, middle, and distal portions of control urethras in the passive state.....	102
Figure A.19: Pharmacological data representing decrease and increase of the outer diameter of the middle portion of control urethras	103
Figure A.20: Pharmacological data representing decrease and increase of the outer diameter of the middle portion of control urethras	104
Figure A.21: Pharmacological data representing decrease and increase of the outer diameter of the middle portion of control urethras	105
Figure A.22: Pharmacological data representing decrease and increase of the outer diameter of the middle portion of control urethras	106
Figure A.23: Pharmacological data representing decrease and increase of the outer diameter of the middle portion of control urethras	107
Figure A.24: Pressure-diameter data for proximal, middle, and distal portions of 3 week DM urethras in the baseline state	108
Figure A.25: Pressure-diameter data for proximal, middle, and distal portions of 3 week DM urethras in the baseline state	109
Figure A.26: Low, middle, and high pressure compliance data for proximal, middle, and distal portions of 3 week DM urethras in the baseline state.....	110
Figure A.27: Low, middle, and high pressure compliance data for proximal, middle, and distal portions of 3 week DM urethras in the baseline state.....	111
Figure A.28: Beta stiffness data for proximal, middle, and distal portions of 3 week DM urethras in the baseline state	112

Figure A.29: Beta stiffness data for proximal, middle, and distal portions of 3 week DM urethras in the baseline state	113
Figure A.30: Pressure-diameter data for proximal, middle, and distal portions of 3 week DM urethras in the passive state.....	114
Figure A.31: Pressure-diameter data for proximal, middle, and distal portions of 3 week DM urethras in the passive state.....	115
Figure A.32: Low, middle, and high pressure compliance data for proximal, middle, and distal portions of 3 week DM urethras in the passive state	116
Figure A.33: Low, middle, and high pressure compliance data for proximal, middle, and distal portions of 3 week DM urethras in the passive state	117
Figure A.34: Beta stiffness data for proximal, middle, and distal portions of 3 week DM urethras in the passive state	118
Figure A.35: Beta stiffness data for proximal, middle, and distal portions of 3 week DM urethras in the passive state	119
Figure A.36: Pressure-diameter data for proximal, middle, and distal portions of 5 week DM urethras in the baseline state	120
Figure A.37: Pressure-diameter data for proximal, middle, and distal portions of 5 week DM urethras in the baseline state	121
Figure A.38: Pressure-diameter data for proximal, middle, and distal portions of 5 week DM urethras in the baseline state	122
Figure A.39: Low, middle, and high pressure compliance data for proximal, middle, and distal portions of 5 week DM urethras in the baseline state.....	122
Figure A.40: Low, middle, and high pressure compliance data for proximal, middle, and distal portions of 5 week DM urethras in the baseline state.....	123
Figure A.41: Low, middle, and high pressure compliance data for proximal, middle, and distal portions of 5 week DM urethras in the baseline state.....	124
Figure A.42: Beta stiffness data for proximal, middle, and distal portions of 5 week DM urethras in the baseline state	124
Figure A.43: Beta stiffness data for proximal, middle, and distal portions of 5 week DM urethras in the baseline state	125

Figure A.44: Beta stiffness data for proximal, middle, and distal portions of 5 week DM urethras in the baseline state	126
Figure A.45: Pressure-diameter data for proximal, middle, and distal portions of 5 week DM urethras in the passive state.....	127
Figure A.46: Pressure-diameter data for proximal, middle, and distal portions of 5 week DM urethras in the passive state.....	128
Figure A.47: Low, middle, and high pressure compliance data for proximal, middle, and distal portions of 5 week DM urethras in the passive state	128
Figure A.48: Low, middle, and high pressure compliance data for proximal, middle, and distal portions of 5 week DM urethras in the passive state	129
Figure A.49: Low, middle, and high pressure compliance data for proximal, middle, and distal portions of 5 week DM urethras in the passive state	130
Figure A.50: Beta stiffness data for proximal, middle, and distal portions of 5 week DM urethras in the passive state	130
Figure A.51: Beta stiffness data for proximal, middle, and distal portions of 5 week DM urethras in the passive state	131
Figure A.52: Pharmacological data representing decrease and increase of the outer diameter of the middle portion of control urethras. Blood glucose levels were (top) 484 mg/dl and (bottom) 462 mg/dl	132
Figure A.53: Pharmacological data representing decrease and increase of the outer diameter of the middle portion of control urethras. Blood glucose levels were (top) 312 mg/dl and (bottom) 300 mg/dl	133
Figure A.54: Pharmacological data representing decrease and increase of the outer diameter of the middle portion of control urethras. Blood glucose levels were (top) 392 mg/dl and (bottom) 396 mg/dl	134
Figure A.55: Pharmacological data representing decrease and increase of the outer diameter of the middle portion of control urethras. Blood glucose level: 458 mg/dl	135
Figure A.56: Pressure-diameter data for proximal, middle, and distal portions of 10 week DM urethras in the baseline state	136
Figure A.57: Pressure-diameter data for proximal, middle, and distal portions of 10-week DM urethras in the baseline state	137

Figure A.58: Pressure-diameter data for proximal, middle, and distal portions of 10-week DM urethras in the baseline state	138
Figure A.59: Low, middle, and high pressure compliance data for proximal, middle, and distal portions of 10-week DM urethras in the baseline state.....	138
Figure A.60: Low, middle, and high pressure compliance data for proximal, middle, and distal portions of 10-week DM urethras in the baseline state.....	139
Figure A.61: Low, middle, and high pressure compliance data for proximal, middle, and distal portions of 10-week DM urethras in the baseline state.....	140
Figure A.62: Beta stiffness data for proximal, middle, and distal portions of 10-week DM urethras in the baseline state	141
Figure A.63: Beta stiffness data for proximal, middle, and distal portions of 10-week DM urethras in the baseline state	142
Figure A.64: Beta stiffness data for proximal, middle, and distal portions of 10-week DM urethras in the baseline state	142
Figure A.65: Pressure-diameter data for proximal, middle, and distal portions of 10-week DM urethras in the passive state.....	143
Figure A.66: Pressure-diameter data for proximal, middle, and distal portions of 10-week DM urethras in the passive state.....	144
Figure A.67: Low, middle, and high pressure compliance data for proximal, middle, and distal portions of 10-week DM urethras in the passive state	145
Figure A.68: Low, middle, and high pressure compliance data for proximal, middle, and distal portions of 10-week DM urethras in the passive state	146
Figure A.69: Beta stiffness data for proximal, middle, and distal portions of 10-week DM urethras in the passive state.....	147
Figure A.70: Low, middle, and high pressure compliance data for proximal, middle, and distal portions of 10-week DM urethras in the passive state	148
Figure A.71: Pharmacological data representing decrease and increase of the outer diameter of the middle portion of control urethras. Blood glucose levels were (top) 540 mg/dl and (bottom) 408 mg/dl	149

Figure A.72: Pharmacological data representing decrease and increase of the outer diameter of the middle portion of control urethras. Blood glucose levels were (top) 479 mg/dl and (bottom) 368 mg/dl	150
Figure A.73: Pharmacological data representing decrease and increase of the outer diameter of the middle portion of control urethras. Blood glucose levels were (top) 480 mg/dl and (bottom) 399 mg/dl	151
Figure A.74: Pharmacological data representing decrease and increase of the outer diameter of the middle portion of control urethras. Blood glucose levels were (top) 479 mg/dl and (bottom) 368 mg/dl	152
Figure A.75: Pharmacological data representing decrease and increase of the outer diameter of the middle portion of control urethras. Blood glucose levels were (top) 355 mg/dl and (bottom) 282 mg/dl	153

1.0 INTRODUCTION

1.1 TYPES AND CLINICAL SIGNIFICANCE OF DIABETES MELLITUS (DM)

It is estimated that 17 million Americans have diabetes mellitus (DM), according to the American Diabetic Association [1]. DM is a condition that involves abnormalities in the body's ability to use sugar [2]. In a healthy person, the pancreas makes extra insulin when they eat. Insulin helps move glucose in the bloodstream to the inside of cells where it is utilized as a key source of energy. A person with diabetes has the inability to produce enough insulin to keep up with their body's demand, and the cells may resist the insulin; thus, glucose cannot be transported into the cells and used.

DM is a disease of complex pathogenesis, which varies with one of three types, juvenile onset diabetes, diabetes mellitus, and gestational diabetes. Type I DM, otherwise known as insulin-dependent diabetes mellitus, involves a pancreas that makes little or no insulin. Type I diabetes is believed to evolve from an autoimmune disorder, in which the body produces antibodies that destroy pancreatic beta cells. The cause of insulin dependent diabetes mellitus remains a mystery, yet genetics, age (usually occurs from spontaneous loss of beta cell function at approximately 11 to 14 yrs), and various viruses are suspected to play a role [3,4].

Type II DM, or non-insulin dependent diabetes mellitus, occurs when the cells in the body become resistant to insulin. As a result, the body cannot consume glucose as well as it should. This is the most common type of DM and risk factors consist of obesity, race, a sedentary lifestyle, high blood pressure, low HDL level, old age, and menopause.

Similarly, gestational diabetes develops in some women during pregnancy, and in most cases, this condition will cease after childbirth [2,5]. Overall, long-term effects of this disease

involve profound damage to the circulatory system, nervous system, and other internal organs resulting in retinopathy, nephropathy, atherosclerosis, and neuropathy [2,3].

1.2 LOWER URINARY TRACT ANATOMY AND FUNCTION

The act of micturition comprises of a storage phase and an expulsion phase, otherwise known as voiding. Micturition is dependent on the coordination of the bladder and the urethra both of which involve opposing function. Essentially, the bladder acts as a reservoir for storing urine and as a pump for expelling it during voiding. On the other hand, the urethra remains closed during filling and controlled dilation provides a conduit for the urinary stream. The bladder and urethra are complex in structure comprised of highly innervated smooth or striated musculature [6].

The bladder is composed of two basic elements: a body (detrusor) and a base (the trigone). The body and base of the bladder are complex, interwoven meshes of smooth muscle fibers that lack discrete layers and are surrounded by collagen and elastin, blood vessels, and nerve axons or terminals. This organization allows the body of the bladder to accommodate increasing amounts of urine during the storage phase of micturition and the base of the bladder to form a vertical funnel to establish a conduit for urine during voiding [6,7].

The urethra (Figure 1) consists of both an internal sphincter composed primarily of smooth muscle and an external sphincter composed primarily of striated muscle. Smooth muscle is found along the entire length of the urethra in the form of a thick inner layer of longitudinally-oriented muscle fibers surrounded by a thin medial layer of circumferentially-oriented muscle fibers. The role of the different layers remains controversial. Most commonly, it is believed that the circumferentially-oriented smooth muscle plays an important role in maintaining urethral pressure during filling and longitudinally-oriented muscle shorten and open the urethra during micturition. Striated muscle, composed of both fast and slow twitch fibers, forms the outer layer of the urethra. The striated urethral sphincter is thought to contribute largely to maintaining tone and high urethral pressure during the storage phase [8].

Parasympathetic, sympathetic, and somatic innervations are responsible for successful storage and voiding. Both sympathetic and parasympathetic nerve fibers innervate the bladder wall, more specifically the detrusor and the trigone. Parasympathetic cholinergic fibers travel via the pelvic nerve to the bladder surface and elicit a smooth muscle contraction during the voiding phase of micturition by release of acetylcholine and activation of muscarinic receptors. Sympathetic noradrenergic innervation, which is present in the bladder, induces detrusor relaxation by release of norepinephrine and activation of beta adrenergic receptors. Somatic innervation is present in the external striated urethral sphincter and the pelvic floor muscles. Somatic innervation, provided by the pudendal nerve, transmits efferent cholinergic impulses to muscles of the pelvic floor, afferent signals from these muscles, and sensory information from the urethra [9]. Although the neural control of the female urethral smooth muscle remains uncertain, many studies have shown that urethral smooth muscle is densely innervated by the parasympathetic and sympathetic nervous systems. Sympathetic activity mediated through alpha adrenergic receptors contribute to the maintenance of high urethral pressure and resistance during the storage phase of micturition; whereas, parasympathetic nerve fibers may contribute to urethral relaxation during voiding [8,10].

1.3 EFFECTS OF DM ON THE LOWER URINARY TRACT

It has been stated in the literature that 52% of randomly evaluated diabetic patients were diagnosed with lower urinary tract dysfunction [11]. Still, it is difficult to estimate the portion of diabetic patients that suffer from urologic disorders, more specifically bladder dysfunction. While DM is a well-defined disease, diabetic cystopathy develops subtly and symptoms do not appear until the disease is in an advanced stage. Moreover, methods of investigation and data collection lack a common criterion; thus, many investigators' definitions of diabetic cystopathy

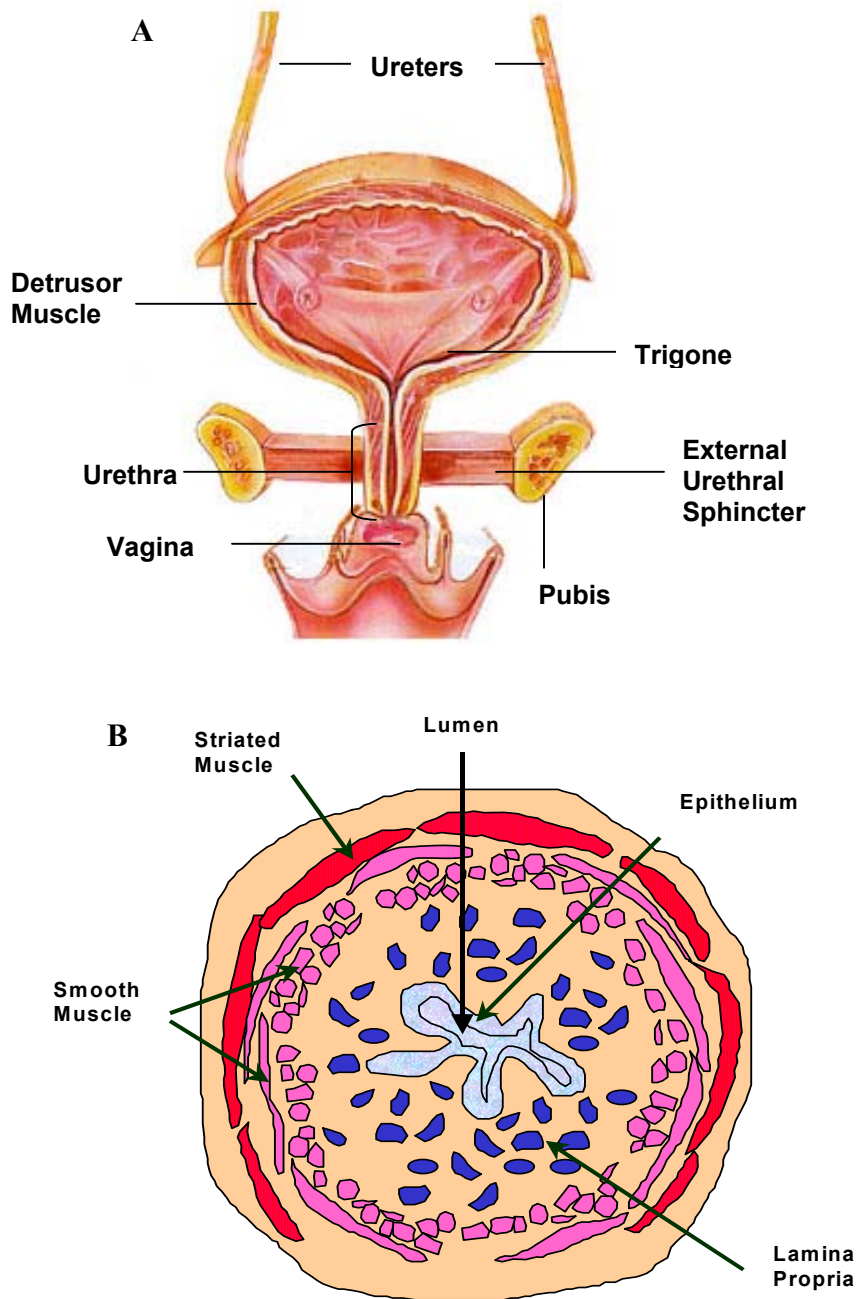


Figure 1.1: A) A basic schematic of the female lower urinary tract; B) A cross section of the female urethra. Both panels adapted from www.beresford.hsc.wvu.edu

vary with factors, such as amount of residual urine, bladder capacity, and first sensation to void [12]. While treatments do exist, diagnosis and pathophysiology need to be better understood in order to more fully accommodate diabetic cystopathy.

Voiding dysfunction is a common finding in patients with diabetes mellitus. Usually, the first manifestation is impaired bladder sensation. Initially, symptoms are infrequent voiding, reduced stream, hesitancy in initiating the urinary flow, dribbling owing to overflow incontinence, sensation of incomplete emptying, and loss of the desire to void. Diagnosis is established by the demonstration of cystometric abnormalities that are associated with residual urine. For example, cystometrograms indicate decreased bladder sensation, increased bladder capacity, and areflexic or hyperreflexic bladders [13]. If addressed early, the condition can be reversed, but if allowed to develop without treatment, the chief complication is infection. The presence of urinary retention inevitably leads to infection of the bladder. Ultimately, the development of bacterial infection will reach the kidney leading to serious consequences, including renal failure [14].

Diabetic cystopathy is attributed to peripheral neuropathy affecting the somatic and autonomic nervous systems and leading to myogenic failure and the inability to mount a satisfactory detrusor contraction. Studies in human diabetes and in experimental animals suggest that the initial site of damage is the axon, which either provides input (afferents) or outputs (efferents) from a neuron. Segmental demyelination occurs which impairs conduction velocity and may result not only in temporary delay, but complete nerve blockade [13,15]. An electrophysiologic evaluation [16] performed on patients with DM showed decreased conduction velocities in patients with detrusor hyper-reflex or areflexia, which are defined as an overactive or non-contractile bladder, respectively. The results of this study indicated the effects of segmental demyelination in the peripheral nerve supply in the bladder and proximal urethra. Other changes that have been found in diabetic neuropathy include alteration in the extracellular matrices surrounding peripheral. It has been found that circular Schwann cell basal laminar tubes occur following axonal degeneration and become crowded with densely packed collagen fibers, which are increased in diameter due to neuropathy also. These findings may play a major role in changes of the urethra and bladder since the extracellular matrix mechanically supports the surrounding cells and regulates their behavior through specific interactions mediated via molecules on the cell surface, such as integrins [17].

1.3.1 Effects of DM on the Bladder

Human urodynamic studies have revealed instability of the detrusor muscle in the bladder wall with the onset of DM which progresses to increased cystometric capacity, decreased bladder contractility, and impaired urination [18,19]. Since the effects of DM on the lower urinary tract are time dependent, researchers have been motivated to study the damaging consequences of DM on the bladder at different time points, i.e. early and end stage intervals in animal models. Early-stage studies have shown that shortly after induction of DM using streptozotocin (STZ) treatment, diabetic rats display increased urine volume. While this study suggests that the bladder is changed to allow greater volumes of urine to be stored and passed, the detrusor muscle of the bladder did not display an impaired response to noradrenaline, acetylcholine, or cholinergic stimulation [20]. Additionally, Pinna et al. [21] showed that 4 weeks after the induction of STZ, the urinary bladder was significantly thicker and heavier and that the ATP contractile response was enhanced compared to controls. There was also no change in contractile response to acetylcholine. On the other hand, research examining the response of a 47 week STZ induced diabetic rat urinary bladder to autonomic stimuli, such as acetylcholine and phenylephrine, exhibited an increase of contractile response when compared to bladder strips of a 6 week diabetic rat [22]. Additionally, Moss et al. [23] examined the early and late effects of DM on an in vitro whole rat bladder preparation. Eight weeks after streptozotocin induction, cystometrogram showed an increase in bladder capacity associated with a decrease in intraluminal pressure, and an increased sensitivity to purinergic (receptors involved in contractile responses in the bladder [39]) agonists and a decreased sensitivity to cholinergic (receptor mechanisms which contract the bladder [39]) agonists. In sixteen week cystometrogram, the bladder capacity had decreased and intraluminal pressure was within normal range, and a greatly reduced response to the purinergic agonists was detected.

1.3.2 Effects of DM on the Urethra

While there have been many studies emphasizing the effect of DM on the bladder, not much is known of the effect of this disease on the urethra. The urethra is more than a simple conduit through which the urine exits. Rather, it is a complicated structure which performs three

functions: a sustained tone to prevent urinary leakage during bladder filling, a transient reflex increased in pressure to prevent opening of the lumen when abdominal pressure rises, and a relaxation preceding micturition [8]. Understanding the effects of DM on this muscular organ may be key to solving problems of diabetic cystopathy. One ex-vivo study scrutinized the response of DM on proximal urethral strips to pharmacological agents, such as ATP, norepinephrine (NE), and potassium chloride (KCL) [21]. DM appeared not to affect the contractile response to NE or ATP, but the contraction to KCL was decreased in DM compared to controls. Another study set out to understand the short and long term effects of DM on the urethra [25]. While onset of DM caused an increase of micturition frequency and volume, findings showed substance P and vasoactive intestinal polypeptide concentration was somewhat higher in 6 week diabetic animals than in age-matched controls, but not statistically significant. These neuropeptides are found in sensory nerve fibers, and an increase in concentration may indicated changes in the bladder and urethra sensation.

Using combined isolated isovolumetric cystometry and anterograde urethral perfusion pressure measurements, an in vivo experiment by Torimoto et al. [24] set out to identify and characterize alterations in physiological properties of the urethra from DM both during the filling and voiding phases. Results indicated impaired smooth muscle urethral relaxation mechanism during micturition in chronic DM rats, as well as a decrease of external urethral sphincter phasic firing and an increase in bladder pressure threshold for urethral relaxation. Consequently, this would be expected to reduce voiding efficiency during a period of diabetic cystopathy development.

1.4 COMPARISON OF EXPERIMENTAL MODELS FOR URETHRAL BIOMECHANICS

Typical urological signals, such as pressure and volume and their respective changes in time, are mechanical parameters. The urethra maintains closure during increases in bladder pressure and volume during filling, characteristics of a load-bearing structure in which collagen and elastin may play a passive role. Additionally, the smooth and striated muscle components of the urethra provide a urethral closure pressure, an active aspect of continence. While no information

currently exists regarding the biomechanical impact of DM on the urethra, biomechanics has been used to characterize the bladder outlet in other types of voiding dysfunction.

1.4.1 Importance of Studying Urethral Biomechanics

The ability to characterize fundamental mechanical tissue properties can be a powerful tool for understanding tissue function and determining origins of dysfunction and the progression of pathological disease states. Only a few studies, which are summarized in section 1.4.2, have attempted to exemplify the fundamental mechanical tissue properties of the urethra, and the dearth of such studies may be attributed to the lack of appropriate experimental systems to perform them [41]. The utilization of experimental devices for other tissue such as the vascular testing systems of Vorp et al.[31] and Brant et al. [30], could produce a more thorough investigation of structure-function relationships for the urethra. Such information is crucial to sufficiently address the role of biomechanics in urinary retention and incontinence as related to diabetic cystopathy.

1.4.2 In Vivo Studies On Urethral Biomechanics

In the following studies, urethral biomechanical has been evaluated mostly to characterize stress urinary incontinence (SUI), an involuntary loss of urine secondary to an increase in abdominal pressure during events such as sneezing, coughing or laughing in the absence of bladder contractions. No studies known to date have concentrated on urethral biomechanics and DM in vivo clinically or in the laboratory.

1.4.2.1 In Vivo Stress Relaxation Tests: Utilizing a special probe developed for the measurement of intraurethral pressure and cross sectional area, Colstrup [42] described the rigidity (change in urethral pressure divided by change in cross sectional area) and urethral hysteresis (e.g. differential pressure at a given volume during inflation versus deflation) of different portions of the resting, healthy female human urethra. The probe consisted of a polyvinyl catheter with a small balloon that was inflated with water and recorded values of

pressures and cross sectional area. Recordings were performed at 0.5 cm intervals from the bladder neck. The results showed that rigidity increased towards the mid and distal portions compared to the proximal portions of the urethra, indicating a rigidity gradient along the urethral length, proximal being the least rigid and distal being the most. In contrast, hysteresis varied little along the length.

This same technique was utilized to assess the value of a stress relaxation parameter ($P_{t0.5}$), which quantifies the dissipation of energy over time from the urethra in conjunction with surrounding anatomical structures stretched by urethral dilation, of healthy and stress incontinent women [43]. It has been found that muscle tissue tends to increase this parameter in comparison to connective tissue. The measurements showed that $P_{t0.5}$ was significantly greater in healthy women than in women with SUI, with the greatest difference at the bladder neck suggesting SUI-induced muscular damage or connective tissue remodeling.

1.4.2.2 In Vivo Animal Model: To quantify urethral wall stiffness for a normal urethra, Yalla et al. [44] used an in vivo female dog model. The dog was anesthetized and the symphysis pubis was excised through a transpubic midline incision in order to expose the urethra. The goal of the study was to examine qualitatively the affects of urethral dilation, urethral myotomy, and tissue death on wall stiffness. The three different variables were assessed via changes in urethral infusion resistance and pressure-volume relationships. A linear variable differential transducer measured changes in the external diameter of the mid urethra. The distal end of the urethra was occluded and continuous infusion of saline at a steady rate was allowed up to 200 mmHg. A polygraph continuously recorded diameter and pressure. This animal model suggested a non-linear pressure-volume relationship, in general for all tissue. Urethral dilation was found to increase compliance (i.e. pressure-volume curves shifted to the right of normal urethral response curves) and slowed the rate of stress relaxation. Urethral myotomy increased compliance, and dead tissue exhibited increased compliance and a slower rate of stress relaxation. This model was able to demonstrate qualitatively the general biomechanical behavior of urethral tissue in three different states, but no quantitative data (e.g. beta stiffness indices, etc.) were derived.

1.4.2.3 Limitations of These Studies: While these in vivo models, described in Sections 1.4.2.1 and 1.4.2.2, initiated biomechanical studies of the urethra, there are several limiting disadvantages to their techniques. The study by Colstrup considered that the urethra was not homogeneous and measured rigidity along the entire length of the urethra, but Yalla et al. neglected this issue and concentrated primarily on the mid portion of the urethra only. On the other hand, the dog model could not provide the researchers with the ability to look strictly at the urethral biomechanical properties since the urethra was still attached to the vaginal wall, and the human model could not discriminate the urethra from peri-urethral structures. If the parameters (infusion rate, volume of fluid, etc.) were identical for both studies, it would have been interesting if one could correlate the two studies. Also, studies by Yalla et al. only demonstrated qualitative endpoints, and neglected to quantify compliance or stiffness in the different urethral states.

In addition, the Colstrup study did not randomize the points at which the urethra was tested. Although these experiments were performed in vivo, consistently evaluating biomechanical properties in the same order (bladder neck, mid portion, then distal portion, for example) may have biased the results. Also, intramural hemorrhaging and edema in the dog model may have created uncontrolled variables, such as spontaneous urethral dilations or wall thickening. Both studies lacked histological or immunohistological evidence of tissue structure and function relations to their results. Finally, the size of the balloon catheters and infusion rates used could have a variable affect on the biomechanical results of these studies and physiological pressures were not used (150 and 200 mmHg).

1.4.3 Ex Vivo Assessment of the Urethra Using Whole Mount Urethral Models

Research to date, has shown little effort to explore urethral biomechanics with the use of whole mount ex vivo studies. Mayo and Hinman [45] utilized an ex vivo model to demonstrate that the female urethra is anisotropic, i.e. the circumferentially-oriented muscle and connective tissue fibers have a decreased compliance compared to longitudinally-oriented ones. The model involved excision of a 3 cm segment of a female dog urethra between the bladder neck and the pelvic floor. The urethra was marked with sutures to carefully maintain in vivo length. One end of the urethra was tied over a glass tube, and a silk thread to the central core of a differential

transformer attached the other end over a low friction pulley where 0.5 g of tension was applied to balance the urethra. The differential transformer (length transducer) provided a linear response and could be calibrated to read to 1 or 2 cm full scale. A 50 ml bath of Locke's solution was oxygenated and circulated for a physiological environment. A static pressure reservoir filled with Locke's solution was used to apply intraluminal pressure. Pressure was measured at a point between the graduated scale and the specimen via a strain gauge transducer.

While this study presented useful information on the anisotropic nature of the urethra, only a 3 cm segment was used, and not the entire organ. It would have been appealing to establish whether inclusion of the distal end would have made a difference in their results. They also allowed the urethra to fully collapse (longitudinal contraction) after excision of the urethra and before restoring it back to in vivo length. This may have impaired the integrity of the tissue. Finally, this study lacked histological or immunohistological evidence of tissue structure and function relations to their results.

Another study that utilized a whole ex vivo mount model [26] used rabbit urethras, which were excised and ligated to a j tube at the distal end and a catheter at the proximal end. The catheter was connected to a three-way stopcock, which enabled a transducer to measure pressure. The diameter measurement was based on increase of pressure at one point proximally which was measured by a transducer output to a grass polygraph recorder. While this was a clever indirect means of measuring the diameter, it was not as accurate as other established techniques (e.g. helium-neon laser micrometer). Also, the experimental system provided continuous flow of saline intralumenally (1 ml/min) via an infusion pump. With only one measurement proximally to the urethra and the distal measurement absent, there was no way of knowing if there was a pressure drop over the urethral length. Of course, the study could have assumed that the flow was minimal enough that it did not pose a differentiating factor.

1.4.4 Ideal Biomechanical Studies for the Urethra

Ex vivo observations allow examination of urethral tissue without potentially confusing effects of the surrounding muscular and other support structures. Urethral strip studies or divided ring segments dominate the small amount of literature dealing with ex vivo studies which examine

pathological states, like DM. Yet, whole mount urethral preparations provide advantages over the segmented tissue models. These preparations provide the three dimensional geometry without any muscle fiber damage that would result from yielding urethral strips or sectored rings. Additionally, the physiological intraurethral pressure may be applied to understand the biomechanical response of the urethra, and the pharmacological function may be understood with the heterogeneous nature of the tissue intact.

An ideal tool to study any changes that may occur in the urethra must have certain attributes. First, unlike any of the systems previously described in Section 1.4, the ideal ex-vivo system would more closely mimic the in vivo environment. Second, it is important to have the ability to separate the urethra from affecting factors, such as biochemical agents released in the body and surrounding structures. Thirdly, the three dimensional geometry must be preserved to account for the fact that the urethra is a heterogeneous complex conduit. Finally, the experimental arrangement must allow for all portions, i.e. proximal, middle, and distal, of the urethra to be assessed for gradients of pharmacological responses or material properties without severing any juxtaposed segments not of interest.

1.5 ANIMAL MODELS FOR DM INDUCTION AND URETHRAL BIOMECHANICS

When considering an animal model for examining any pathological state, the investigator must control for a wide array of variables, such as age, hormonal status, sex, strain, and habitat. Some previous types of animal models used for diabetes are alloxan injection [3,69,79,85] and NOD mice [3,85] and BB Wistar rats [3,85] where the pancreatic beta cells are spontaneously abolished upon birth. While the diabetogenic effect of STZ is more reproducible and less influenced by changes in the nutritional status of the animals, the metabolic changes are closer to those existing in human diabetes than the response of alloxan (a drug that completely eliminates the pancreatic function) induced diabetes [47]. For this study, the female rat offers an inexpensive and versatile species to investigate the effects of DM on the urethra. While neural pathways are less complex than that of humans, nevertheless, the female rat lower urinary tract

closely replicates that of the female human. Certain important issues of this animal model are discussed in the following sections.

1.5.1 Comparisons of the Rat Lower Urinary Tract vs. Human Lower Urinary Tract

While the rat offers an important animal model to induce DM and subsequently investigate bladder and urethral function, this animal model does have certain differences in the lower urinary tract from the human. These differences deal with transmitter mechanisms and coordination of voiding [32]. Pharmacological evidence suggests that adenosine triphosphate (ATP) may be the transmitter responsible for atropine resistant bladder contractions, but, on the other hand, humans hold a small component of atropine resistance, which is also independent of neural firing.

As for the coordination of voiding, lower urinary tract of the adult rat displays reflex bladder contractions that occur simultaneously with rhythmic contractions of the external urethral sphincter (EUS). Rhythmic contractions of the EUS have been thought to promote voiding by creating a urethral pumping action or by inducing temporary isometric contractions of the bladder [10]. However, this characteristic of voiding is reminiscent of detrusor sphincter dyssynergia, which is the loss of coordination of the bladder and its outlet, observed following lesions of the spinal cord in humans.

1.5.2. Female versus Male: Anatomical Considerations

As mentioned previously, the lower urinary tract anatomy of the female rat has proven to be a useful model for studying pathology induced changes in lower urinary tract function. Although, the male has also been used for to evaluate genito-urinary tract disorders with studies such as urethral reconstruction, erectile dysfunction, and effects of DM, the female rat lower urinary tract was more suitable both experimentally and anatomically for present studies.

The rat male genito-urinary tract (Figure 1.2) basically consists of bladder, ureters, urethra, vas deferens, bulbourethralis, and the prostate. Many of these elements may cause problems for the experimental set up. For example, biomechanical and pharmacological data are

based on outer diameter measurements; thus, in vivo length must be maintained since the diameter is largely dependent on its length. That is, if the urethra is stretched further than its in vivo length, biomechanical data will be skewed and any diameter response from pharmacological agents will be smaller. In the male urethra, it would be difficult to maintain in vivo length. The lumen of the urethra drastically varies in segments ranging from large (e.g., proximal urethra) to exceptionally small sizes (e.g., the prostatic urethra). These varied segments make it difficult to use one appropriate sized catheter to insert into the lumen, and it is crucial to match up the size of the catheter with the inner diameter of the lumen to avoid any collapsing of the tissue, which would damage the urothelium. Also, since the prostatic urethra is extremely tiny in diameter, it can damage very easily when surgically manipulated.

In the female, the ureters are tubes leading to the bladder neck, which need to be tied off to prevent leakage and serve as anatomical landmarks for in vivo length. Since the ureters are located at the bladder neck, suture ligations will not affect the integrity of the urethra, nor skew any outer diameter data. Despite the fact that the ureters and the vas deferens can be sutured in the male urethra, there still remain tiny tubes leading to the bulbourethralis, which will need to be ligated. Since the urethra is so small in diameter, and the locale of these tubes are at a midpoint along the urethra, these ligations would have a major affect on any deformations that are a result of applying static pressure and would ultimately affect the biomechanical properties. This could also pose a problem for measuring the outer diameter with the laser micrometer.

Finally, one last consideration that deals with muriform rodents entirely is the vaginal plug that is present within the male pelvic urethra. This anatomical component resides in a rather vacuous (relative to the rest of the urethral diameter) outpouching that runs the length of the post-prostatic and pre-penile urethra. Moreover, there are many conduits that make large holes along the length from which the prostatic and seminiferous tubule secretions pour in to solidify and form the eosinophilous, proteinaceous, solid, sperm shuttle. Also, the prostatic urethra could potentially serve as the proximal tying off point, but it is thin and weak and could easily be damaged. As well, the urethra exiting the pelvic floor makes a sharp, perpendicular turn to become fairly the rigid, spring-loaded penis where most mammals, other than humans, have penile bones or at least rigid cartilage, and at this juncture lies a diverticulum. Therefore, the muriform urethra with its specialized sperm delivery system makes it quite difficult for urethral biomechanical studies using this experimental set up.

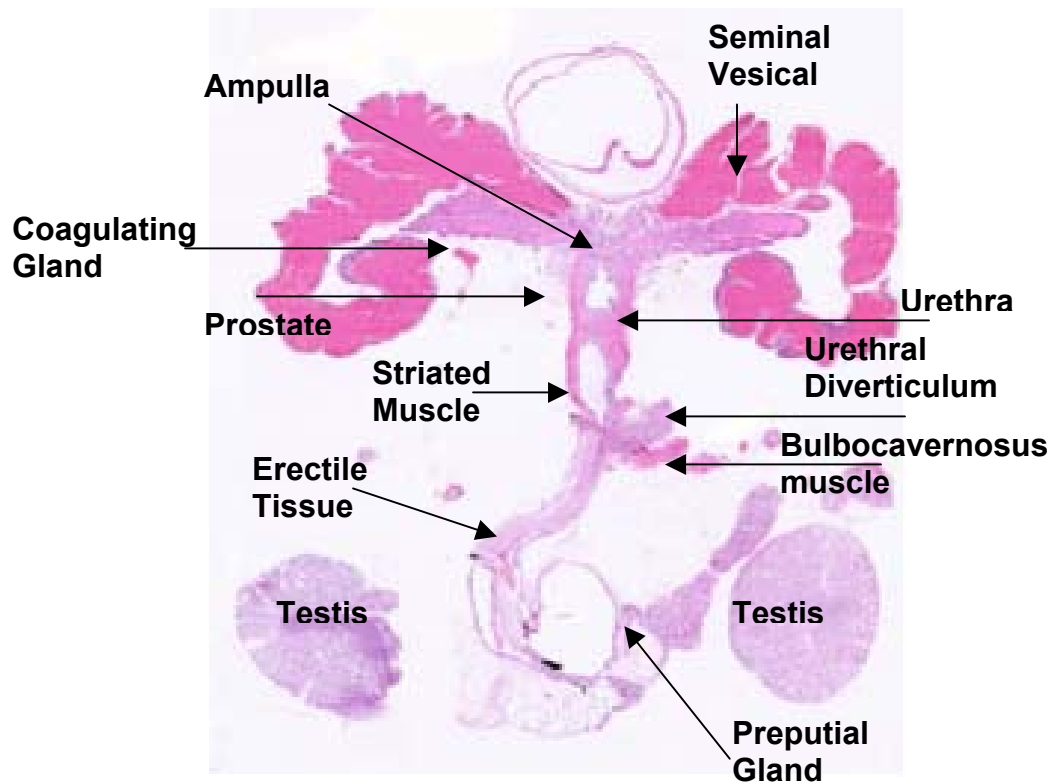


Figure 1.2: Depiction of the lower urinary tract of a male muriform rodent. The female muriform rodent lower urinary tract is more comparable to that of the female human. Adapted from www.uscd.edu/jpathology

A.6 SCIENTIFIC OBJECTIVES AND HYPOTHESES

One of the main outcomes of DM is autonomic neuropathy, which can greatly affect the urinary bladder and the urethral sphincter. While it is clear that many urinary problems occur due to neurological complications, it is also important to evaluate any structural changes to the connective tissue and smooth muscle from diabetes mellitus. The diabetic bladder has been widely studied; yet, understanding the affects of DM on the urethra may be key to solving problems of diabetic cystopathy.

Therefore, the objective of this thesis was to evaluate the effects of DM on the urethral biomechanical properties and pharmacological response of the female rat urethra ex-vivo. Employing techniques discussed in Section 1.5 [87], the biomechanics and smooth muscle function of diabetic rat urethras at three different time points after the onset of induction of diabetes mellitus (3, 5, and 10 weeks) were compared to healthy age-matched controls. These studies were performed in three different states: passive, active, and baseline.

The **Hypotheses** that were addressed in this project are:

- 1) DM urethras are stiffer (less compliant) when compared to healthy controls, and these changes are due to an alteration of tissue musculature and connective tissue components.
- 2) The pharmacological response of DM urethras is impaired in comparison to that of healthy control urethras.

The **Specific Aims** executed to evaluate these hypotheses were:

- 1) A. Experimentally determine the compliance and beta stiffness values of the urethra for normal and DM rats.
B. Perform histological analysis to assess the possible differences of musculature and connective tissue among healthy and DM urethras.
- 2) Compare measurements and observations from 1) A. and B. for three different states, passive with tone, active, and passive without tone, among DM and healthy controls

- 3) Measure contractility and relaxation of the healthy and DM urethras in response to pharmacologic stimulation

2.0 METHODS

2.1 DM INDUCTION AND URETHRAL HARVEST

DM was induced in female rats by intraperitoneal injection of streptozotocin (STZ) at a concentration of 65 mg/kg, which is a standard protocol [85]. STZ abolishes beta cell function of the pancreas, which ceases insulin production, a trait common in patients with DM [38]. Previous to tissue removal, blood sugar was assessed. Rats were considered diabetic with levels above 300 mg/dl. At three different time points following STZ treatment (3, 5, and 10 weeks), animals were anesthetized with urethane (1.2 g/kg), and the urethra was immediately excised. An intraluminal catheter was inserted into the urethra, and an incision at the apex of the bladder dome was made, and the bladder was ligated, as well as the distal external meatus. The ureters were tied off to prevent leakage and to serve as anatomical landmarks for in vivo length measurement, which were made prior excision. The maintenance of in vivo length is important since each animal will have a different sized urethra; thus, all tests were standardize by keeping each specimen at its own specific in vivo length. For transport, urethral specimens were then placed in media 199 that was bubbled for a minimum of 30 minutes with a gas mixture (95% oxygen and 5 % carbon dioxide) in order to prevent anoxia.

2.2 EX VIVO URETHRAL TESTING SYSTEM

The idyllic factors stated Section A.5 served as motivation for the modification of an existing ex vivo vascular testing system [26,42-45] in order to test intact urethras both biomechanically and

pharmacologically [87]. The resulting new urethral testing system [87] is described in this Section.

2.2.1 Static Pressure Measurements

System modifications were required in order to accommodate the urethral tissue. Several constraints were considered when making alterations. First, the system previously had been used to mimic the arterial environment, with applied pressures of 100 mmHg or more, as well as the application of pulsatile pressure. For the rat urethra, the maximum pressure experienced is approximately 25 mmHg [28], and flow is not continuous, but rather intermittent during time of voiding. Thus, it would be appropriate to apply hydrostatic pressure and ignore the effects of flow.

In these studies, stepwise pressure was held constant. Therefore, it was appropriate to measure pressure at one location and this was achieved just proximally to the urethra (Figure 2.1 and 2.2) via a strain gauge transducer (model #: PX272, Baxter Healthcare Co.), which output a signal to a pressure monitor (Model #: 90603A, Space Labs Inc.). Pressure was applied by clamping off the distal tubing (i.e. the exit for the urethra) and by utilizing a hydrostatic pressure reservoir attached to a graduated ring stand. The reservoir was manually displaced to establish graduations, which were calibrated by a manometer for intervals of 2 mmHg using the pressure height relation.

$$\text{Equation 2.1: } p-p_0 = \Delta p = \rho gh$$

The range of intraluminal pressure applied was 0 to 20 mmHg. As for the working fluid, which was cell culture media, the density was taken as $\rho = \rho_{H_2O} = 1000 \frac{kg}{m^3}$. For a change an incremental change in pressure of 2mmHg, the change in height (h) necessary was calculated as 2.7 cm. The applied intraluminal pressure was continuously recorded via computer.

2.2.2 Measurement of Outer Diameter

The outer diameter of the urethra was measured using a helium-neon laser micrometer (laser Model # 162-100, Beta Lasermike) [30]. The laser emits monochromatic light at 632.8 nm and has a scanning range from .254 to 50 mm (+/- .01 mm accuracy). A urethra is placed in the

path of the beam preventing light from reaching the photocell opposite the emission source (Figure 2.1 and 2.2). Using the time interval for a scanning segment and sweep velocity (9800 cm/s), the laser calculates the blocked distance (i.e. the outer diameter). Analog laser voltages are digitized through a 16 channel A/D converter in order to output the measurement to the computer (Pentium II 266 MHz) where it continuously records the data^{27,29,30}. The laser micrometer is calibrated with the use of precisely machined tubes of known diameter.

2.2.3 Components of the Ex Vivo Perfusion System

Due to the small size of the urethras, specially fabricated attachment/infusion tees with an outer diameter of approximately 1.25 mm were used. Pressure ports were attached to the tees with transparent polyethylene tubing (3/16" inner diameter). The tissue housing chamber (Figure 2.1) was composed of plexi-glass with glass windows inserted into the side panels. The glass windows are offset at 5° to minimize diffraction of the laser that scans through the chamber for the purpose of diameter measurement [31]. The lid to the housing chamber consisted of plexi-glass with a gas exchange port attached to the top.

It is important to maintain physiological pH of 7.4 and temperature of 37°C. Media 199 (Sigma Chemical Co., #M3769) was used for the adventitial bath to provide nutrients to the

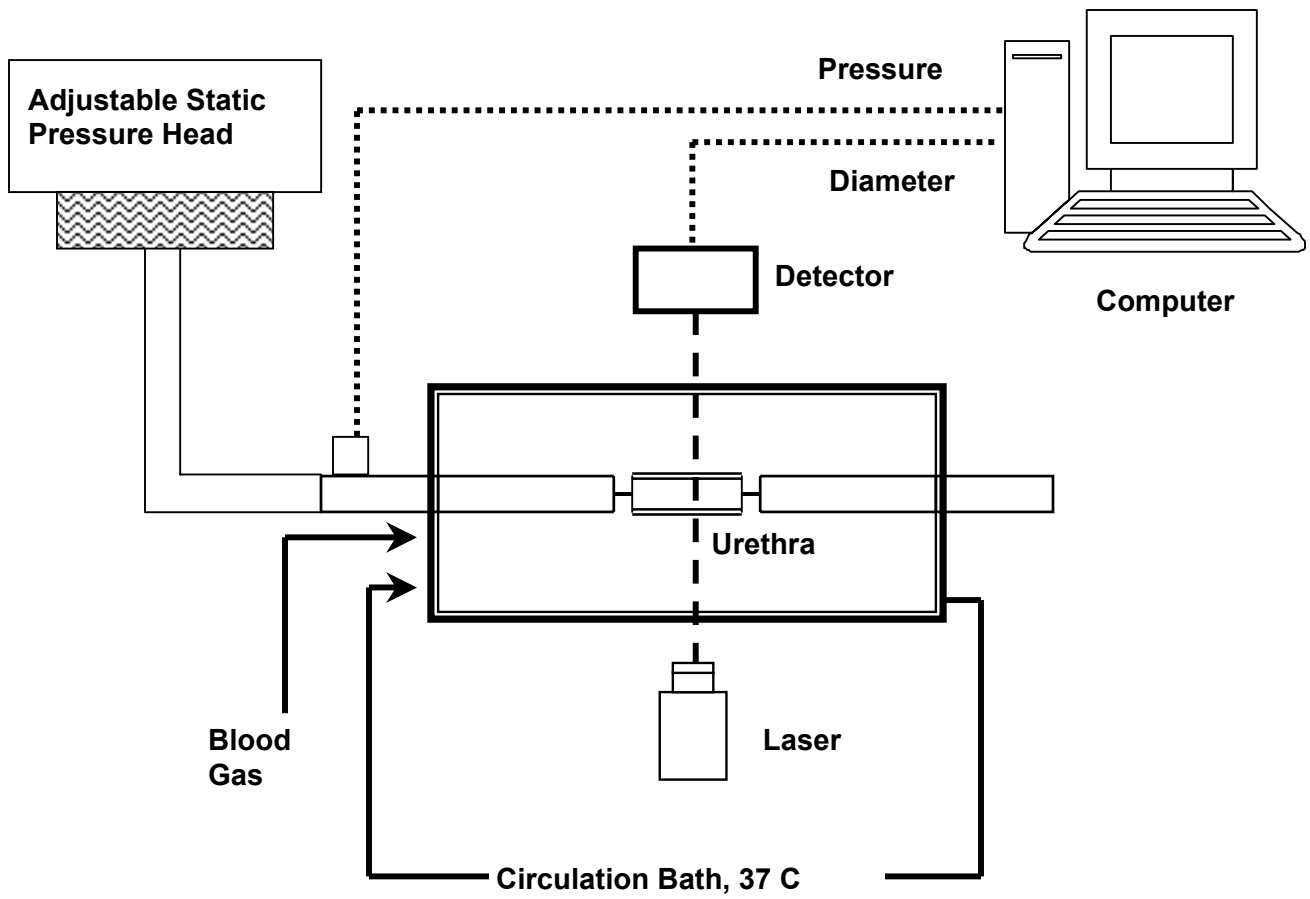


Figure 2.1: A schematic of the modified ex vivo urethral testing system

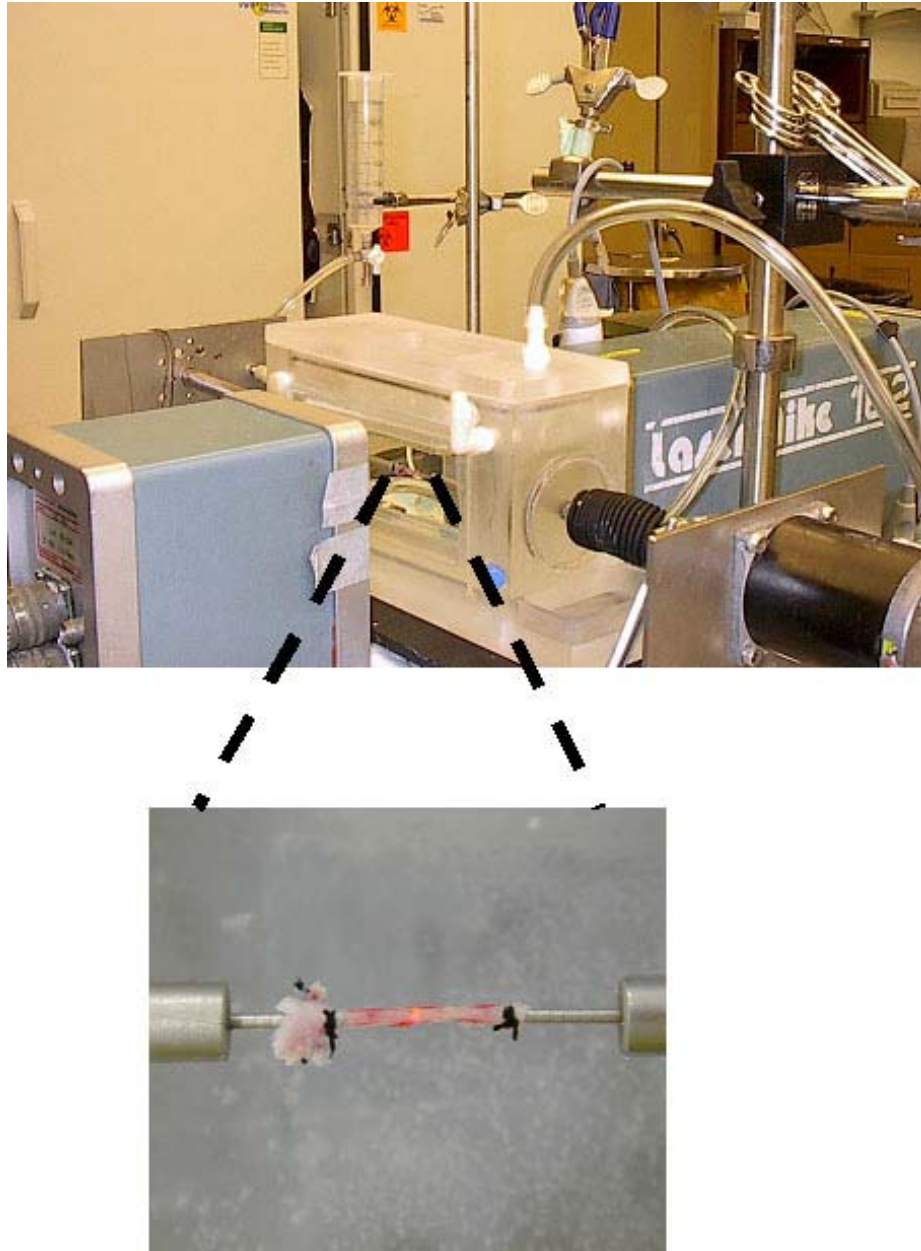


Figure 2.2: A photograph of the entire testing system (top), and a female rat urethra mounted onto the attachment/infusion tees (bottom). The urethras tested had an average length of approximately 20mm.

specimen. This was continuously circulated through a heat exchanger and water bath (Model #: 13000, Lab-Line instruments) by way of a roller pump (model #: 7553-20, Cole Parmer instrument Co). A blood gas mixture (Nationally Valley Gas), consisting of 74% nitrogen, 21% oxygen, and 5% carbon dioxide was directly bubbled into the bathing and reservoir medium in order to maintain physiologic gases.

2.3 BIOMECHANICAL TESTING

In order to assess the affects of DM, biomechanical and pharmacological tests were used. Biomechanical tests were executed in two separate states, baseline and passive. Baseline tone refers to a tissue state in which no attempt was made to either stimulate or eliminate contraction of either muscle component, and passive tone is used to describe the state in which induced muscle contractions, as well as any endogenous tissue tone was eliminated. Pharmacological evaluations were performed to assess alterations to smooth muscle function caused by DM. In this section, the methodology utilized for these measurements is described.

2.3.1 Parameters for Biomechanical Studies

Before performing our biomechanical studies, it was first necessary to establish two testing parameters: the maximum number of cycles needed for preconditioning (i.e. to obtain a repeatable curve) and the duration of each step of pressure. Initially, specimens were preconditioned between 0 and 16 mmHg. The range was decreased to between 0 and 8 mmHg because it was felt that the higher pressure of 16 mmHg might disrupt the muscle fibers, which would skew any biomechanical properties. It was determined that 6 to 7 cycles of this pressurization was sufficient to obtain a repeatable curve (Figure 2.3).

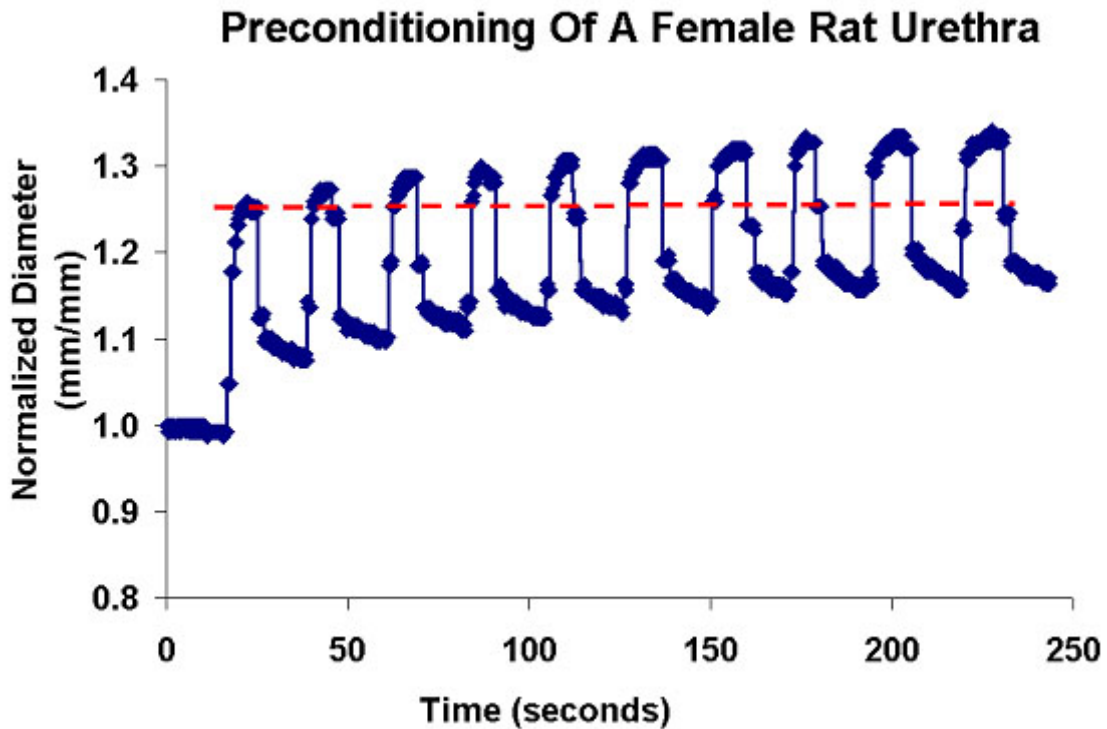


Figure 2.3 : The above picture represents the results of the preconditioning regimen of the middle region for a female rat urethra in the baseline state. The dotted line indicates the diameter of the urethra after the first cycle's pressure step, illustrating the change in peak diameter over from the first cycle to the tenth. Note that by the sixth or seventh cycle the cycles begin to appear repeatable.

Similarly, preliminary step experiments were performed in order to determine the duration needed for the diameter measurement to become stable after each 2 mmHg increment of pressure. This was completed by holding each pressure for a duration of 1.5 minutes and observing the extent to which the diameter became constant. From Figure 6, one may see that the diameter did reach a constant value at lower pressures as soon as 1 minute after application, but this held true only for pressures up to approximately 6 mmHg. Beyond this pressure, the diameter remained constant for 2 minutes and increased a minimal amount (roughly less than 1%) by the end of the 1.5 minute interval. Thus, the time parameter for each step in the static pressure experiment was a 1-minute interval.

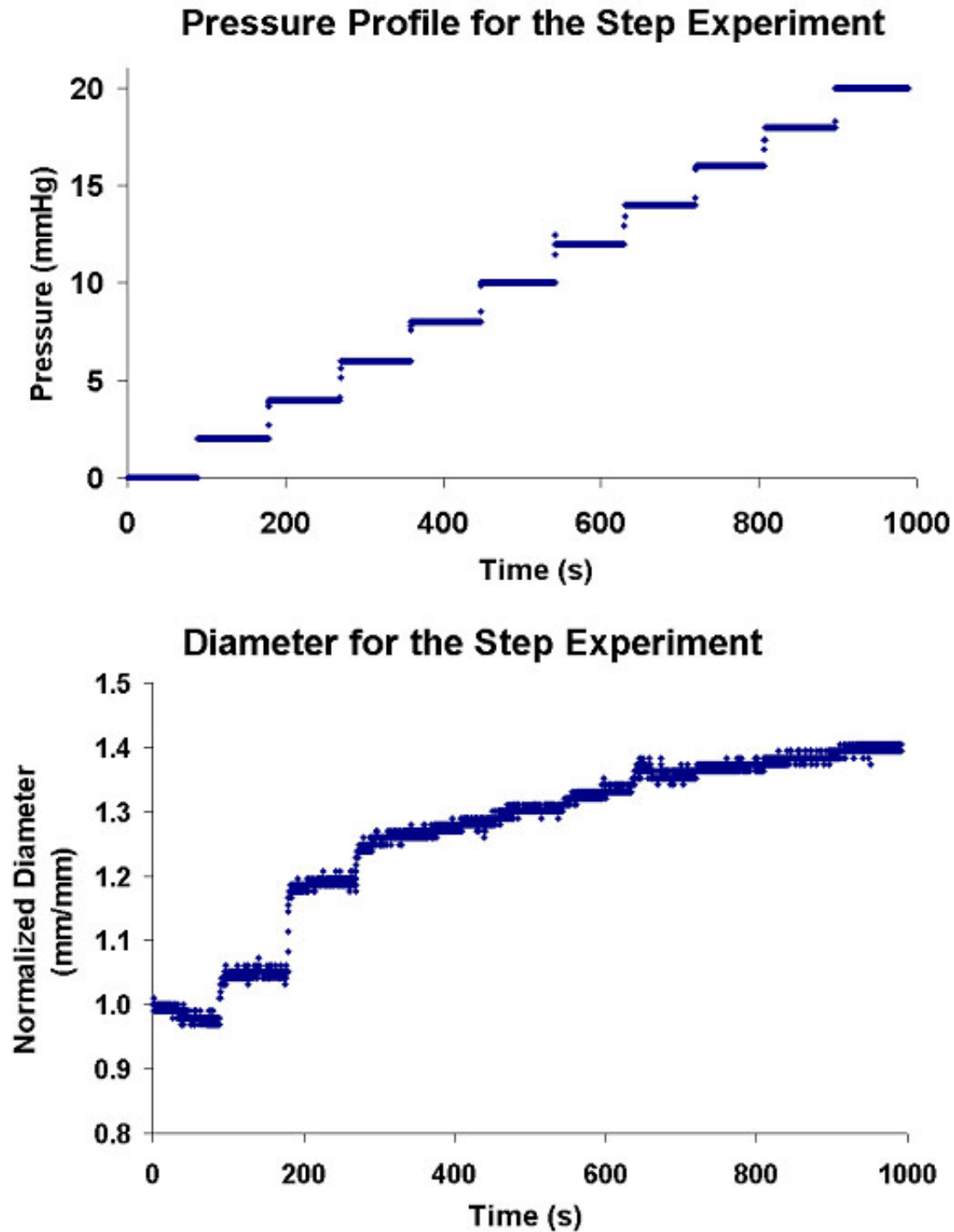


Figure 2.4: *Top*: The pressure profile for a static pressure experiment holding each increment of pressure for 5 minutes. *Bottom*: The resulting outer diameter measurement for the proximal portion of a female rat urethra.

2.3.2 Baseline Biomechanical Studies

Upon arrival to the laboratory, specimens were mounted onto the tees of the ex vivo testing system described in Section 2.1. The hydrostatic pressure reservoir was manually displaced about the calibrated ringstand in order to apply intraluminal static pressure. First, the tissue was preconditioned as described in Section 2.2.1 (Figure 2.3). Next, the urethra was subjected to the step experiment described in Section 2.2.1 (Figure 2.4).

Due to the fact that the tissue is non-homogeneous, measurements were taken at three positions along the length (L) of the urethra (Figure 2.5): the proximal (a distance of $L \cdot 0.3$ from the proximal end of the specimen), middle (a distance of $L \cdot 0.5$ from the proximal end of the specimen) and distal (a distance of $L \cdot 0.7$ from the proximal end of the specimen) positions.

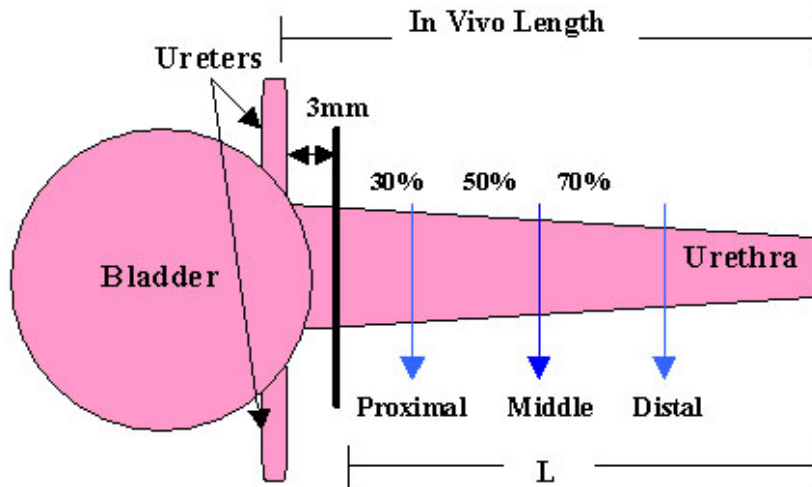


Figure 2.5: Schematic depicting the identification of the three positions used for measurement along the length of the urethra. L was taken as 3mm less than the measured in vivo length. neck, the value of ' L ' used here was 3mm less than the in actual measured in vivo length. L was actually considered to be the length of the urethra.

It should be noted that in order to take into account that the ureters are integrated with the bladder. From the pressure and diameter data gathered, compliance (C; equation 2) and beta stiffness [34] (β ; equation 3) values were calculated to quantify the biomechanical properties of the urethra.

Equation 2.2 :

$$C = \frac{(D_{Max} - D_{Min}) / D_{Min}}{(P_{max} - P_{min})}$$

Equation 2.3:

$$\beta = \frac{\ln\left(\frac{P}{P_s}\right)}{\left(\frac{D}{D_s} - 1\right)}$$

C, is the fractional change in volume that occurs in response to changes in pressure where D_{max} and D_{min} represent the measured diameters corresponding to the maximum and minimum pressures, P_{max} and P_{min} , used to define the range over which the compliance is calculated. The incremental compliance was evaluated for the following pressure ranges: 0-6 mm Hg, 6-12 mmHg and 12-18 mmHg. This approach permitted correlations of differences in biomechanical behavior with tissue microstructure [88]. Beta stiffness, β , is a dimensionless parameter which may be utilized to describe non-linear pressure-diameter responses and incorporates all pressure-diameter values over the range of physiologic pressure examined. P_s and D_s are a standard pressure and paired corresponding diameter, respectively, which is chosen by the investigator to be within the average physiologic pressure range. Since 10mmHg fell at a mid point of the physiological range, it was chosen as P_s for this experiment.

2.3.3 Passive Biomechanical Studies

Studies on the biomechanics of the passive urethra were performed in the same manner as for the baseline studies described in Section 2.3.1 with the exception of the addition of 3mM ethylenediamine tetraacetic acid (EDTA), a calcium and magnesium chelator, into the bath with a syringe. The incorporation of this agent occurred prior to mechanical testing and the tissue was allowed to equilibrate for 30 to 45 minutes in order to ensure that muscle contractions were completely blocked and the tissue is completely passive. Compliance and beta stiffness were calculated and quantified as in Section 2.2.2.

2.4 PHARMACOLOGICAL ASSESSMENT OF URETHRAL SMOOTH MUSCLE FUNCTION

Tissue responses were measured at the middle portion of the urethra following addition of muscle agonists or antagonists for both healthy urethras and urethras after 5 and 10 weeks of DM. For these experiments, the urethra was exposed to a fixed intraluminal pressure of 8 mmHg, which caused the tissue to be pre-dilated and allowed for a measurable amount of contraction to take place. Upon pressurizing the urethra at 8 mmHg, 30 minutes was allowed in order for the specimen to reach a baseline diameter ($D_{8\text{mmHg}}$). This measurement allowed the determination of the relative percentage change ($\% \Delta D$) in outer diameter, following the addition of muscle-responsive agents, added consecutively: 100 μM [36] N ω -Nitro-L-arginine (NLA), a nitric oxide synthase (NOS) inhibitor; 40 μM [35] phenylephrine (PE), a nonselective alpha-adrenergic receptor agonist; and 3 Mm [37] ethylenediamine tetraacetic acid (EDTA), a calcium chelator, (n=6-9). Specifically, $\% \Delta D$ was calculated as:

Equation 2.4:

$$\% \Delta D = \left(\frac{D_{drug} - D_{8mmHg}}{D_{8mmHg}} \right) \times 100\%$$

where D_{drug} represents the diameter response to each respective pharmacologic agent, and D_{8mmHg} is defined as the baseline diameter measured at an intraluminal pressure of 8mmHg prior to addition of any pharmacological agents. In order to ensure full effect on the urethra, a time interval of 20 to 30 minutes was permitted after administration each pharmacological agent, with the exception of EDTA where the interval was increased to 30 to 45 minutes to ensure the fully passive state for biomechanical testing.

At the time of pressure application or drug addition, the pressure was measured from the transducers and the diameter was taken as an average of the last 100 diameter data points recorded before the addition of the next drug. Calculations for % ΔD were performed for the maximal diameter response to 8 mmHg, NLA, and EDTA. Both the maximum magnitude of contraction (PE-Max) and the magnitude of contraction value just before addition of EDTA (PE-End) was calculated for diameter response to PE.

2.5 MICROSTRUCTURAL ANALYSIS

For immunohistological and histological evaluation, upon the termination of experiments, urethras were removed from the experimental testing system, re-tied onto the intraluminal catheter at in vivo length, and placed in 10% formalin in phosphate buffered saline (PBS) overnight. Specimens were then subjected to ascending sucrose solutions of, 10%, 20%, and 30% sucrose in PBS, which served as a ‘cryoprotectant’ to the tissue. Histological assessment was performed in order to examine and quantify the microstructure; more specifically the collagen, elastin, and smooth muscle components. Alterations to these constituents were compared to the results of the biomechanical and pharmacological data. For example, an

increase in stiffness of DM tissue may be a result of an increase in collagen present, or conversely, a decrease in elastin. The following sections describe the methods used for microstructural analysis of all urethral specimens studied.

2.5.1 Identification of Smooth Muscle

Quantifying the smooth muscle may aid the understanding any impairment of urethral smooth muscle function due to DM. Both smooth muscle types, i.e. longitudinally- and circumferentially- oriented, may be identified with smooth muscle alpha actin antibody staining. Alpha actin is a cross-linking protein, which helps to form a loose contractile bundle of actin filaments. This protein is concentrated in stress fibers in contractile bundles of the smooth muscle. Thus, this method is suitable for specifying smooth muscle in the urethra.

First, urethras were divided into proximal, middle, and distal portions as defined in Section 2.2.2. Each section was placed vertically into a cryomold and saturated with TBS freezing medium (Fisher Co) where it was then snap frozen in liquid nitrogen in order to avoid any deterioration of the tissue due to ice crystal formation. Next, 8 to 11 μm cross sections of the proximal, middle, and distal portions of the urethra were cut with a cryostat (Thermoshandon) and placed onto gel-coated slides to increase the adherence of the section to the slides. Each section was circled with PAP-pen, a hydrophobic marker.

Prior to immunohistochemistry, the tissue was fixed in 2% paraformaldehyde for 1 hour at room temperature. Goat serum was used to block any non-specific protein binding (45 minutes). Primary antibodies (Chemicon) for the smooth muscle alpha actin were diluted 1:100 with bovine serum albumin (BSA) and left on the sections for 1 hour. Subsequently, the secondary antibody for fluorescence, TRITC, was placed on the sections for another hour in dilutions of 1:200 with BSA. Finally, for a secondary stain of cell nuclei, Hoescht was placed on the sections for 15 to 30 seconds. All slides were coverslipped with gelvatol and protected from light. All washes between steps were performed with PBS and BSA.

2.5.2 Identification of the Connective Tissue

Collagen and elastin are the two major connective tissue matrix proteins that were quantified in this study. Two separate histological staining methods were used to designate each protein.

The tissue was embedded and prepared for microscope slides in the same manner as in Section 2.5.1 with the exception that sections were 20 μm thick, and slides were not gel coated. (The gelatin coated slides were found to non specifically bind to the stains resulting in a high degree of background staining.) For collagen, Masson's trichrome stain was used. First, slides were placed in Bouin's solution overnight at room temperature. Slides were washed in running tap water and kept in Weigert's hemotoxylin (Sigma Chemical Co.) for 5 minutes. After washing in running tap water, Biebrich scarlet-acid fuchsin (Sigma, #HT-151-250) was used for 5 minutes, and a wash with deionized water followed. Phosphomolybdic/phosphotungstic acid (Sigma, #224200 #P0550) solution prepped the sections for the aniline blue solution (Sigma, #41,504-9). Slides were then submerged in 1% acetic acid solution for 5 minutes, dehydrated in ascending alcohols (95% and 100%), cleared in xylene, and coverslipped with gelvatol.

Elastin was differentiated from collagen by using Weigert's resorcin fuchsin. The tissue was prepared for microscope slides in the same manner as for the collagen stain. First, sections were hydrated with tap water, then subjected to acidified potassium permanganate (Aldrich, #31,941-4), 1 % oxalic acid (Sigma, #O-0376), and 70% alcohol, sequentially. Next, the sections were stained in Weigert's resorcin fuchsin (Sigma, #R-5645; Aldrich, #85,734-3) at room temperature followed by a differentiation step in acid alcohol. Finally, slides were dehydrated with ascending alcohols, cleared in xylene, and coverslipped.

2.5.3 Quantification of Tissue Constituents

Pictures were taken of each circular section using a fluorescent (immunostaining; Nikon Eclipse, model E800, Tokyo, Japan) and light (histological stains; Olympus, model BX51, Japan) microscope at 20x magnification at four positions along the circumference, i.e., at the 12 o'clock, 3 o'clock, 6 o'clock, and 9 o'clock positions. Smooth muscle was identified by the red fluorescence emitted by the Tritc secondary antibody. Collagen was identified by the blue color

and elastin by its deep purplish black color. Smooth muscle, collagen, and elastin were separately quantified using Bioquant Nova software (NOVA 4.00.8 for Windows 98, vol.1581, Nashville, TN). The software measured the area for each portion of interest based on their respective colors and exported this data to a Microsoft Excel workbook where it was subsequently analyzed. The total area of the section was also measured. The total areas calculated for the four clockwise positions were added for total area (A_{total}), and the amount of stained areas for collagen, elastin, or smooth muscle was added together in the same manner (A_{stain}). The percentage of each component ($A_{stain}\%$) was then calculated by:

Equation 2.5:

$$\%A_{Stain} = \left(\frac{A_{stain}}{A_{total}} \right) \times 100\%$$

An average was taken between two separate sections for each position for all specimens, so that each of the three constituents of interest were expressed as a percentage of total area.

2.6 STATISTICAL ANALYSIS

For both baseline biomechanical studies and passive biomechanical studies, three different time points were compared to healthy controls. Statistical analysis was performed with Sigma Stat Software (Aspire Software Int., Leesburg, VA) using a one-way analysis of variance (ANOVA) with repeated measures to compare the compliance and beta stiffness values of the portions (i.e., proximal, middle, and distal) within the specimen. A one-way ANOVA was used to compare each portion separately among time points and healthy controls. Finally, a two-way ANOVA was used to evaluate which factor played a larger role in any differences, onset of DM (i.e. DM vs. control), positions within the tissue, or both.

For pharmacological data, as well as tissue constituent data, one way ANOVA was used to analyze whether there were any differences between controls, 5 and 10 weeks DM at the middle position. A Student Newman Keuls test was used for post-hoc testing.

3.0 RESULTS

3.1 THE DIABETIC RAT MODEL

Approximately three weeks post-STZ injection, Sprague-Dawley female rats began to show rapid weight loss and emaciation, but this characteristic did not hold true for all animals injected with STZ. Some of the animals did not show this characteristic until after 6 weeks post-STZ injection. Other than high blood sugar (Figure 3.1), anatomical features of diabetic rats exhibited large bowels, largely distended urinary bladder, little surrounding adipose tissue, soft fecal matter, and enlarged ureters and urethras.

3.2 BIOMECHANICAL STUDIES

3.2.1 Baseline Biomechanics

All urethras, whether DM or healthy, had non-linear, sigmoidal pressure-diameter curves which is characteristic of biological tissues. Such data is a useful indication of tissue compliance or distensability, with a leftward shift of the pressure-diameter curves indicating a decrease in this property. Averaging all pressure-diameter data of healthy controls indicated a trend of a proximal-to-distal compliance gradient, proximal being the most compliant and distal being the least (Figure 3.2). Comparing the averaged pressure-diameter response curves of DM and

healthy urethras suggests that proximal 3-week DM urethras are more distensible than control and 5 and 10-week DM urethras (Figure 3.3). While this trend seemed to hold for middle portions, the control distal portion was less distensible compared to all three time-points of DM.

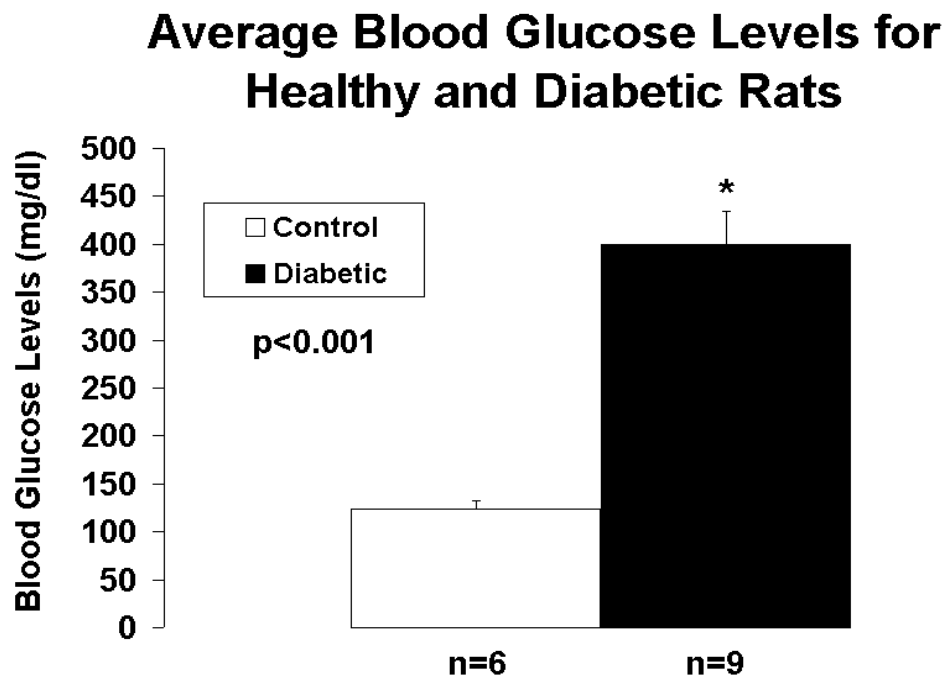


Figure 3.1: Blood glucose levels of DM rats compared to healthy controls

Pressure-Diameter Response For A Healthy Urethra At Baseline State

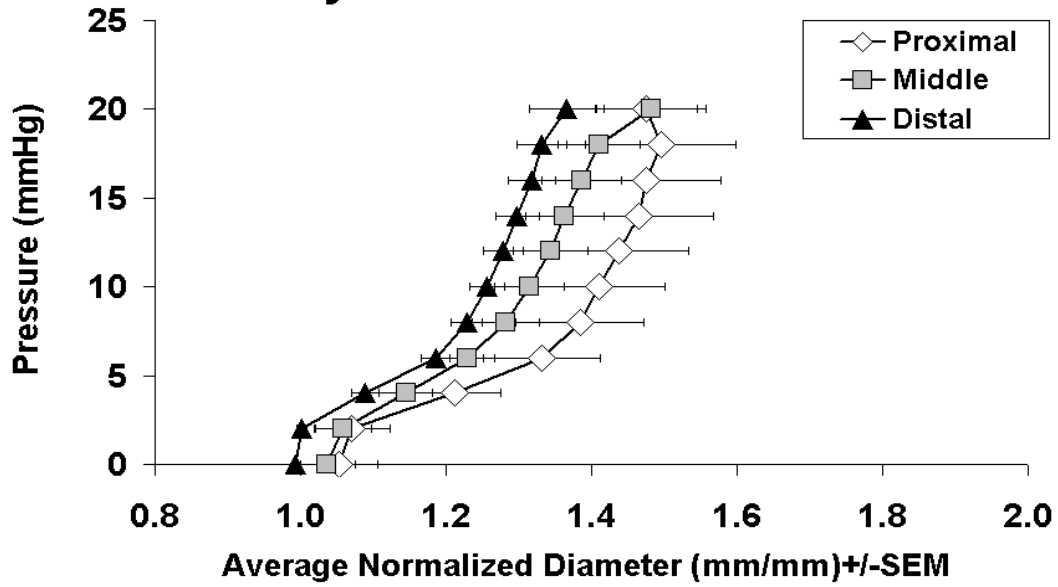


Figure 3.2: The average pressure-diameter data for 11 healthy urethras in the baseline condition. Note the proximal to distal stiffening effect as indicated by the leftward shift of the curves.

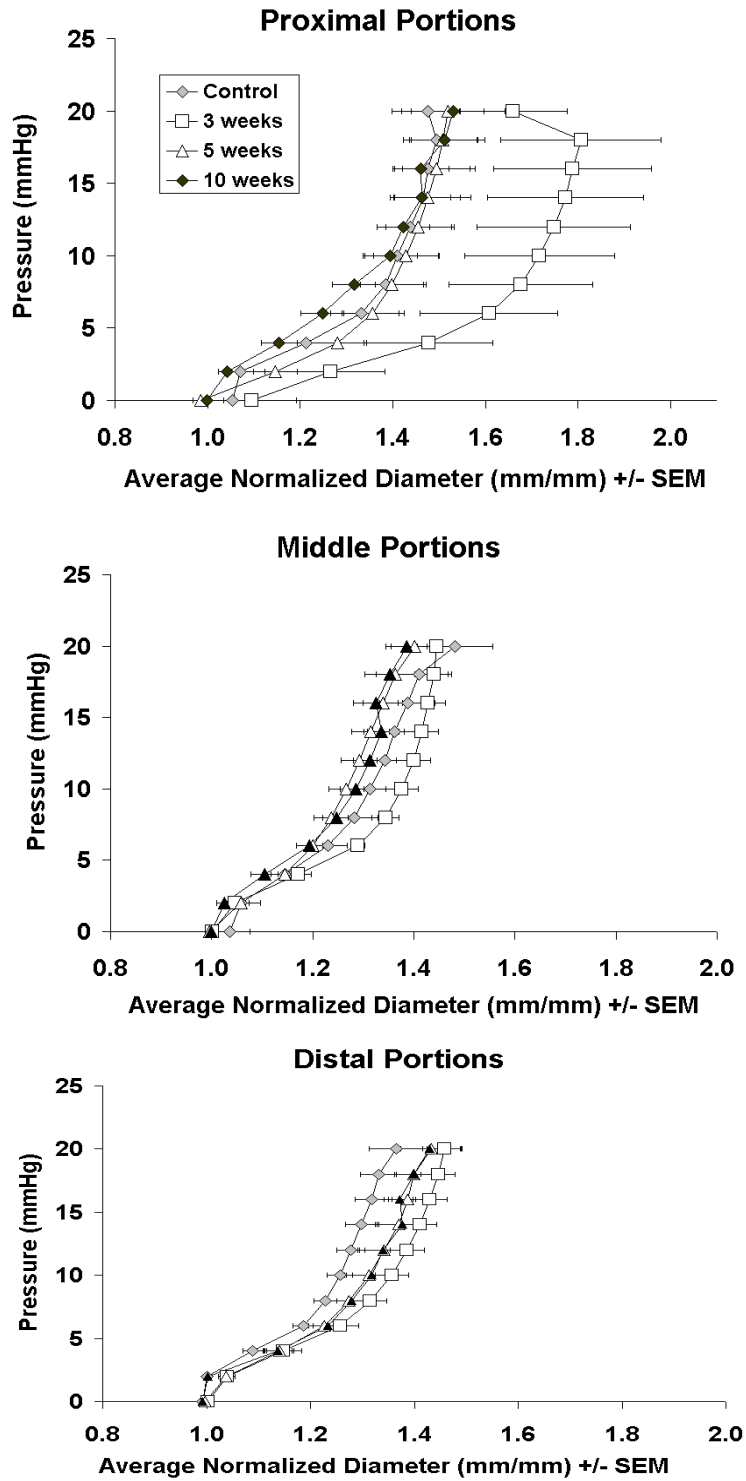


Figure 3.3: Average pressure-diameter response of proximal (top), middle (middle) and distal (bottom) portions of DM urethras and controls in the baseline state.

As one general comparison, the 3-, 5-, and 10-week DM urethras were combined into a single group of DM data (n=31) and compared to healthy controls (n=11) for both the baseline and passive states. For low-pressure (0 to 6 mmHg) incremental compliance, the proximal portion ($0.062 \pm 0.006 \text{ mmHg}^{-1}$) was significantly more compliant than middle ($0.037 \pm 0.003 \text{ mmHg}^{-1}$) and distal ($0.039 \pm 0.003 \text{ mmHg}^{-1}$) portions ($p < 0.001$; Figure 3.4A) in control tissues. The DM proximal portion was significantly more compliant than that of the control proximal (0.062 ± 0.006 versus $0.046 \pm 0.006 \text{ mmHg}^{-1}$; $p < 0.05$). All other comparisons in the other pressure ranges (6 to 20 mmHg) among control middle ($0.032 \pm 0.006 \text{ mmHg}^{-1}$) and distal ($0.032 \pm 0.004 \text{ mmHg}^{-1}$) and DM middle and distal displayed no statistical significance.

Separating the time points of DM for low-pressure incremental compliance, the progressive changes in the disease state were observed (Figure 3.4B). For within-tissue differences at low-pressure compliance, statistical analysis via one-way ANOVA with repeated measures indicated that the proximal portions of the 3-week ($0.077 \pm 0.013 \text{ mmHg}^{-1}$) and 5-week ($0.062 \pm 0.009 \text{ mmHg}^{-1}$) DM urethras were significantly more compliant than their middle (0.048 ± 0.002 versus $0.034 \pm 0.006 \text{ mmHg}^{-1}$, respectively; $p < 0.01$) and distal (0.042 ± 0.006 ; $0.038 \pm 0.005 \text{ mmHg}^{-1}$) portions. Low pressure compliance also revealed that the proximal and middle portions of the 3-week DM urethra were significantly more compliant than control proximal (0.077 ± 0.013 versus $0.046 \pm 0.006 \text{ mmHg}^{-1}$, respectively; $p < 0.05$) and middle ($0.032 \pm 0.006 \text{ mmHg}^{-1}$) portions ($p < 0.05$ and $p < 0.01$, respectively), and that middle portions of 10-week DM were significantly less compliant than 3-week mid portion (0.030 ± 0.005 versus $0.048 \pm 0.002 \text{ mmHg}^{-1}$, respectively; $p < 0.01$).

Middle pressure (6 to 12 mmHg) incremental compliance for the baseline state showed no within-tissue differences for either control or DM urethras (Figure 3.5). Proximal, middle, and distal areas compared among control (0.011 ± 0.002 , 0.016 ± 0.002 , $0.013 \pm 0.001 \text{ mmHg}^{-1}$) and DM (0.018 ± 0.003 , 0.015 ± 0.002 , 0.02 ± 0.002) were not significantly different either. High-pressure (12 to 20 mmHg) compliance values for control (0.007 ± 0.002 , 0.008 ± 0.002 , $0.007 \pm 0.001 \text{ mmHg}^{-1}$) and DM (0.007 ± 0.001 , 0.007 ± 0.001 , $0.008 \pm 0.001 \text{ mmHg}^{-1}$) proximal, middle, and distal segments displayed no within-tissue differences or between DM and control (Figure 3.6).

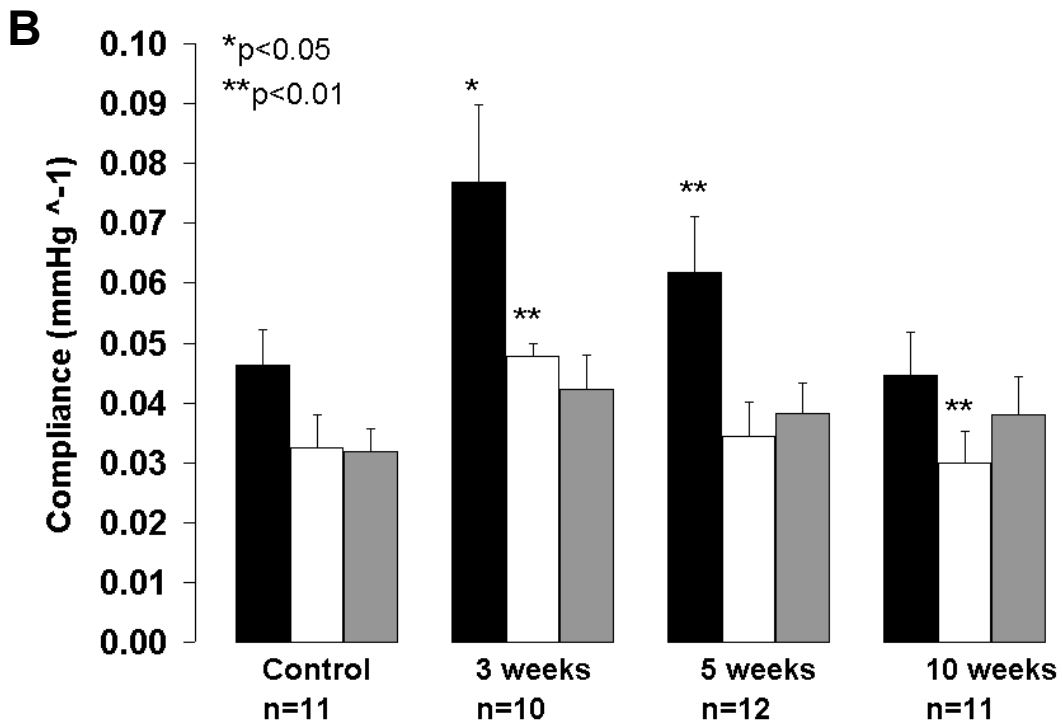
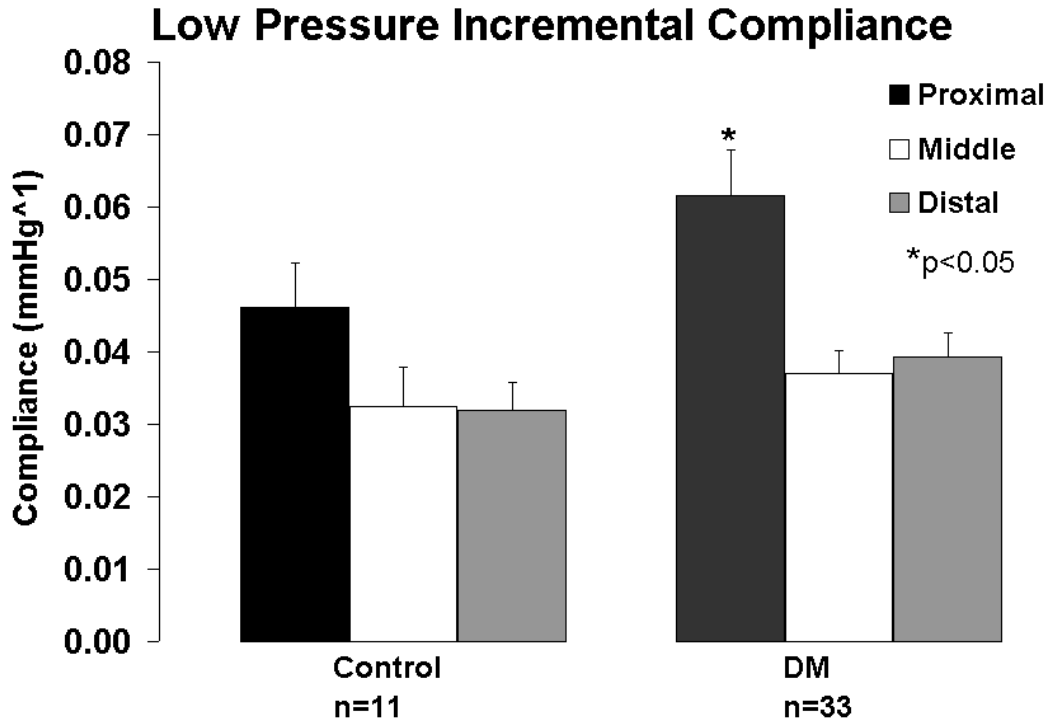


Figure 3.4: Low pressure incremental compliance (0 to 6 mmHg) values for DM (A) and three time points of DM (B) in comparison to control values in the baseline state. Error bars represent standard error of the mean.

The middle (Figure 3.5) and higher pressure (Figure 3.6) compliances revealed no statistical differences among positions within the specimens of each time point compared with the control group. Comparing proximal positions for middle pressure compliance among controls ($0.011 \pm 0.002 \text{ mmHg}^{-1}$), 3-week ($0.017 \pm 0.005 \text{ mmHg}^{-1}$), 5-week ($0.012 \pm 0.001 \text{ mmHg}^{-1}$), and 10-week ($0.025 \pm 0.006 \text{ mmHg}^{-1}$), one-way ANOVA indicated a trend where 10-week DM proximal portions were more compliant than proximal portions of controls ($p = 0.06$). The middle portions and distal portions for, 3-week, 5-week, and 10-week had no significant differences among the groups at both middle and high pressure compliances. Two way ANOVA analysis showed that onset of DM played a large role in significant differences found for middle pressure incremental compliance. This indicated that 10-week DM was significantly more compliant from both 5-week ($p = 0.026$) and controls ($p = 0.021$), more specifically for the proximal portions. Two way ANOVA indicated no difference among the groups for high pressure incremental compliance.

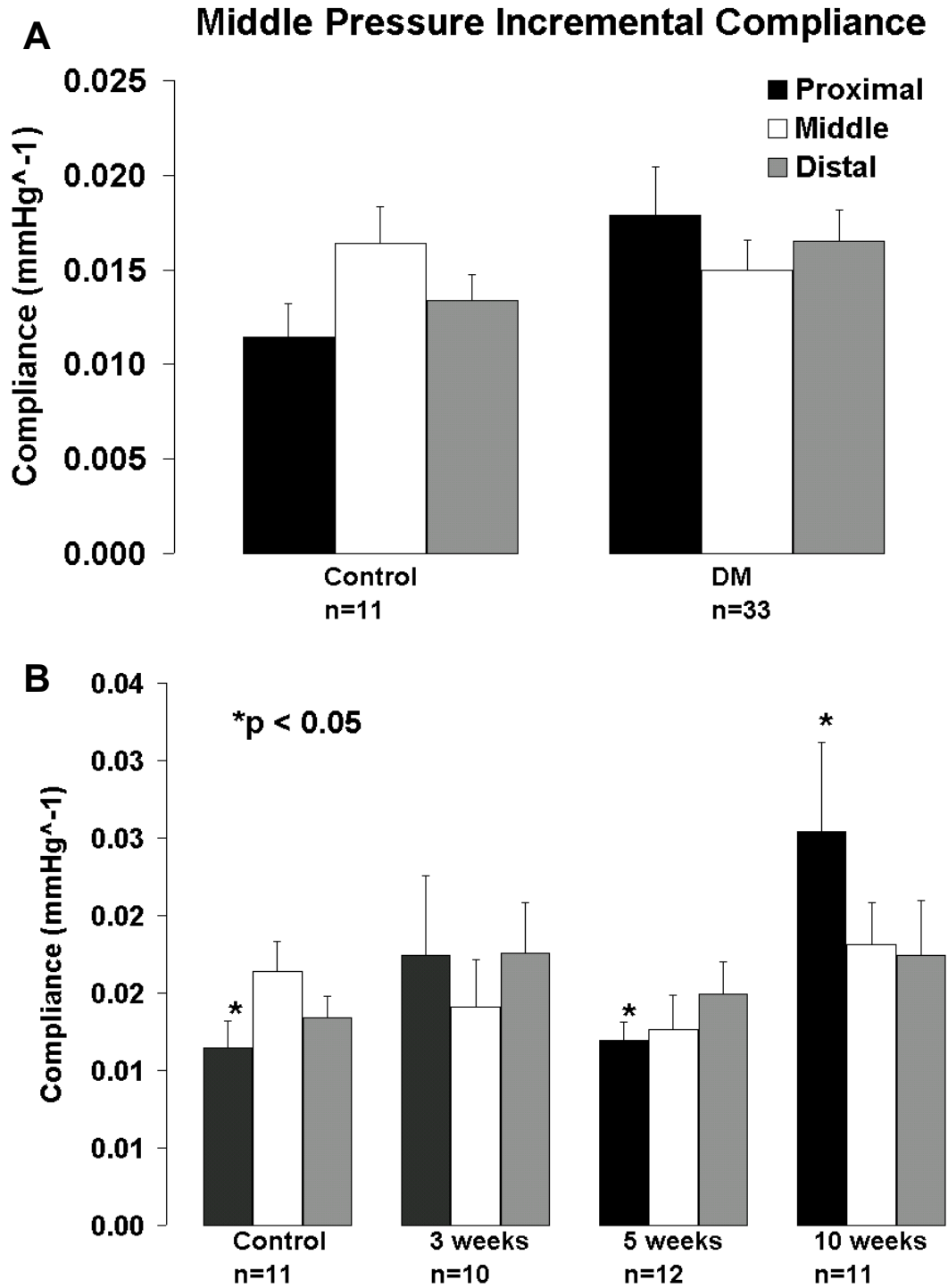


Figure 3.5: Middle-pressure incremental compliance (6 to 12 mmHg) values for DM (A) and three time points of DM (B) both in comparison to control values in the baseline state. Error bars represent standard.

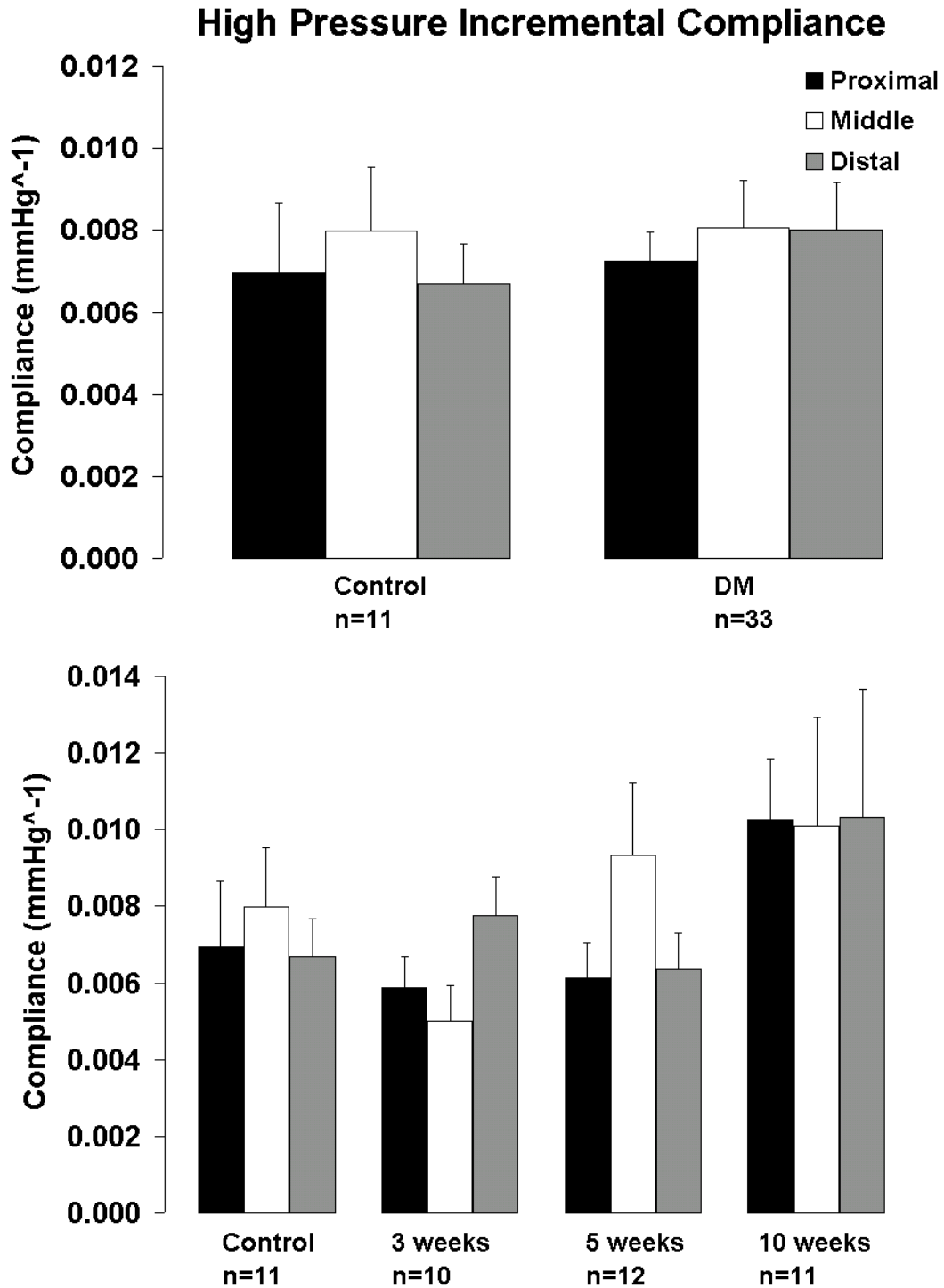


Figure 3.6: High-pressure incremental compliance (12 to 20 mmHg) values for DM (A) and three time points of DM (B) both in comparison to control values in the baseline state. Error bars represent standard error of the mean.

Beta Stiffness values calculated for all three portions of controls (7.3 ± 0.9 , 7.8 ± 0.8 , 7.6 ± 0.8) and DM (8.0 ± 0.4 , 8.6 ± 0.5 , 8.1 ± 0.5) displayed no significant within-tissue differences and no significant differences between DM and controls (Figure 3.7). On the other hand differences were found when the time points of DM were compared to controls (Figure 3.7). Beta stiffness values for the proximal and middle portions of 5-week DM (9.1 ± 0.5 , 9.8 ± 0.8 ; $p < 0.05$) were significantly stiffer (less compliant) than that of 10-week DM (6.9 ± 1.0 , 7.8 ± 0.5 ; $p < 0.05$). Beta stiffness showed no significant differences amongst positions within the tissue in any of the groups (Figure 3.7).

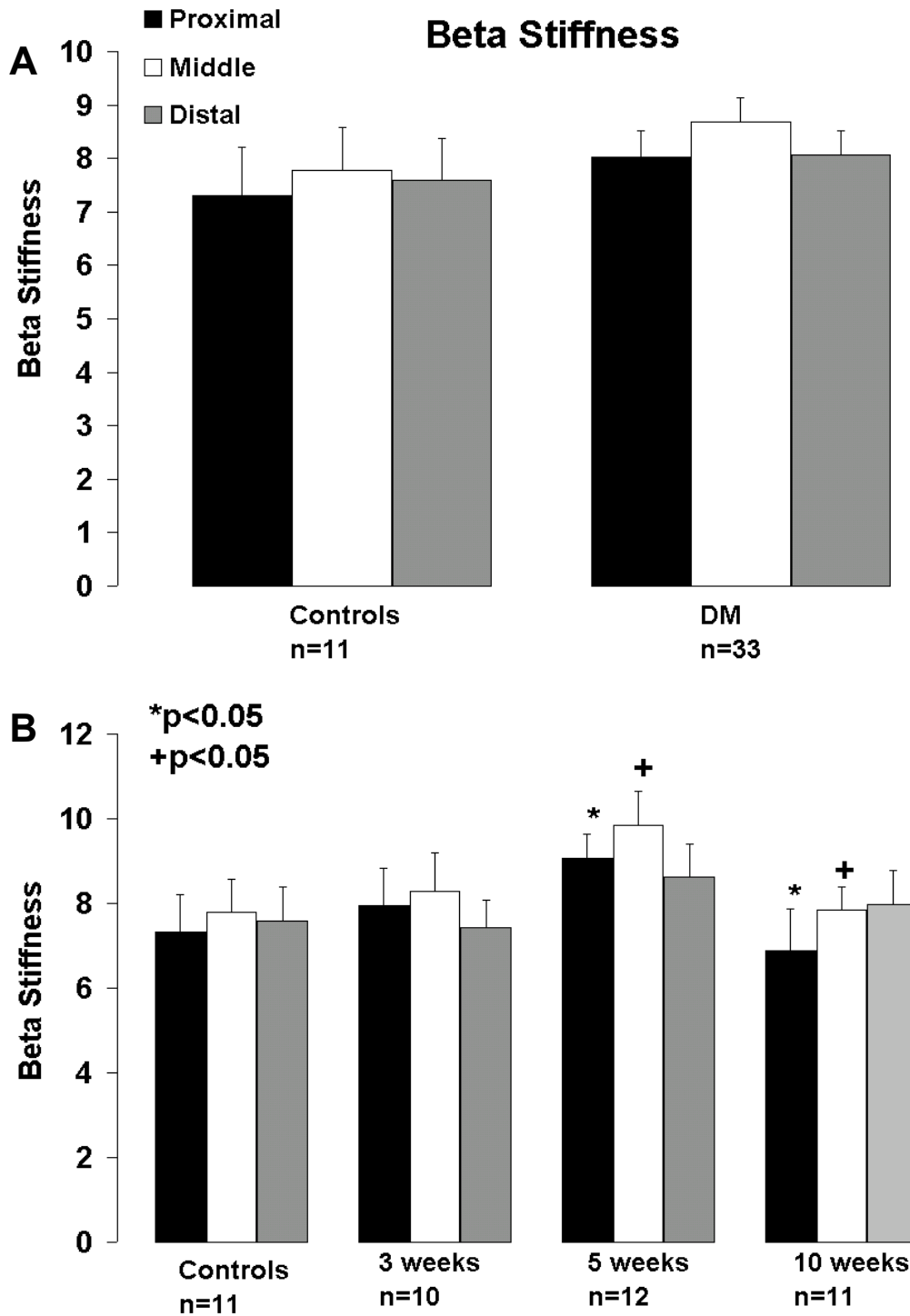


Figure 3.7: Beta Stiffness values for DM (A) and three time points of DM (B) both in comparison to control values in the baseline state. Error bars represent standard error of the mean.

3.2.2 Passive Biomechanics

Pressure-diameter curves for healthy urethras showed a nonlinear, exponential curve often characteristic of biological tissues (Figure 3.8). For control tissue, the proximal-to-distal compliance gradient - which was also seen in the baseline state (recall Figure 3.2) - became statistically significant ($p = 0.001$), with the proximal significantly more compliant than the mid and distal portions.

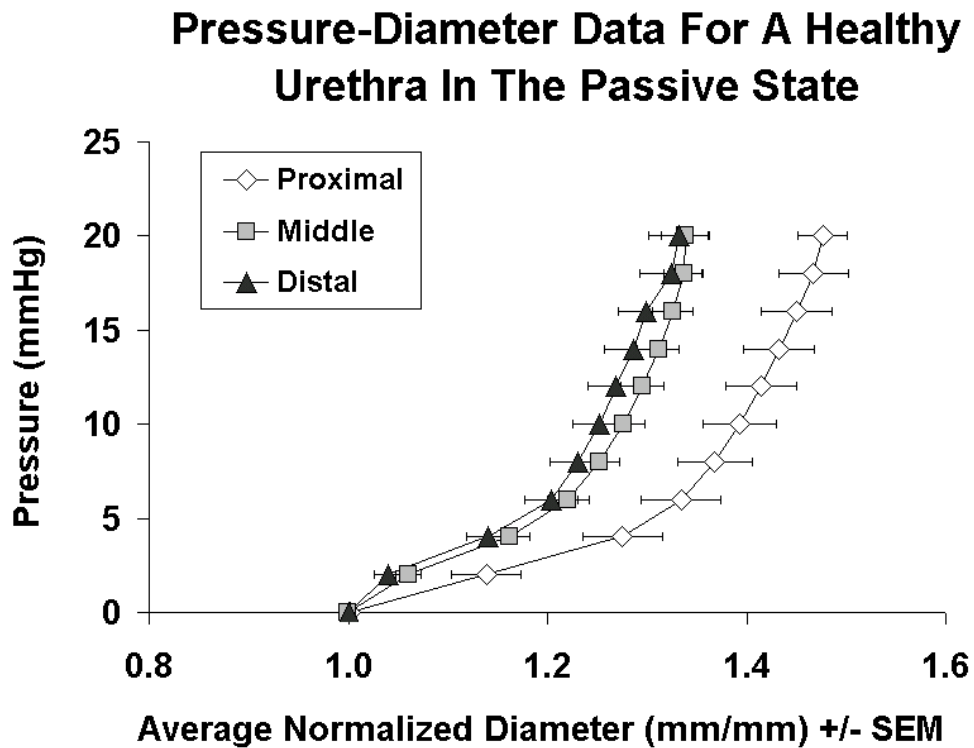


Figure 3.8: Pressure-diameter curves for the three different positions along the length of the urethra. With a proximal-to-distal shift to left, this data suggests that the proximal portion is more compliant than both the mid and distal portions.

Comparing each portion separately among groups, the normalized and averaged pressure-diameter plots distinguished some differences in the passive state between controls and diabetic urethras at different time points (Figure 3.9). For proximal portions, the 3 and 10-week DM had a more compliant response than control and 5-week. With middle and distal portions, all time points of DM displayed a marked shift to the right (i.e. increase in compliance or reduction in stiffness) compared to controls.

Initially, comparisons were made simply between control biomechanical data and all time points of DM as a group. As stated previously, passive data for low pressure incremental compliance (Figure 3.10) indicated within-tissue differences with proximal compared to middle and distal portion, and there was a significant difference among dm portions (0.082 ± 0.009 , 0.057 ± 0.003 , 0.057 ± 0.004 mmHg⁻¹; $p < 0.01$). Comparing portions between groups in this pressure range, proximal portions for controls (0.058 ± 0.007 mmHg⁻¹) and DM (0.082 ± 0.009 mmHg⁻¹) were not significantly different. For the middle portions controls (0.037 ± 0.004) were significantly different from DM ($p < 0.001$), and distal portions of controls (0.034 ± 0.005 mmHg⁻¹) were significantly less compliant, also ($p = 0.003$). Two-way ANOVA indicated that both state and position of the tissue were factors in any differences that occurred ($p < 0.001$); yet, there was no significant interaction between the two factors ($p = 0.96$).

As with baseline data, DM data was separated into time points 3, 5, and 10-week DM and compared to healthy controls in order to study biomechanical changes with the onset of DM. Low-pressure compliance for the passive state indicated opposite results than that of baseline. That is, for within-tissue differences, the control (0.058 ± 0.007 mmHg⁻¹) and 10-week (0.090 ± 0.01 mmHg⁻¹) proximal portions were significantly different from middle (0.037 ± 0.003 ; 0.055 ± 0.005 mmHg⁻¹, respectively) and distal (0.033 ± 0.004 ; 0.055 ± 0.008 mmHg⁻¹, respectively) portions ($p < 0.001$, $p < 0.05$, respectively), and there was no within-tissue differences indicated for 3-week and 5-week DM urethras. Low-pressure incremental compliance indicated trends developed with the proximal portions. Though only closely significant ($p = 0.095$) 3-week and 10-week DM proximal portions were more compliant than control and 5-week DM proximal portions. With one-way ANOVA, middle and distal portions of controls proved to have significant differences in compliance compared to all time points of DM. Middle portions of 3-week (0.056 ± 0.006 mmHg⁻¹), 5-week (0.059 ± 0.005 mmHg⁻¹), and 10-week (0.055 ± 0.005 mmHg⁻¹) DM were more compliant than controls ($p = 0.009$).

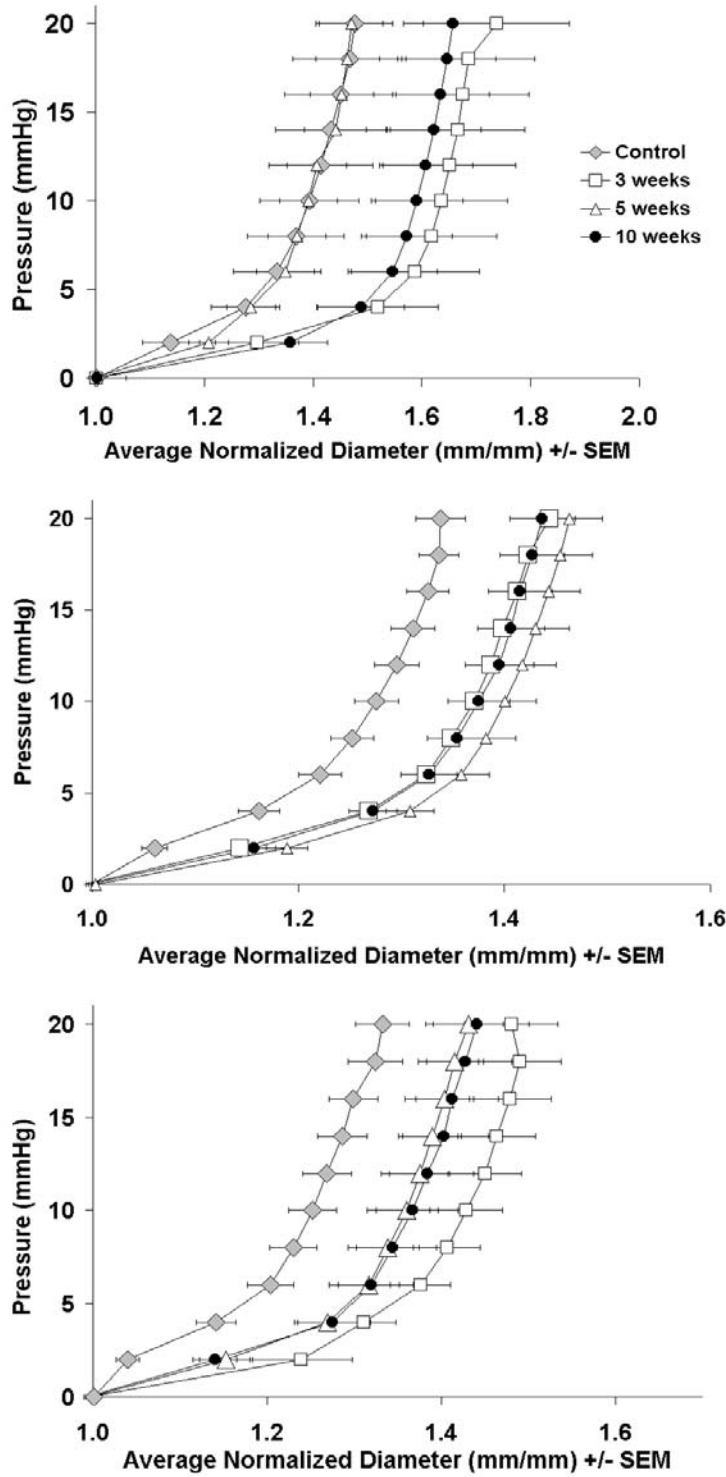


Figure 3.9: The average and normalized pressure-diameter response of proximal (top), middle (middle) and distal (bottom) portions of 3, 5, and 10-week DM urethras and controls in the passive state.

The same was found for distal portions of 3-week ($0.064 \pm 0.006 \text{ mmHg}^{-1}$), 5-week ($0.053 \pm 0.006 \text{ mmHg}^{-1}$), and 10-week ($0.054 \pm 0.008 \text{ mmHg}^{-1}$) DM urethras, as well ($p=0.02$). Two way ANOVA indicated that both position ($p<0.001$) and onset of DM ($p<0.001$) had major roles in significant differences found, especially between controls and all time points of DM. Our data suggests that interaction between these two factors played no role in any observed differences ($p=0.3$; Figure 3.10).

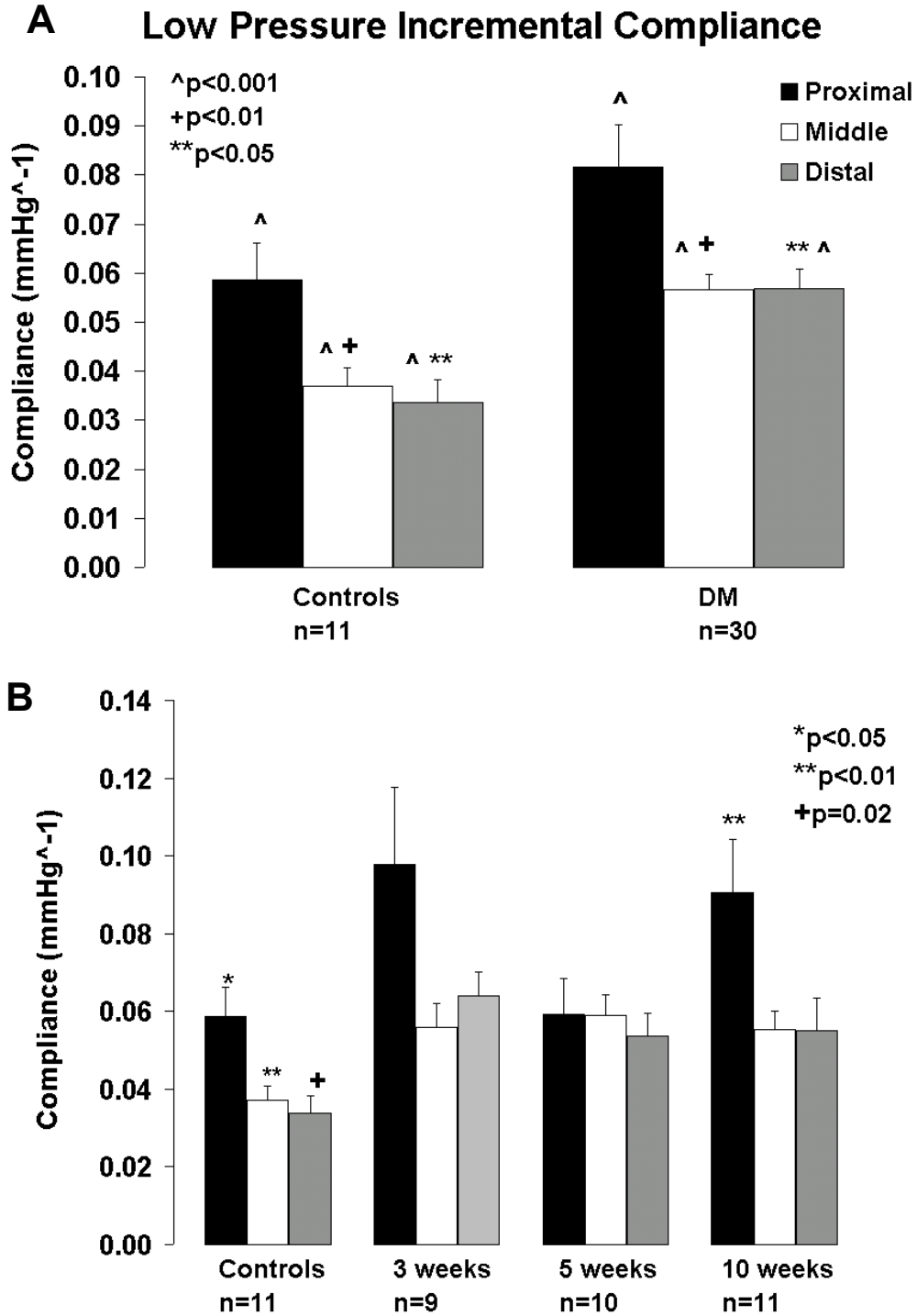


Figure 3.10: Low pressure incremental compliance (0 to 6 mmHg) values for combined DM (A) and three time points of DM (B) compared to control values in the passive state. Error bars represent standard error of the mean.

Middle incremental compliance showed no differences among positions within the same tissue, but proximal ($0.009 \pm 0.006 \text{ mmHg}^{-1}$) and middle ($0.010 \pm 0.004 \text{ mmHg}^{-1}$) controls were significantly more compliant than proximal ($0.006 \pm 0.004 \text{ mmHg}^{-1}$) and middle ($0.007 \pm 0.003 \text{ mmHg}^{-1}$) DM ($p=0.006$, $p=0.02$). Distals were not significantly different. Additionally, no differences were seen for high-pressure compliances for comparisons between proximal, middle, or distal portions (Figures 3.11 and 3.12).

For comparisons between separated time points of DM and controls, incremental compliance for the middle pressure ranges indicated that no within tissue differences were seen among the portions along the length of the urethra in any of the groups. Still, the proximal to distal compliance gradient for controls was maintained as proven by the compliance values in the bar graph. Actually, this gradient was preserved for high-pressure incremental compliance, as well. With the onset of DM, this proximal to distal gradient was no longer present. Middle pressure incremental compliance (Figure 3.11) showed that proximal control ($0.055 \pm 0.005 \text{ mmHg}^{-1}$) values were more compliant than 10-week DM ($0.005 \pm 0.001 \text{ mmHg}^{-1}$) proximal ($p=0.012$). Control and 10-week DM middle portions were found to be closely different ($p = 0.096$) with controls more compliant than all time points of DM. Distal portions of each group showed no significant difference ($p=0.237$). Two way ANOVA indicated a loss of position as a factor of differences ($p = 0.725$), but onset of DM was sustained as a significant factor ($p<0.001$) where controls were significantly different from all time points of DM. There was no role of interaction between position and onset of DM ($p = 0.81$). Comparisons for compliance values in the high-pressure ranges (Figure 3.12) indicated a significant difference ($p = 0.023$) for proximal portions of controls ($0.007 \pm 0.001 \text{ mmHg}^{-1}$) and 10-week DM ($0.004 \pm 0.001 \text{ mmHg}^{-1}$). Middle ($p=0.161$) and distal ($p=0.845$) portions of all urethras showed no significant differences among each group. As well, a two way ANOVA denoted that both position ($p 0.262$) and time ($p=0.181$) did not have a role in any variations perceived.

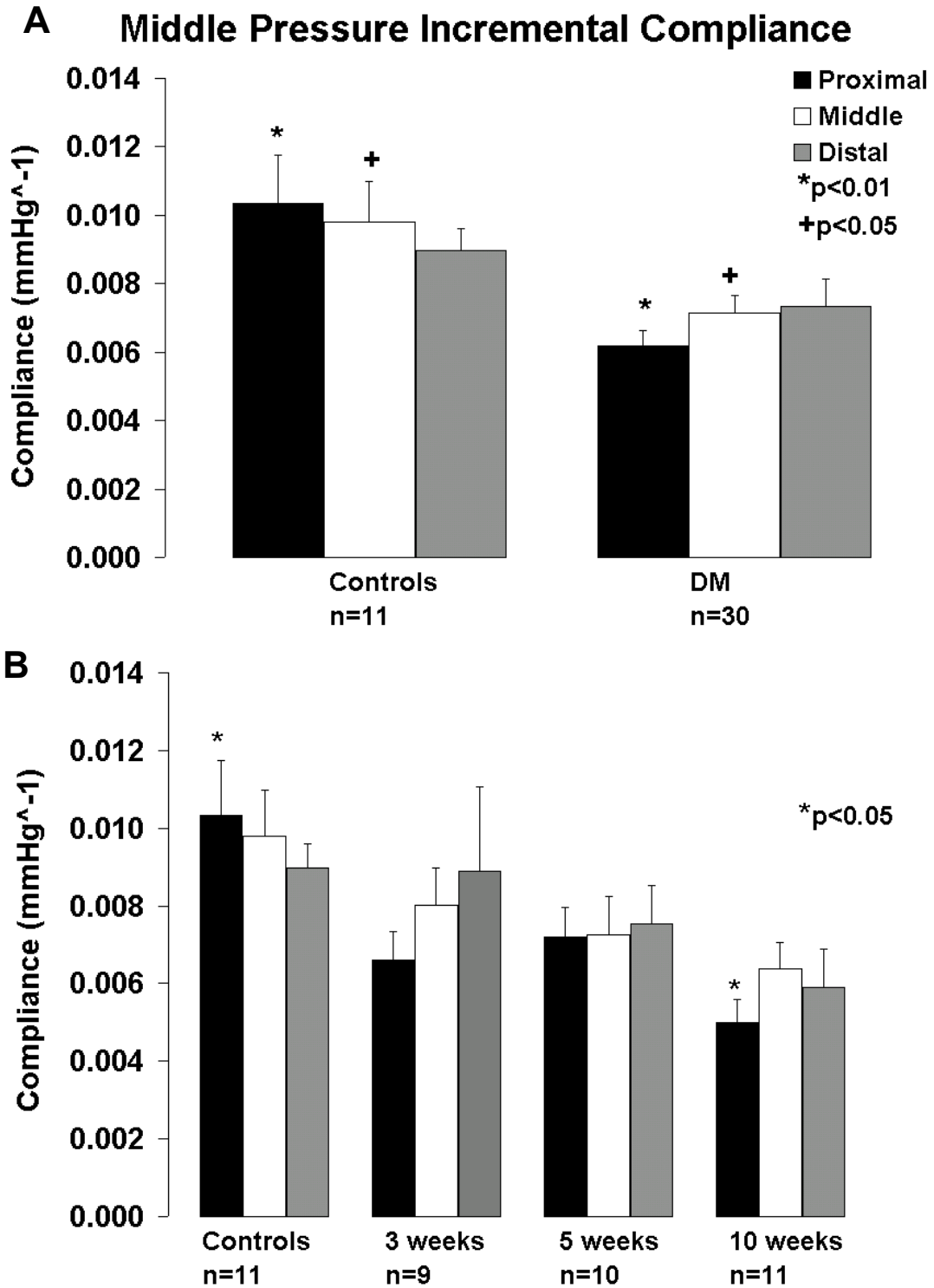


Figure 3.11: Middle pressure incremental compliance (6 to 12 mmHg) values for combined DM (A) and three time points of DM (B) compared to control values in the passive state. Error bars represent standard error of the mean.

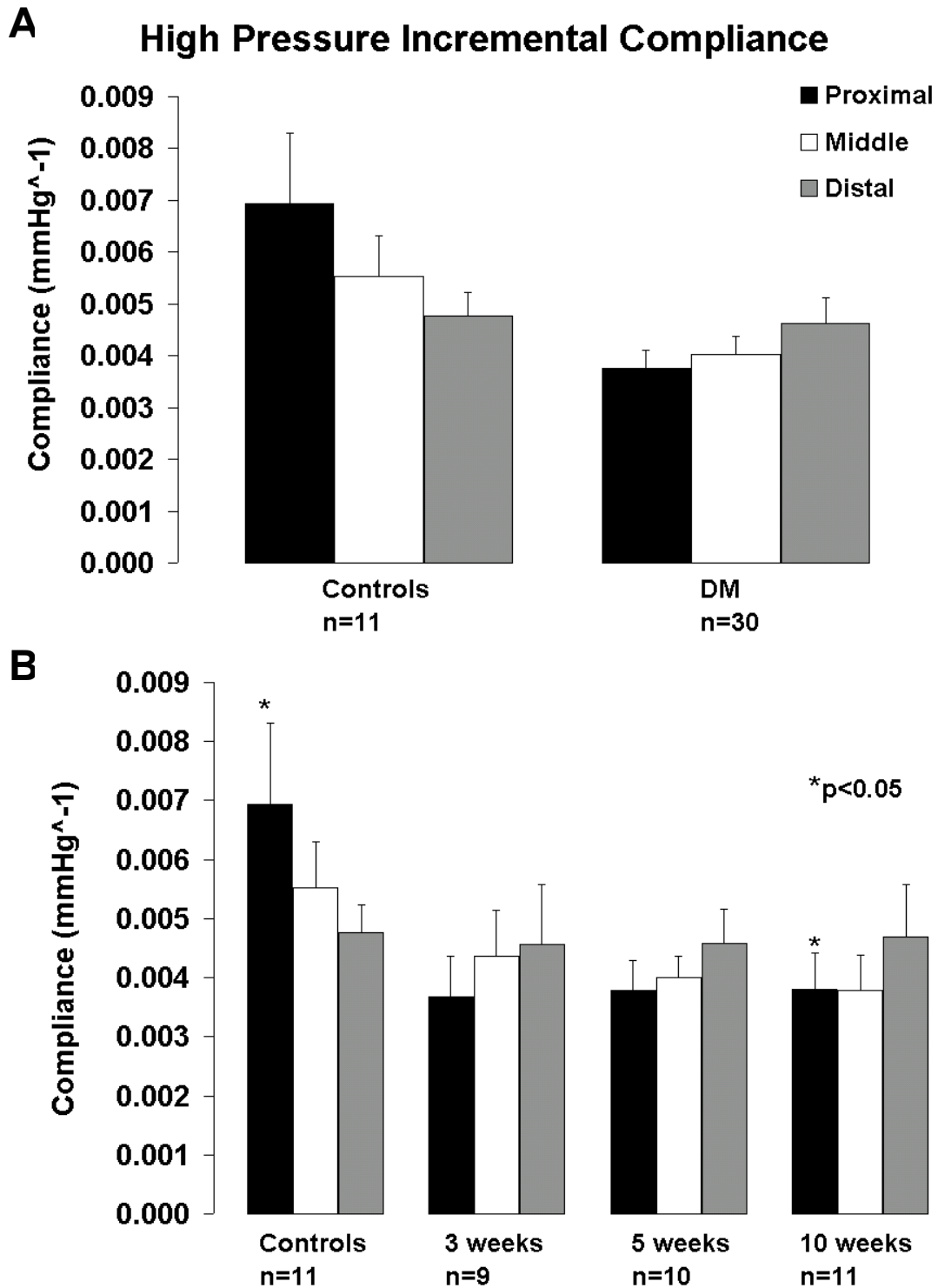


Figure 3.12: High-pressure incremental compliance (12 to 20 mmHg) values for combined DM (A) and three time points of DM (B) compared to control values in the passive state. Error bars represent standard error of the mean.

Beta stiffness values indicated that DM urethras were stiffer than controls in the passive state (Figure 3.13A). The only significant comparison was between proximal (10.1 ± 2.9 , 12.8 ± 3.4) portion of controls and DM ($p=0.02$). Two way ANOVA suggested that the state of the tissue (healthy versus diseased) was the only factor which played a role in any significant differences.

Beta stiffness values in the passive state showed no within tissue differences between proximal, middle and distal portions for controls (10.1 ± 0.85 , 10.6 ± 0.68 , 10.69 ± 0.76 ; $p=0.78$), 3-week DM (10.2 ± 1.0 , 11.8 ± 0.9 , 13.7 ± 1.9 ; $p=0.237$), 5-week DM (14.4 ± 1.1 , 12.7 ± 0.9 , 12.3 ± 0.9 ; $p=0.223$), and 10-week DM (13.4 ± 1.0 , 12.0 ± 1.1 , 12.1 ± 1.0 ; $p=0.21$; Figure 20B). Comparing the positions of each group, one way ANOVA confirmed a difference in the proximal portions ($p=0.004$). Furthermore, the pairwise comparison indicated that 5 ($p=0.009$) and 10 ($p=0.045$) week DM were significantly stiffer than controls, and 3-week DM were less stiff than 5 ($p=0.017$) and 10 ($p=0.041$) week DM. Two way ANOVA suggests that position was not a determining factor in significant differences ($p=0.844$), but, on the other hand, DM took part in significant differences ($p=0.007$). More specifically, controls were significantly less stiff (more compliant) than 5 ($p=0.005$) and 10 ($p=0.029$) weeks of DM. Additionally, there was not a statistically significant interaction among the two factors ($p=0.21$).

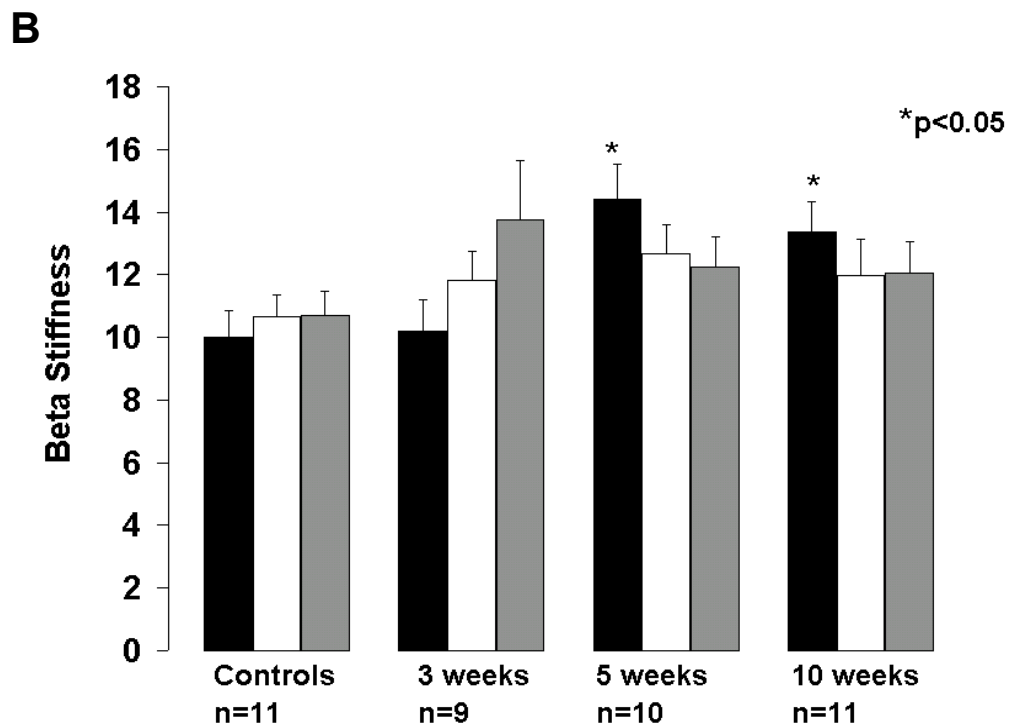
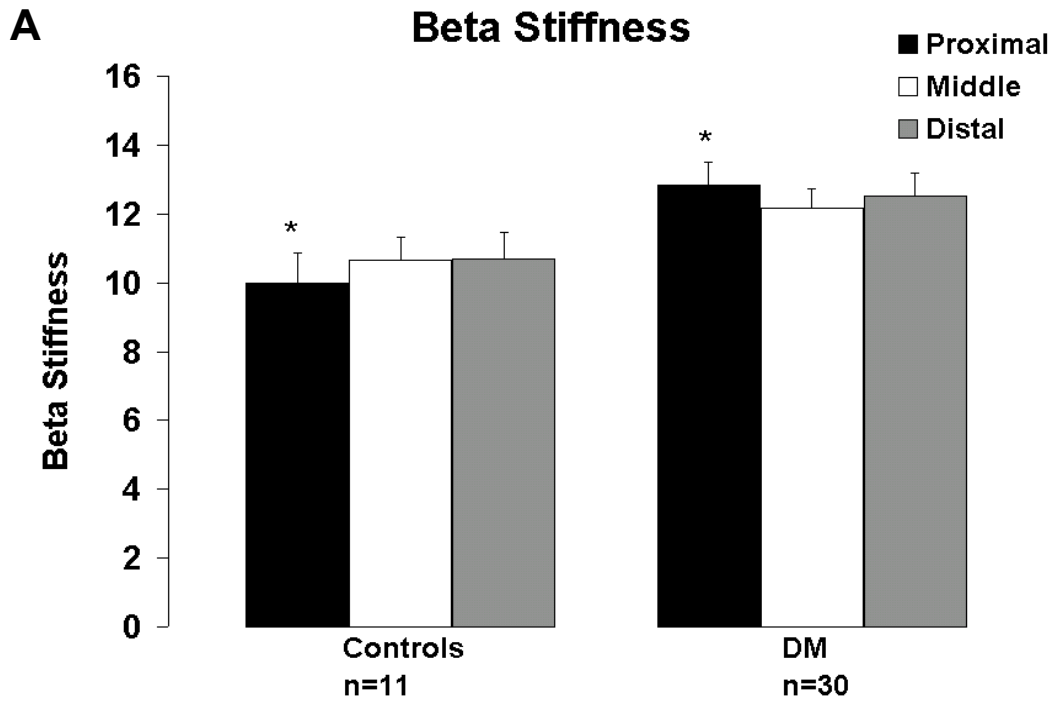


Figure 3.13: Beta Stiffness values for combined DM (A) and three time points of DM (B) compared to control values in the passive state. Error bars represent standard error of the mean.

3.3 PHARMACOLOGICAL ASSESSMENT

With the contractile responses of the DM urethras grouped, there was a significant gradual decrease in diameter response to N ω -nitro-L-arginine between control (-2.9 +/- 1.3 %) and DM (-0.1 \pm 0.4 %) urethras (p=0.04; Figure 3.14). On the other hand, the maximal contraction to phenylephrine (PE-max) for DM (-9.1 \pm 2.2 %) urethras appeared to be greater than that of controls (-8.2 \pm 1.6 %). While this difference was not significant (p=0.8), the same result was maintained for the relaxation response to EDTA.

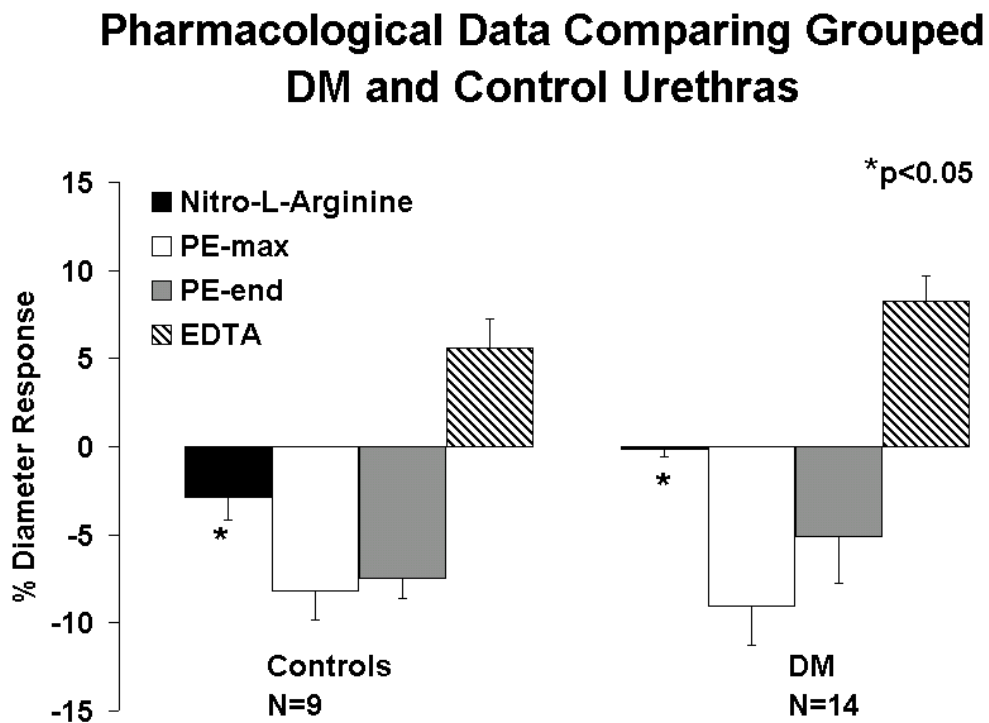


Figure 3.14: Urethral response to N ω -nitro-L-arginine, phenylephrine and EDTA. The error bars represent SEM.

The control (5.6 ± 1.6 %) relaxation was less than that of DM (8.2 ± 1.4 %). Additionally, the control (-7.4 ± 1.1 %) urethras displayed a stronger maintenance of the contractile response (PE-end) compared to DM (-5.1 ± 2.7 %), although this observation was not significant.

Comparing 5 and 10-week time points of DM separately to controls provided a further insight to the progressive loss of smooth muscle function, but no significant differences were found (Figure 3.15). Response to the N ω -nitro-L-arginine was progressively abolished at 5-week (-0.6 ± 0.5 %) and 10-week DM (0.3 ± 0.7 %) compared to the control response (-2.9 ± 1.3 %), and statistical analysis indicated that this observation was a trend ($p=0.08$).

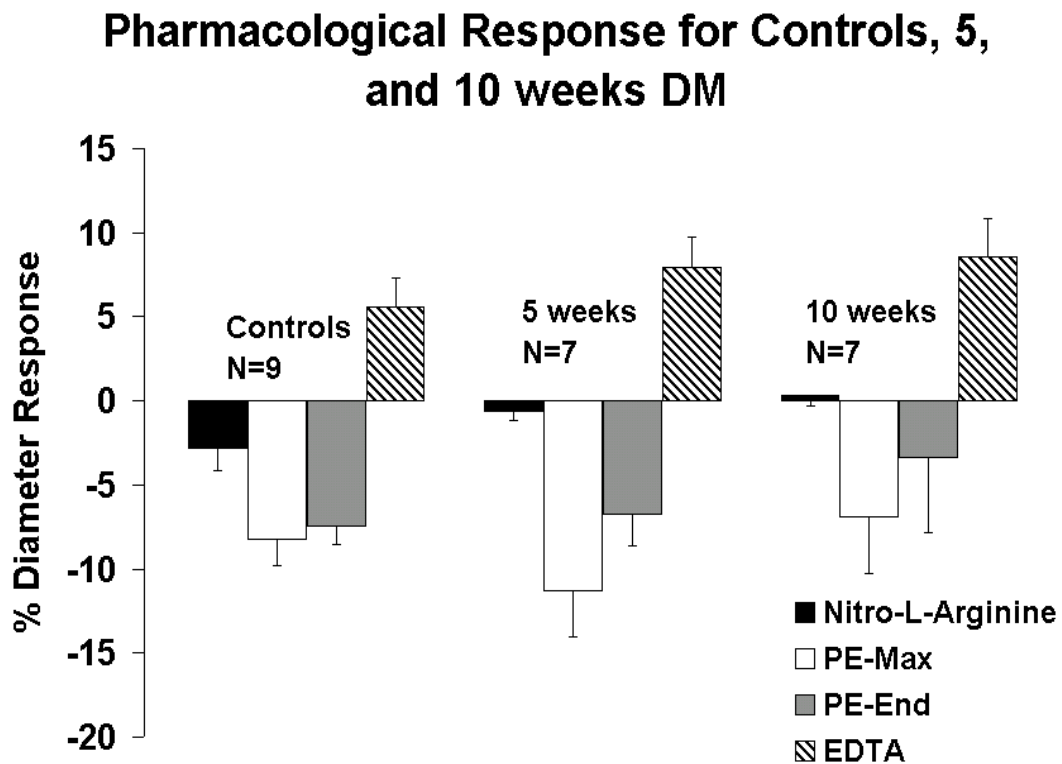


Figure 3.15: Urethral response to nitric oxide inhibitor (N ω -nitro-L-arginine), contractile (PE) and relaxation agents (EDTA). The error bars represent SEM.

For PE, mean values indicate that the maximal response increased by 5-week DM and weakened to less than control values by 10-week DM. Unlike control urethras, DM urethras were unable to maintain the contractile response for a period of 20 to 30 minutes. Finally, the relaxation response increased with 5-week DM ($7.9 \pm 1.8\%$) and even more so with 10-week DM ($8.6 \pm 2.3\%$). The observations of PE and EDTA were also not statistically significant.

Due to animal to animal variability with measured weight gain or loss and blood sugar levels (BG) of the diabetic animals, the pharmacological responses were separated into four groups: weight loss/ blood glucose less than 400, weight gain/ blood glucose less than 400, weight loss/ blood glucose greater than 400, and weight gain/ blood glucose greater than 400 (Figure 3.16).

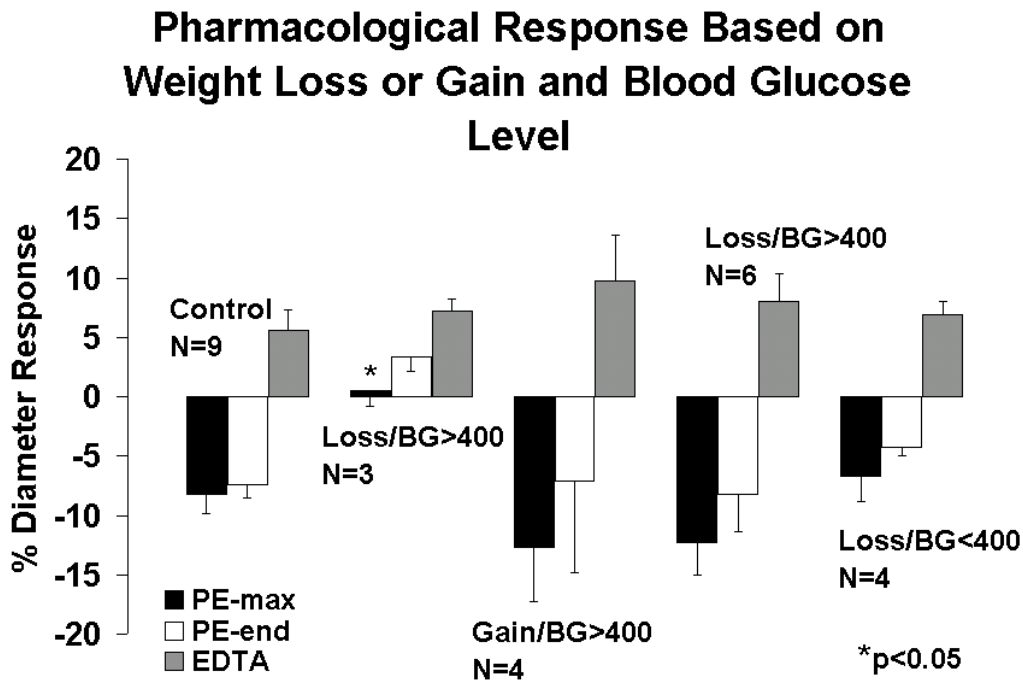


Figure 3.16: Urethral response to contractile (PE) and relaxation agents (EDTA). The error bars represent SEM.

Weight loss or gain was dependent on the weight measured during the first three days after injection of STZ, which has a maximal three day delay before its effects ensue [40]. The maximal response to PE was greatest from the groups of animals that gained weight with $BG > 400$ ($-12.7 \pm 4.5\%$) and lost weight with $BG < 400$ ($-12.3 \pm 2.7\%$). The animals, which lost weight with $BG > 400$, had a contractile response which was significantly less in magnitude than all other groups. From PE-end values, the controls ($-7.4 \pm 1.1\%$) appeared to maintain the contractile response more than all diabetic groups; yet, this development was not significant. Finally, the largest relaxation response from EDTA arose from the group, which gained weight with $BG > 400$ ($9.8 \pm 3.7\%$), but one-way ANOVA did not reveal a statistically significant difference for this result.

The amount of time to reach maximal response between controls and DM animals was different, as well. The control (4.2 ± 1.1 minutes), 5-week (4.2 ± 1.8 minutes) and 10-week (2.6 ± 4.3 minutes) DM middle urethral response to PE exhibited no significant differences ($p=0.78$; Figure 3.17). On the other hand, the control (8.7 ± 1.4 minutes) EDTA response was significantly less than that of 5 (18.9 ± 3.4 minutes) and 10-week (12.1 ± 2.3 minutes) DM.

Amount of Time For Maximum Response

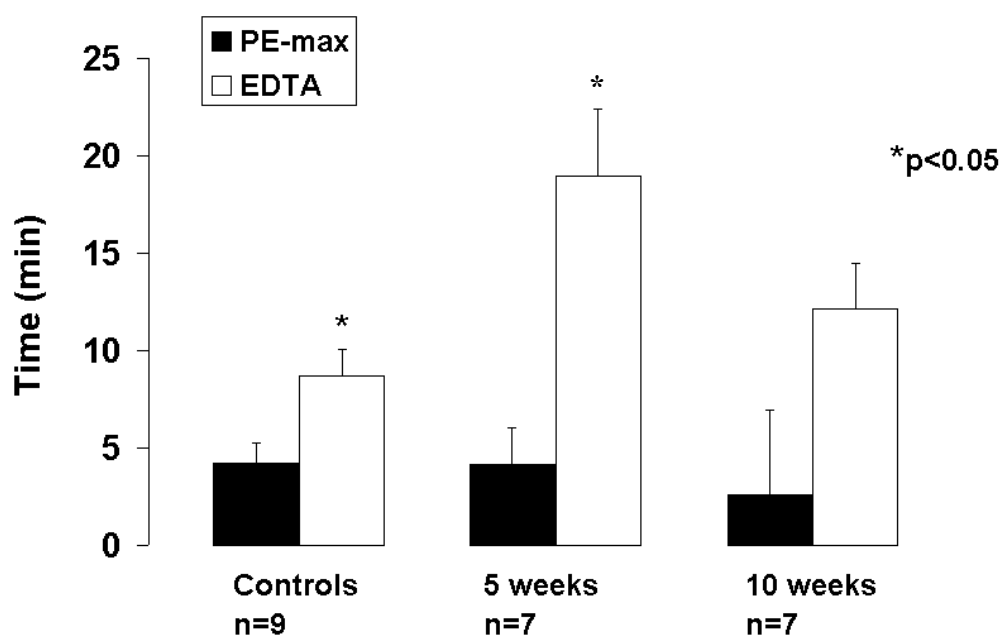


Figure 3.17: The time to reach maximal response to PE and EDTA for each group. No differences were seen for PE, but DM increased the time for relaxation in response to EDTA.

3.4 HISTOLOGICAL RESULTS

3.4.1 Smooth Muscle Quantification

Representative immunohistochemical staining for smooth muscle α -actin results appear in Figure 3.18. The amount of smooth muscle ranged between 15 and 30% dependent upon the portion of the urethra (Figure 3.19). No apparent differences in the amount of smooth muscle were noted between control and DM groups. For controls, proximal ($21.4 \pm 3.5\%$) and distal

($21.7 \pm 4.8\%$) portions had larger smooth muscle quantities than middle ($18.7 \pm 2.7\%$; $p=0.8$), though this was not statistically significant. For 3-week DM, the amount of smooth muscle decreased along the length of the urethra proximally to distally ($20.8 \pm 5.9\%$, $19.7 \pm 0.8\%$, $14.9 \pm 1.1\%$; $p=0.3$), but was not significant.

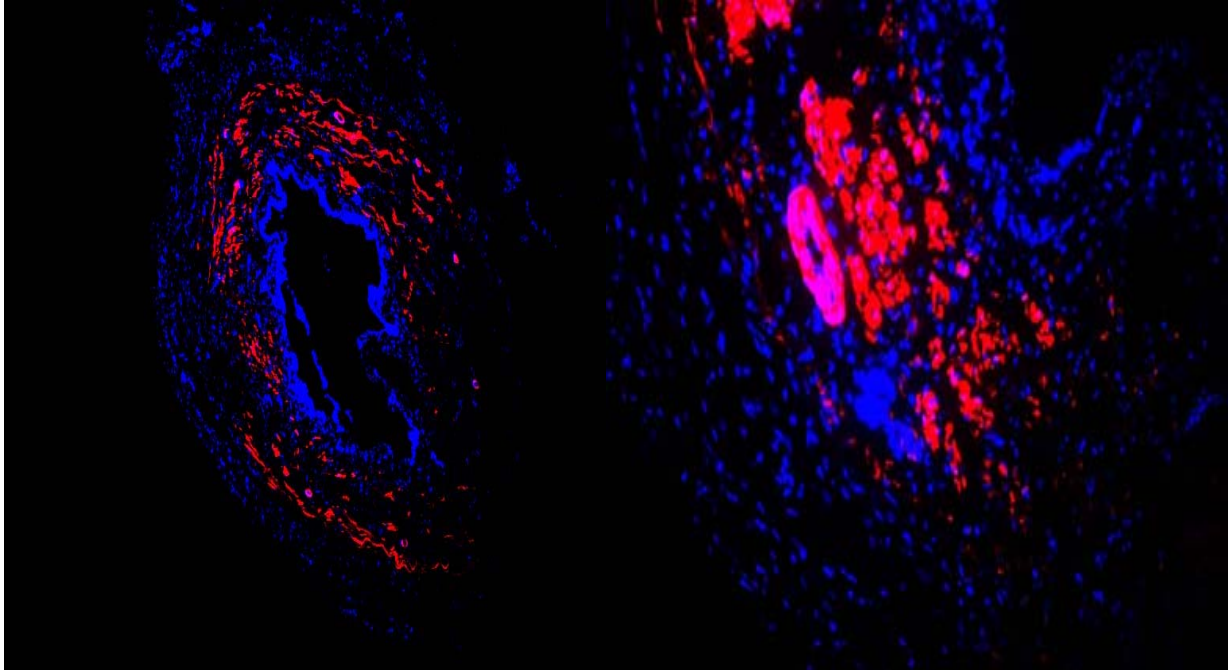


Figure 3.18: (Left) Smooth muscle alpha actin antibody staining of a proximal urethra (red) with the background of Hoescht (blue) at 5x using a Nikon fluorescent microscope. (Right) A closer view at (20x)

Additionally, 5-week ($p=0.12$) and 10-week ($p=0.13$) DM urethras showed no differences of smooth muscle quantities between proximal ($15.9 \pm 4.1\%$, $18.9 \pm 1.4\%$), middle ($17.1 \pm 1.8\%$, $16.4 \pm 2.1\%$), and distal ($21.3 \pm 3.3\%$, $15.0 \pm 0.3\%$) portions. However, both 3-week and 10-week DM showed a trend of proximal having more smooth muscle compared to middle and distal.

Smooth Muscle Quantification

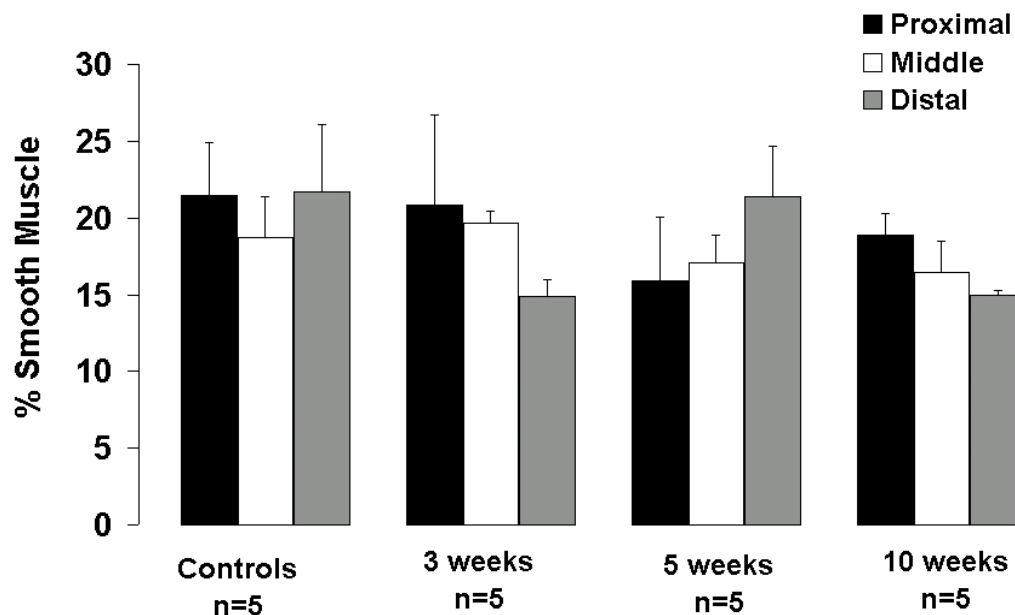


Figure 3.19: The amount of smooth muscle alpha actin in the proximal, middle, and distal portions of control and DM urethra. Error bars represent standard error. No significant differences were noted in any comparisons.

Between groups, the average amount of smooth muscle in the proximal portion decreased, but, statistically speaking, the amount of smooth muscle in the proximal and middle portions of the urethra remained unaffected by the onset of DM ($p=0.63$ and $p=0.65$). In the distal portion, the amount of smooth muscle decreased at 3 and 10-week DM compared to controls and 5-week indicating a possible trend, but this observation was nearly significant ($p = 0.095$).

3.4.2 Collagen Quantification

Collagen in the urethra was found abundantly in the lamina propria and surrounds both types of smooth muscle components (Figure 3.20). As with smooth muscle quantification, collagen quantification (Figure 3.21) yielded no differences among proximal, middle, and distal portions

in controls ($34.8 \pm 3.9\%$, $38.2 \pm 2.7\%$, $45.0 \pm 4.1\%$; $p=0.17$), 3 ($41.5 \pm 5.8\%$, $33.8 \pm 3.7\%$, $40.3 \pm 3.8\%$; $p=0.42$), 5 ($37.2 \pm 2.6\%$, $38.7 \pm 3.5\%$, $43.2 \pm 3.4\%$; $p=0.41$) and 10 (40.7 ± 2.3 , 32.2 ± 3.6 , 38.8 ± 2.9 ; $p=0.15$) weeks DM. The amount of collagen in the urethras averaged between 35 and 45%. Among diabetic and control groups, there were no differences among proximal ($p=0.55$), middle ($p=0.46$), or distal ($p=0.62$) portions.

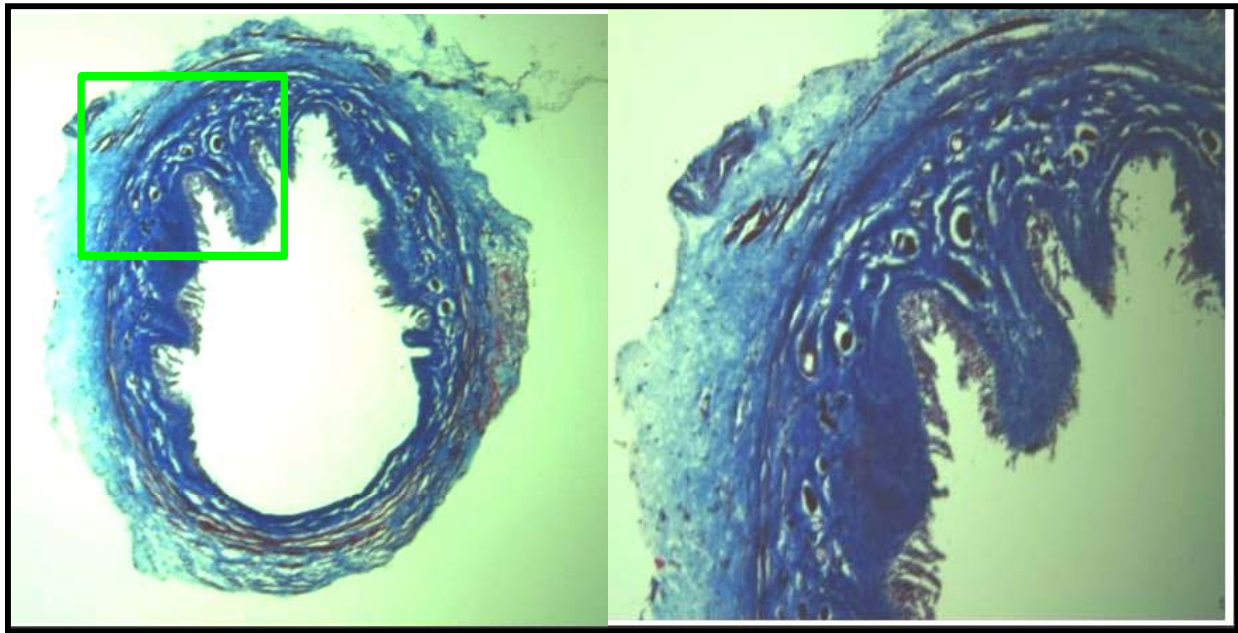


Figure 3.20: (Left) Masson's trichrome histological stain of a proximal urethra, collagen (blue) with muscle (red/brown) at 5x using a light microscope. (Right) A closer view of the region within the green box of the figure to the left (20x)

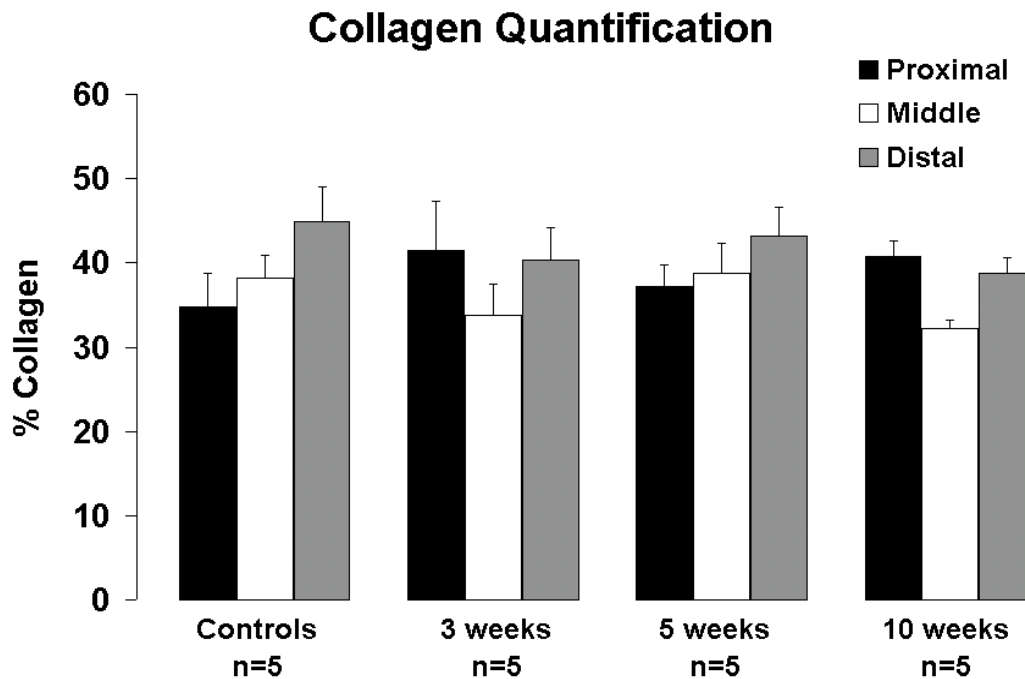


Figure 3.21: The amount of collagen in the proximal, middle, and distal portions of control and DM urethra. Error bars represent standard error. No significant differences were noted in any comparisons.

3.4.3 Elastin Quantification

The amount of elastin was less than that of collagen and smooth muscle, between 15 and 18% on average, in the urethra, and most elastin was located in the adventitial area or around the musculature, both smooth and striated (Figure 3.22 and 3.23). The presence of elastin increased along the length of the urethra proximally to distally in controls ($12. \pm 2.8$, 16.2 ± 1.3 , 17.6 ± 2.2). No differences were found among the portions within the tissue, with the exception of 3-week DM where the mid portion ($12.8 \pm 1.4\%$) had less elastin than the distal portion ($18.7 \pm 2.4\%$; $p = 0.05$). While the elastin remained unchanged in the proximal and distal portions, a statistically significant decrease could be seen in the middle portion for 10-week DM ($10.9 \pm 1.0\%$) compared to controls ($p=0.01$).

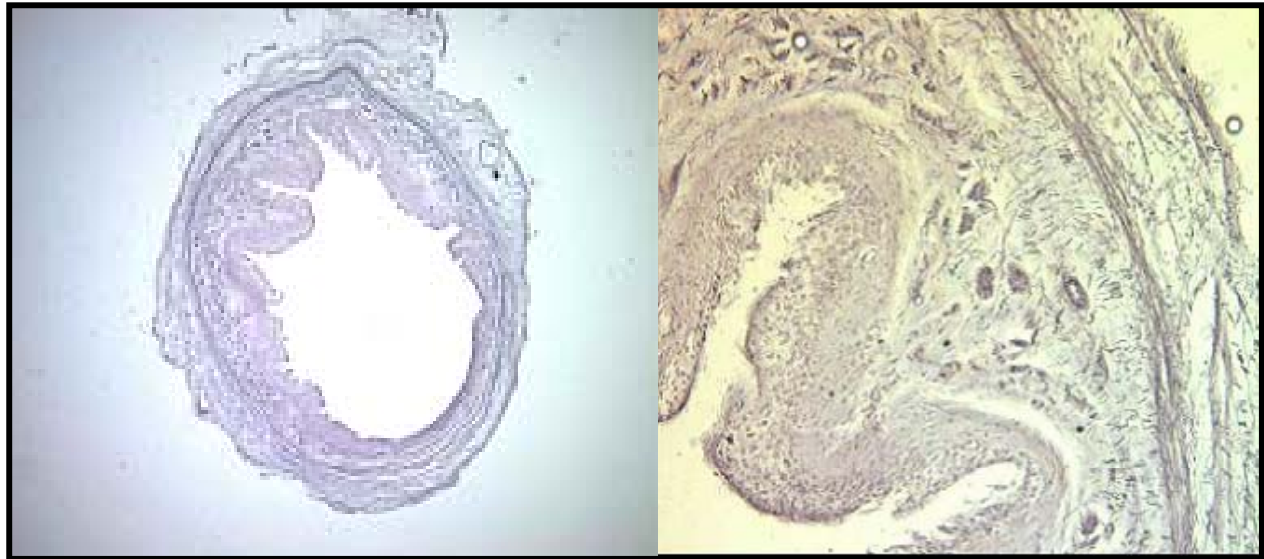


Figure 3.22: (Left) Weigert's Recorsin Fuschin histological stain of a proximal urethra, elastic fibers, dark purple/ black at 5x using a light microscope (Right) A closer view (20x) Note: no background stain was performed.

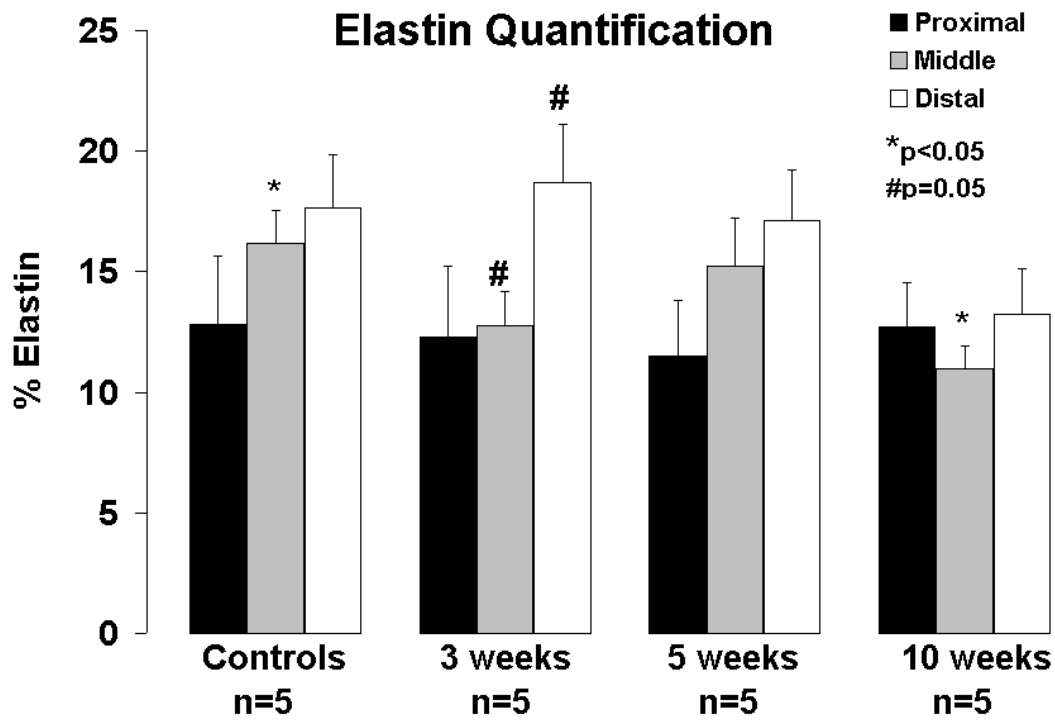


Figure 3.23: The amount of elastin in the proximal, middle, and distal portions of the urethra and the effects from DM. Error bars represent standard error.

4.0 DISCUSSION

While the bladder has remained the investigative focus of diabetic cystopathy [11-16,20,23], the urethra has been largely ignored. A small number of pharmacological studies have been performed on the urethra exposed to DM [21,22,25] but, to our knowledge, no studies have concentrated on the effects of DM on the biomechanical properties of the urethra. This investigation hypothesized that the biomechanical properties of the urethra - namely, incremental compliance and beta stiffness - as well as the pharmacological function of urethral smooth muscle are altered due to DM.

4.1 BIOMECHANICAL RESULTS

As with most biological tissues, the pressure-diameter response was non-linear for both control and DM tissue (Figures 3.2, 3.3, 3.8 and 3.9). Both types of tissue also exhibited creep due to their viscoelastic nature. More specifically, the response was sigmoidal in shape for the baseline tissue and exponential in shape for the passive state. Most likely, the presence of the smooth muscle function in the baseline tissue was responsible for this difference. That is, smooth muscle was free to “act” as summarized in Section 2.3, and with both control and DM specimens, the urethra would resist initial intraluminal pressures applied (0 to 4 mmHg) with a decrease or maintenance in diameter; thus, preventing any distension of the external diameter (Figure 4.1A). Similar to these findings, Yalla et al. [44,50] discovered a non-linear pressure-diameter response in vivo as well. Since the urethra is comprised mostly of smooth and striated muscle, collagen and elastin, the initial, easily-distensible phase of the passive curve (also known as the toe region

[51]) is attributed to the stretch of the smooth muscle and elastic fibers. The non-linear region where the stiffness of the tissue decreases with increasing distension is attributed to the sequential uncrimping of the collagen fibers. The relatively indistensible linear region occurs when the load is transferred completely to the collagen, causing the collagen fibers to fully straighten from their tortuous form at low stress (Figure 4.1B).

At the baseline state, controls displayed a proximal-to-distal compliance gradient at low pressures (0 to 6 mmHg), where the proximal portion was more compliant than middle and distal portions (Figure 3.2). While this observation was not significant in the baseline state at low pressures, this proximal-to-distal gradient was significant in passive control tissue at low pressures, where the proximal portion was more compliant than middle and distal portions (Figure 3.4 and 3.10). This significant gradient is likely due to the absence of the contribution of the smooth and striated muscle. Since the muscle is “free” to act in the baseline condition, the muscle may have been contracting in response to the intraluminal pressure applied; thus, rendering the urethra a more homogeneous structure.

The proximal-to-distal compliance gradient seen in the passive state was not verified by any significant differences in the structural analysis of the collagen and elastic fiber components of the extra-cellular matrix. However, perhaps a further analysis utilizing spectrophotometry assays to measure actual weights of collagen in the tissue could authenticate this finding. A similar observation was distinguished in urethras of healthy women in vivo [43,52]. The results of this previous study showed that in response to forced dilatation via balloon catheter in vivo, the portion of the urethra near the bladder neck had a significantly higher elastic coefficient and dissipated energy compared to the distal portion, thus indicating a urethral stiffening at positions further from the bladder neck. While no pharmacological agents were added to inhibit or promote muscle contraction, the researchers attributed this finding to the position of the peri-urethral structures and the involvement of the external urethral sphincter.

The significant compliance gradient in passive control tissue may be due to the varied smooth muscle density along the length of the urethra (i.e. less smooth muscle might be present in the proximal portion than in the middle and distal portions). However, the data from the smooth muscle quantification in this study (Figure 3.19) does not support such a variation. The analysis not only displayed no significance of the amount of smooth muscle present in each portion, but the proximal and distal portions appeared to have comparable amounts while the

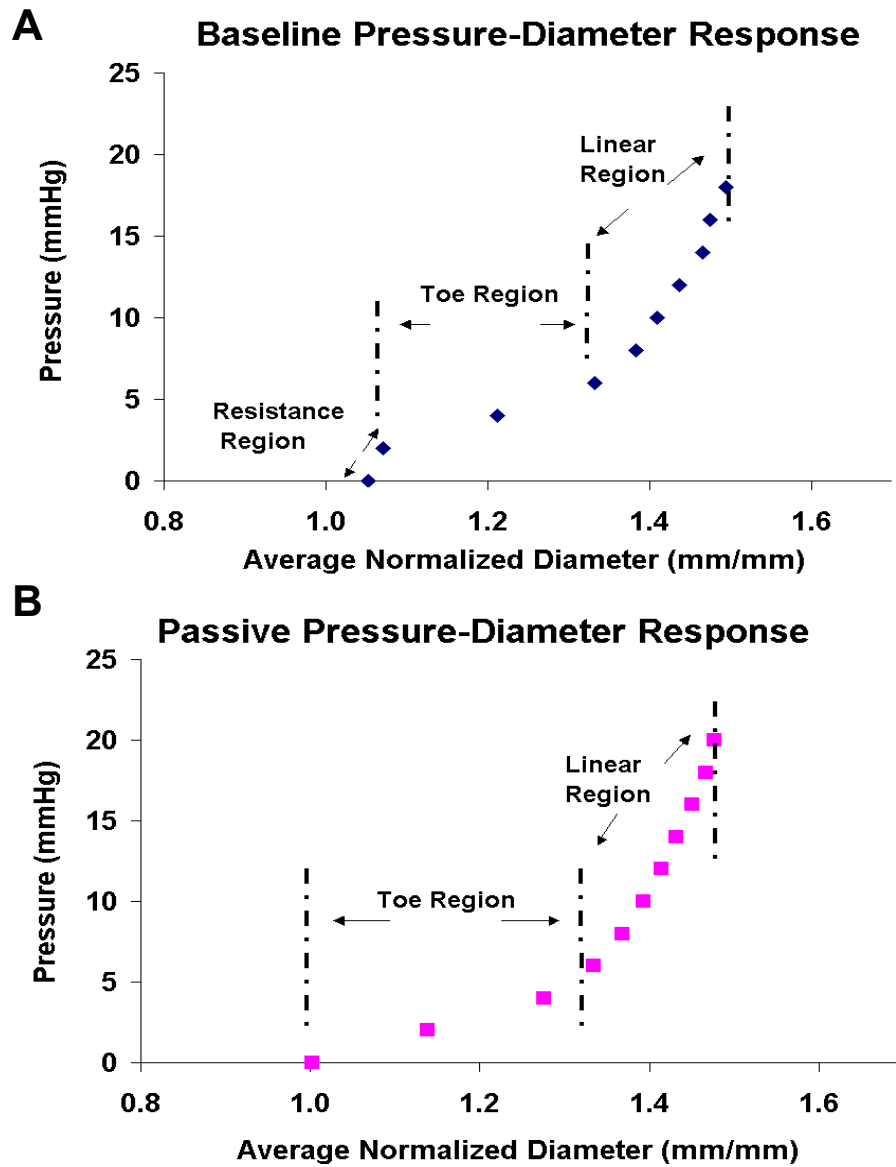


Figure 4.1: Typical proximal pressure-diameter responses which are sigmoidal for baseline tissue (A) and exponential for passive tissue (B)

middle portion had less. The other reason might be that the amount of collagen, a relatively stiff structural protein, in the proximal portion of the urethra was less than that of middle and distal portions (Figure 3.21). Microstructural analysis confirmed these trends, though it was not significant.

DM urethras were also found to have a significant compliance gradient for both baseline (especially for 3- and 5- week DM) and passive conditions (especially for 10- week DM). Since the passive state represents mostly the extracellular matrix properties, this would suggest some differences in the amount or structure of collagen along the length of the 10-week DM urethra as was found with control passive tissue. However, this was not supported by the data shown in Figure 3.22. Instead, microstructural analysis indicated no differences for collagen or elastin along the length of the 10-week DM urethra compared to healthy controls. The alternative reason for this observation may be the changes in extracellular matrix structure due to DM. It has been established that advanced glycation end products (AGEs), which are elevated in DM [59], can affect the properties of collagen in a number of ways. It can alter charge profiles, act as an oxidizing agent, and form precise supramolecular aggregates [59]. Also, cross-linking AGEs that cause the most damaging effects have been related to DM. This type of AGE form intermolecular cross links between molecules in the collagen and elastin fibers [60,61]. In relation to this possibility, many past studies, including one from our laboratory [91], have indicated blood vessel stiffening from the state of DM and attribute these findings to a large contribution of AGEs [62-64]. AGEs may also contribute to the progressive significant increase in stiffness (decrease in compliance) of the 10-week DM proximal urethra.

The reason for the proximal portion displaying a higher compliance than middle and distal portions of 3- and 5-week DM in the baseline state may be due to regional variations in smooth muscle since this observation was not seen in passive 3- and 5-week DM urethras. Additionally, the proximal and middle portions of 3-week DM urethras were significantly more compliant at low pressures than that of controls (Figures 3.4 and 3.10). Either the viscoelastic properties of the smooth muscle may have been altered due to DM or there may be alterations of smooth muscle function in the proximal and middle portions of the urethra with this disease. Since compliance measurements are based on the size of the lumen [53], as well as the elastic properties of the urethral wall, the smooth muscle may be stimulated into the dilatory state. A major contribution to the increase in low pressure baseline compliance for the proximal portions

was the absence of a resistance region displayed by pressure diameter data which was seen in controls (Figure 4.1). The failure of smooth muscle to correspond to the intraluminal pressure may have been due to smooth muscle cell apoptosis from hyperglycemic conditions [54] or alteration of smooth muscle physiology due to diabetic neuropathy [55]. On the other hand, the middle portion for 3-week DM urethras displayed the resistance region in pressure diameter curves for low pressure baseline compliance, but mid portion resistance may not have been as strong for 3-week DM as for controls. By 6 mmHg, the outer diameter for middle portions for 3-week DM increased 6% more than that of controls. For increases in low pressure baseline compliance between 3-week and 10-week DM, this may also serve as a possible explanation where diameter measurements 10-week DM middle portions were similar to that of controls at 6 mmHg in the baseline state (Figures 3.3-3.5).

Low-pressure compliance values indicated an increase for DM urethras in middle and distal portions in the passive state. Although elastin resides in urethral tissue only in small amounts [56], this increase in compliance may be due to a local alteration or increase in the amount of elastin, which dominates biomechanical behavior at low-pressure. Studies have found that DM induces a change in the amounts of collagen and elastin when compared to normal tissues [17,57,58]. However, there was a decrease, instead of an increase, for the amount of elastin between the middle portions of controls, 3 and 10-week DM (Figure 3.23). While this may have contributed to the overall stiffness increase seen in middle and high pressure compliance and beta stiffness for DM tissues, this does not explain the increase of low pressure compliance for DM tissue. The other factor could have been the amount of smooth muscle present, but the only trend that would support this is the decrease in the quantity of smooth muscle in the distal portion of 3- and 10-week DM urethras compared to controls (Figure 3.19), though this was not statistically significant.

4.2 PHARMACOLOGICAL FUNCTION OF SMOOTH MUSCLE

Analyses of smooth muscle function were performed at the mid point of both control and DM urethras. The pharmacological regimen assessed smooth muscle contractility via phenylephrine,

a non-selective α 1-adrenoceptor agonist, and relaxation via EDTA, a magnesium and calcium chelator to inhibit any muscle contraction. Nitric oxide (NO) release was also examined with the use of a nitric oxide synthase (NOS) inhibitor, N ω -Nitro-L-arginine, which was applied before assessment of phenylephrine. This preparation ensured maximal smooth muscle contraction.

In this study, the addition of the NOS inhibitor resulted in a gradual decrease of diameter, indicating a tonic relaxation due to the release of nitric oxide. There could be several possible sources of nitric oxide (NO): efferent or afferent nerves, the urothelium, urethral smooth muscle, the external urethral sphincter, or endothelial cells in the blood vessels in the urethra [65]. NOS has been identified in neurons innervating the lower urinary tract. NOS is most prominent in parasympathetic innervation of the urethra [98]. Functional experiments have shown that these nerves have an inhibitory urethral sphincter function [99]. In this case, nerve endings that have survived the isolation process may be the source of the NO release causing an inhibitory relaxation of the urethra in response to the increase of intraluminal pressure (0 to 8 mmHg) during our pharmacological testing.

As with the endothelial layer of blood vessels, the urothelium can synthesize and release NO. Pinna et al. demonstrated that NO dependent relaxations observed in hamster proximal urethra were diminished following urothelial cell denudation [66]. Although the reasons for NO presence in the urothelium remain a mystery, there could be some relations of the urothelium to the function of NO within the endothelium. Since shear stress, as well as stretch, has been found to stimulate nitric oxide production in endothelial cells [67], the urothelial layer could be stimulated by shear stress from the actual preparation of tying the tissue onto the tees of the ex-vivo perfusion system. That is, the system is filled with media to calibrate pressure and set the physiological environment. Once the urethra is tied in, the specimen is exposed to a small amount of shear stress when the media must be passed through in order to rid the system tubing of any air bubbles. On the other hand, one factor that may indicate that the urothelium is not

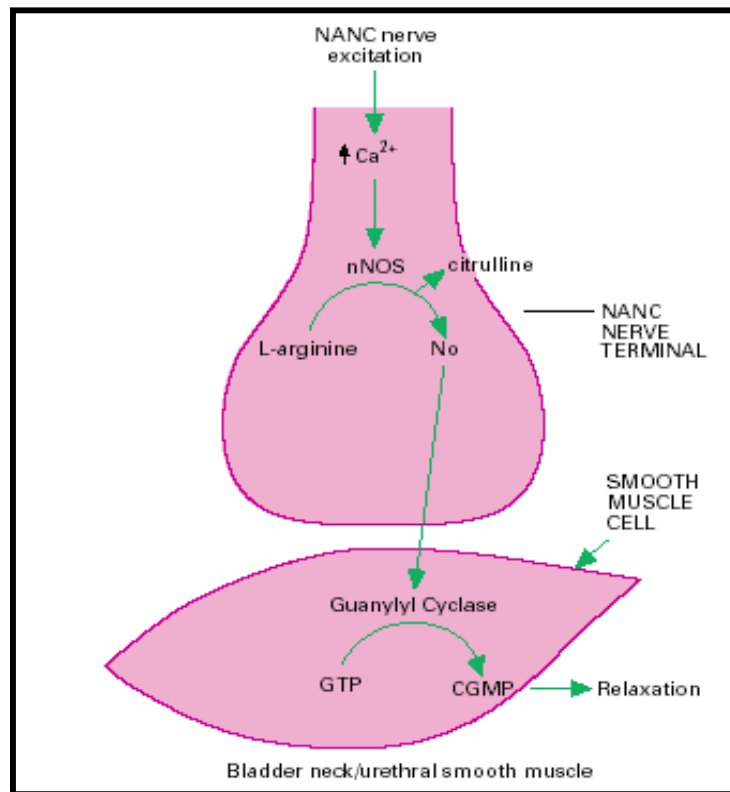


Figure 4.2: Depiction of the pathway of nitric oxide in urethral smooth muscle or the bladder neck (From Mumtaz et al, 2000 [65])

responsible for the production of NO, is that it may be injured and impaired due to the insertion of an intraluminal catheter. Of course, from histological observation, this is only true for a portion of the specimen. Urethral smooth muscle and external striated sphincter could also be a possible source of NO release. There is no direct evidence that NO is produced by urinary tract smooth muscle, but it has been discovered that there is a prominent orientation of cGMP-ir in the urethral smooth muscle by NO in guinea pigs (Figure 4.2) [65]. For the striated sphincter, NOS activity has been evident in the sarcolemma of the intramural striated muscle fibers and the nerve fibers. Recent observations suggest that NO has a role in the control of the external urethral sphincter [68]. The final and most likely source could be the blood vessels, which can be found

throughout the urethra. Due to dissection of the urethra and any handling, the blood vessels could be releasing NO as a response to injury [67].

This response to the NO inhibitor was significantly abolished in urethras from severely diabetic animals; thus, indicating that NO release was absent in these preparations. First, it must be known that STZ is an NO donor, which contributes to the pancreatic destruction of islet cells. Although not likely since STZ was administered many weeks prior to testing, the absence of the release of NO observed in DM urethras could be due to the STZ and not due to the effects of DM. In order to make certain that the DM is at fault, the rats that were injected, but had blood glucose levels less than 400 could be compared to animals with blood glucose levels greater than 400 mg/dl (Figure 4.3).

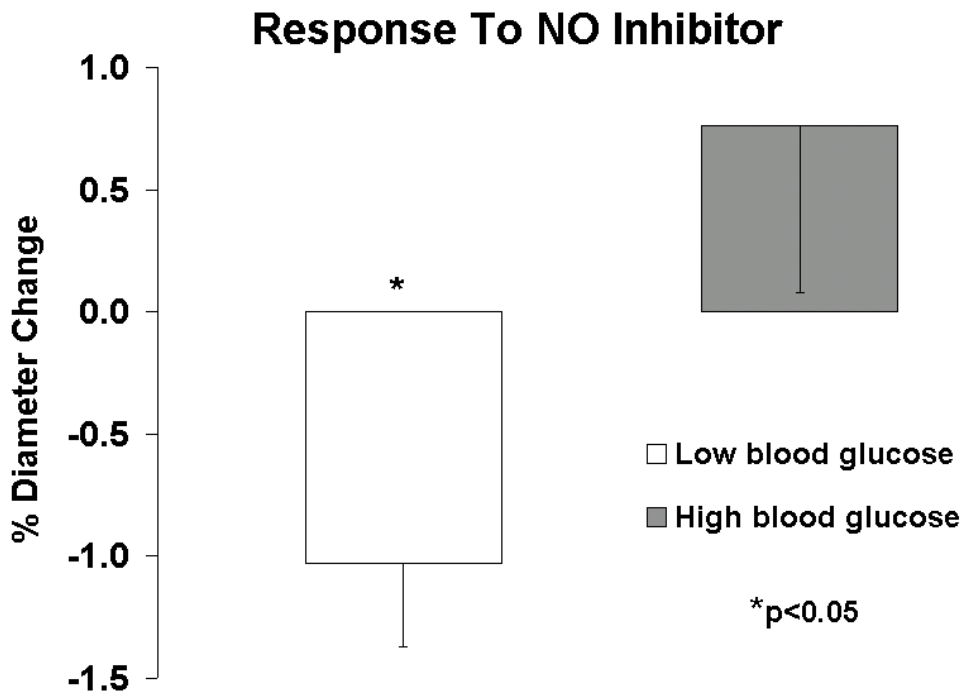


Figure 4.3: The STZ injected animals were grouped into high (less than 400 mg/dl) blood glucose (n=7) and low (greater than 400 mg/dl) blood glucose (n=7) in order to assess whether the absence of NO were due to DM or STZ. (*p<0.05)

The figure conveys that STZ has not altered the effect in low blood sugar animals, which were not truly diabetic compared to animals of high blood sugar levels. Therefore, the absence of NO is due to the effects of experimental DM.

What could cause this absence of NO release? Depending on the source of the NO, it could be due to a number of factors. Nitroergic nerves could be damaged by the diabetic state where protein crosslinking by DM induced AGEs can interfere with axonal transport and intracellular trafficking by physical blockage. Studies have shown that in smooth muscle of other DM tissues, such as the penis [100], there is a decrease of neuronal NOS due to selective damage of nitroergic neurons in the DM rat.

With blood vessels as the source, NO production was found to be reduced in vascular smooth muscle and the endothelium exposed to experimental DM [70]. Few studies have observed effects of DM on NO synthesis. Mumtaz et al. (1999) [101] found that DM decreased cGMP formation, which is the product of NO release, in the bladder neck and urethra of the rabbit. In addition, it has been found that urethral NO relaxation is impaired, and the cause may be due to lower cGMP formation or increased levels of advanced glycosylation end product (AGE's), which causes increase crosslinks of the extracellular matrix making it difficult for ion channels and membrane bound receptors to become stimulated [71]. Furthermore, it has been discovered in vascular smooth muscle that there is a marked increase in superoxide production. An interaction between NO and superoxide is very rapid and leads to the inactivation of NO and production of an oxidant of peroxynitrite [80]. As a result, this reaction would result in the absence of NO, and therefore, to inhibitor response from the NO inhibitor.

There are two types of smooth muscle in the urethra, longitudinally-oriented and circumferentially-oriented. The longitudinal layer is the inner most layer, and separated from a thin layer of collagen, the circumferential layer follows. Being that the longitudinal direction was set at a fixed in vivo length, the laser micrometer could only assess the circumferential smooth muscle direction. Whether they act separately to contract and relax the urethra during micturition or in a coexisting manner remains highly controversial [72]. The smooth muscle was assessed pharmacologically with phenylephrine, an α 1-adrenoceptor agonist. Non-selective agonists were not used, such as epinephrine and norepinephrine, because they can also activate α 2-receptors, which causes contraction, and β -receptors, which causes relaxation [73]. Addition

of these non-selective agents would cause a mixed response, and a complete contractile response could be measured [74]. It is possible that $\alpha 1$ -adrenoceptors are mainly responsible for mediating the effects of sympathetic nerves in the urethra. Also, this class of receptors has the highest population density in the mid urethral region [75], which is one of the main reasons why the middle point of the urethra was chosen to test pharmacologically.

The contractile response to phenylephrine seemed not to change when basing the comparison on controls and 5 and 10-week DM. Although, a trend was observed that the healthy urethras could maintain the contractile response more efficiently than DM urethras. Due to the variability of this diabetic rat model, discussed in the limitations (Section 4.5.2), the pharmacological data were evaluated on two populations of DM rats: those that severely diabetic (e.g. high blood glucose levels (B.G. \geq 400 mg/dl and dramatic loss of weight) or only mildly diabetic (e.g. low blood glucose levels (B.G. \leq 400 mg/dl and gain and marginal loss of weight) and compared (Figure 3.17). Results showed that the maximal phenylephrine contraction was significantly less than all of the other groups signifying that this observation may be correlated to the severity of DM. This may be due to the hyperglycemic condition brought on by DM's characteristic loss of the production of insulin. Much of this result may be due to the interaction of the cell surface with the altered extracellular matrix due to non-enzymatic glycosylation reactions. AGEs in diabetes have been shown to bind cell surface receptors including the receptor for AGEs (RAGE), which has been modified on vascular smooth muscle cells setting the stage for excessive tissue damage [76]. Furthermore, studies have shown that AGE's impair arteriolar smooth muscle mechanotransduction by alteration of intracellular calcium handling, and this occurs in the endothelium, as well [76,77]. This could also be the reason for urethral smooth muscle impaired response to phenylephrine in the severely diabetic state. It has been revealed that extracellular and intracellular calcium release play a role in $\alpha 1$ -adrenoceptor activated contraction (Figure 4.4) [78].

The results of this study showed that the magnitude of relaxation induced by calcium and magnesium chelation had no effect in DM urethras compared to controls. On the other hand, the amount of time to reach maximal relaxation was significantly longer for DM urethras. Like with contractility, this difference may be due to the non-enzymatic glycosylation reactions of the ECM; thus, impairment of ion release of the voltage gated ion channels occurs. Still, studies on blood vessels exposed to DM conditions have been conflicting [79]. Much of this may be due

different diabetic animal models used, i.e. alloxan versus STZ, or testing at varied times whether in the early, intermediate, or late stages of DM.

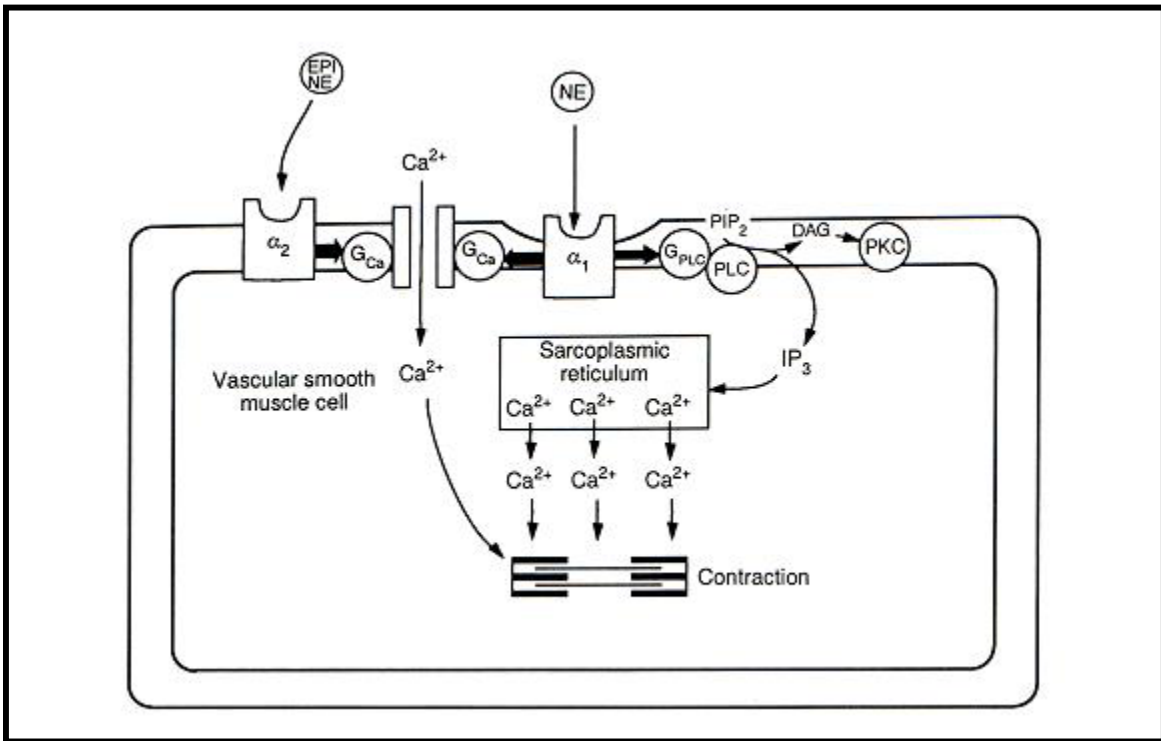


Figure 4.4: A schematic representing the mechanism behind the activation of alpha 1-adrenoceptor smooth muscle contraction. Note: this mechanism is dependent upon both intra- and extra-cellular calcium levels (From Ruffolo et al. 1991 [78]).

4.3 EXPERIMENTAL LIMITATIONS

While these experiments provided much insight to the pathology of diabetic cystopathy, some experimental limitations need to be distinguished.

4.3.1 Limitations to the Ex-Vivo Experiments

One of the most important disadvantages was the uncertainty and potential error in maintaining the urethral in vivo length. For example, the urethra was measured at the time of dissection, but the sutures, which ligated the urethra at in vivo length, were untied in order to tie the urethra onto the tees of the ex vivo system. With hindsight, it would have been more appropriate to develop an adjustable apparatus that could be used at the time of dissection, and versatile in a way that the proposed apparatus may fit into the perfusion system. A similar system has been described in the past for vascular segments [30]. Another limitation to the experimental set up was that the proximal, middle, and distal portions could not be measured at the same time. The laser could only be positioned at one point during testing. Thus, mechanical testing needed to be performed at one position at a time and in random order each time in order to avoid any variations in the results due to the strain history effects of biological viscoelastic tissue. A similar problem occurred during pharmacological testing. This not only increased the number of animals needed for experiments, but also specimen-to-specimen variability.

The outer diameter was utilized for the calculations of incremental compliance and beta stiffness. Conversely, most studies use the mid wall diameter range to calculate beta stiffness and inner diameter (for lumenal volume) to calculate compliance [34]. Under the thin wall assumption, where the thickness is less than .10 of the radius, the outer diameter could be a fit measure for these calculations, but this is not the case for the urethra, which has been calculated to be a thick walled tube [102]. However, beta stiffness values for the baseline and passive proximal urethra are compared to previously calculated values for other tissues [Table 1; 103-104], and the values are similar in range. Table 2 represents compliance values for the baseline

Table 4.1: Beta stiffness values for the proximal urethra for baseline and passive states compared to values calculated for arterial tissues in past literature.

TISSUE SPECIMEN	BETA STIFFNESS VALUE
Baseline Control Proximal Urethra	7.31 ± 0.89
Passive Control Proximal Urethra	10.00 ± 0.86
Human Common Carotid Artery (in vivo) [103]	10.30 ± 0.05
Passive Rat Aorta [104]	1.4 ± 0.4

Table 4.2: Compliance values for low (0-6 mmHg), middle (6-12 mmHg), and high (12-20 mmHg) pressure compliance for the proximal urethra compared to that calculated in past literature for passive porcine coronary arteries

TISSUE SPECIMEN	LOW PRESSURE COMPLIANCE (mmHg⁻¹)	MIDDLE PRESSURE COMPLIANCE (mmHg⁻¹)	HIGH PRESSURE COMPLIANCE (mmHg⁻¹)
Baseline Control Proximal Urethra	0.046 ± 0.006	0.011 ± 0.002	0.007 ± 0.002
Passive Control Proximal Urethra	0.059 ± 0.007	0.010 ± 0.001	0.007 ± 0.001
Passive Porcine Coronary Arteries [105]	$3.086 \pm 4.473 \cdot 10^{-4}$ (at 10 mmHg)	$0.718 \pm 5.522 \cdot 10^{-5}$ (at 30 mmHg)	$0.426 \pm 5.020 \cdot 10^{-8}$ (at 50 mmHg)

and passive proximal urethra compared to values previously calculated for porcine coronary arteries [105]. These inconsistencies may not only be due to the use of outer diameter versus inner diameter, but different pressure ranges for low, middle, and high pressure compliance values were used, as well. Although the data is not shown, the middle and distal urethral compliance and beta stiffness values exhibited the same comparisons, as the proximal urethra values.

Another assessment that was neglected was the accuracy of measurement. For future studies propagation of error analyses will be performed in order to assess error in the results. The analyses that will be performed are derived in Appendix B.

For future experiments, one might also consider altering the system so that the urethra is exposed to continuous flow, yet minimal flow (approximately 1.5 ml/min). The system used in this work was set up so that the distal end was clamped off to allow application of intraluminal pressure. With this approach, the media contained within the urethra was not being circulated as was the adventitial bathing media. As a result, the tissue may not have received sufficient gas balance or nutrients. This may have contributed largely to any inconsistencies seen in the functional data. Another concern dealing with dissolved gases may have been another limitation. Although the media was bubbled with an oxygen mixture for 20 minutes and the urethra was placed in a conical tube filled with the oxygenated media during transport, the average transportation time was 30 minutes. Tissue viability is a limitation to *ex vivo* systems, also. This obstacle may contribute to possible variations for the biomechanical and functional results. Kwon et al. [46] found that urethral strips exposed to anoxic conditions exhibited an immediate decrease of contractile response to phenylephrine. Steps should be taken to understand affects on the healthy tissue from factors, such as isolation of the tissue, duration of time after excision, time in the perfusion system, and distension of the tissue. This may be achieved with the use of a live/dead stain to assess necrosis or assessment of lactate dehydrogenase, which indicates the amount of cell death by the release of lactate dehydrogenase from the cytosol of the damaged cell.

Other limitations relate to the *ex vivo* nature of the experiments. The urethra is a highly innervated structure involving both somatic (external striated sphincter via pudendal nerve) and autonomic (sympathetic and parasympathetic) nervous systems. By excising the urethra and

testing it *ex vivo*, all neural input to the urethra is eliminated, except for possible spontaneous release of transmitter from intramural nerve terminals. Future work might examine the effects of electrical stimulation to provide a model of the urethra that is closer to its *in vivo* environment and to maintain the integrity of the nerve tissue. Also, the urethra is composed of both longitudinally- and circumferentially- oriented muscle. However, the laser micrometer can assess only circumferential contractile response, but longitudinal contraction also plays a large role in urethra functionality. As evidence of this, it was observed that the urethra became largely elongated and kinked within the experimental system once it completely relaxed with the addition of EDTA. A suggestion to solve this problem would be to attach two force transducers to the tees and connect via A/D conversion board to the computer. Thus, the longitudinal tension and relaxation could be measured with the addition of each pharmacological agent, as well as the circumferential response.

Finally, another limitation to this study involved the application of pressure. As described in Section 1.4, a reservoir filled with media 199 attached to a graduated ringstand was manually displaced to apply intraluminal pressure. While much care was taken to calibrate each graduation to increments of 2 mmHg using a water manometer, there still was more likely error of achieving exact increments of 2 mmHg. Also, by using manual displacement, the preconditioning regimen could only be performed at an approximate maximal rate of 0.5 Hz. Much faster strain rates are typically employed for mechanical testing of soft biological tissues [92,93]. An automated system involving a computer controlled stepper motor could possibly solve this problem, and could also allow the application of the pressure in smaller increments (1 mmHg).

4.3.2 Limitations to Microstructural Analysis

Microstructural quantification of the tissue components did not agree with the biomechanical findings. But, the techniques used were not sensitive and had their disadvantages. First, cryosectioning produces some voids in the tissue. The purpose of subjecting the tissue to ascending sucrose solutions was to provide a ‘cryoprotectant’ for the tissue before freezing the tissue for sectioning. However, this tissue can still exhibit freeze-induced damage, including local disruption by ice crystals, thus producing holes and affecting measurement of the entire

urethral cross sectional area. Secondly, while immunohistochemistry is highly specific with the use of antibodies, results from histological staining are quite varied depending on the type of animal tissue and method of fixation. Another disadvantage is that methods used for Masson's trichrome stain and Weigert's resorcin fuschin were very sensitive to the washing times, staining times, dehydration times, and clearing times. Holes seen in the tissue could also have been a result of the many washes required for the immunohistochemical and histological methods. For the future, analyses using enzymatic digestions should be considered, as well as methods involving three dimensional reconstruction.

4.3.3 Limitations of the Diabetic Rat Model

Rakieten et al. (1963) [38] were the first to report that streptozotocin exerts diabetogenic activity in rats, amongst other animals. Since then, this diabetic animal model has been largely used to replicate type I DM. Unfortunately, the experience with this particular model was not repeatable. Depending on the dosage, studies claim that signs of DM, e.g. high blood glucose levels, take effect 8 to 48 hours post STZ induction [38, 47-49]. The dose for these experimental studies was on the higher end of that typically used (65 mg/kg), but only a portion of the rats exhibited symptoms of STZ-induced DM (e.g. soft fecal matter and weight loss). For the other portion of rats, such effects took much longer (on the order of weeks) before they were noticeable. While the rats in this study that were deemed diabetic did meet the blood glucose criteria (>300 mg/dl), there was much variability. The blood glucose levels ranged from <300 to 555 mg/dl in those DM rats which had this measurement made. Much of this variability was likely due to the vehicle that was used to administer the drug and its preparation. The STZ was dissolved in saline and made fresh immediately before induction. Although this method has been previously used [85,89], most studies dissolved STZ into citrate buffer (pH adjusted to 4.5) [85]. Since STZ has an extremely short half-life (15 minutes), the method described may aid the stability of the drug and provide the more consistency vis-à-vis blood glucose level with this experimental diabetic model. Thus, while it was certain that the DM rats used here were diabetic (i.e. they exhibited all of the characteristics summarized in Section C.1), there was no certainty as to whether the rats were exposed to exactly 3, 5, or 10-week DM since blood glucose levels were measured only at those times following STZ administration.

5.0 CONCLUSIONS AND FUTURE WORK

Diabetes mellitus is the leading cause of peripheral neuropathy in the western world [86]. Cardiovascular, gastrointestinal, and neurological systems, to name a few, are seriously damaged, and patients with DM suffer health problems leading to a compromising lifestyle. A dysfunctional bladder has been the focus of diabetic cystopathy, and not much research has been aimed at an understanding of the role of the urethra in this voiding dysfunction. The experiments described here have attempted to answer the biomechanical and functional changes due to the onset of this disease.

First, a biomechanical testing regimen was implemented to assess the linear elastic properties of the urethra in both the diseased and healthy states. By gaining pressure vs. diameter data *ex vivo*, both the beta stiffness and compliance were quantified and compared. From the biomechanical data, the first conclusion stands that significant stiffening occurs with the onset of DM, most markedly in the proximal portion. Additionally, increased passive compliance occurs in DM animals at the middle and distal portions at low pressures. These changes in biomechanical properties may reflect the alterations of three primary tissue constituents: smooth muscle (longitudinally- and circumferentially- oriented), collagen, and elastin. With an increase in beta stiffness and decrease in middle and high pressure compliance values, it is likely that collagen remodeling is a consequence of DM. Likewise, a significant increase in low compliance for DM specimens could represent derangements in elastin that is present, as well. Unfortunately, with the exception of the decrease of elastin in the mid portion of 10 week DM specimen, histological analyses described here did not reveal any significant changes in the amount of any tissue constituent or in the orientation of connective tissue fibers. These methods have some inadequacies as described in Section 4.3.2. As described previously in Sections 4.1 and 4.2, DM has been associated with advanced glycation endproducts (AGEs) and reactive oxygen species (ROS). As with the vasculature, oxidative stress may cause cellular damage and

AGEs are known to initiate connective tissue crosslinking. Histological methods for collagen and elastin could not reveal this type of alteration or different types of collagen present, and smooth muscle alpha actin staining was not capable of assessing cellular damage. It would be important to assess any increase in the amount of varied collagen types. It is well established that collagen fibril diameters become enlarged from diabetes [94], but it has also been established that there are increased amounts of different types of collagens which can indicate alterations of diabetic tissues down to the cellular level. Renal, hepatic, and cardiac tissues have exhibited alterations in cell production of collagens type I and III indicating that DM may cause changes in cell phenotype [95,96,97]. Further work in the area must be carried out in order to assess these possibilities.

A pharmacological assessment of mid urethral smooth muscle was performed on both control and DM specimens. Similar to blood vessels, nitric oxide release was absent for DM specimens due to the fact that there was no response to the NO inhibitor. This finding suggests that DM might cause an impairment of urethral relaxation. In agreement with this, it was observed that the DM urethra endured a significantly longer relaxation period than controls, although the magnitude of relaxation was unaffected (Figures 3.14-3.17). EDTA is a calcium and magnesium chelator indicating that there might be impaired extracellular calcium release. Finally, phenylephrine response was also impaired, but this factor was largely related to the severity of the diabetic state of the animal, and the extent of the blood glucose levels. For high blood glucose levels, the maximal contraction in response to phenylephrine stimulation was significantly impaired. However, this becomes a question of whether or not this discrepancy was due to the state of DM or the state of hyperglycemia, and if not either, how much of a role the two play in this damage. To determine this, pharmacological assessments should be performed on the urethras of sucrose fed animals. Additionally, it would also be important to assess the effects of other smooth muscle contractile agents in order understand the portion of the $\alpha 1$ -adrenoceptor pathway that is damaged.

Clearly, the urethra is considerably affected structurally and functionally by the state of DM. Future studies addressing each of the limitations summarized in Section 4.4 should be considered. Efforts should also be made to relate these studies to in vivo experiments of DM and sucrose-fed control animals, as well. Additionally, ex-vivo biomechanical and pharmacological assessments should be compared with assessments made in vivo, such as leak point pressure tests

and urodynamic analysis. Correlating these comparisons with protein assays and gene or protein analyses will further aid the understanding of the tissue remodeling that appears to occur in the lower urinary tract from DM, and pave the way for future therapies for diabetic cystopathy. Furthermore, enhancing our comprehension of the pathogenesis of voiding dysfunction in DM may ultimately help in developing a therapy for these patients who suffer from lower urinary tract dysfunction, potentially serving hope for a better lifestyle and a promising future.

APPENDIX A. INDIVIDUAL DATA

A.1 CONTROL DATA

A.1.1 Baseline State

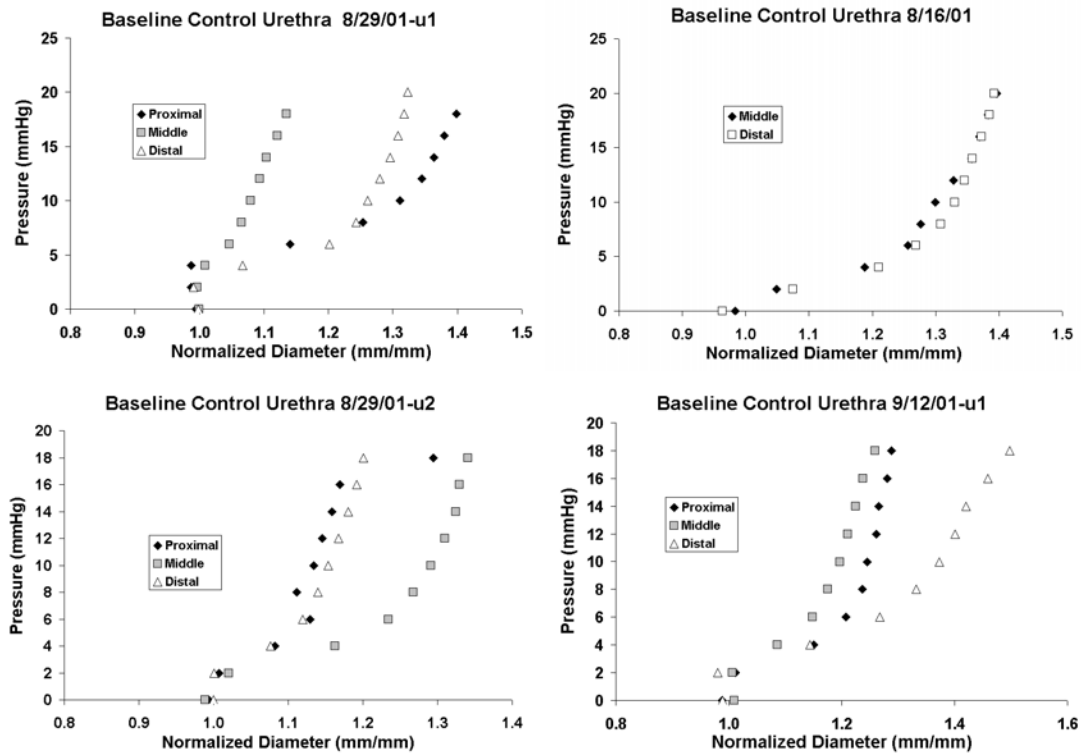


Figure A.1: Pressure-diameter data for proximal, middle, and distal portions of control urethras in the baseline state

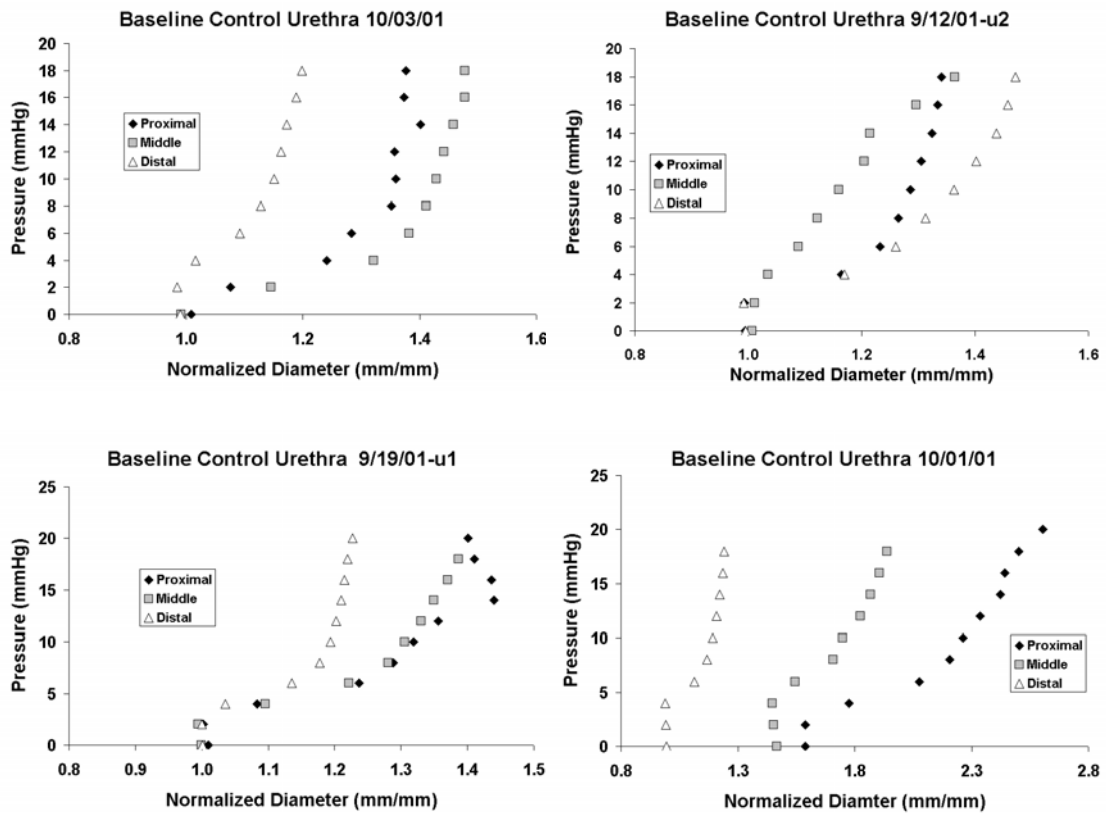


Figure A.2: Pressure-diameter data for proximal, middle, and distal portions of control urethras in the baseline state.

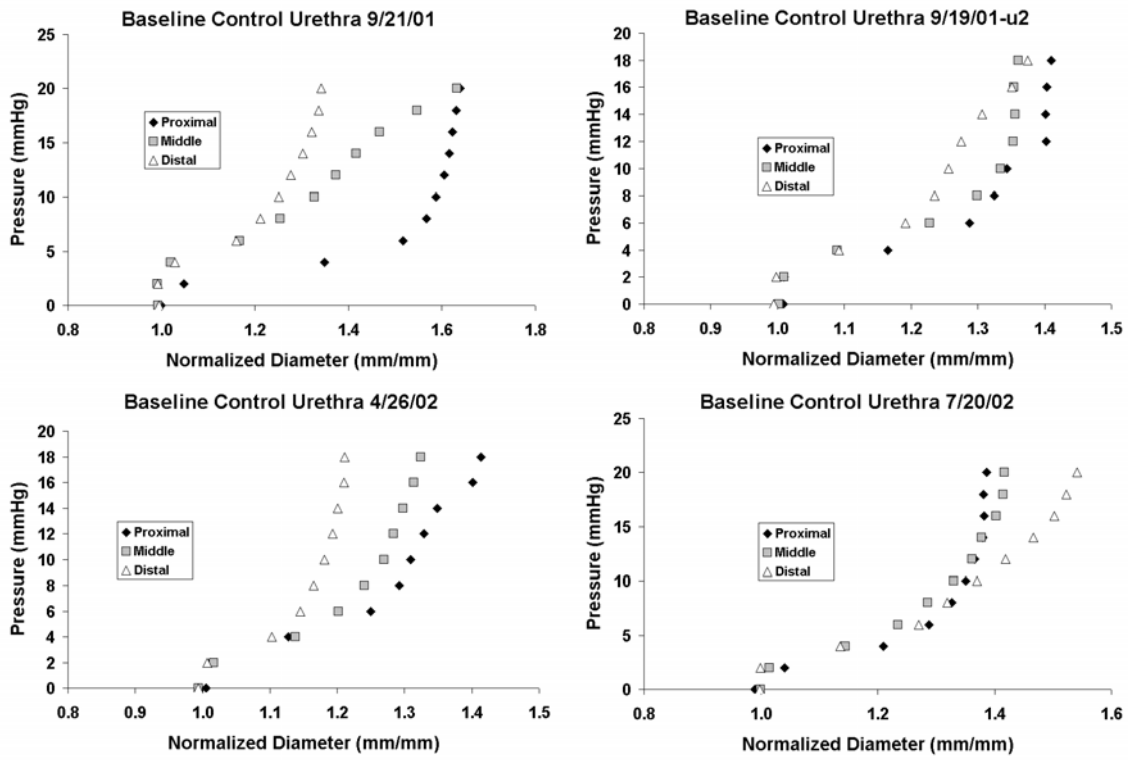


Figure A.3: Pressure-diameter data for proximal, middle, and distal portions of control urethras in the baseline state

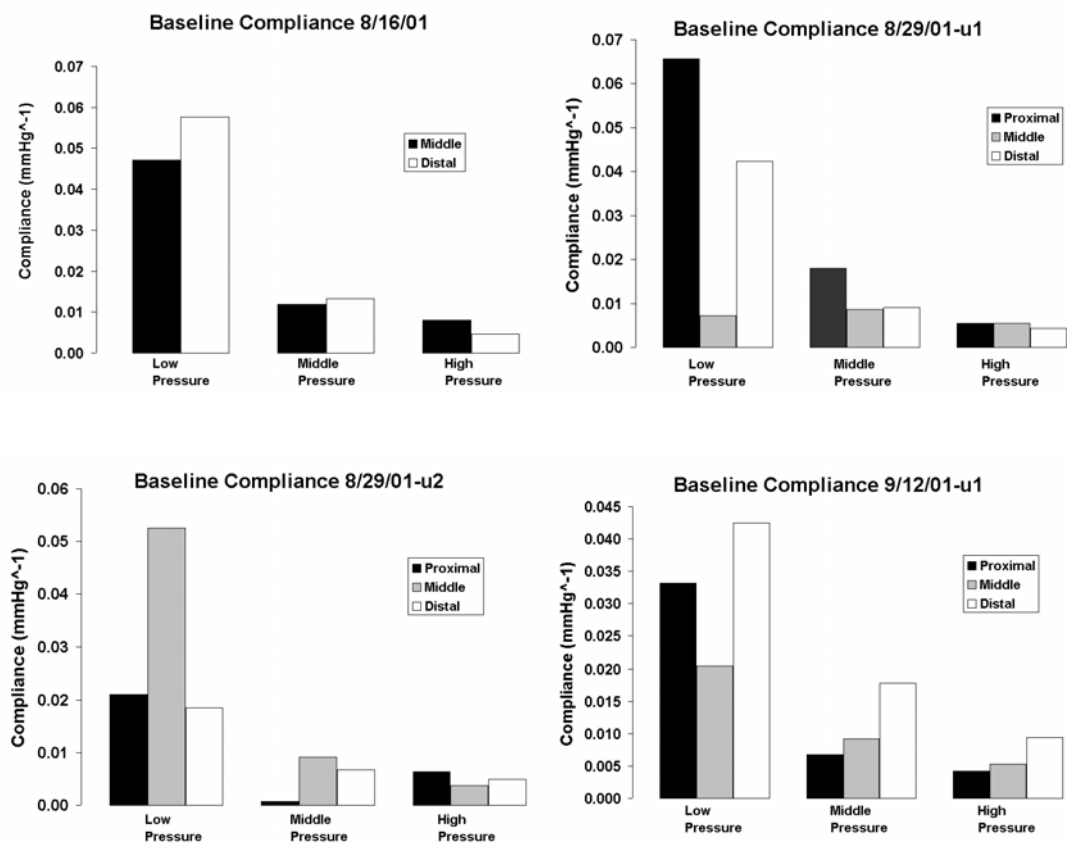


Figure A.4: Low, middle, and high pressure compliance data for proximal, middle, and distal portions of control urethras in the baseline state

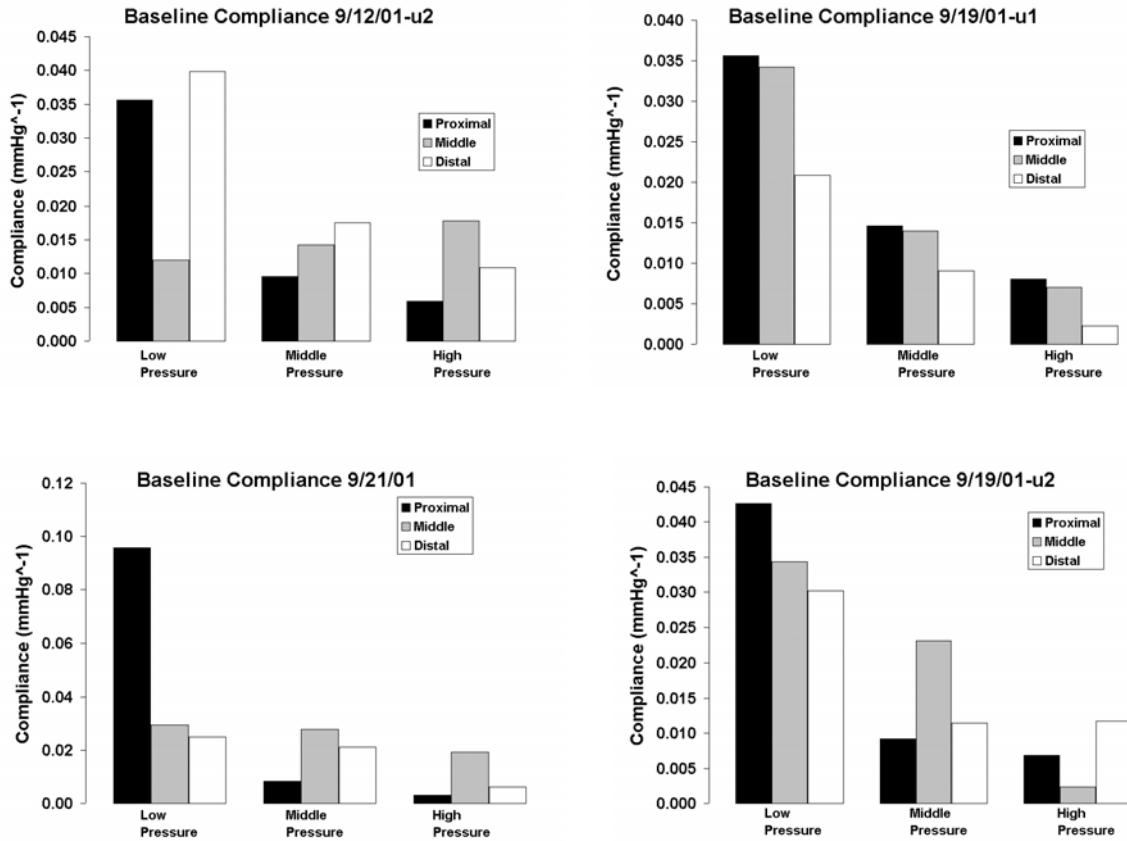


Figure A.5: Low, middle, and high pressure compliance data for proximal, middle, and distal portions of control urethras in the baseline state

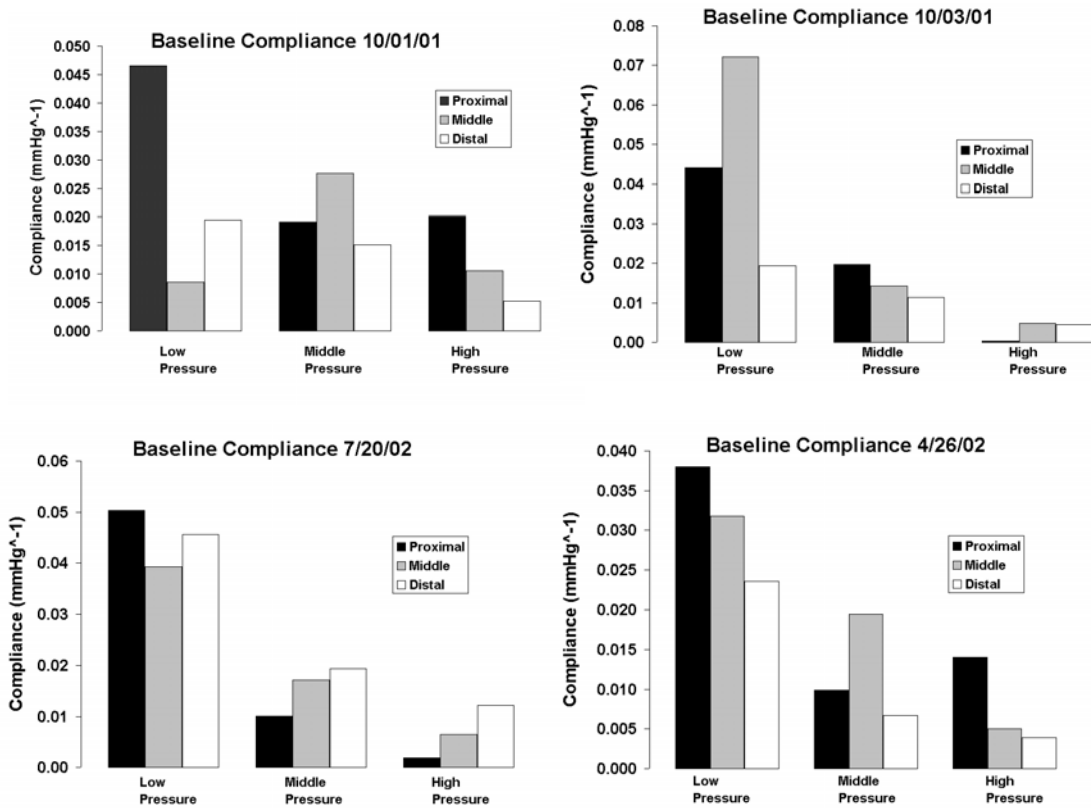


Figure A.6: Low, middle, and high pressure compliance data for proximal, middle, and distal portions of control urethras in the baseline state

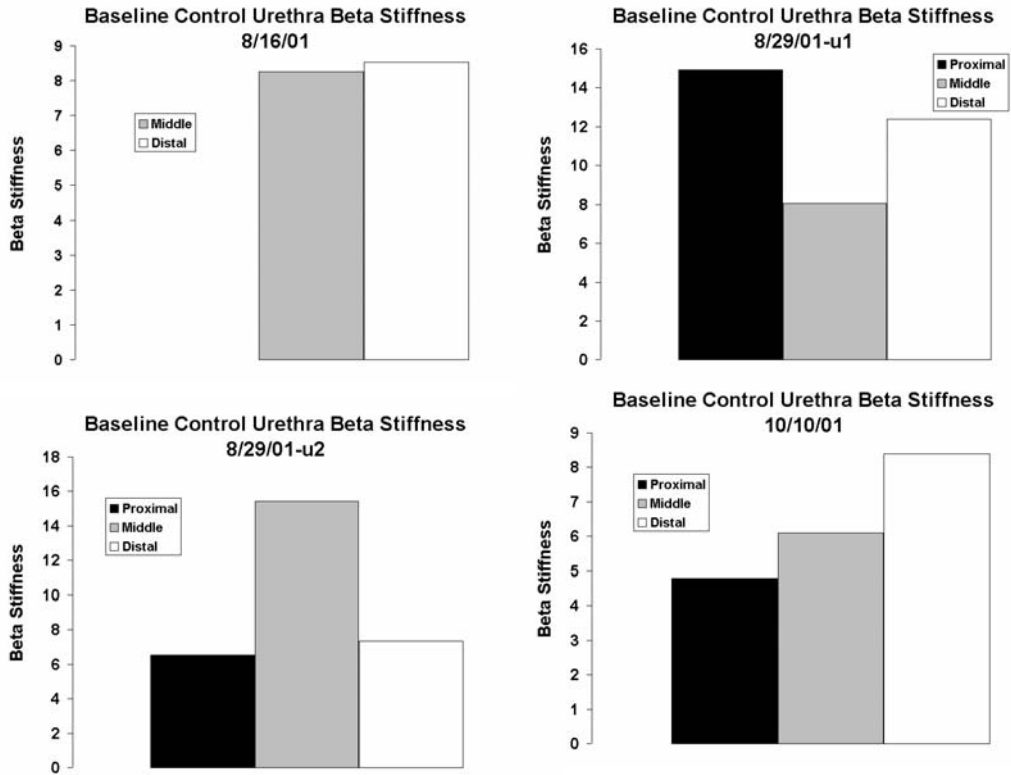


Figure A.7: Beta stiffness data for proximal, middle, and distal portions of control urethras in the baseline state

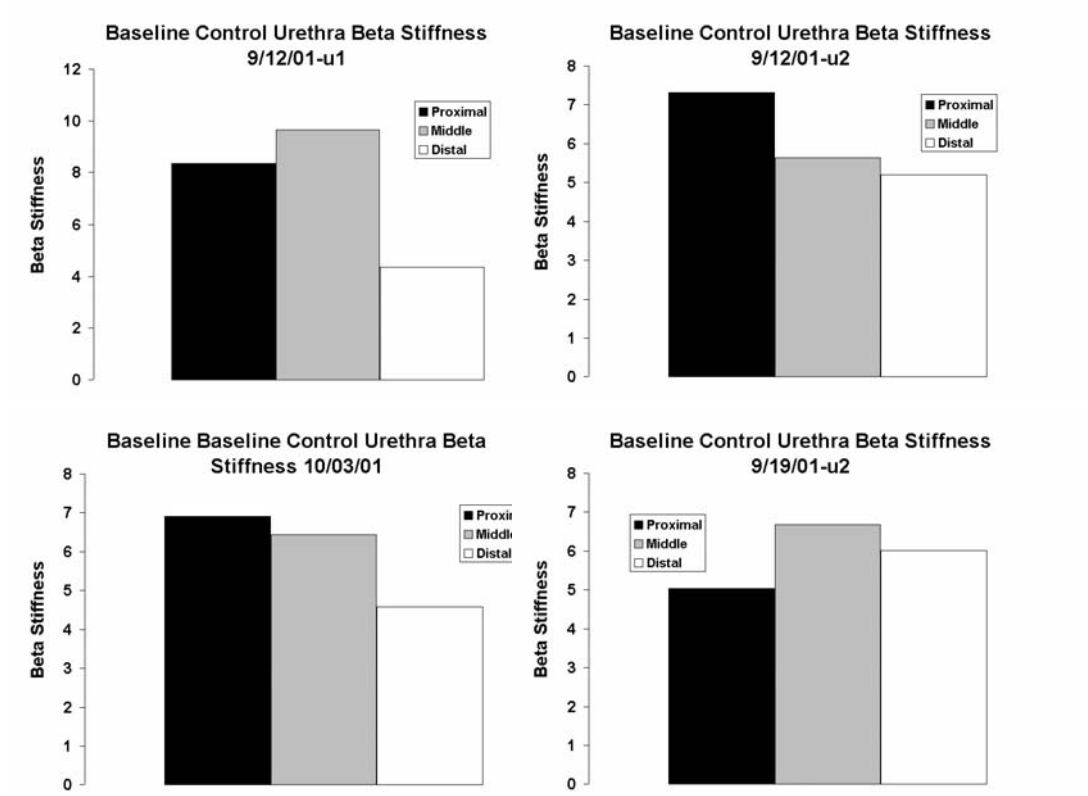


Figure A.8: Beta stiffness data for proximal, middle, and distal portions of control urethras in the baseline state

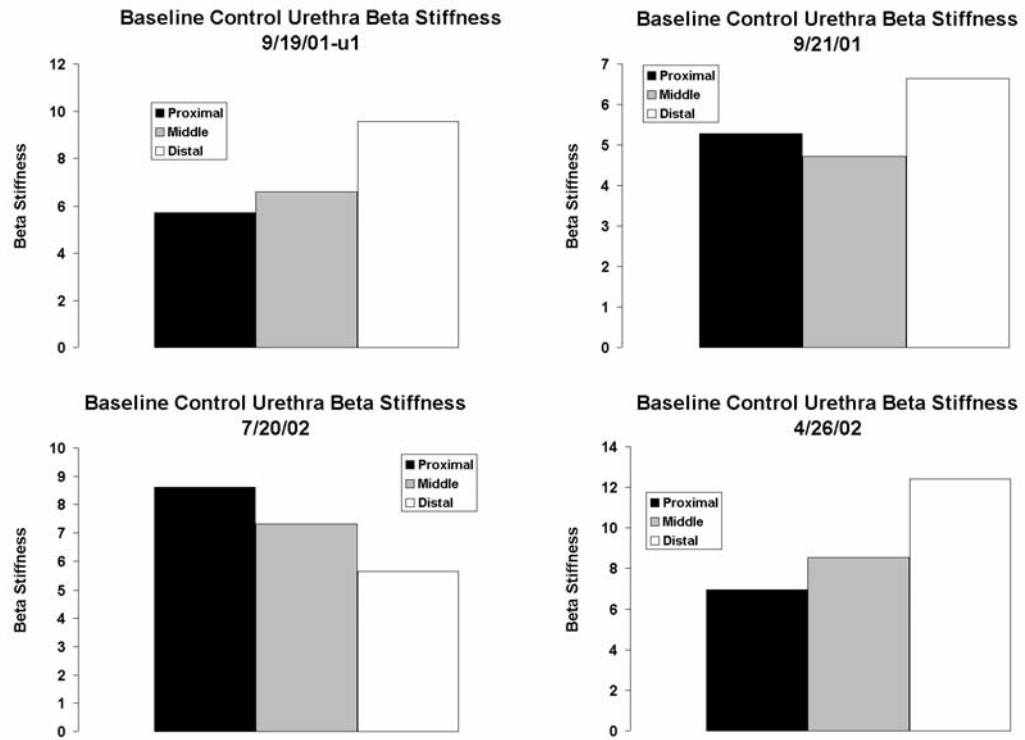


Figure A.9: Beta stiffness data for proximal, middle, and distal portions of control urethras in the baseline state

A.1.2 Passive State

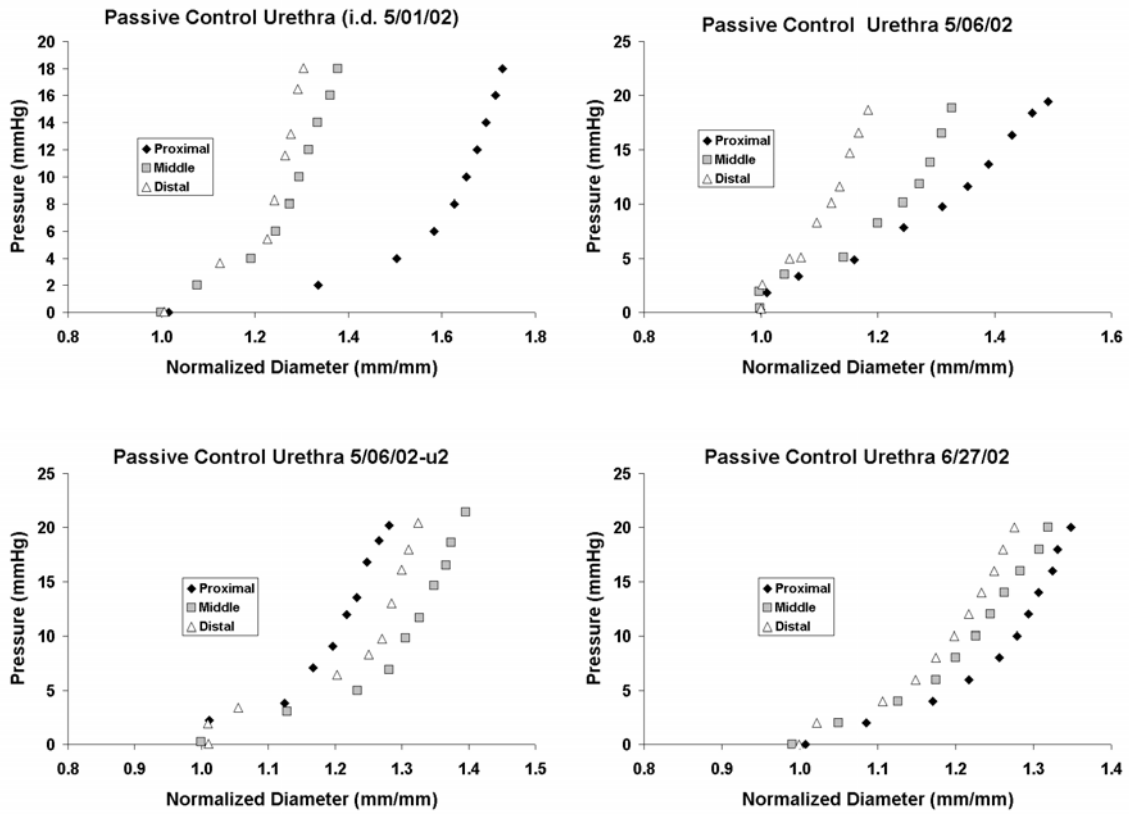


Figure A.10: Pressure-diameter data for proximal, middle, and distal portions of control urethras in the passive state

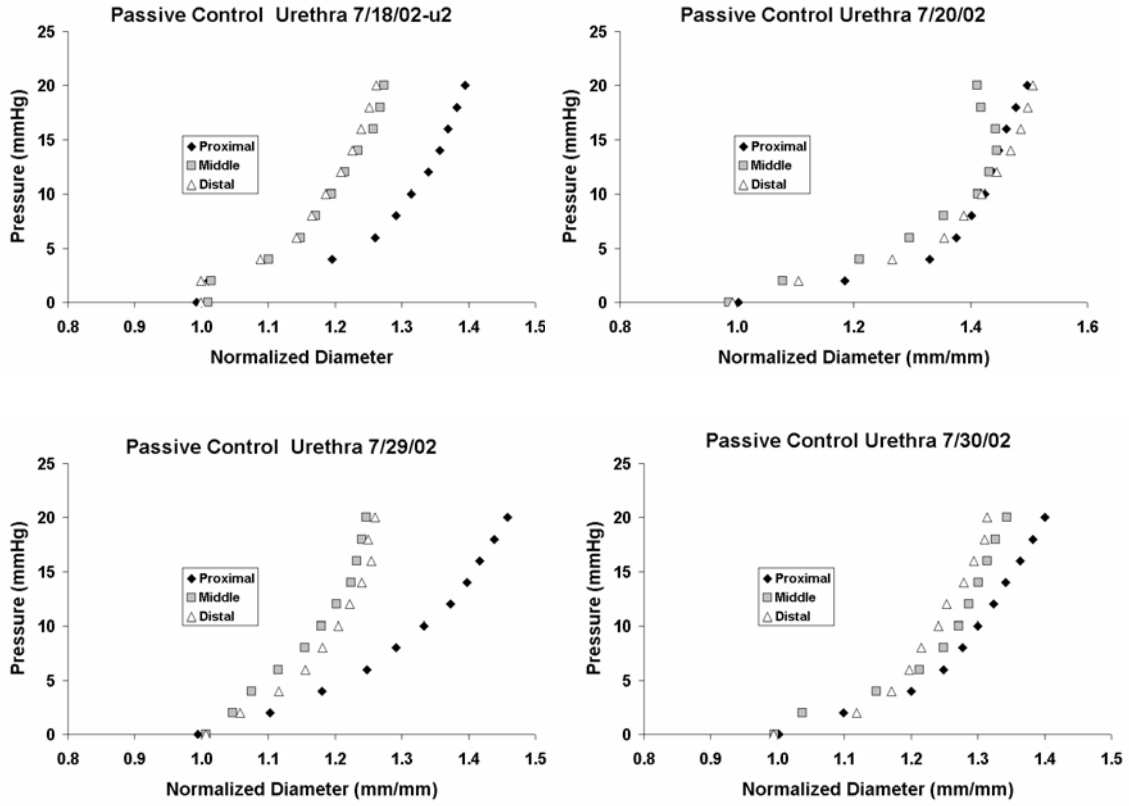


Figure A.11: Pressure-diameter data for proximal, middle, and distal portions of control urethras in the passive state

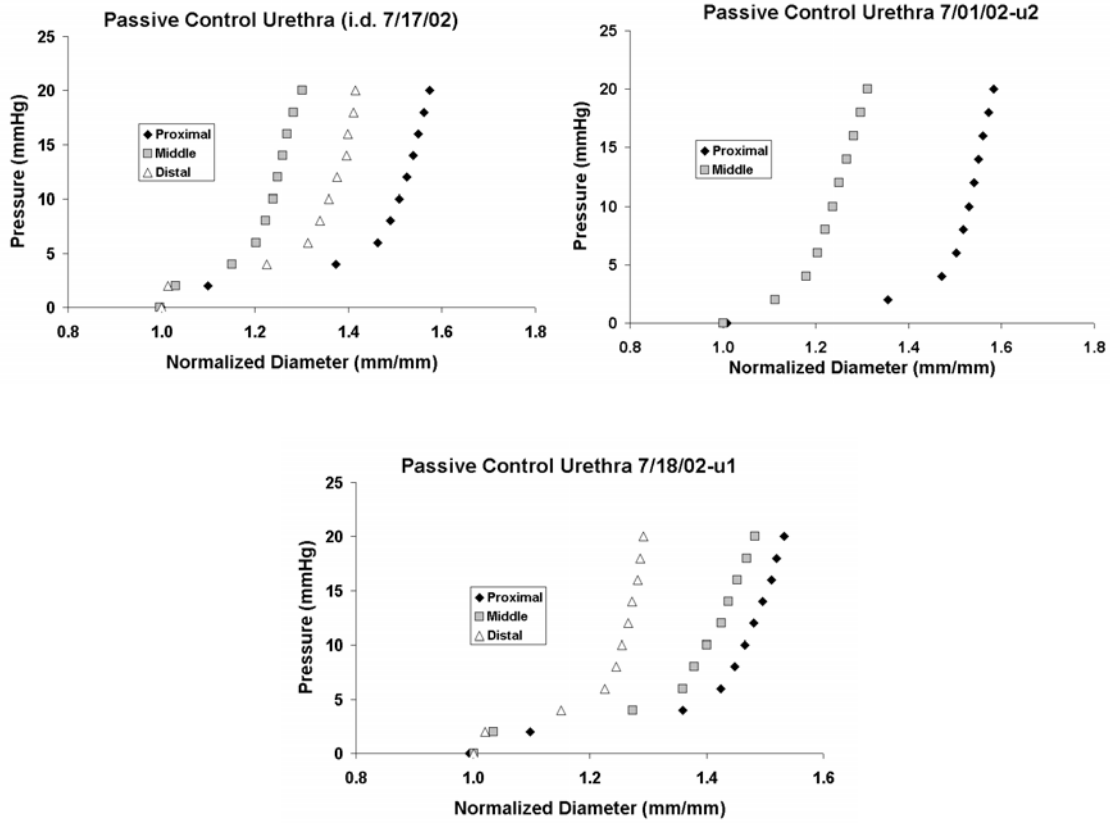


Figure A.12: Pressure-diameter data for proximal, middle, and distal portions of control urethras in the passive state

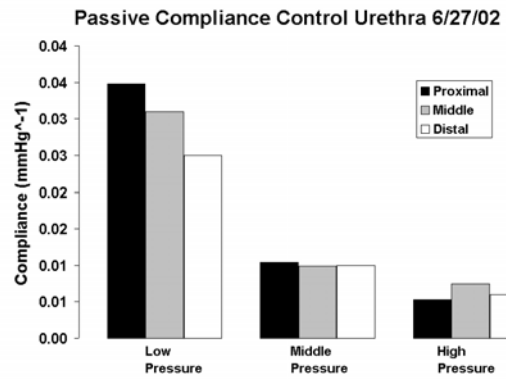
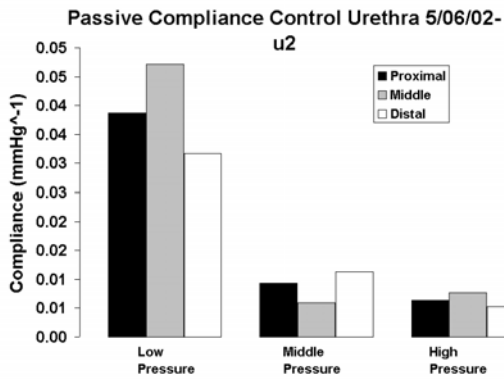
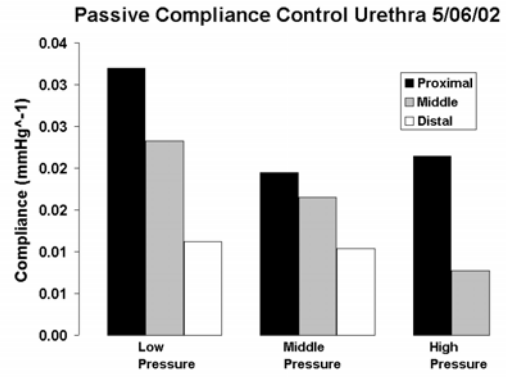
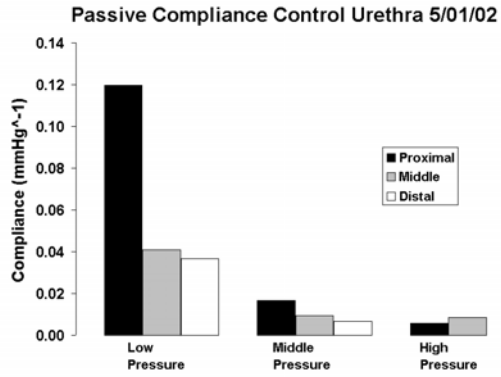


Figure A.13: Low, middle, and high pressure compliance data for proximal, middle, and distal portions of control urethras in the passive state

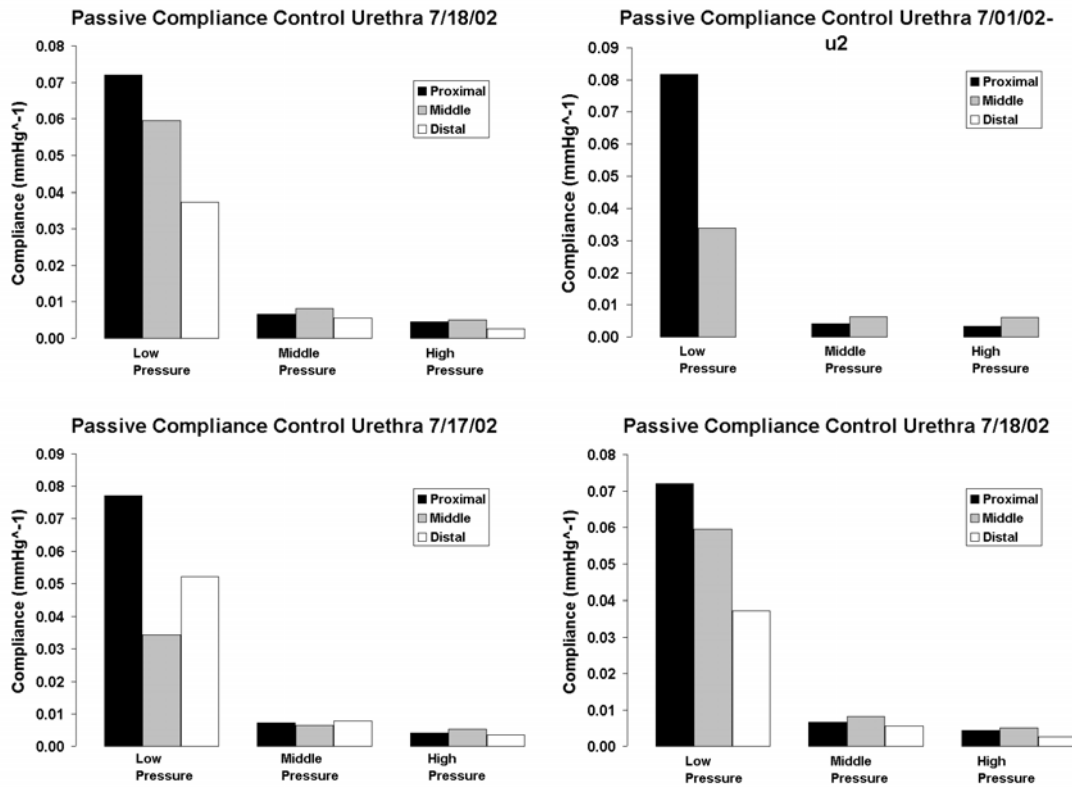


Figure A.14: Low, middle, and high pressure compliance data for proximal, middle, and distal portions of control urethras in the passive state

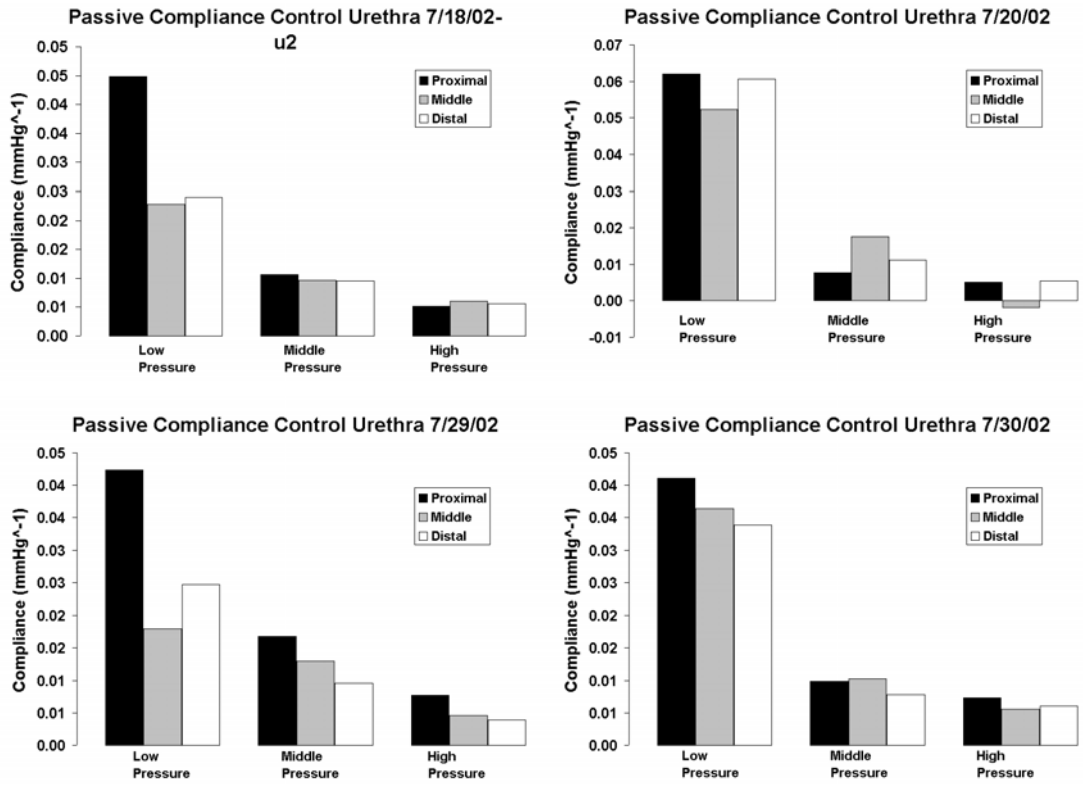


Figure A.15: Low, middle, and high pressure compliance data for proximal, middle, and distal portions of control urethras in the passive state

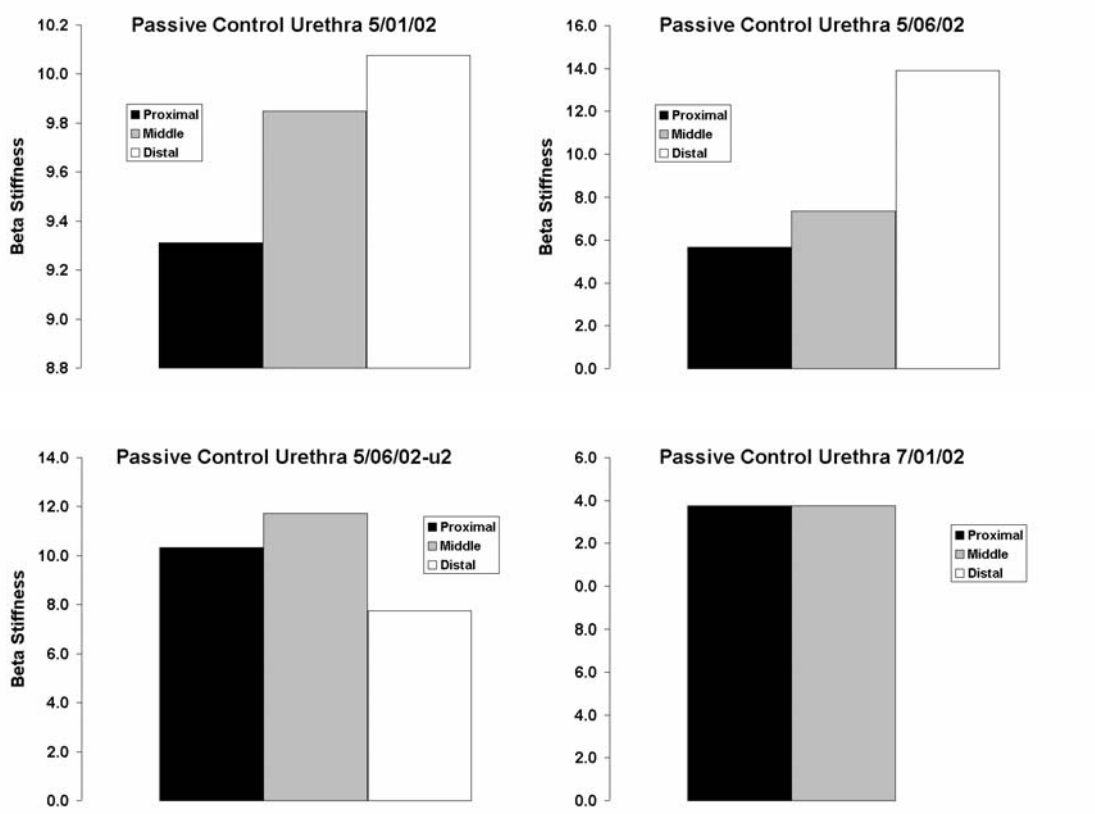


Figure A.16: Beta stiffness data for proximal, middle, and distal portions of control urethras in the passive state

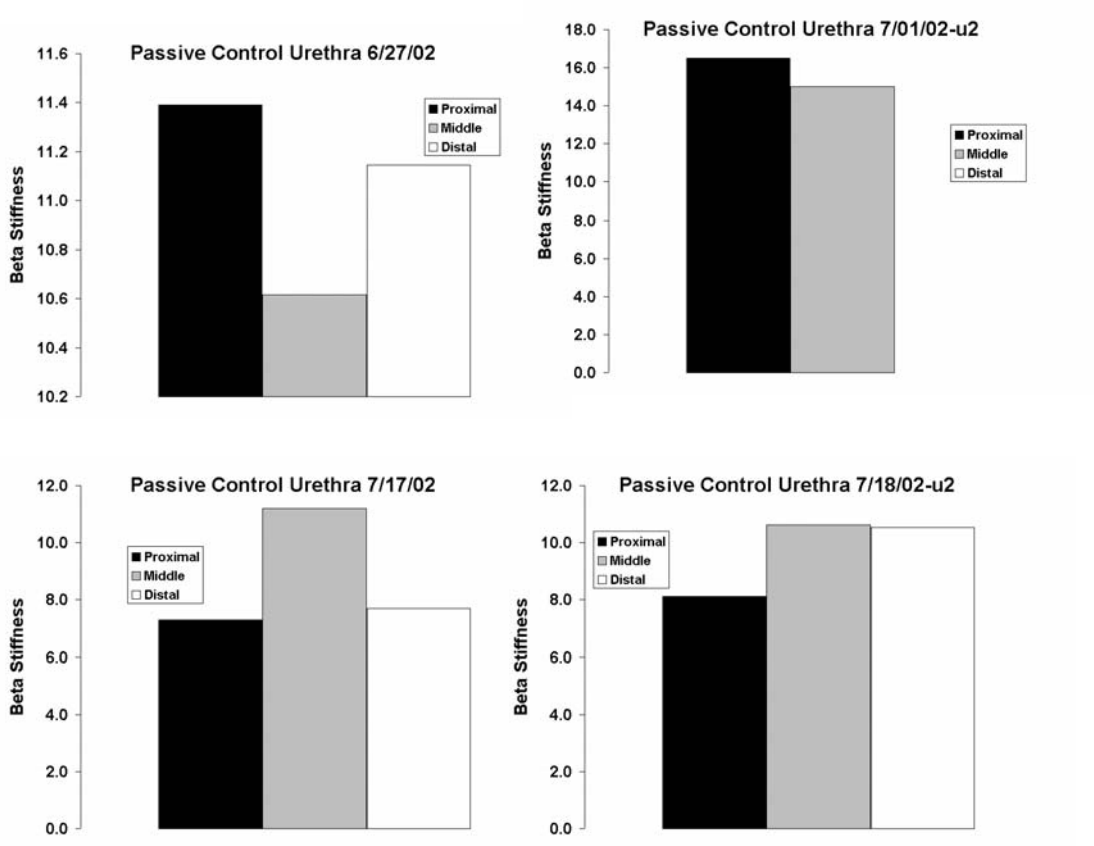


Figure A.17: Beta stiffness data for proximal, middle, and distal portions of control urethras in the passive state

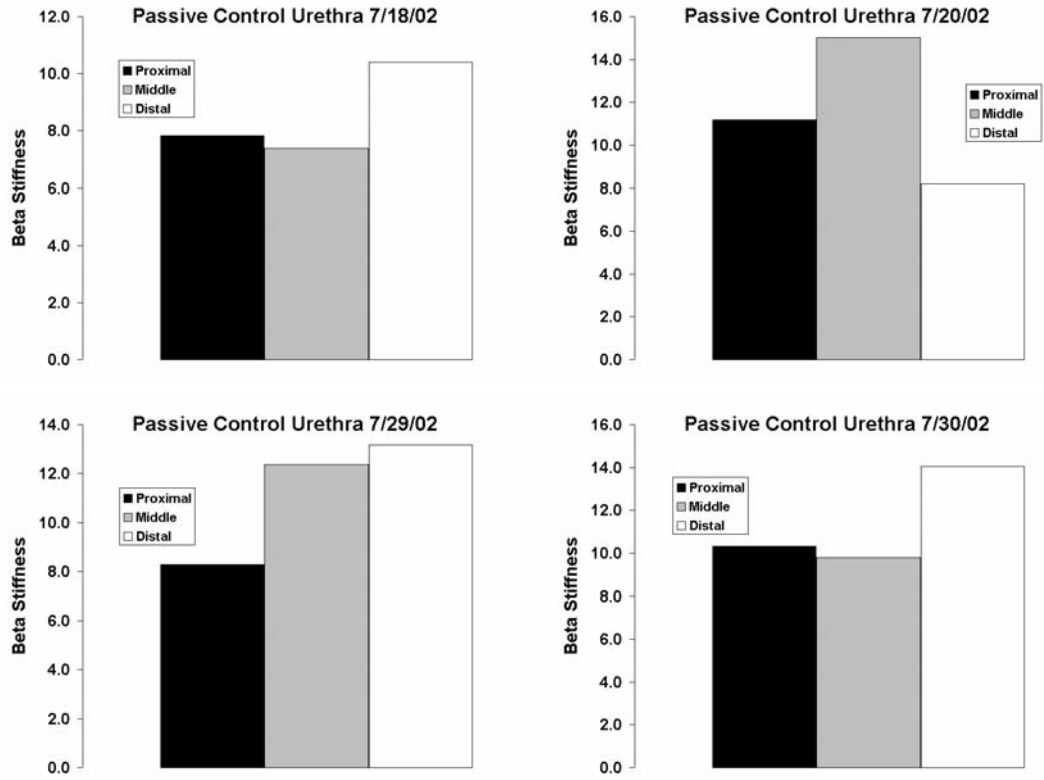


Figure A.18: Beta stiffness data for proximal, middle, and distal portions of control urethras in the passive state

A.1.3 Pharmacological Data for Control Urethras

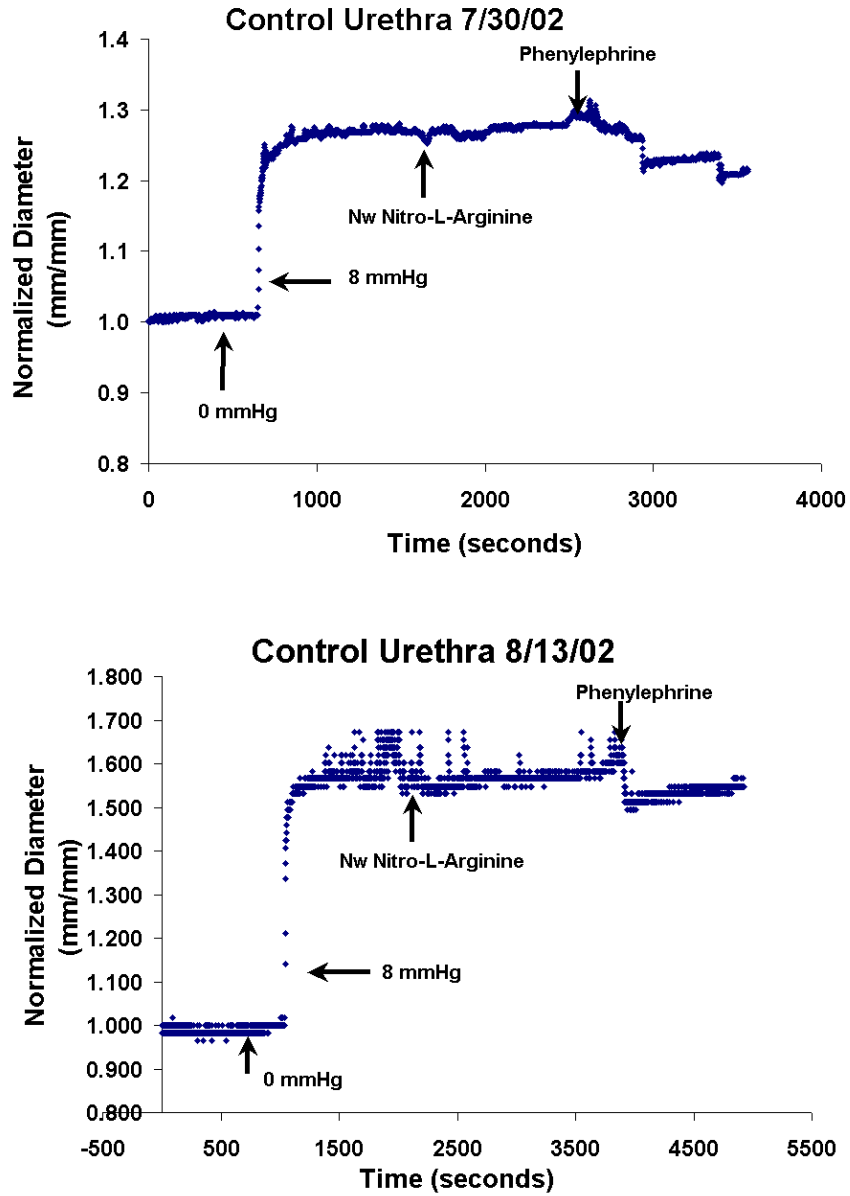


Figure A.19: Pharmacological data representing decrease and increase of the outer diameter of the middle portion of control urethras

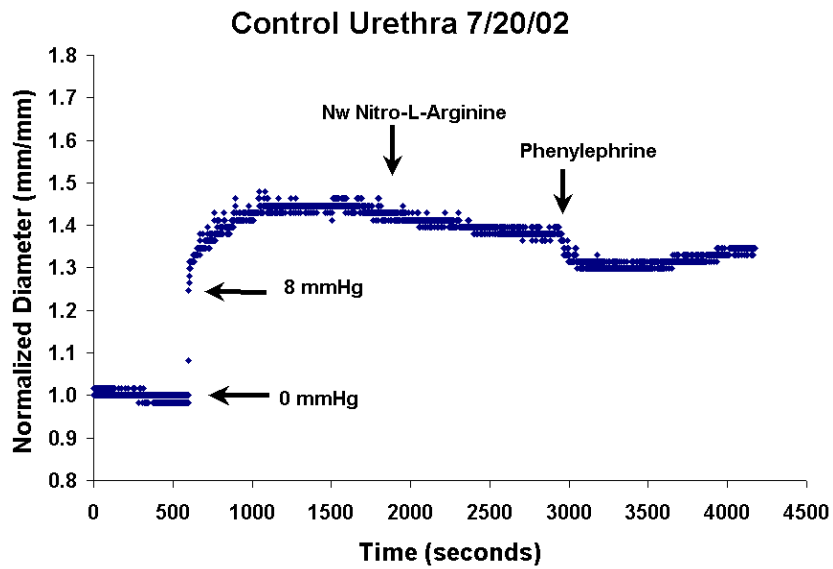
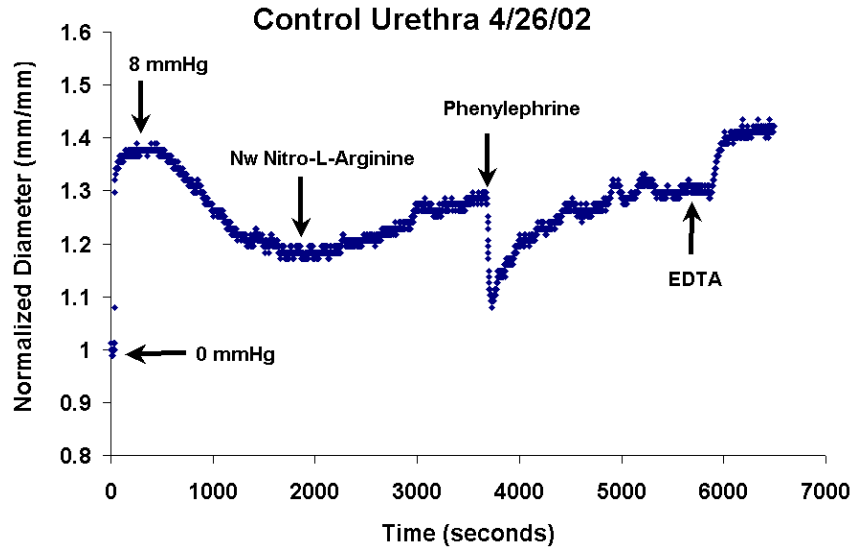


Figure A.20: Pharmacological data representing decrease and increase of the outer diameter of the middle portion of control urethras

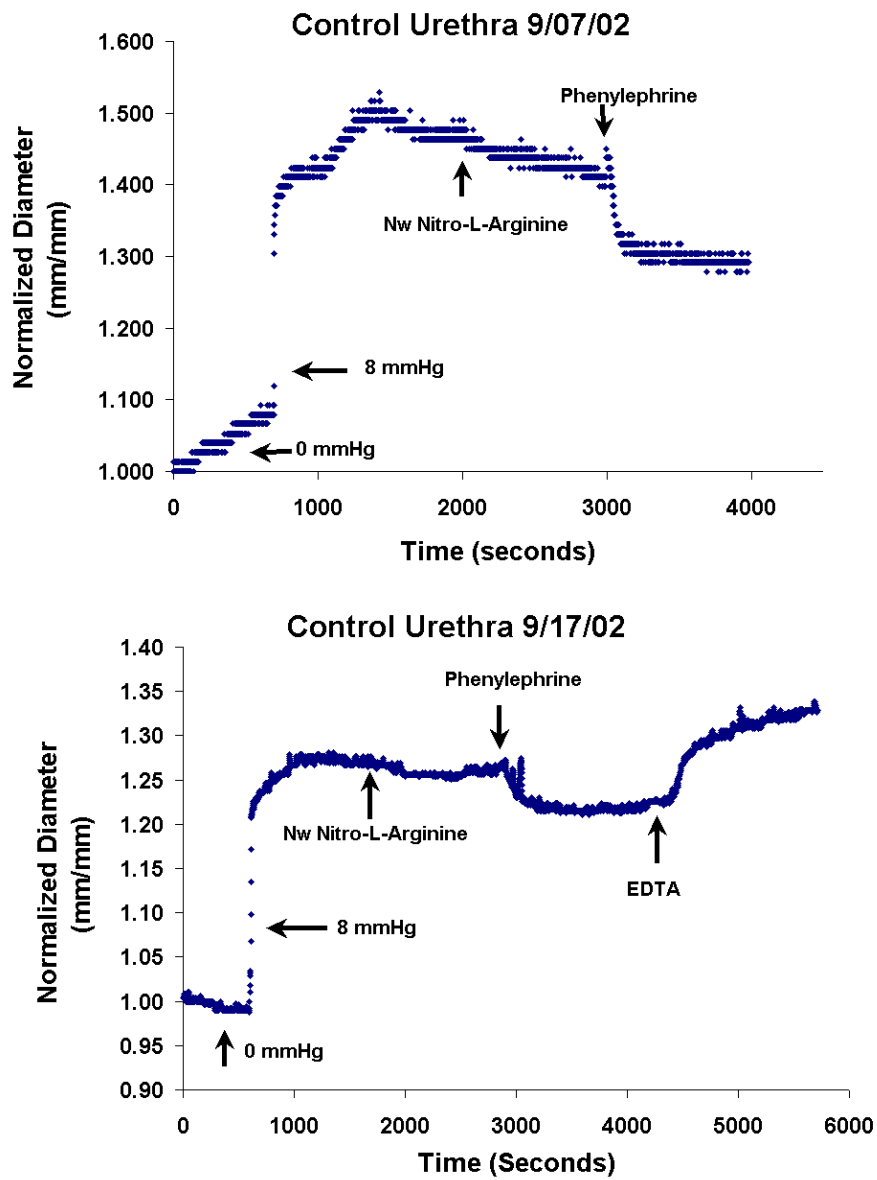


Figure A.21: Pharmacological data representing decrease and increase of the outer diameter of the middle portion of control urethras

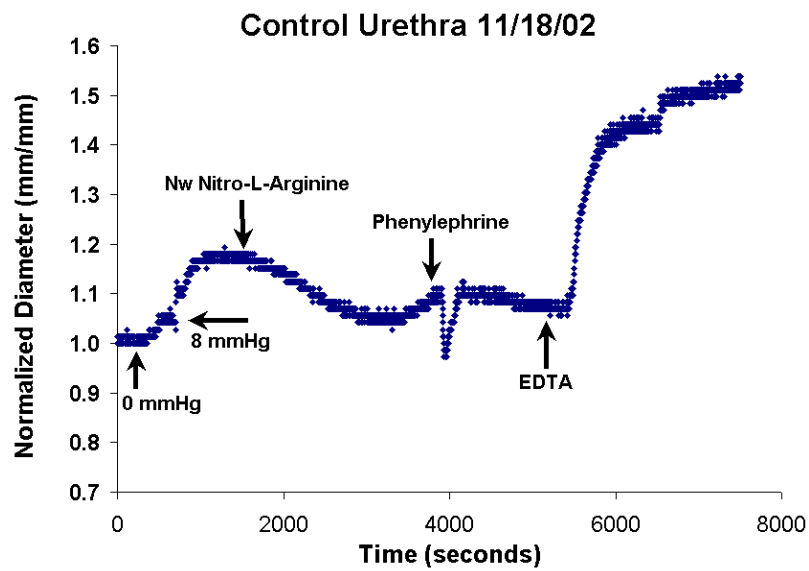
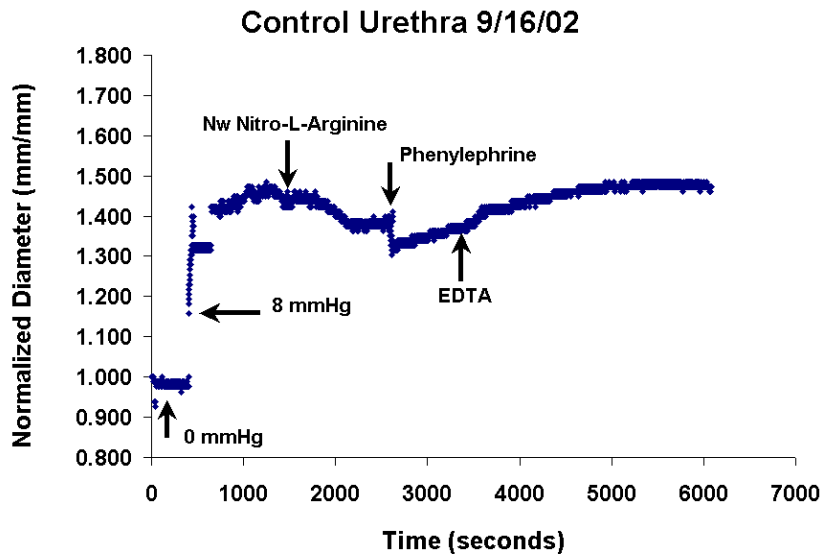


Figure A.22: Pharmacological data representing decrease and increase of the outer diameter of the middle portion of control urethras

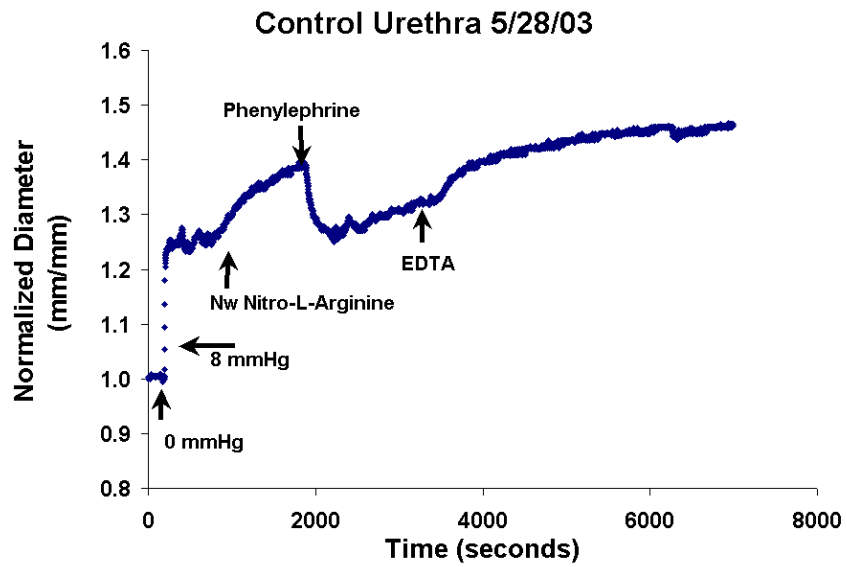
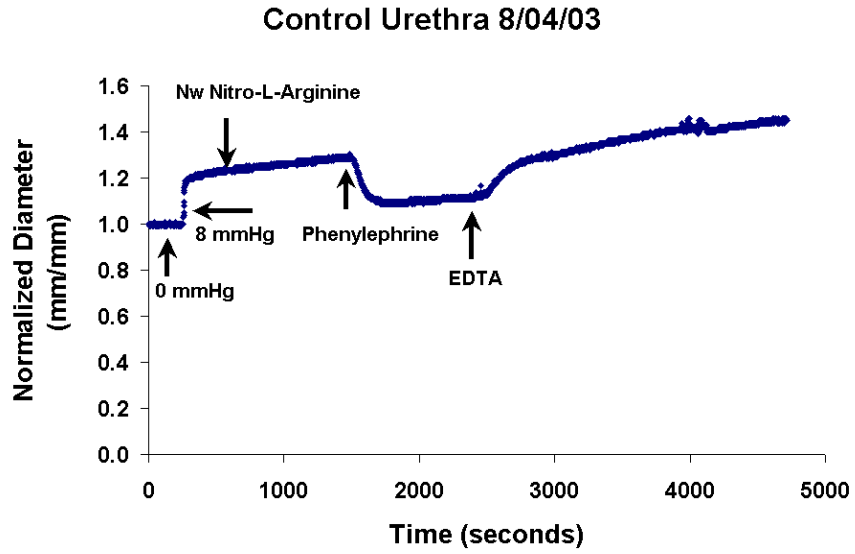


Figure A.23: Pharmacological data representing decrease and increase of the outer diameter of the middle portion of control urethras

A. 2 3-WEEK DM DATA

A.2.1 Baseline Data

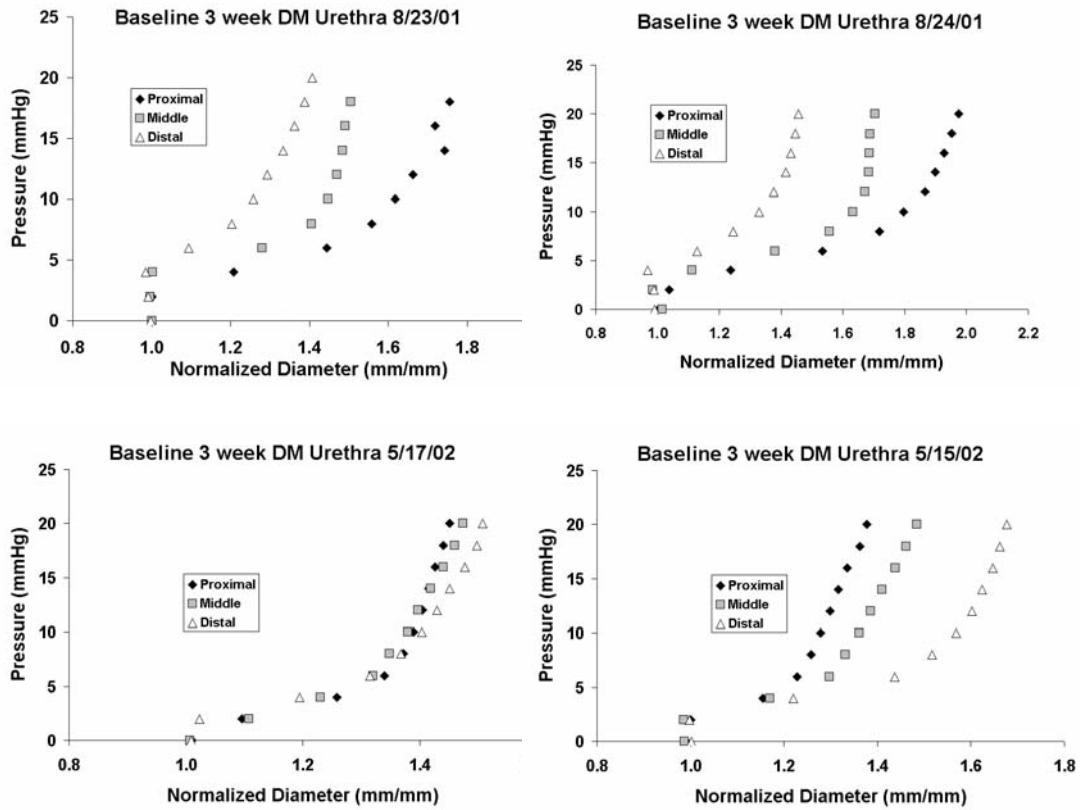


Figure A.24: Pressure-diameter data for proximal, middle, and distal portions of 3 week DM urethras in the baseline state

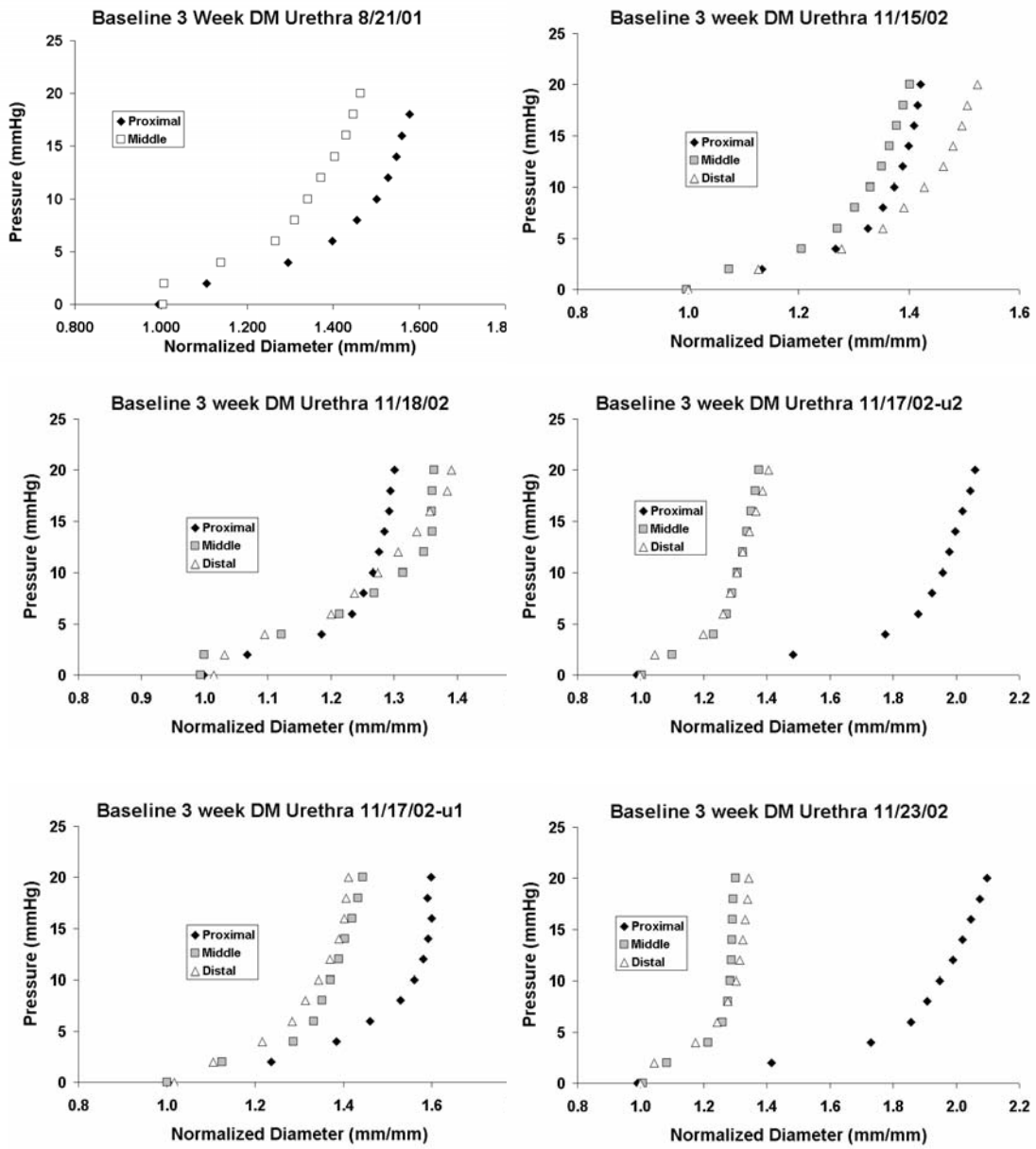


Figure A.25: Pressure-diameter data for proximal, middle, and distal portions of 3 week DM urethras in the baseline state

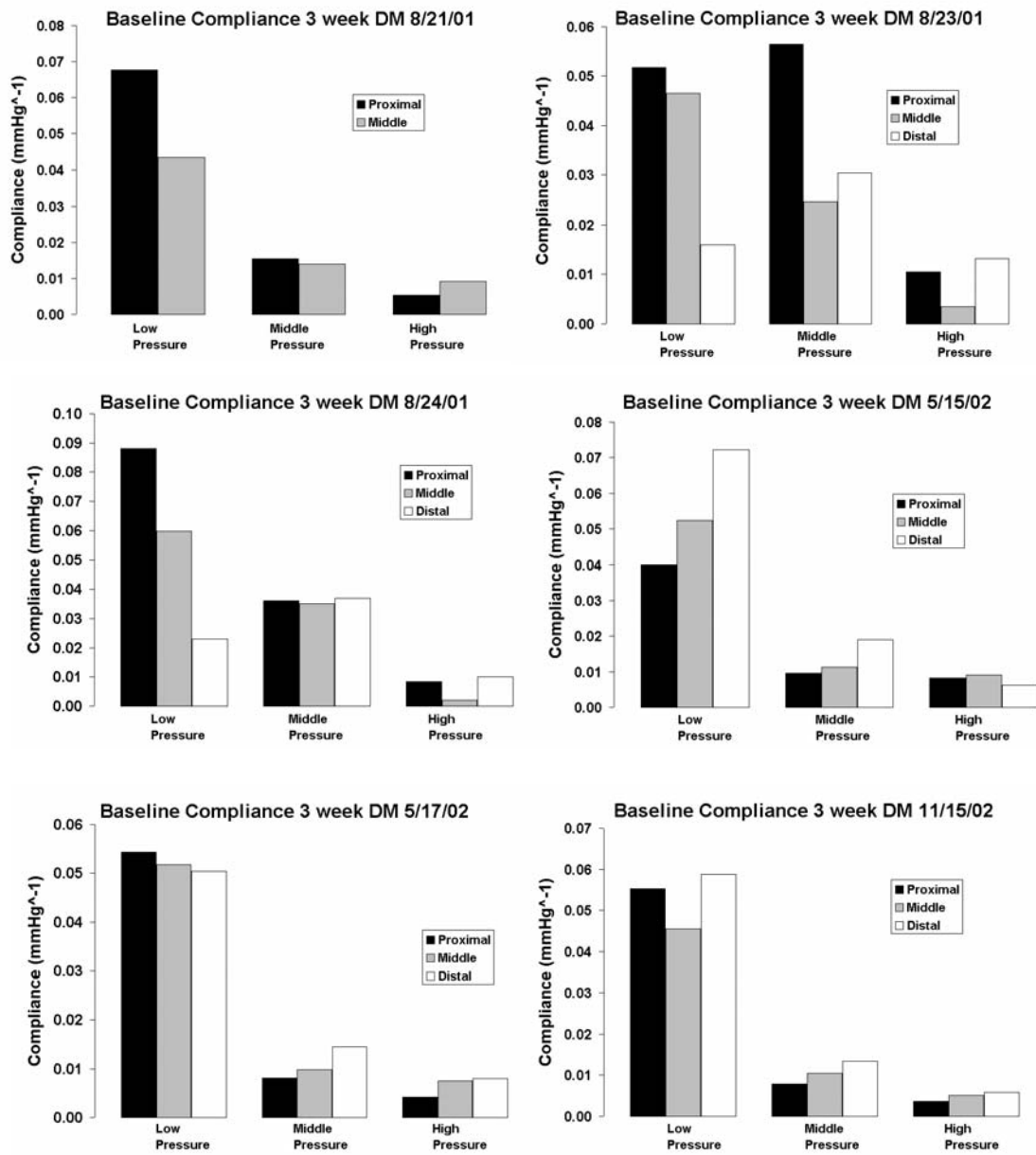


Figure A.26: Low, middle, and high pressure compliance data for proximal, middle, and distal portions of 3 week DM urethras in the baseline state

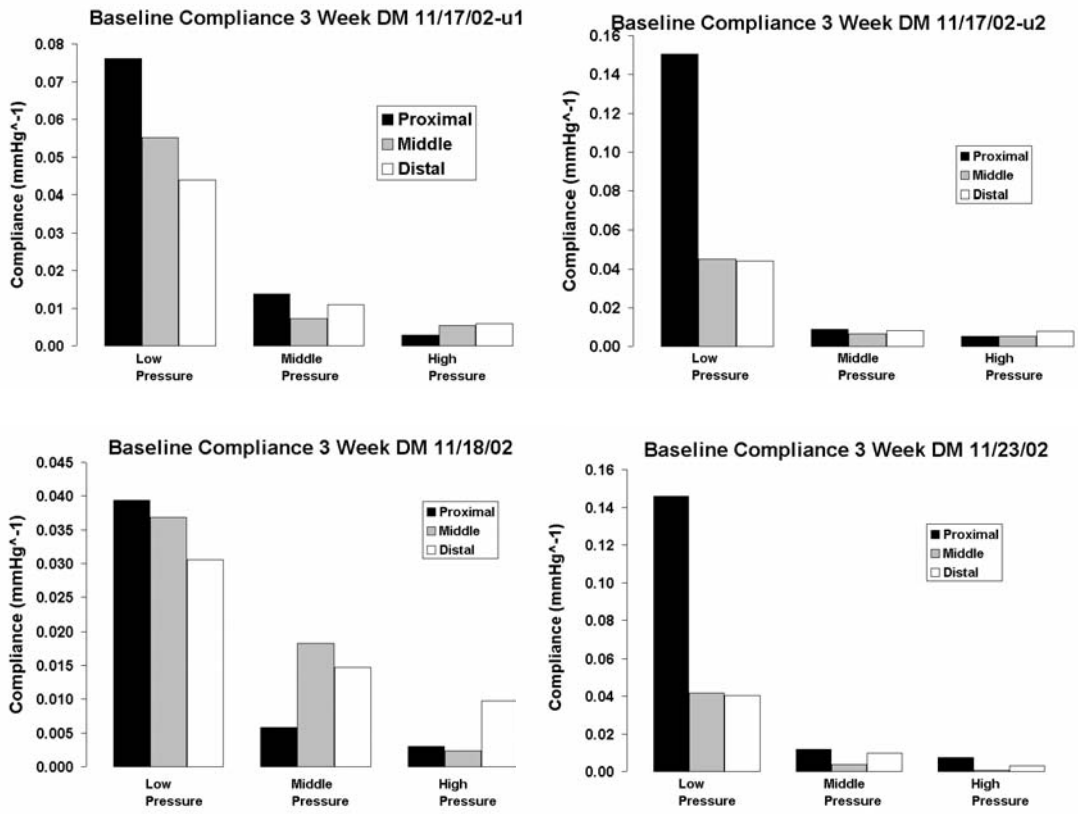


Figure A.27: Low, middle, and high pressure compliance data for proximal, middle, and distal portions of 3 week DM urethras in the baseline state

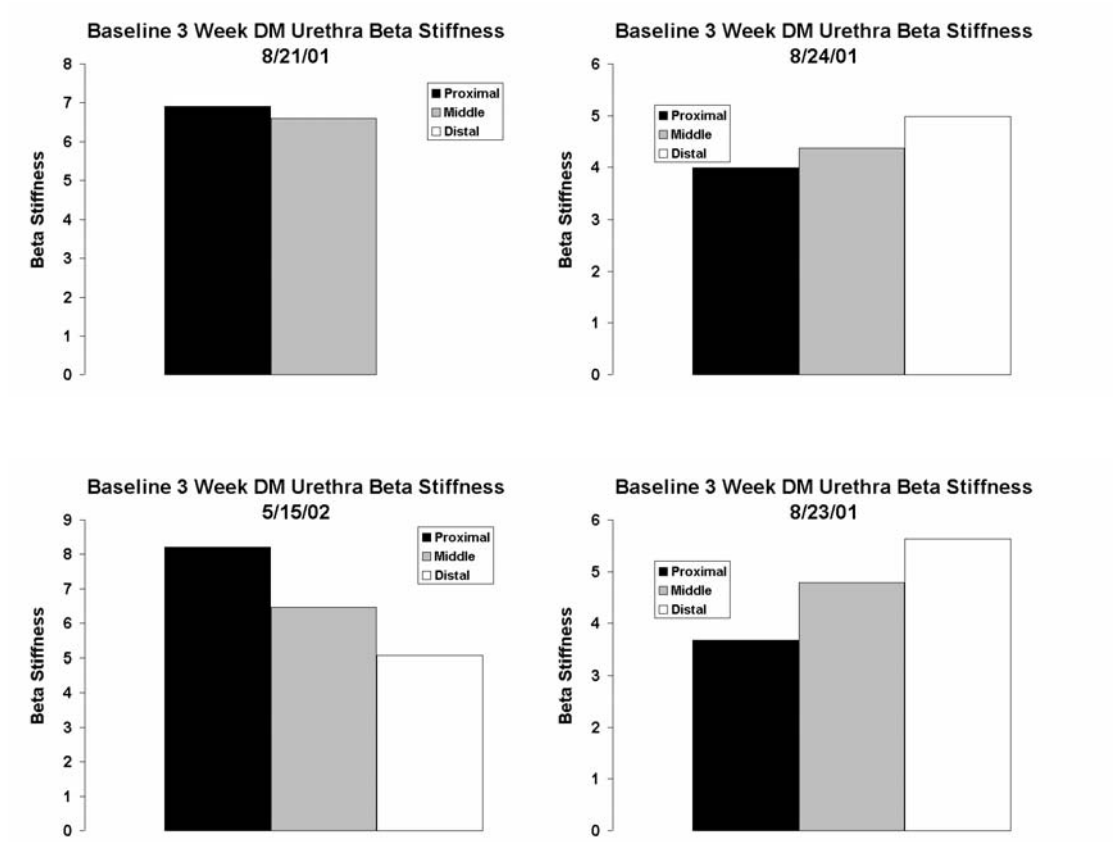


Figure A.28: Beta stiffness data for proximal, middle, and distal portions of 3 week DM urethras in the baseline state

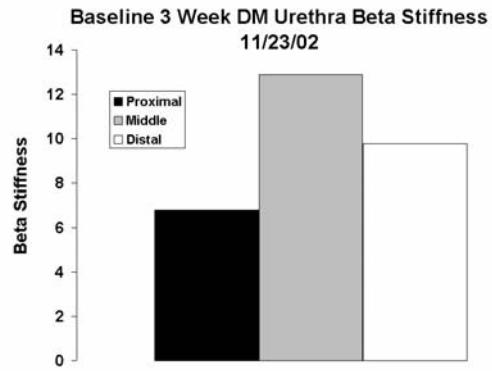
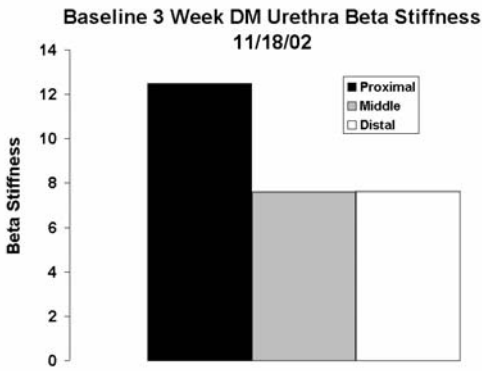
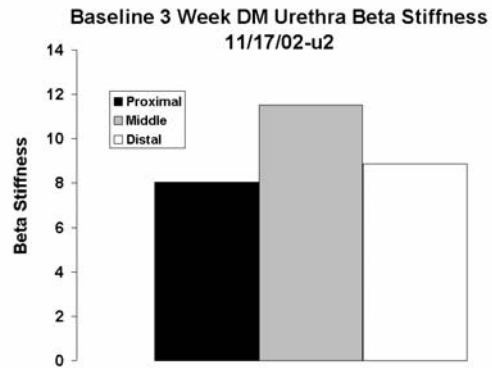
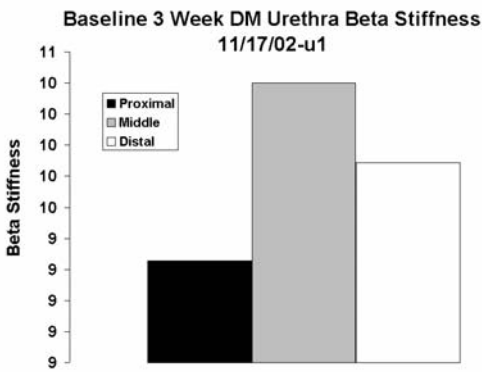
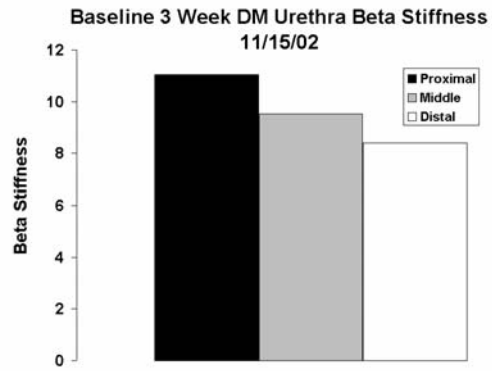
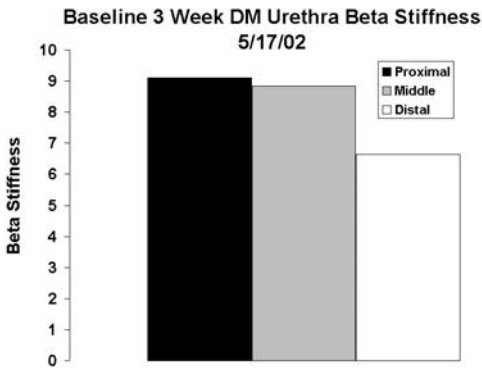


Figure A.29: Beta stiffness data for proximal, middle, and distal portions of 3 week DM urethras in the baseline state

A.2.2 3-week DM Passive Data

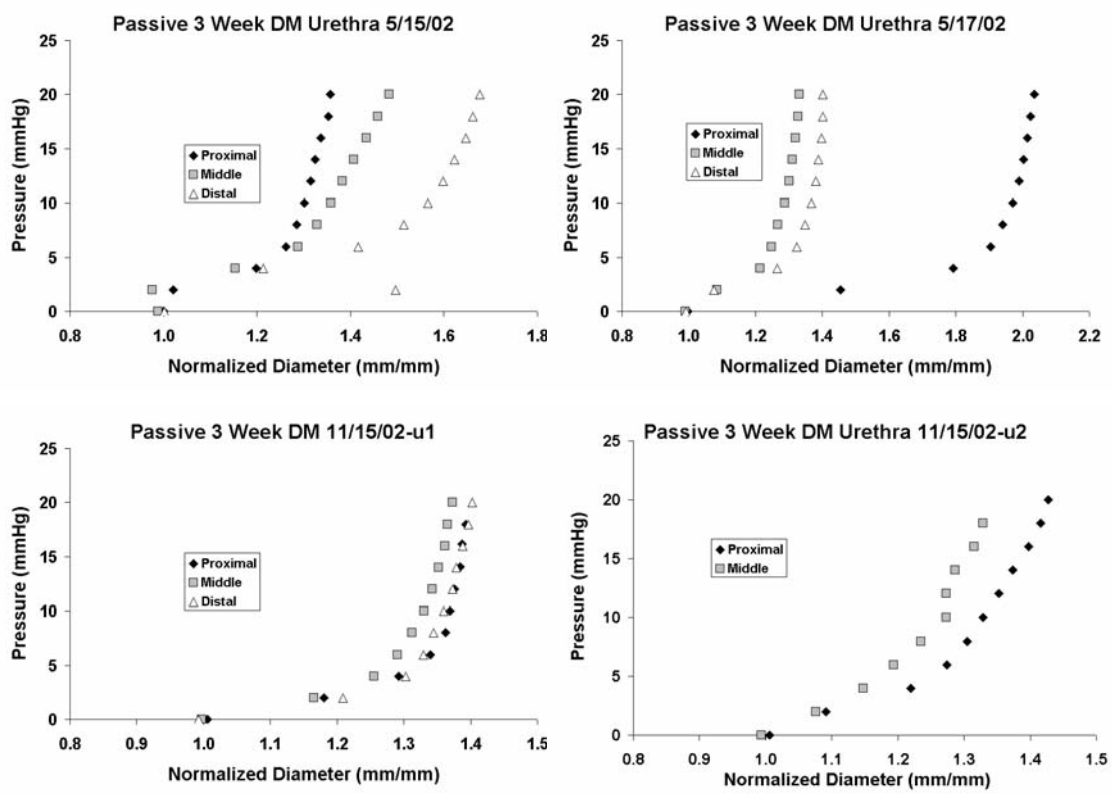


Figure A.30: Pressure-diameter data for proximal, middle, and distal portions of 3 week DM urethras in the passive state

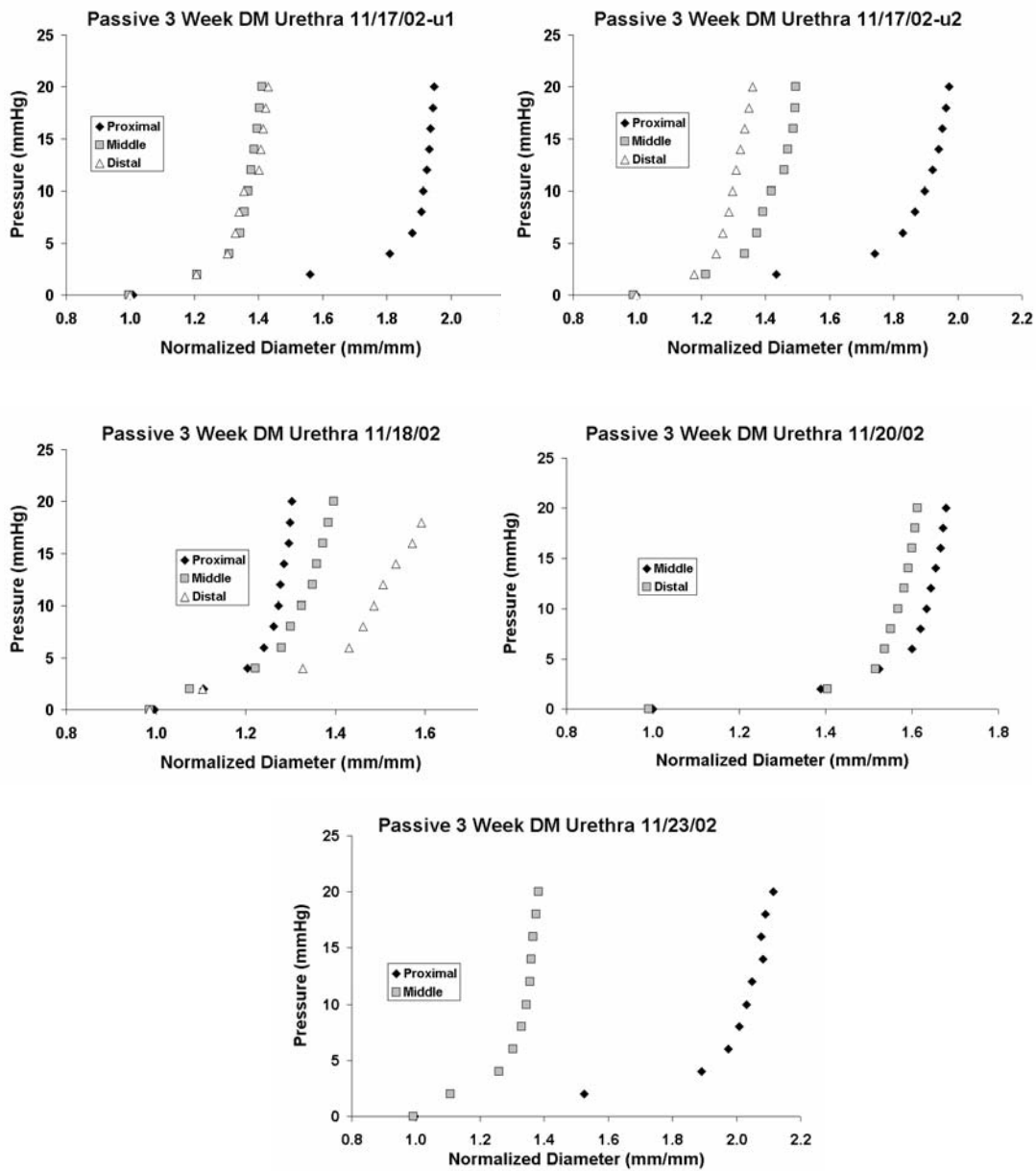


Figure A.31: Pressure-diameter data for proximal, middle, and distal portions of 3 week DM urethras in the passive state

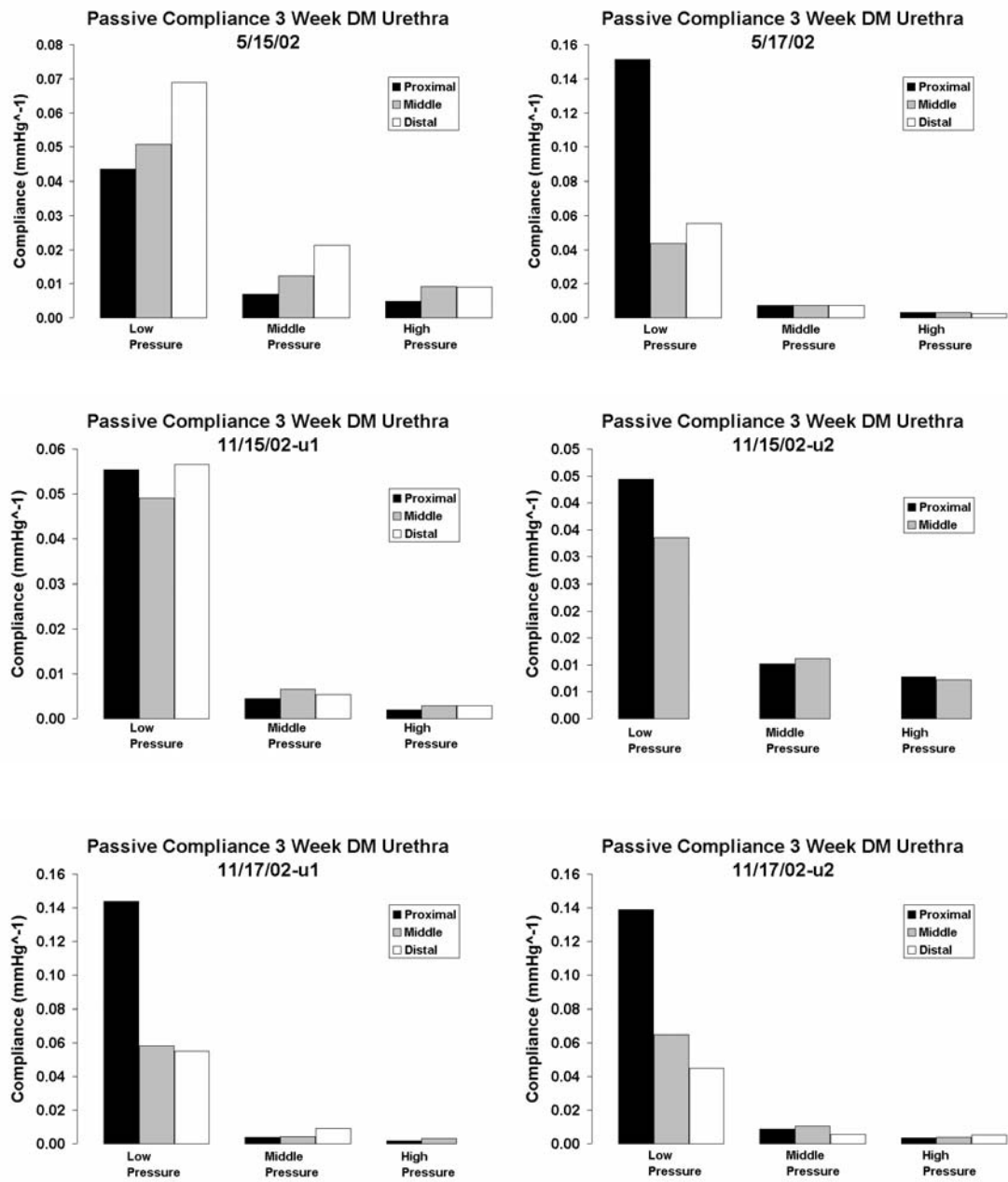


Figure A.32: Low, middle, and high pressure compliance data for proximal, middle, and distal portions of 3 week DM urethras in the passive state

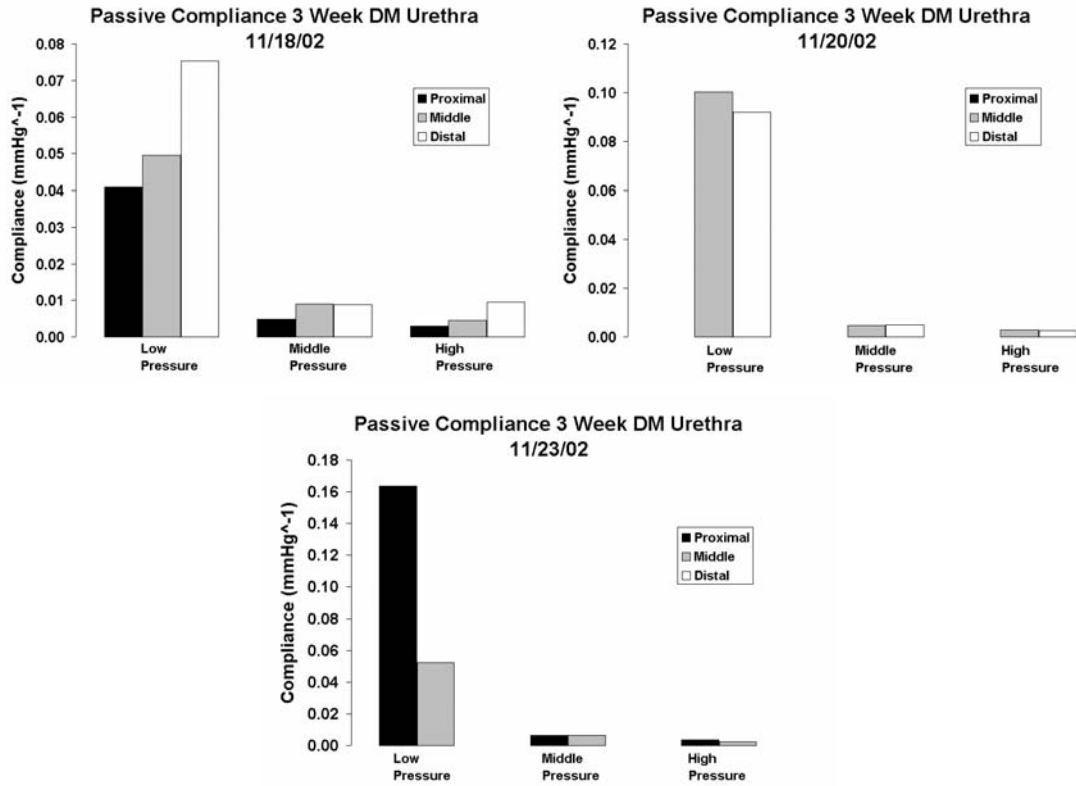


Figure A.33: Low, middle, and high pressure compliance data for proximal, middle, and distal portions of 3 week DM urethras in the passive state

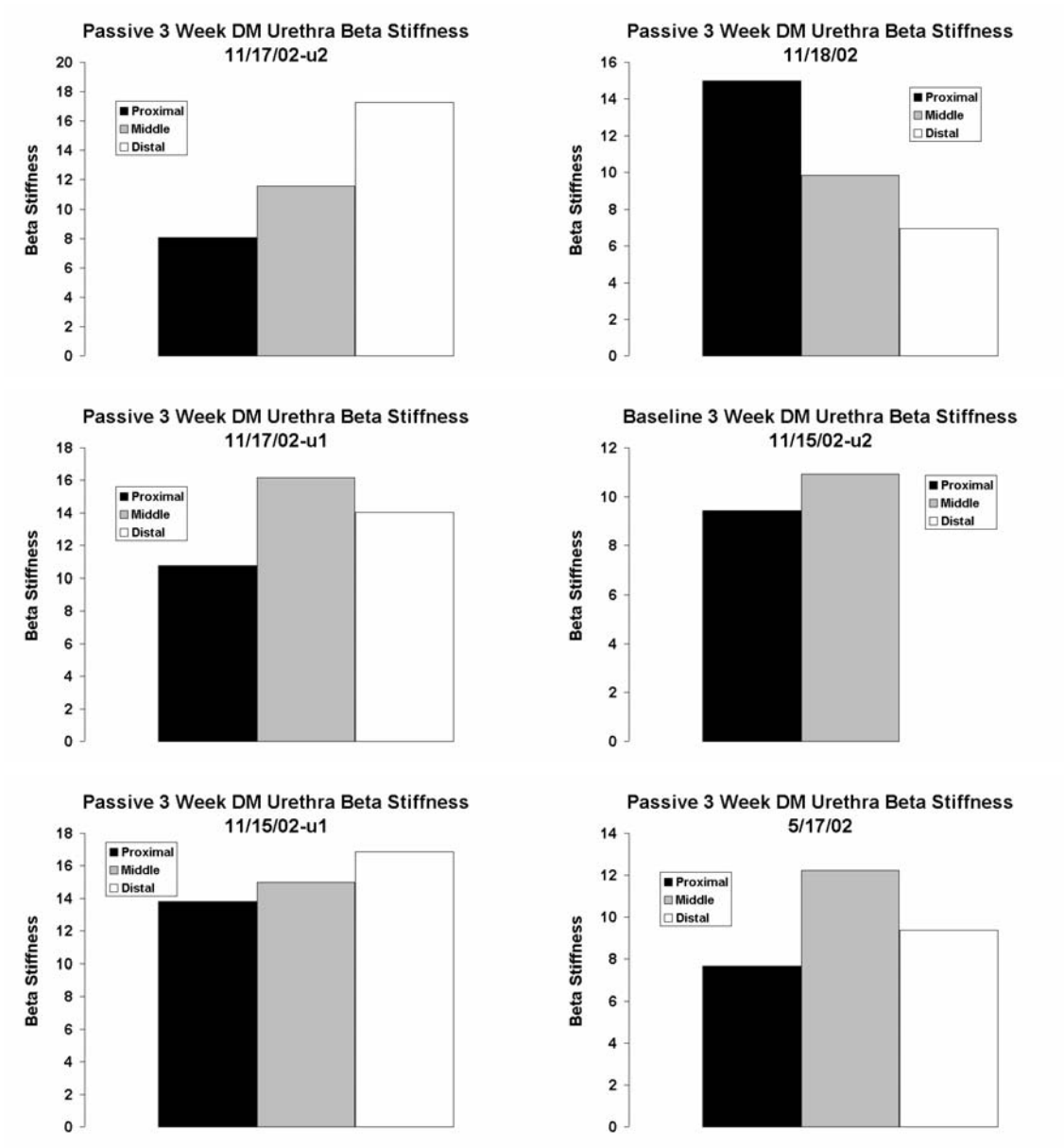


Figure A.34: Beta stiffness data for proximal, middle, and distal portions of 3 week DM urethras in the passive state

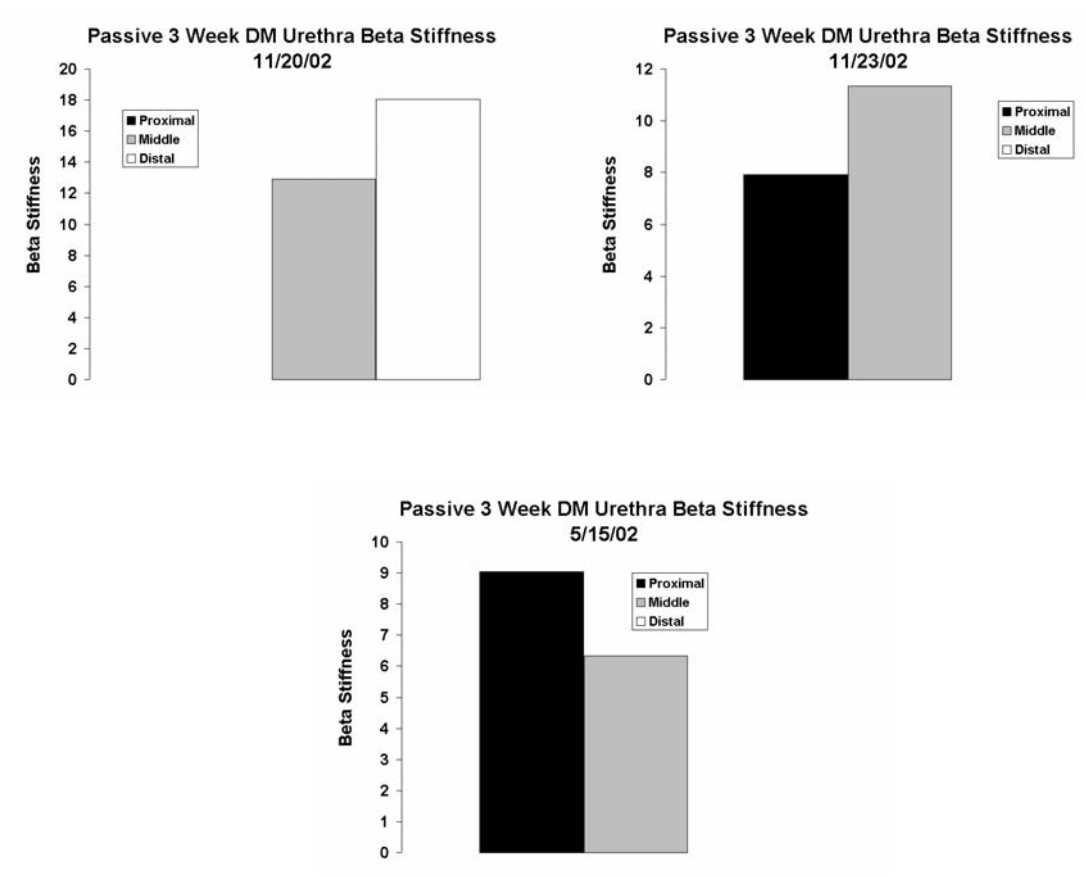


Figure A.35: Beta stiffness data for proximal, middle, and distal portions of 3 week DM urethras in the passive state

A.3 5-WEEK DM DATA

A.3.1 Baseline State

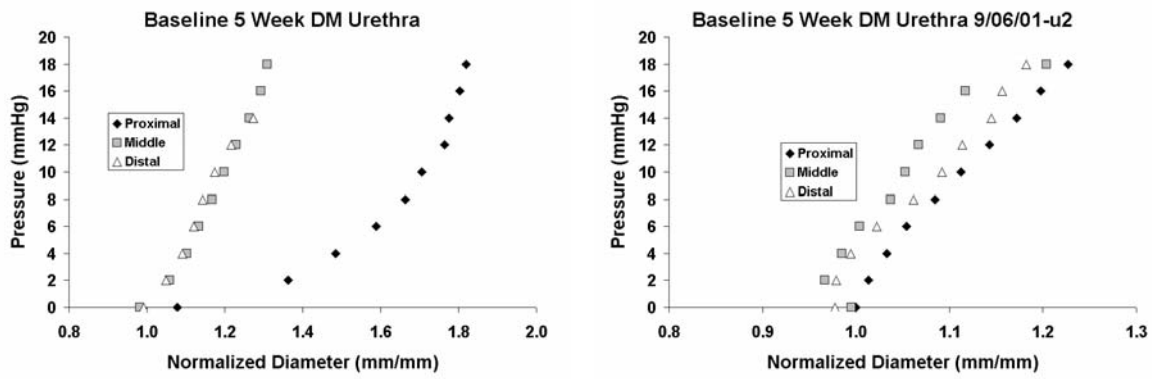


Figure A.36: Pressure-diameter data for proximal, middle, and distal portions of 5 week DM urethras in the baseline state

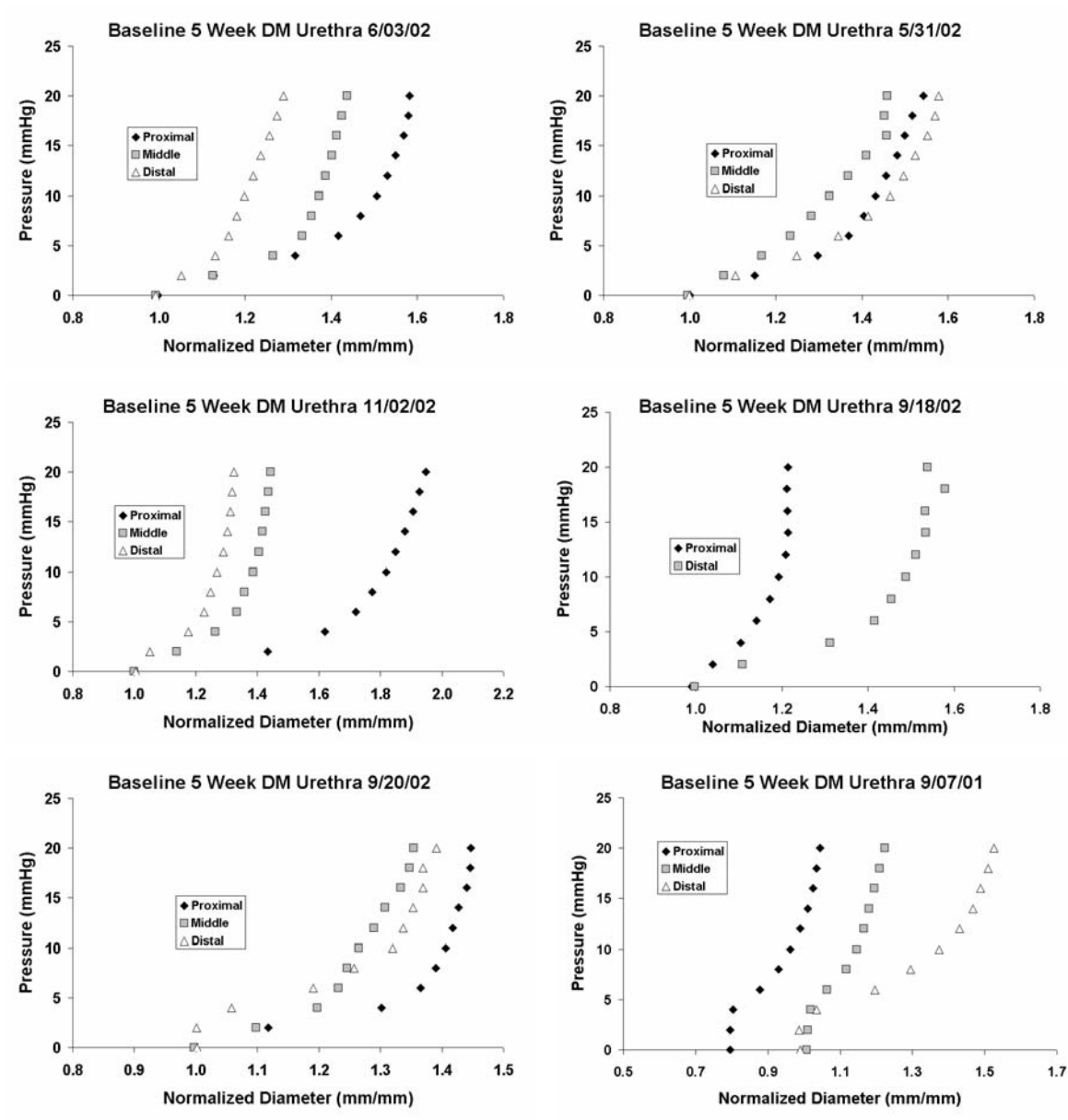


Figure A.37: Pressure-diameter data for proximal, middle, and distal portions of 5 week DM urethras in the baseline state

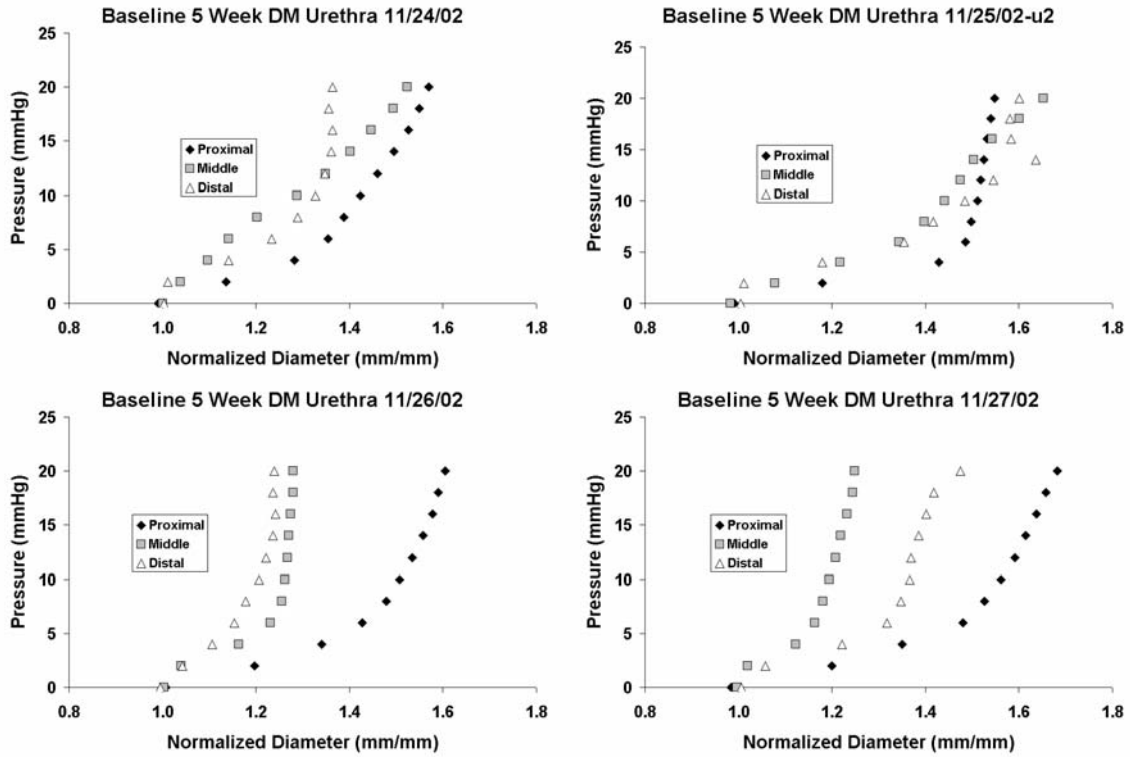


Figure A.38: Pressure-diameter data for proximal, middle, and distal portions of 5 week DM urethras in the baseline state

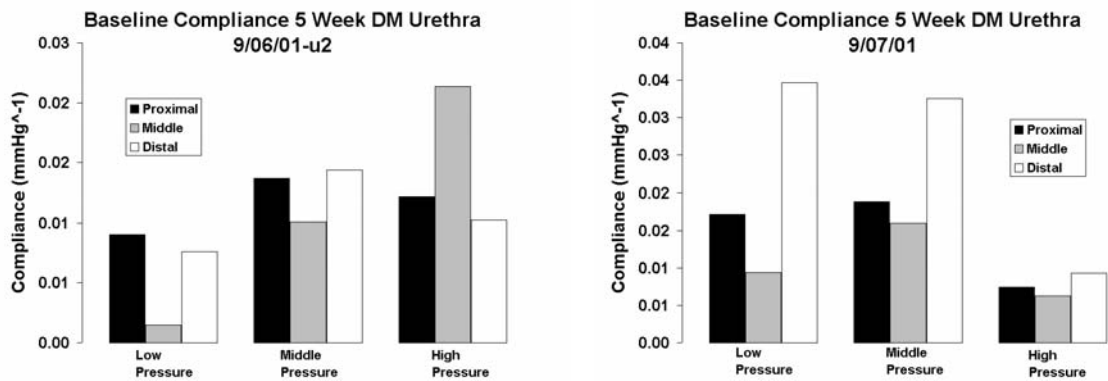


Figure A.39: Low, middle, and high pressure compliance data for proximal, middle, and distal portions of 5 week DM urethras in the baseline state

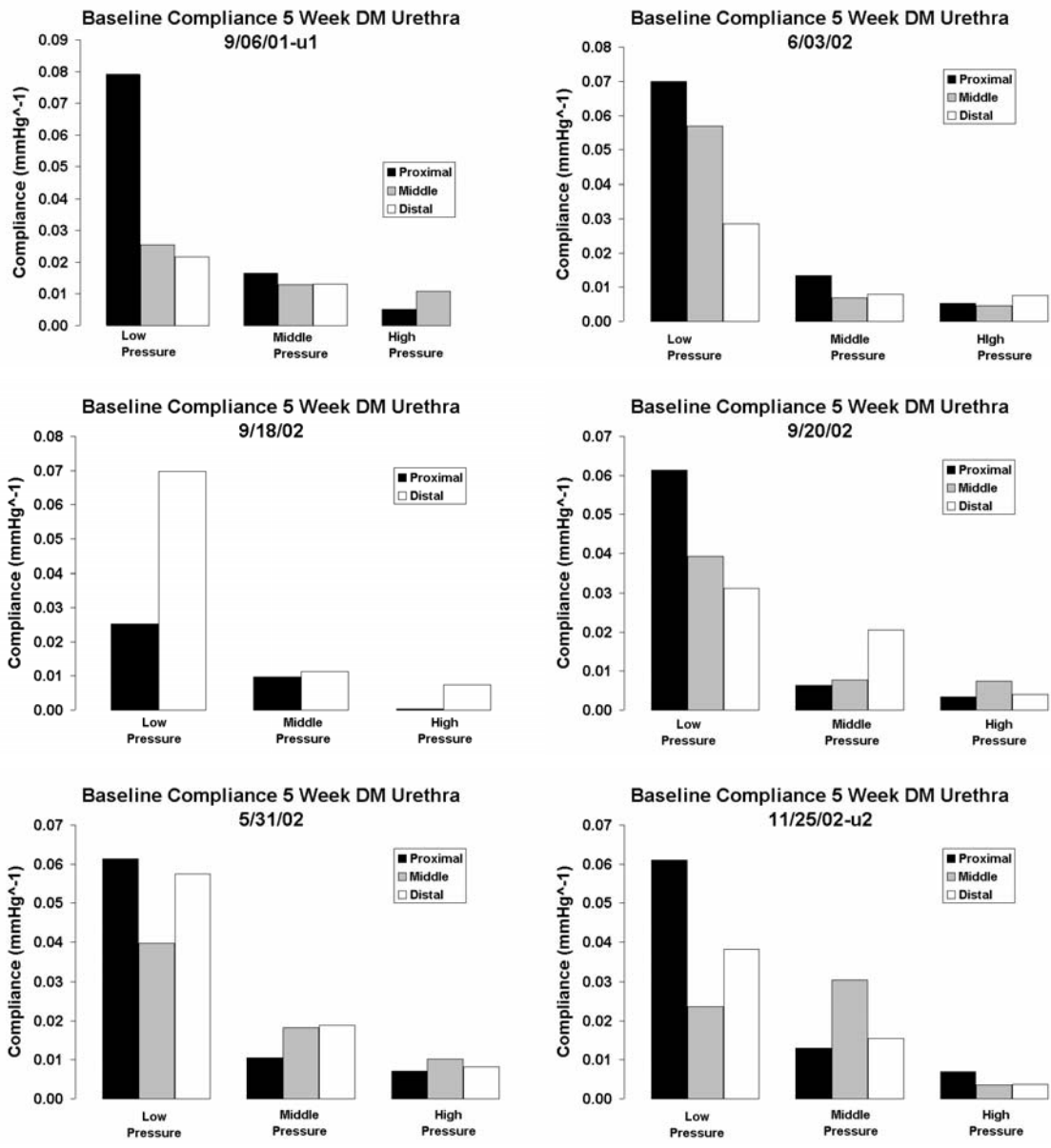


Figure A.40: Low, middle, and high pressure compliance data for proximal, middle, and distal portions of 5 week DM urethras in the baseline state

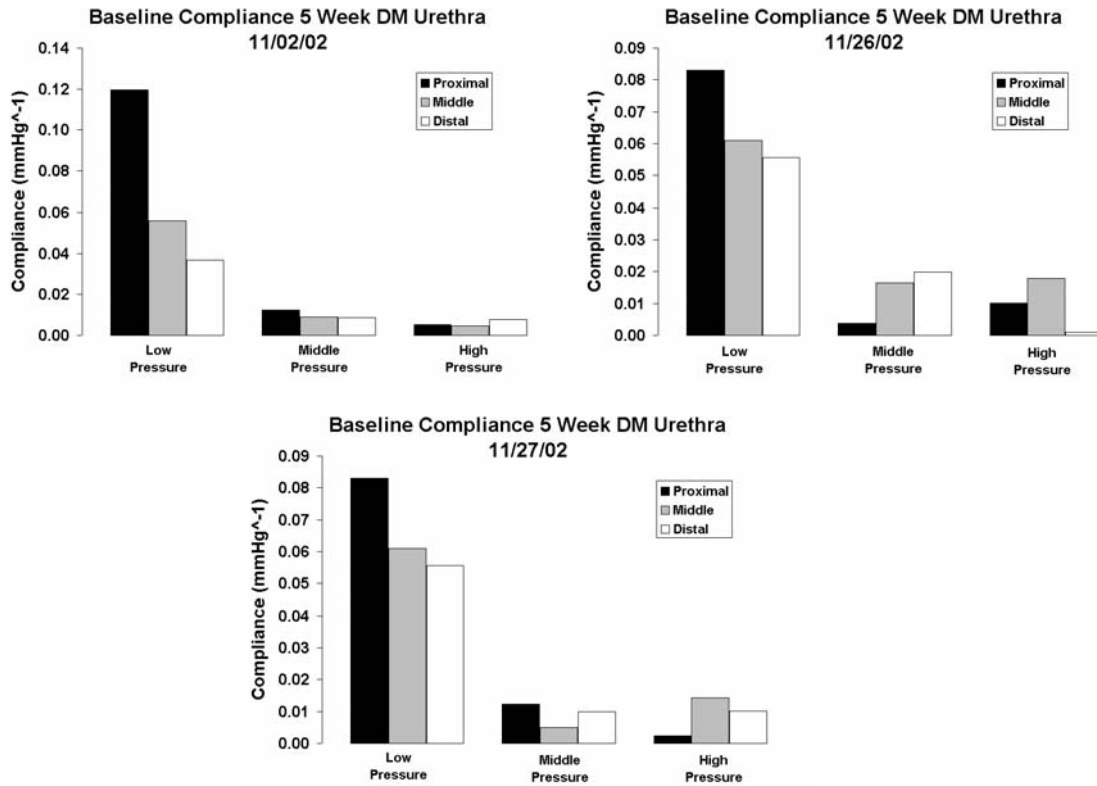


Figure A.41: Low, middle, and high pressure compliance data for proximal, middle, and distal portions of 5 week DM urethras in the baseline state

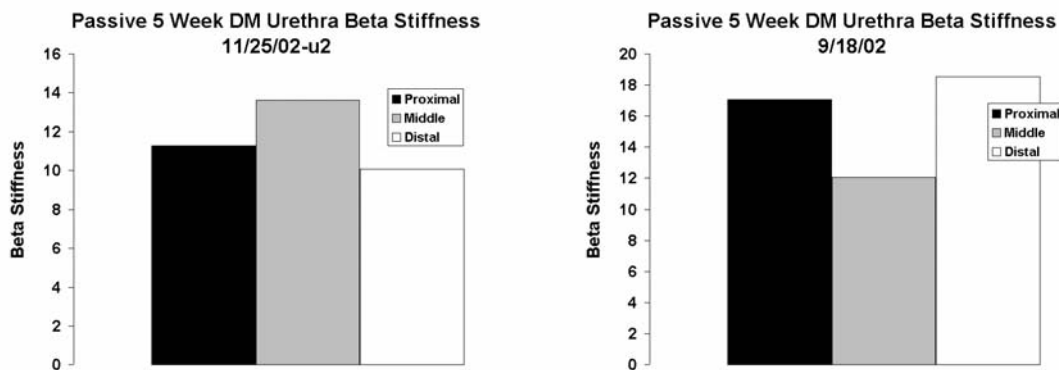


Figure A.42: Beta stiffness data for proximal, middle, and distal portions of 5 week DM urethras in the baseline state

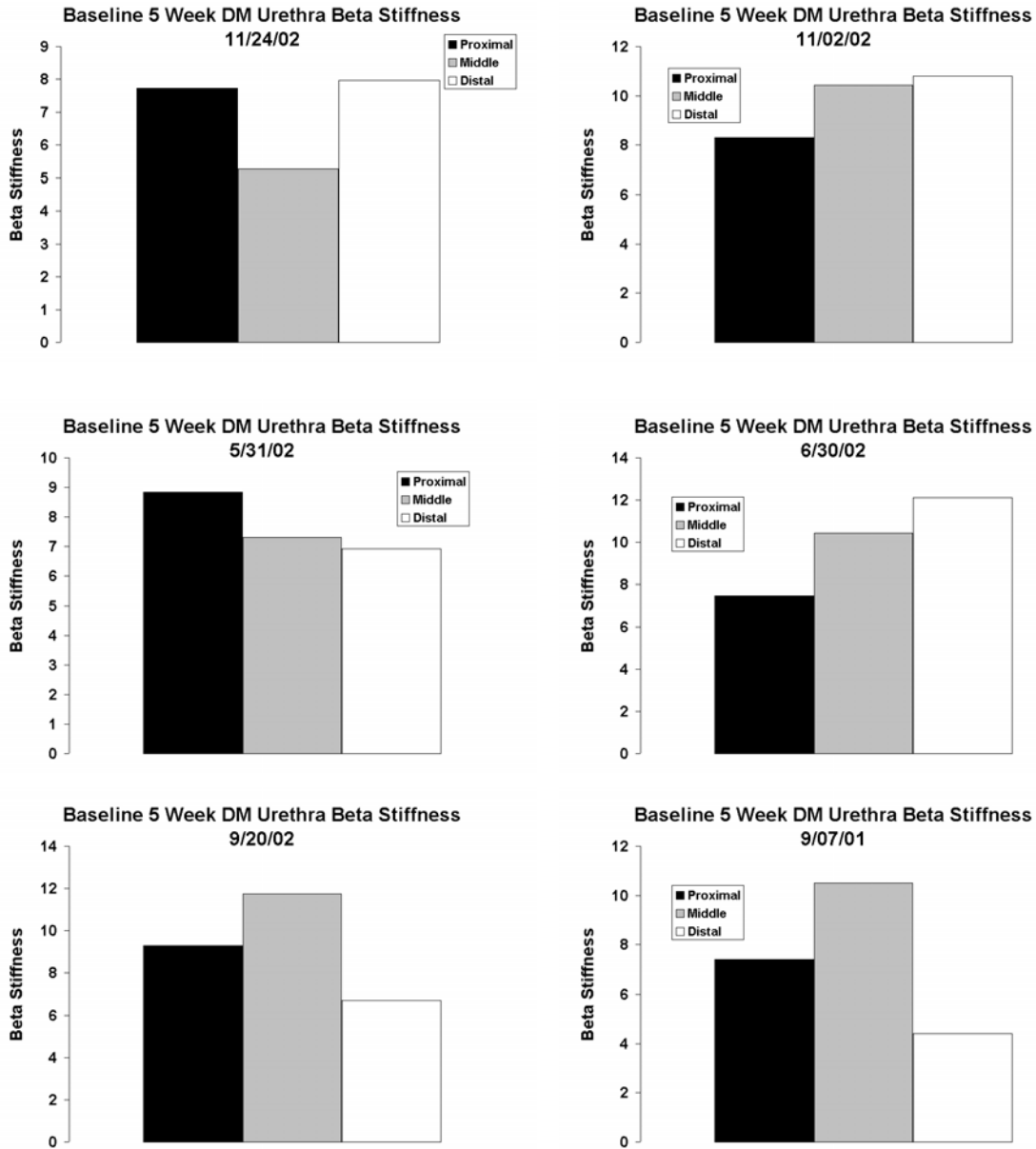


Figure A.43: Beta stiffness data for proximal, middle, and distal portions of 5 week DM urethras in the baseline state

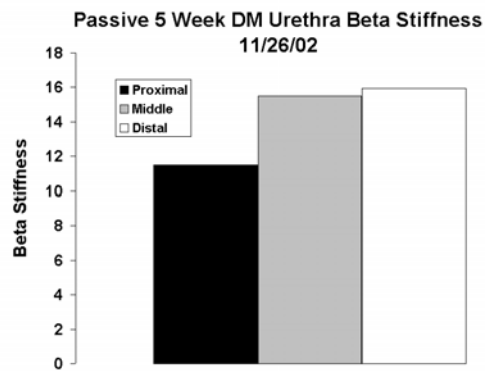
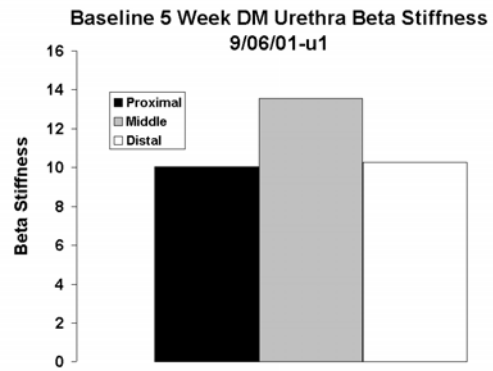
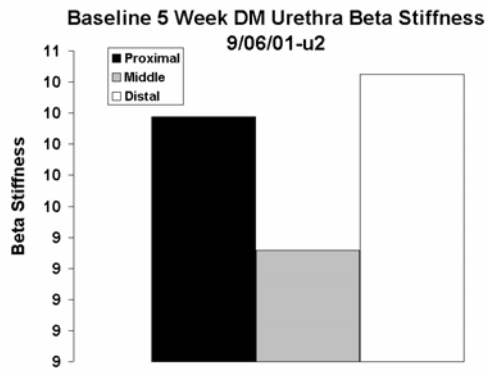


Figure A.44: Beta stiffness data for proximal, middle, and distal portions of 5 week DM urethras in the baseline state

A.3.2 Passive State

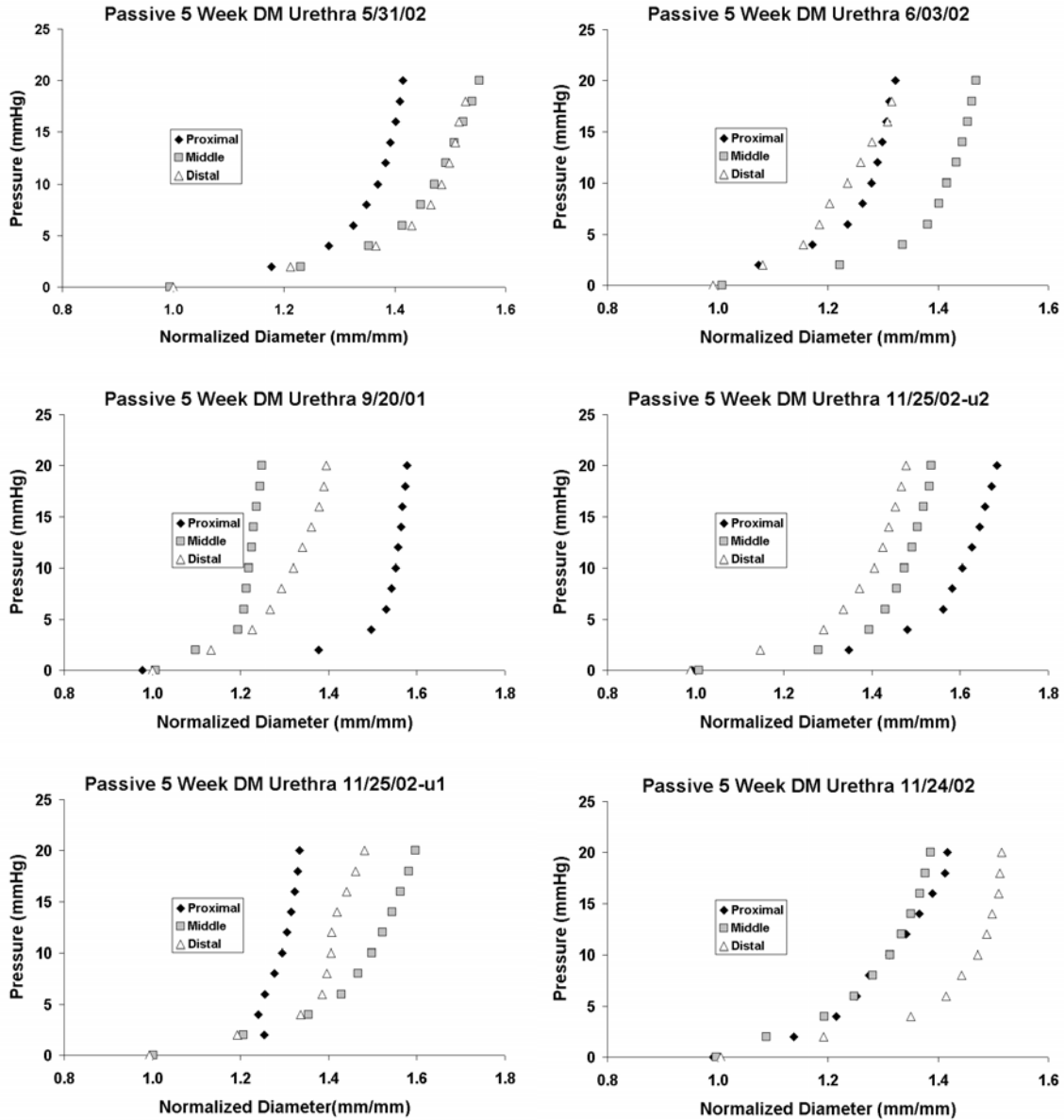


Figure A.45: Pressure-diameter data for proximal, middle, and distal portions of 5 week DM urethras in the passive state

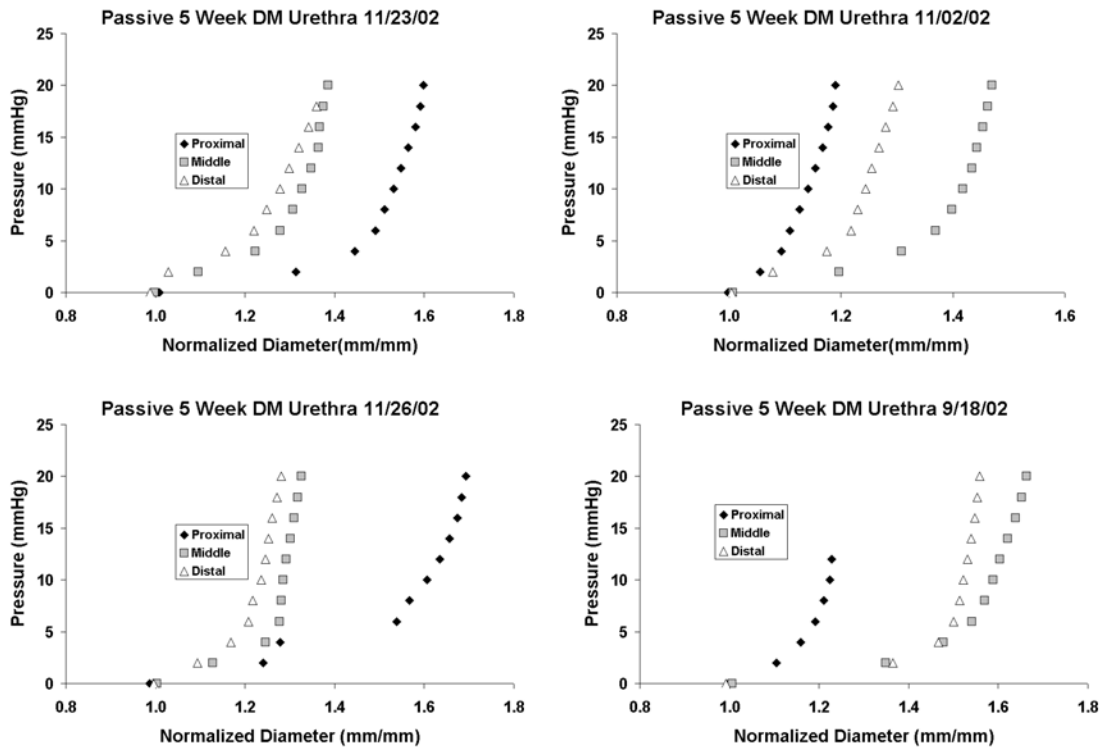


Figure A.46: Pressure-diameter data for proximal, middle, and distal portions of 5 week DM urethras in the passive state

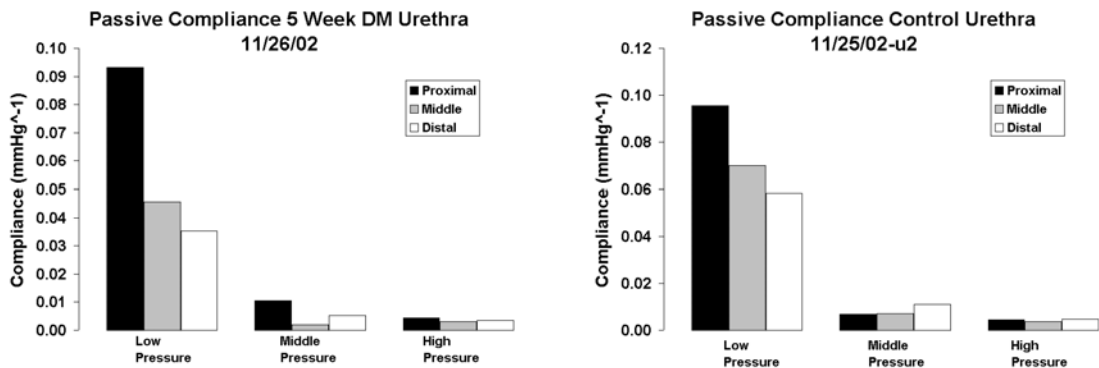


Figure A.47: Low, middle, and high pressure compliance data for proximal, middle, and distal portions of 5 week DM urethras in the passive state

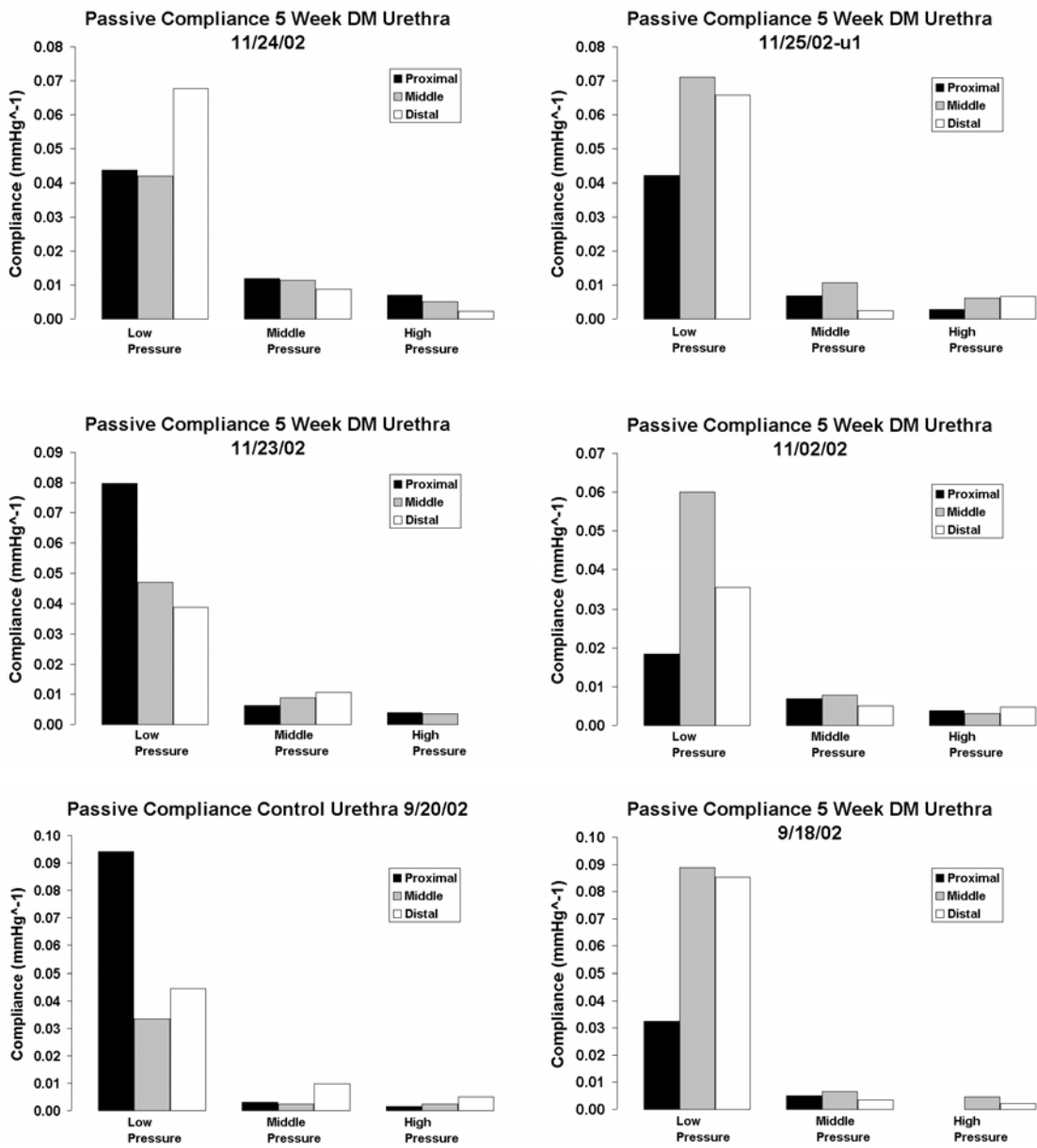


Figure A.48: Low, middle, and high pressure compliance data for proximal, middle, and distal portions of 5 week DM urethras in the passive state

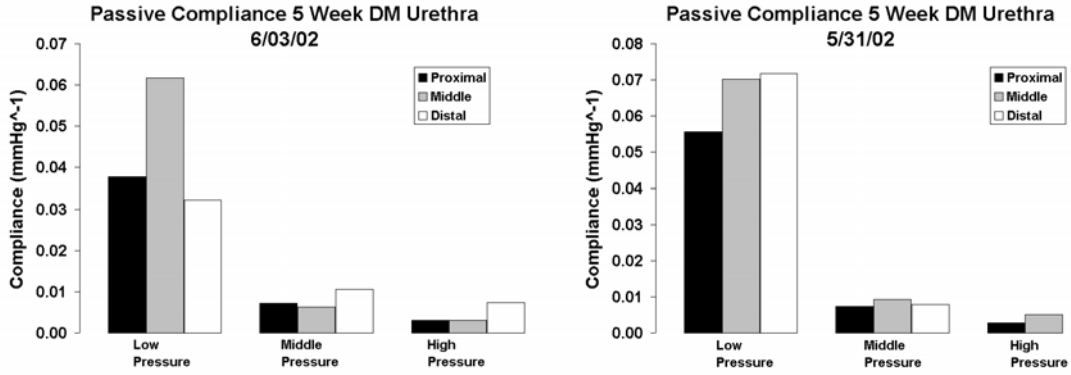


Figure A.49: Low, middle, and high pressure compliance data for proximal, middle, and distal portions of 5 week DM urethras in the passive state

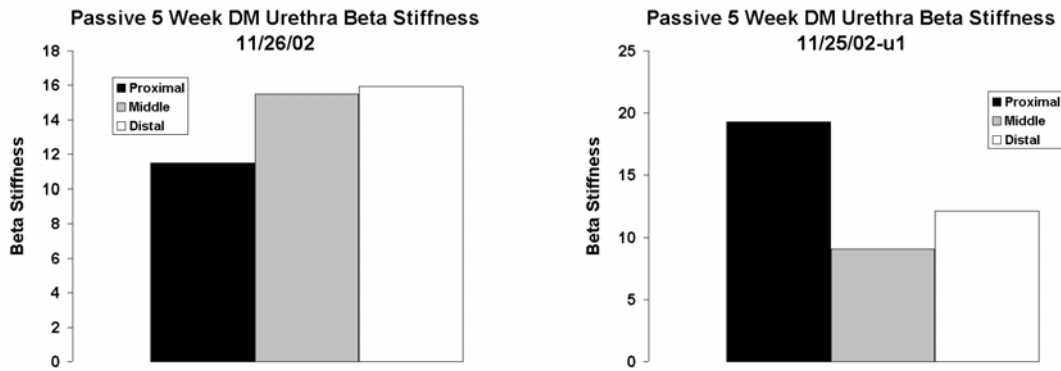


Figure A.50: Beta stiffness data for proximal, middle, and distal portions of 5 week DM urethras in the passive state

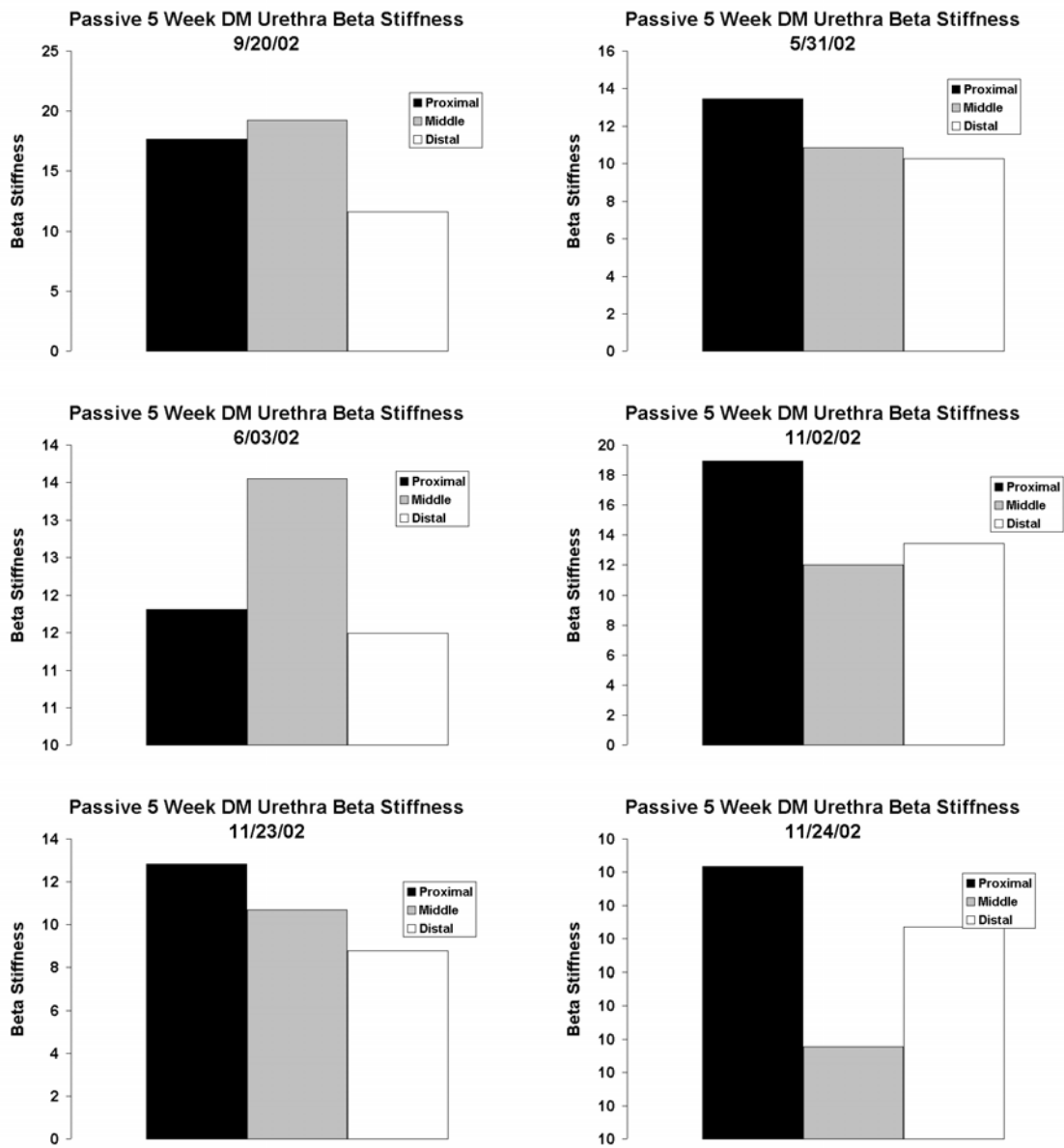


Figure A.51: Beta stiffness data for proximal, middle, and distal portions of 5 week DM urethras in the passive state

A.3.3 Pharmacological Data for 5-week DM Urethras

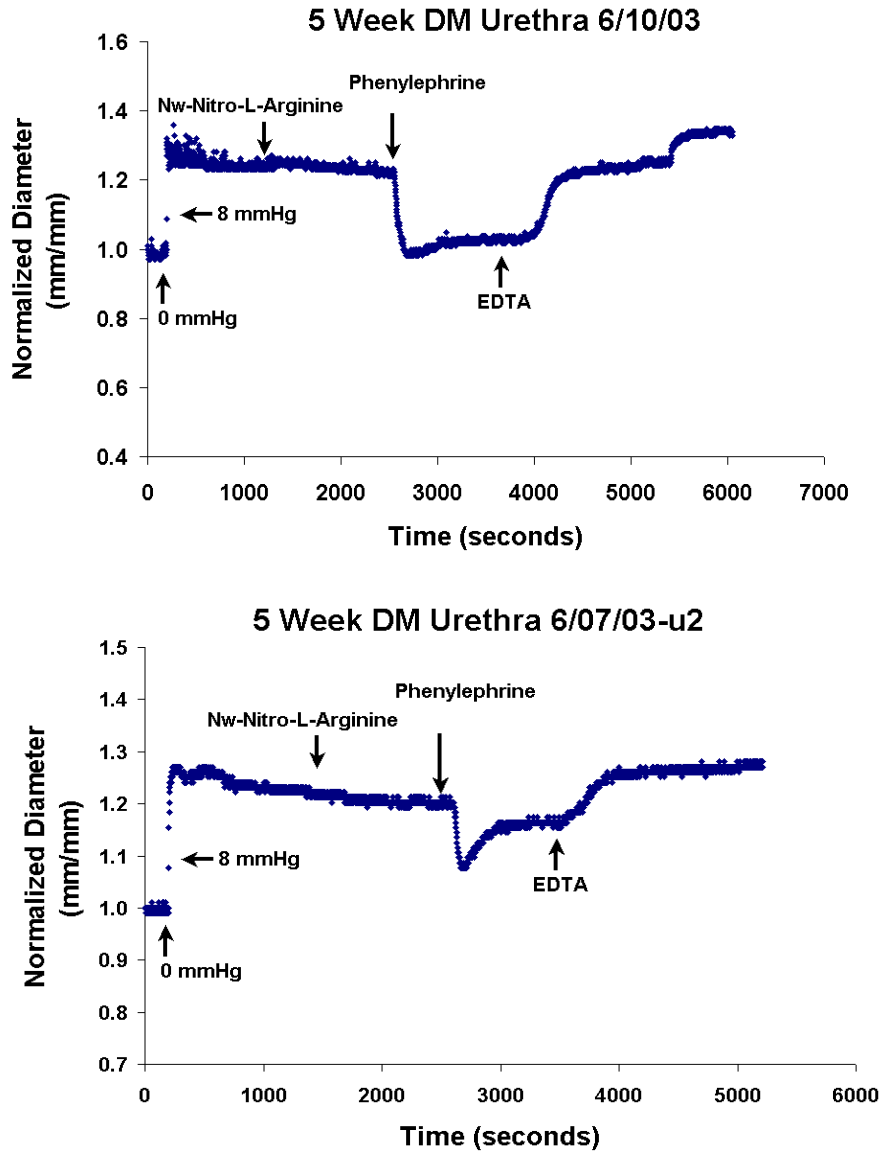


Figure A.52: Pharmacological data representing decrease and increase of the outer diameter of the middle portion of control urethras. Blood glucose levels were (top) 484 mg/dl and (bottom) 462 mg/dl

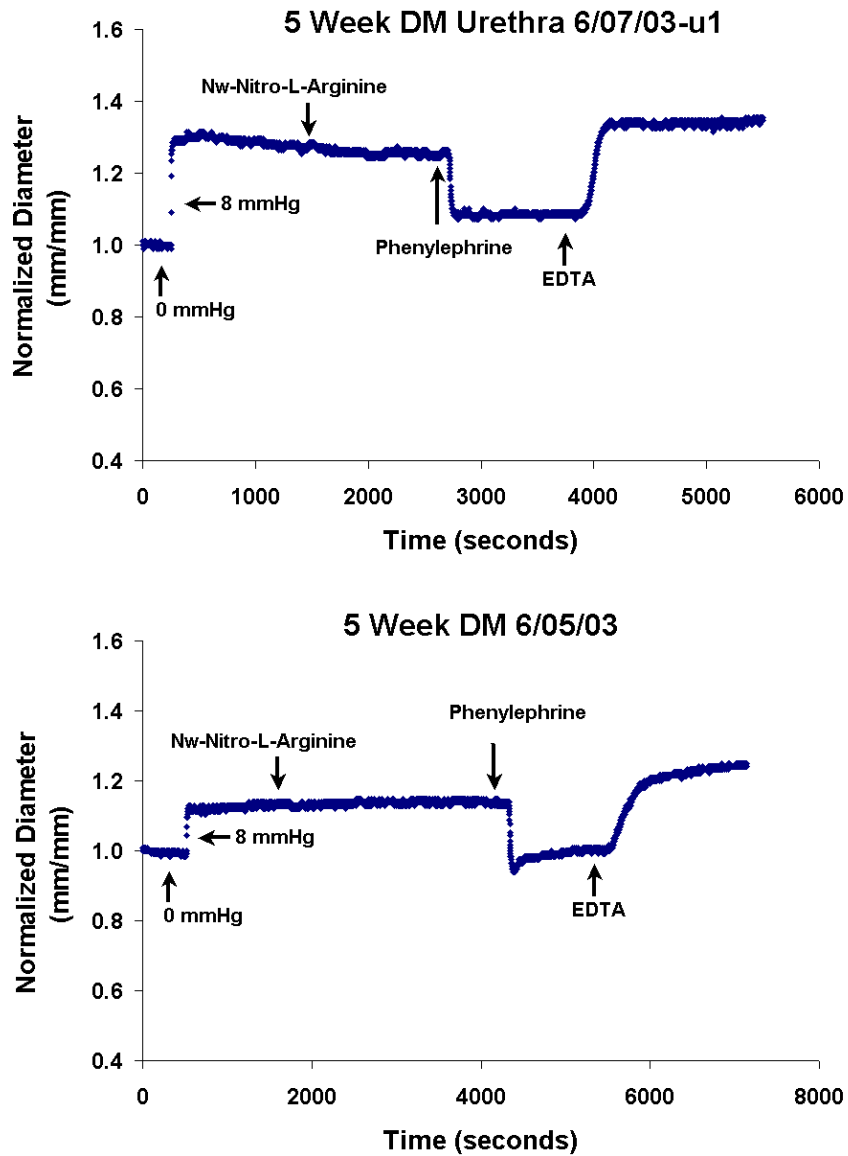


Figure A.53: Pharmacological data representing decrease and increase of the outer diameter of the middle portion of control urethras. Blood glucose levels were (top) 312 mg/dl and (bottom) 300 mg/dl

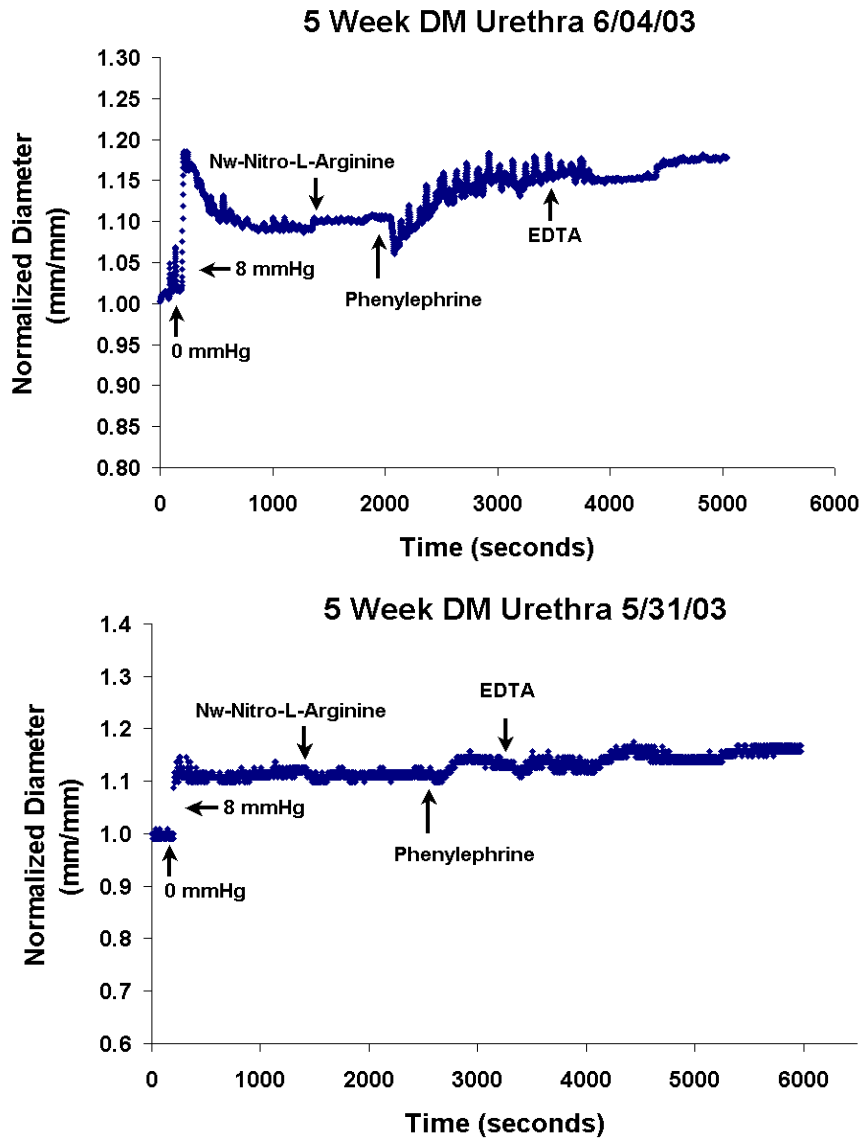


Figure A.54: Pharmacological data representing decrease and increase of the outer diameter of the middle portion of control urethras. Blood glucose levels were (top) 392 mg/dl and (bottom) 396 mg/dl

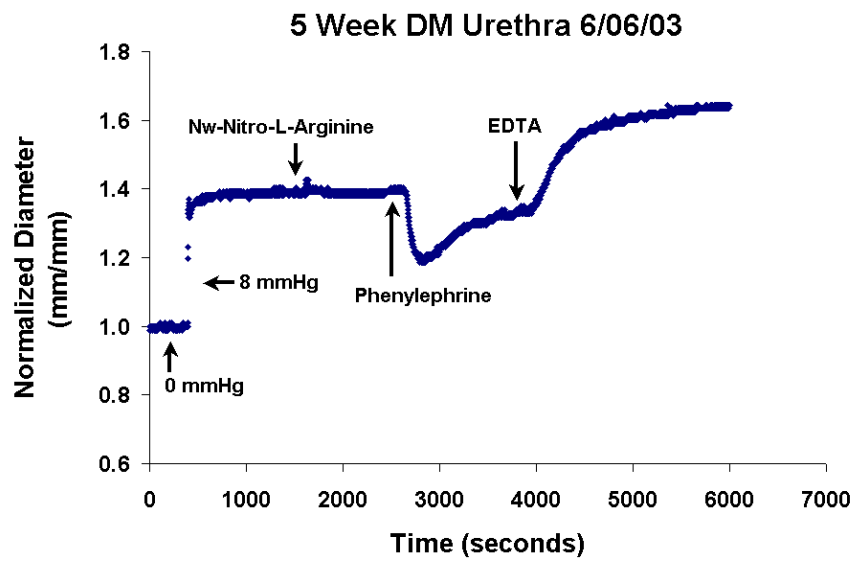


Figure A.55: Pharmacological data representing decrease and increase of the outer diameter of the middle portion of control urethras. Blood glucose level: 458 mg/dl

A.4 10-WEEK DM DATA

A.4.1 Baseline Data

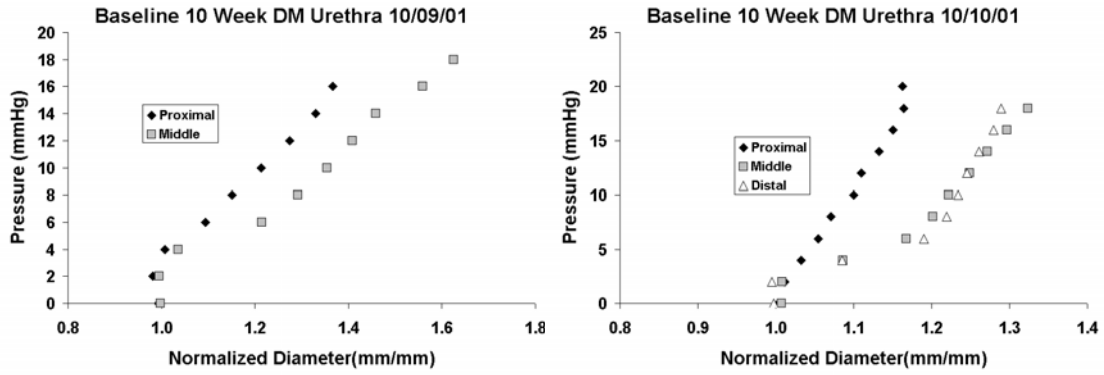


Figure A.56: Pressure-diameter data for proximal, middle, and distal portions of 10 week DM urethras in the baseline state

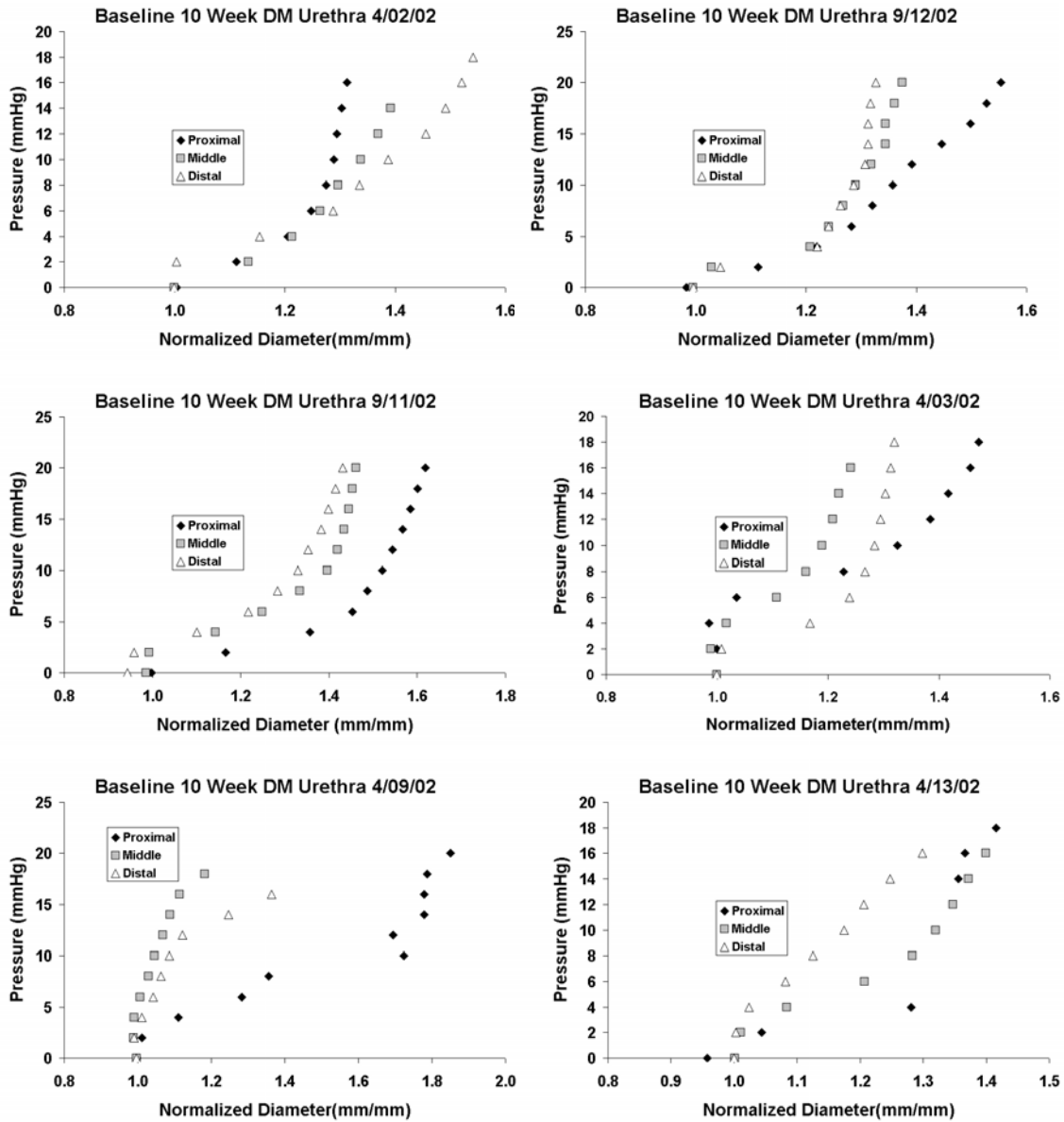


Figure A.57: Pressure-diameter data for proximal, middle, and distal portions of 10-week DM urethras in the baseline state

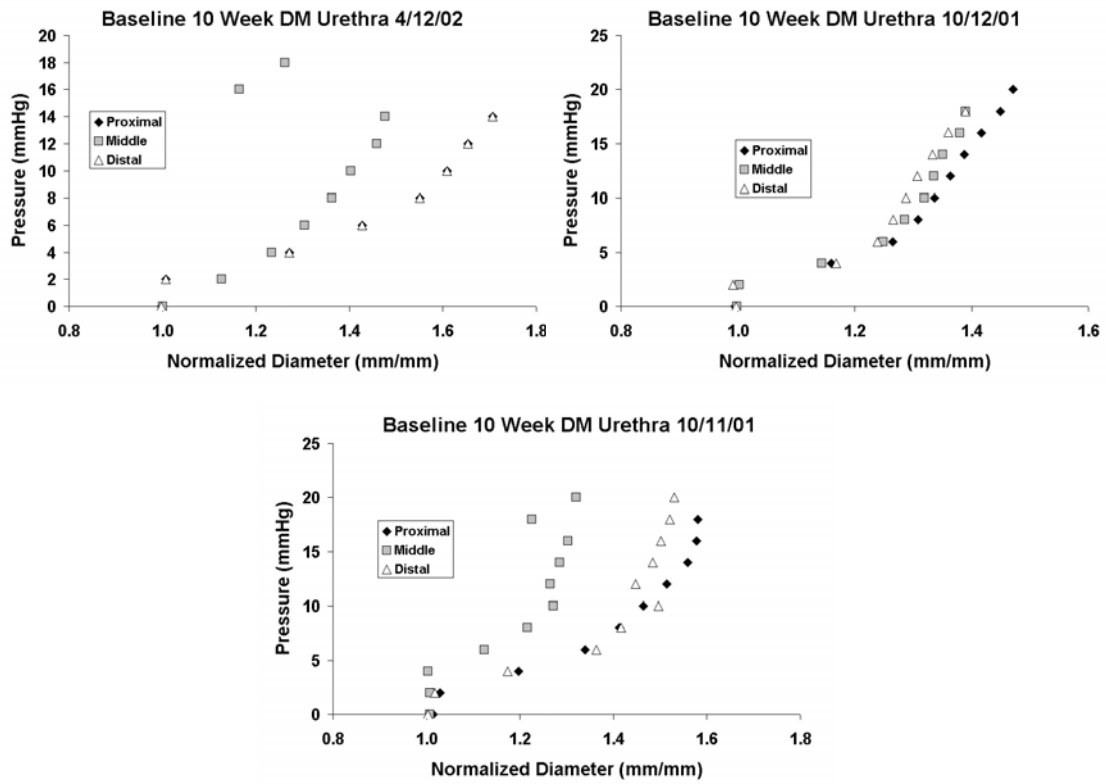


Figure A.58: Pressure-diameter data for proximal, middle, and distal portions of 10-week DM urethras in the baseline state

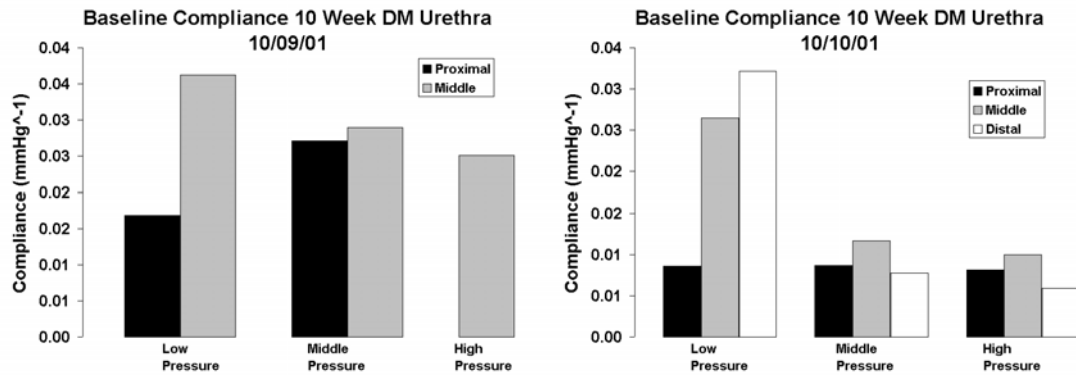


Figure A.59: Low, middle, and high pressure compliance data for proximal, middle, and distal portions of 10-week DM urethras in the baseline state

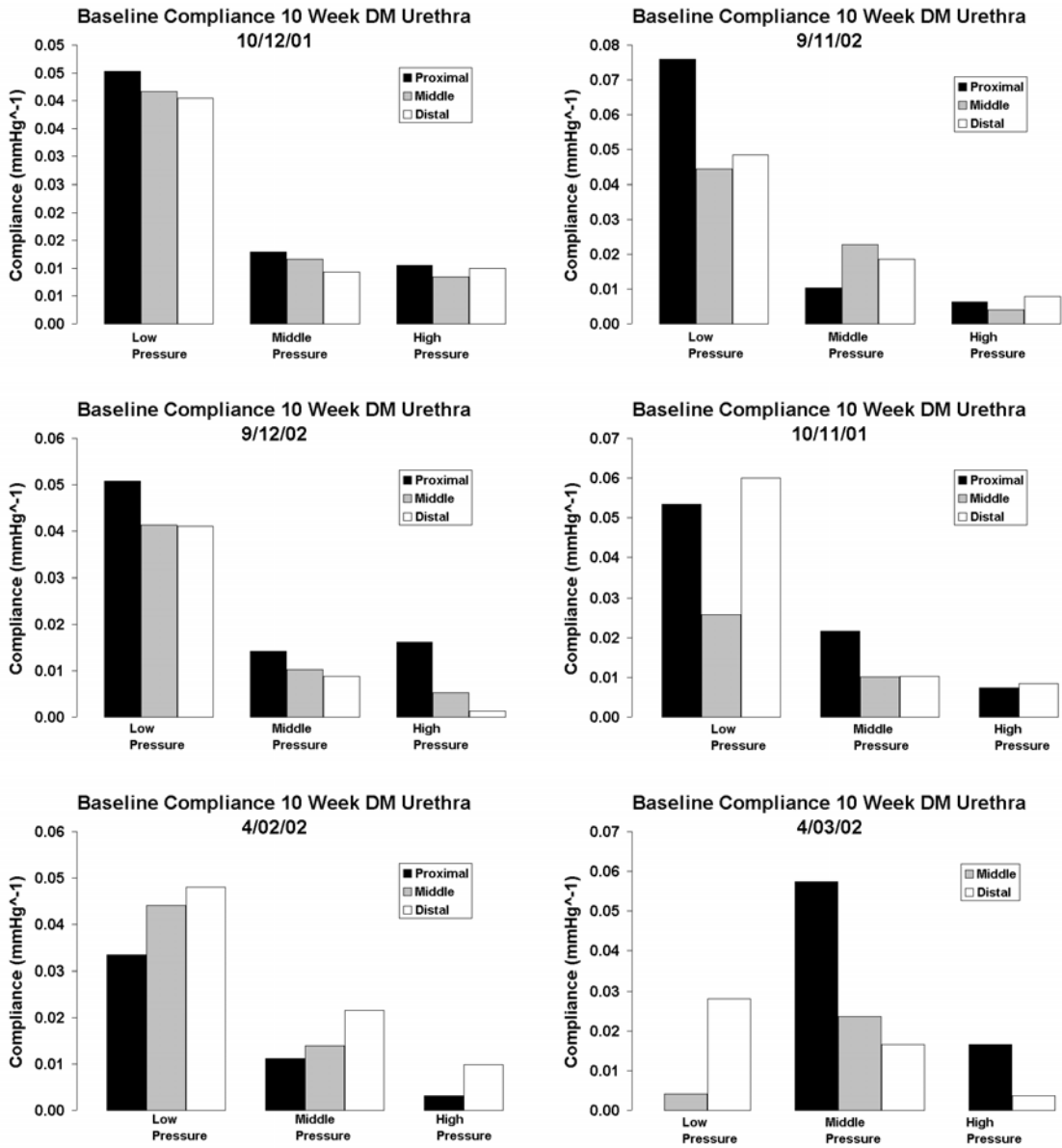


Figure A.60: Low, middle, and high pressure compliance data for proximal, middle, and distal portions of 10-week DM urethras in the baseline state

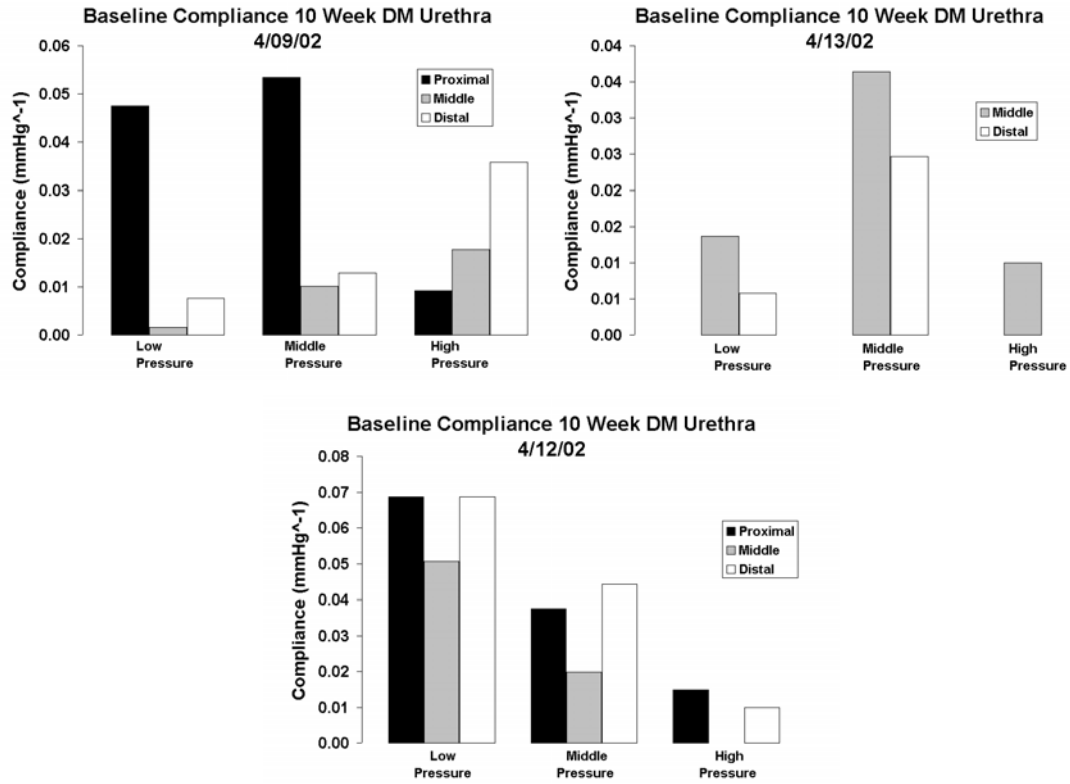


Figure A.61: Low, middle, and high pressure compliance data for proximal, middle, and distal portions of 10-week DM urethras in the baseline state

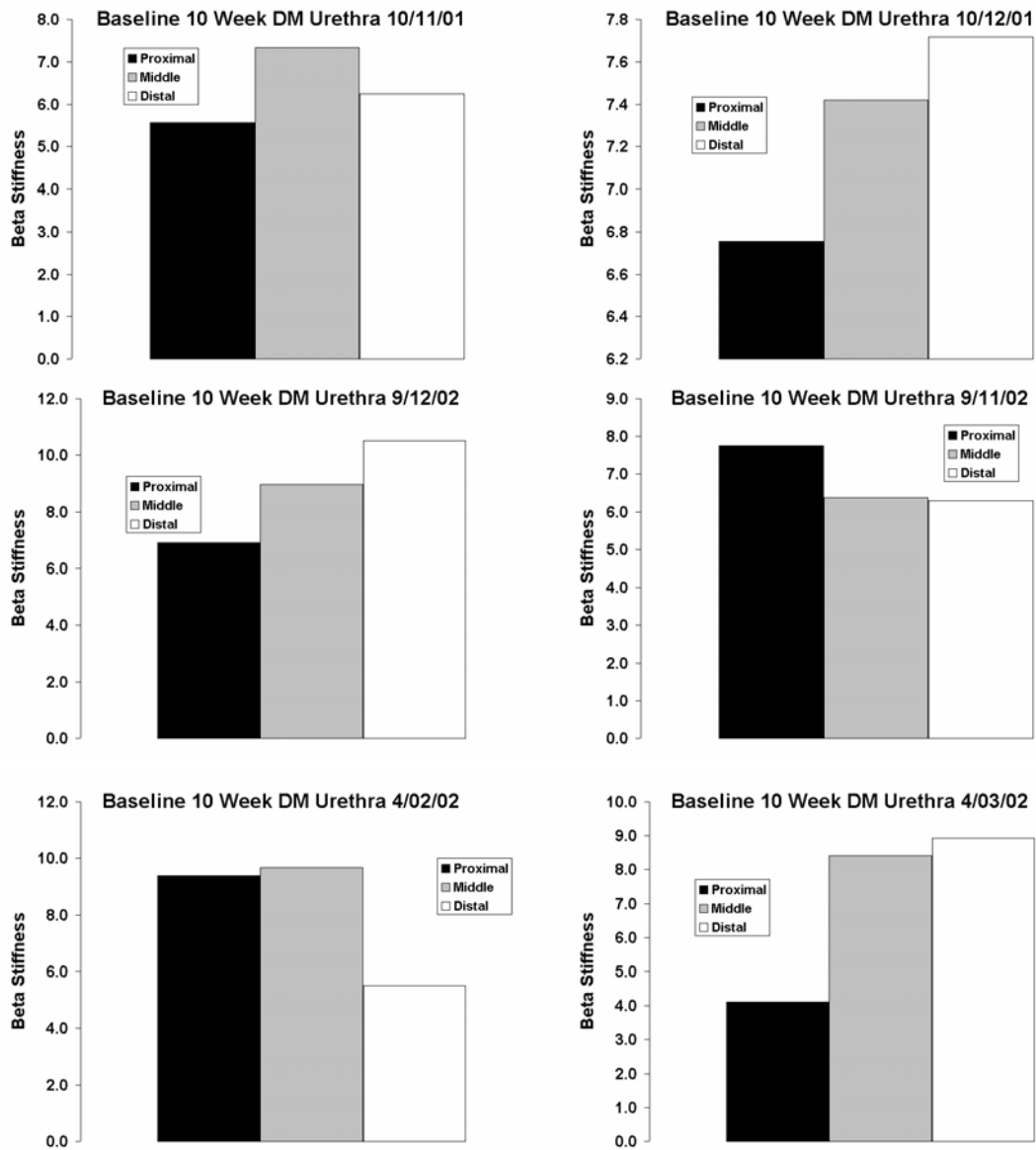


Figure A.62: Beta stiffness data for proximal, middle, and distal portions of 10-week DM urethras in the baseline state

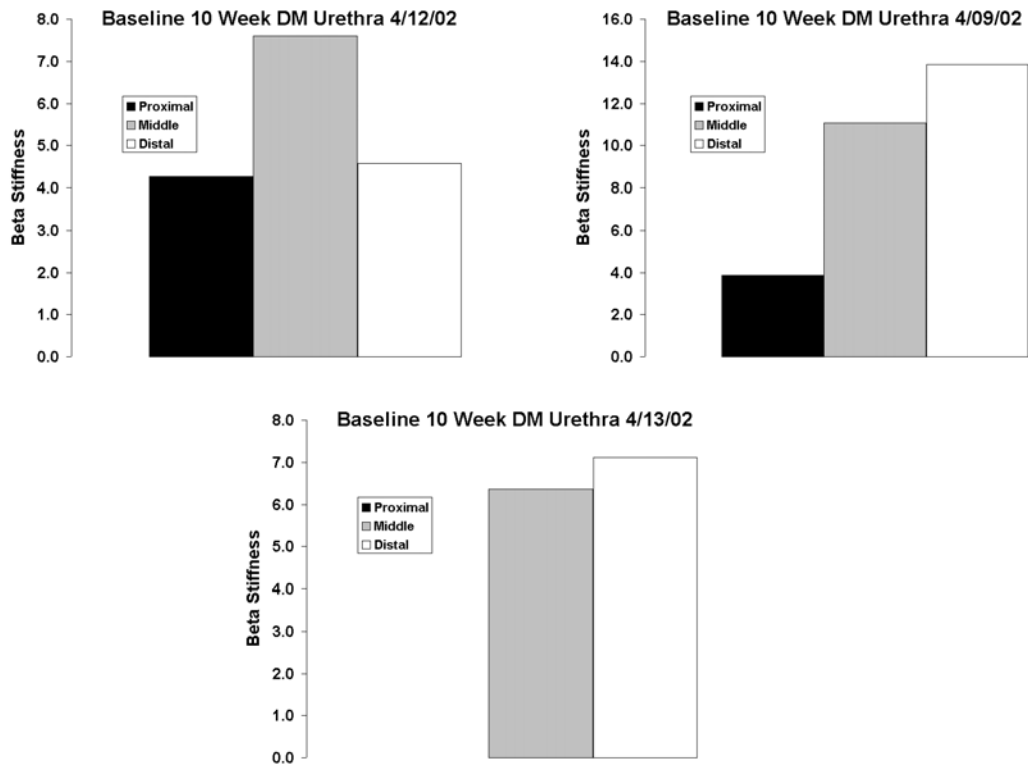


Figure A.63: Beta stiffness data for proximal, middle, and distal portions of 10-week DM urethras in the baseline state

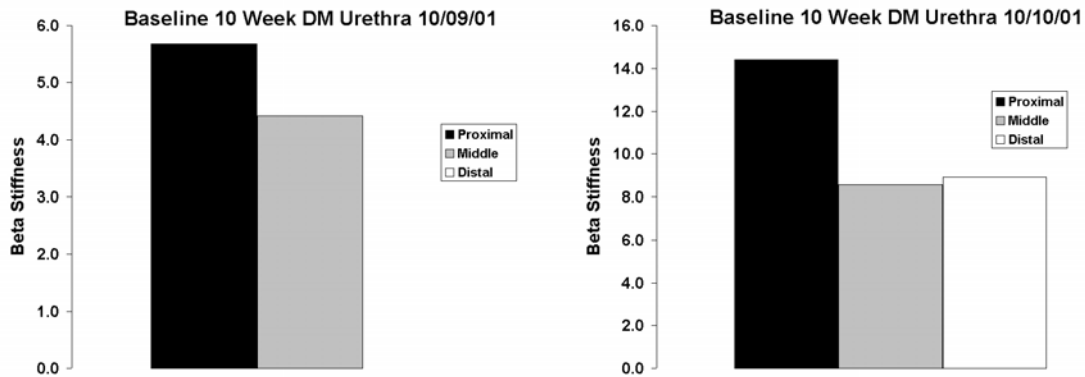


Figure A.64: Beta stiffness data for proximal, middle, and distal portions of 10-week DM urethras in the baseline state

A.4.2 Passive Data

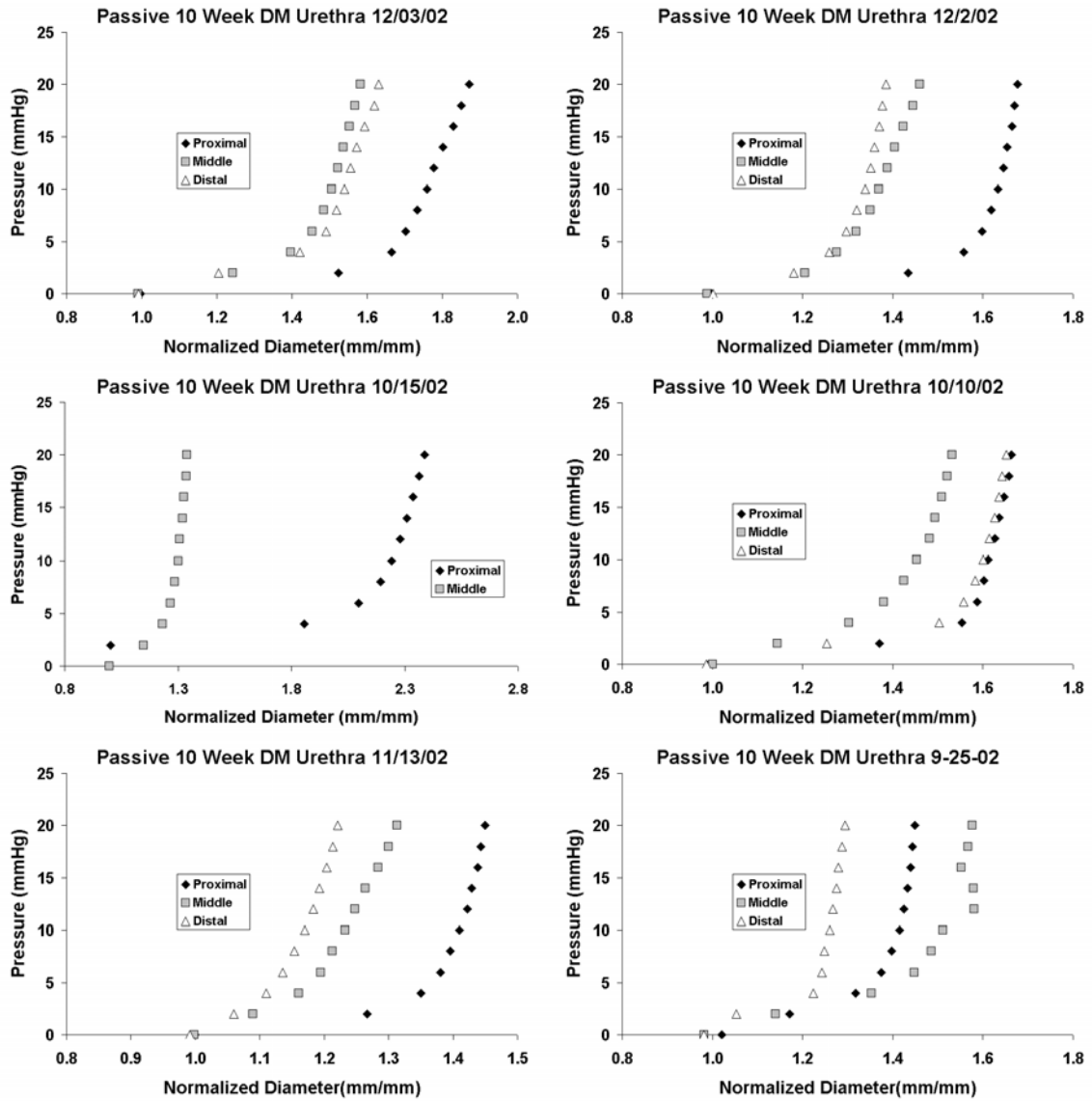


Figure A.65: Pressure-diameter data for proximal, middle, and distal portions of 10-week DM urethras in the passive state

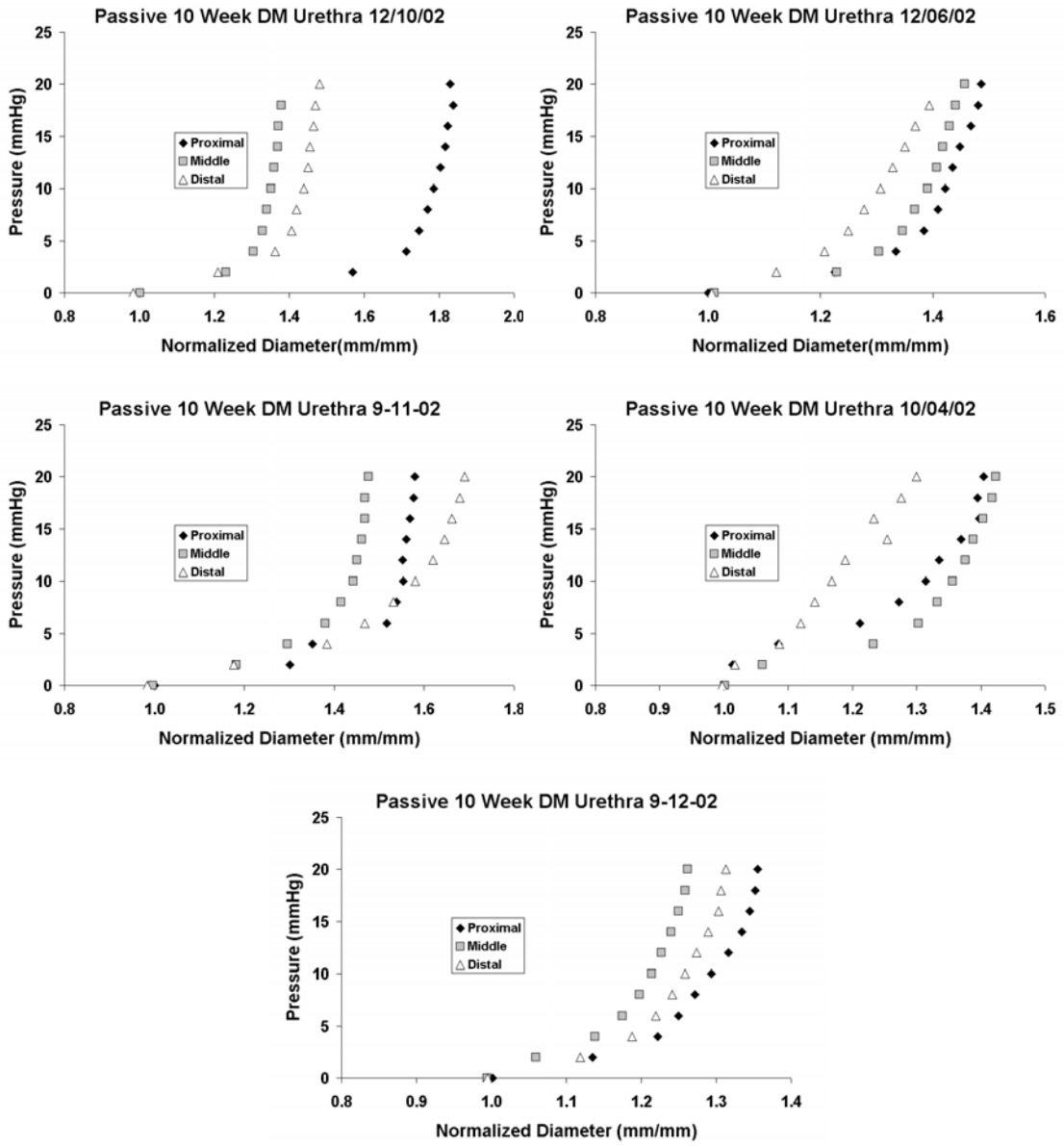


Figure A.66: Pressure-diameter data for proximal, middle, and distal portions of 10-week DM urethras in the passive state

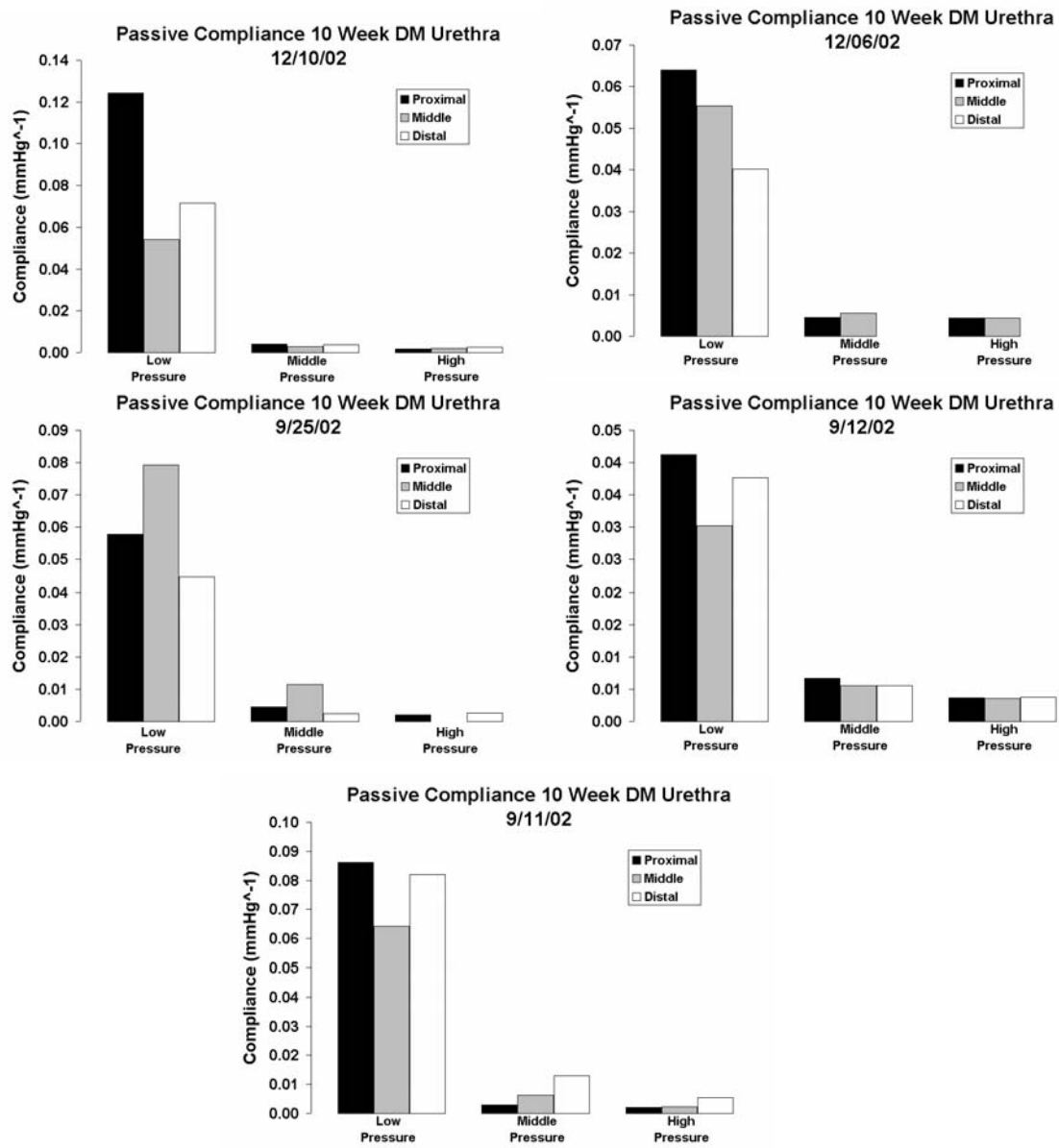


Figure A.67: Low, middle, and high pressure compliance data for proximal, middle, and distal portions of 10-week DM urethras in the passive state

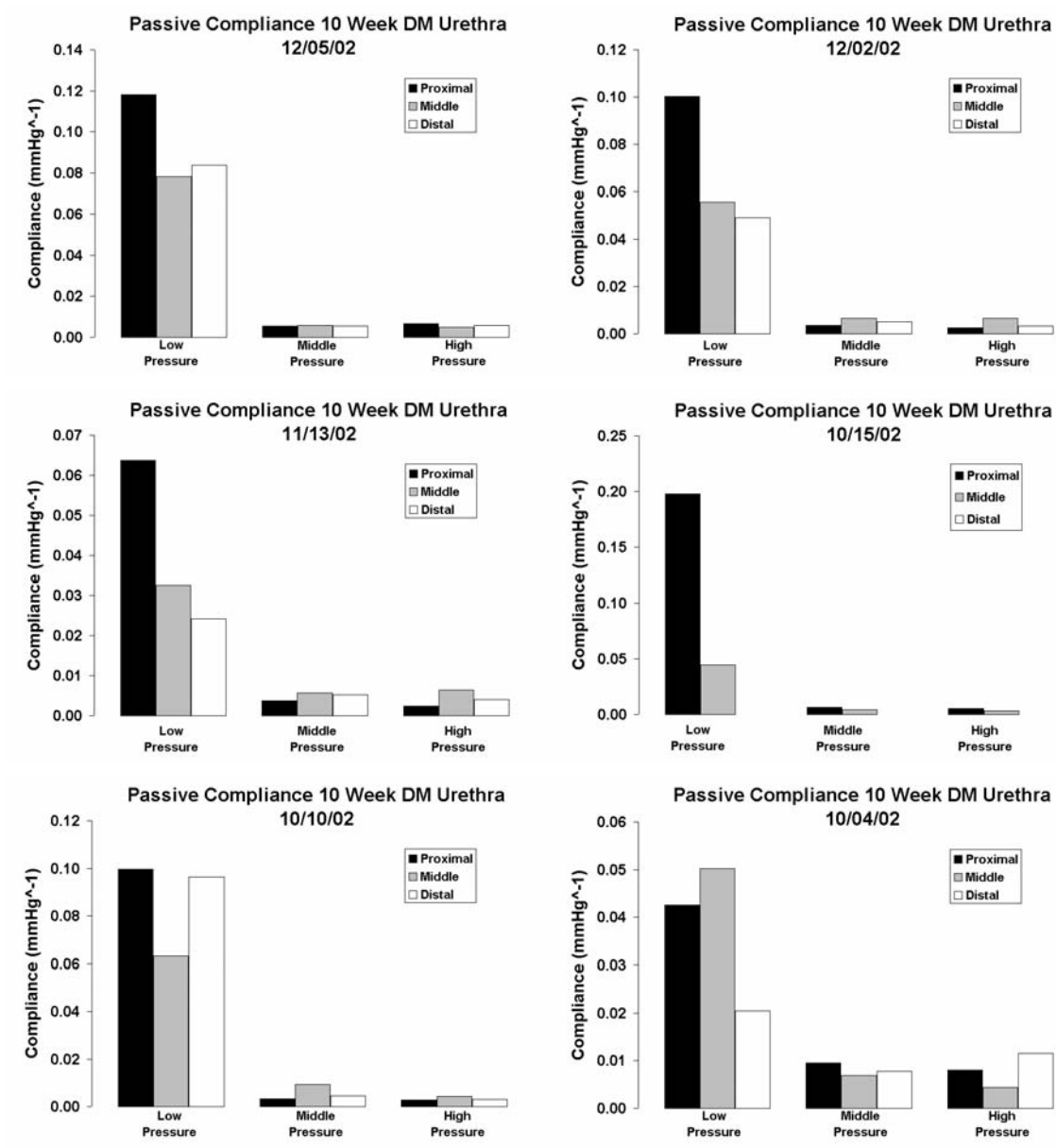


Figure A.68: Low, middle, and high pressure compliance data for proximal, middle, and distal portions of 10-week DM urethras in the passive state

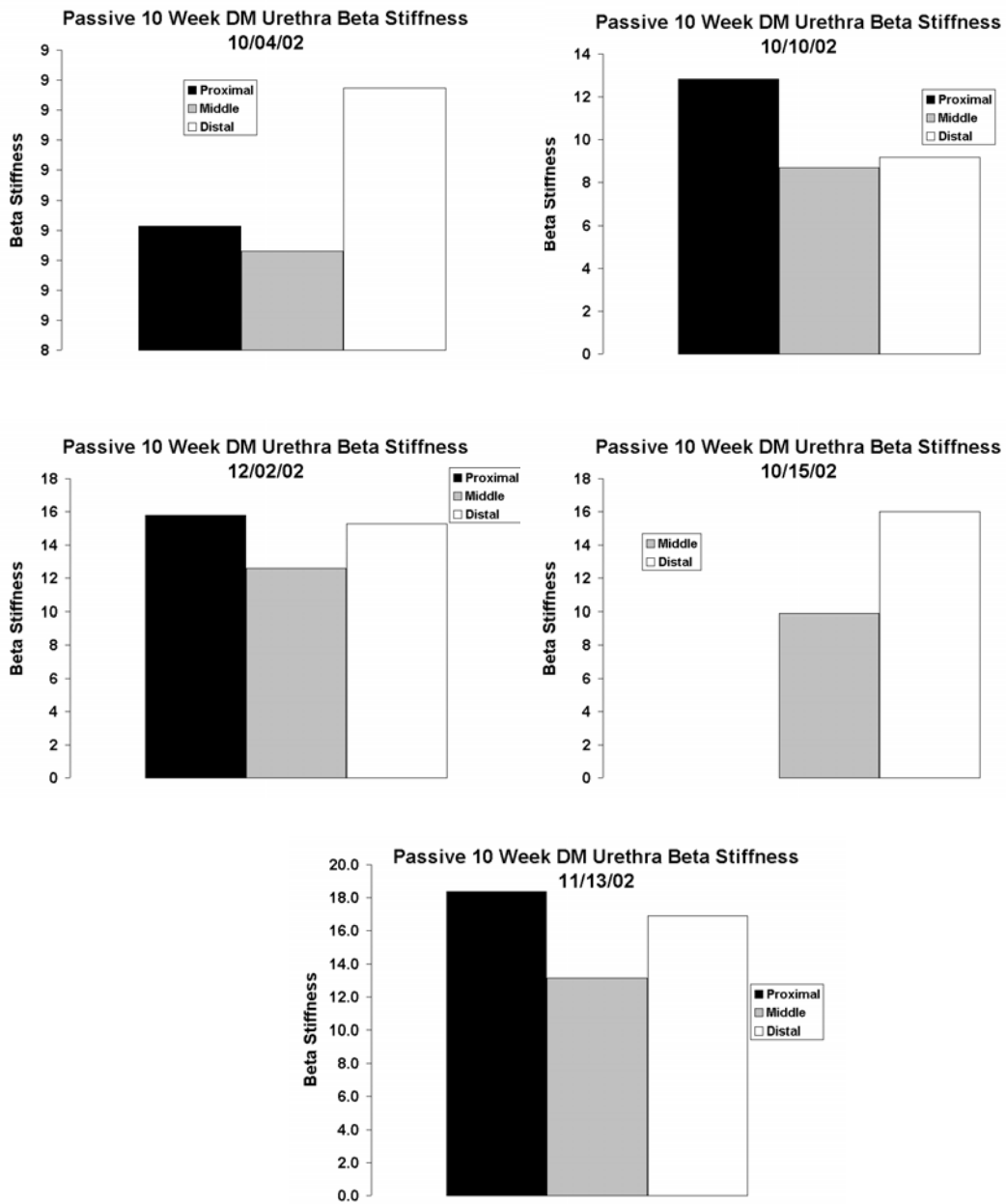


Figure A.69: Beta stiffness data for proximal, middle, and distal portions of 10-week DM urethras in the passive state

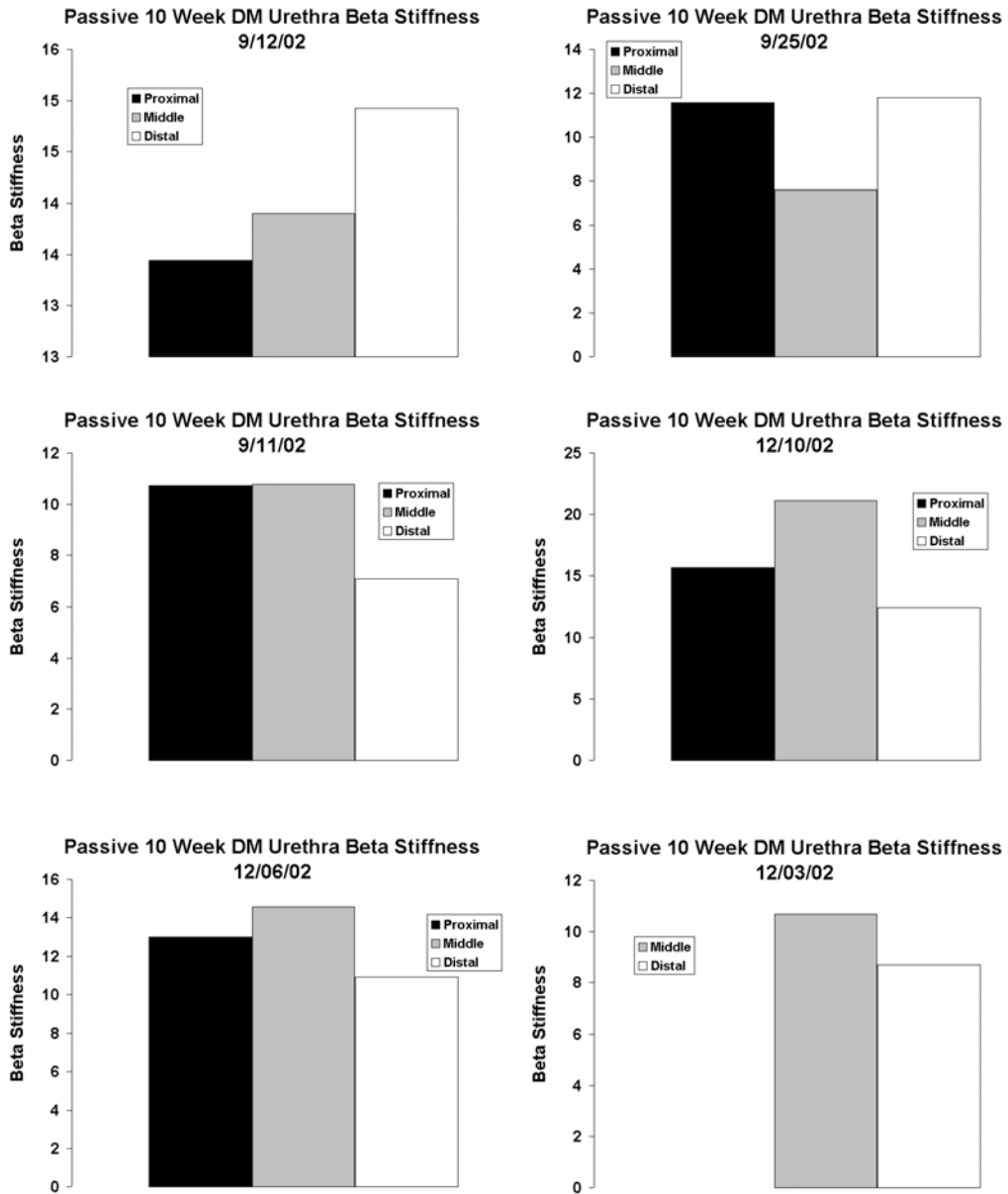


Figure A.70: Low, middle, and high pressure compliance data for proximal, middle, and distal portions of 10-week DM urethras in the passive state

A.4.3 Pharmacological Data

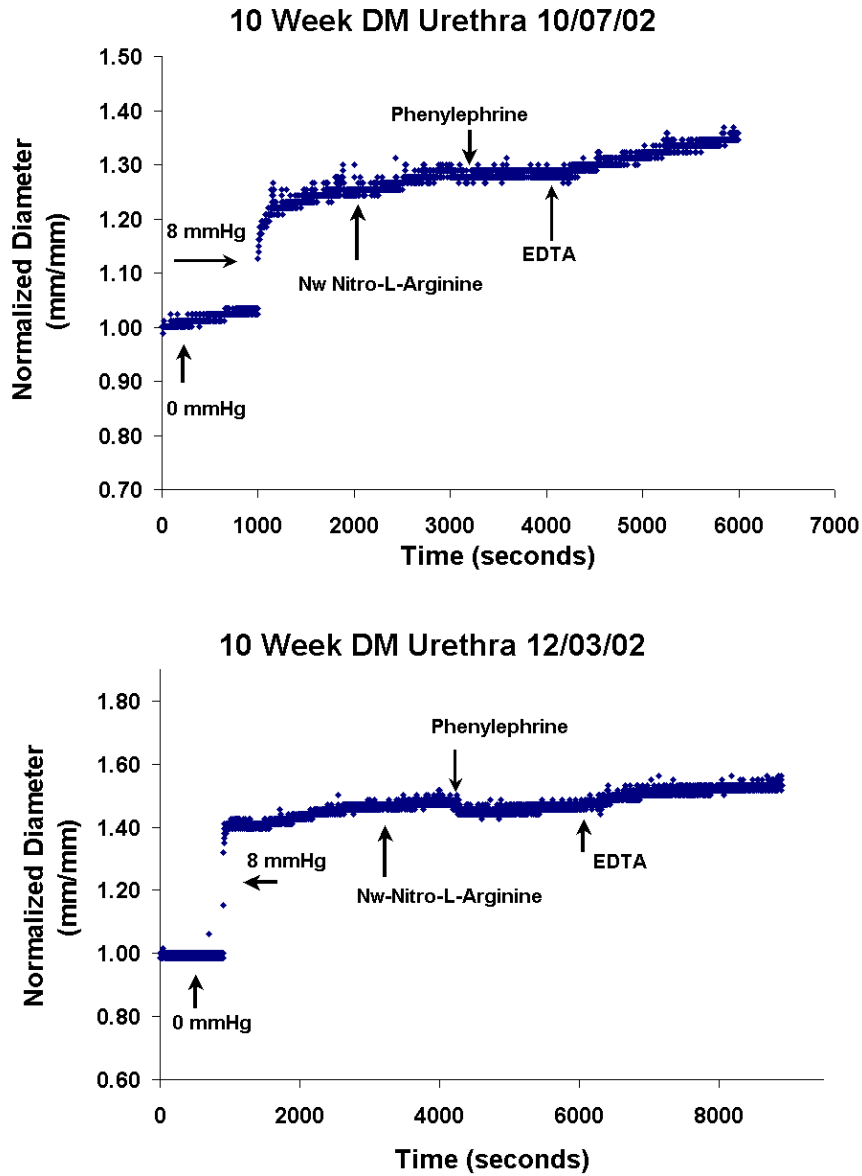


Figure A.71: Pharmacological data representing decrease and increase of the outer diameter of the middle portion of control urethras. Blood glucose levels were (top) 540 mg/dl and (bottom) 408 mg/dl

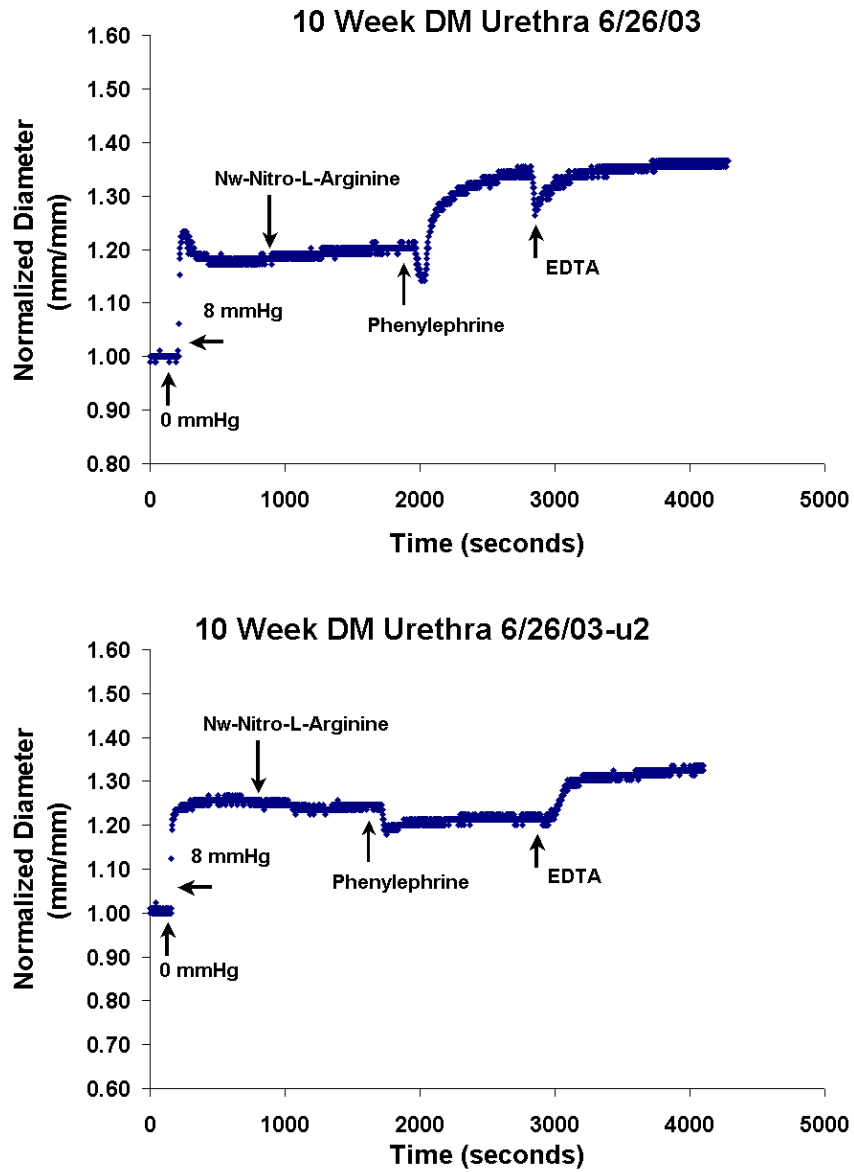


Figure A.72: Pharmacological data representing decrease and increase of the outer diameter of the middle portion of control urethras. Blood glucose levels were (top) 479 mg/dl and (bottom) 368 mg/dl

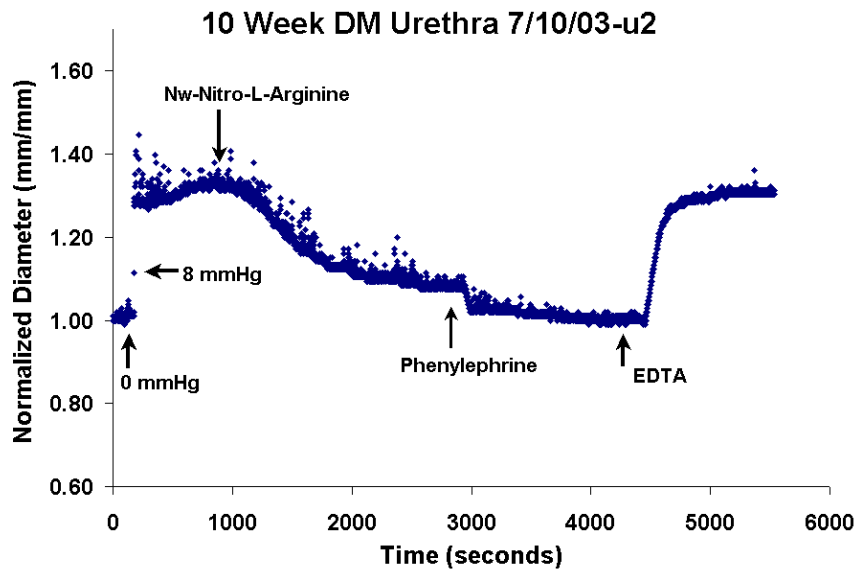
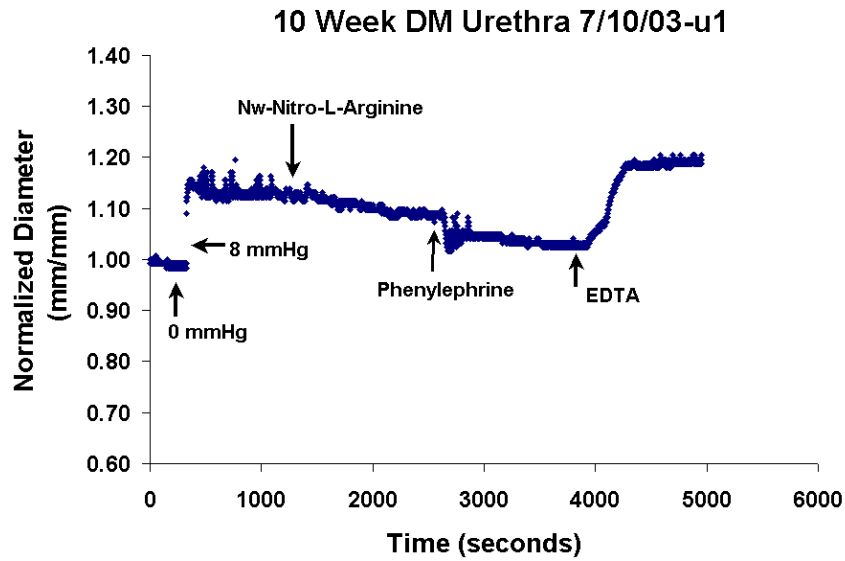


Figure A.73: Pharmacological data representing decrease and increase of the outer diameter of the middle portion of control urethras. Blood glucose levels were (top) 480 mg/dl and (bottom) 399 mg/dl

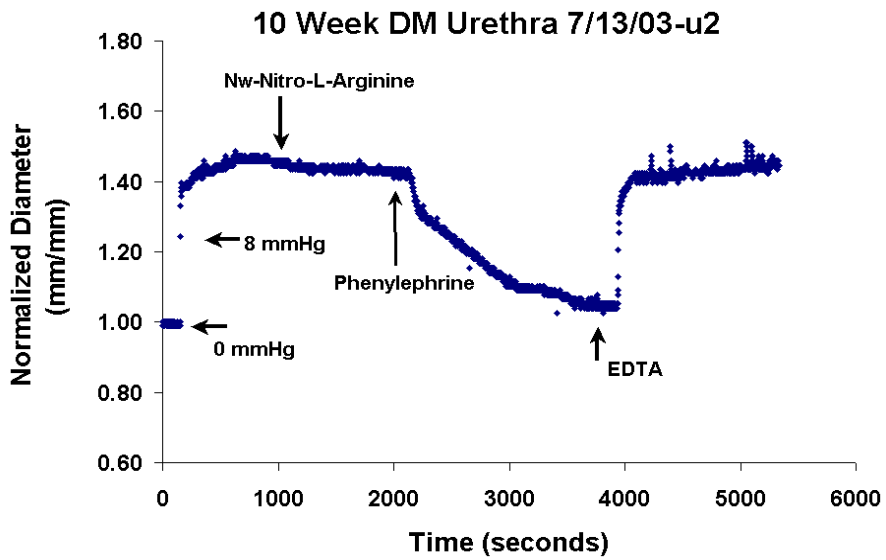
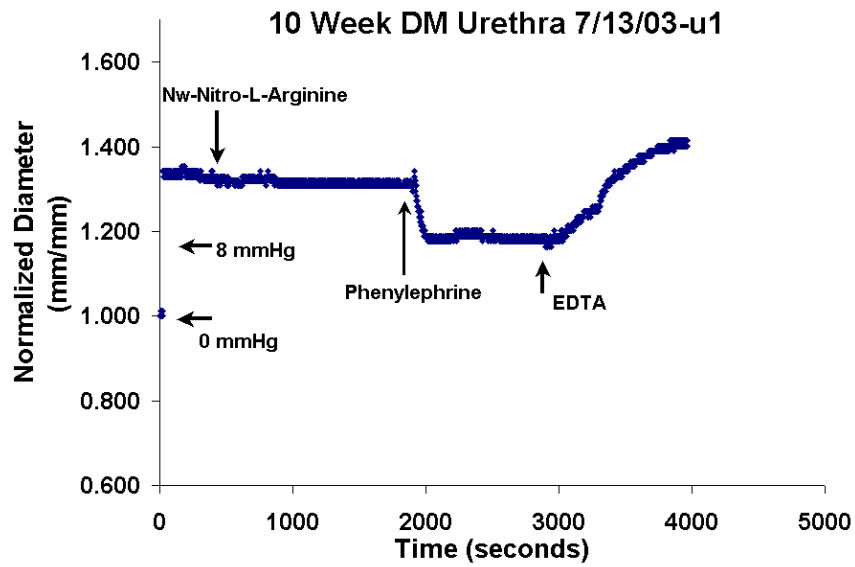


Figure A.74: Pharmacological data representing decrease and increase of the outer diameter of the middle portion of control urethras. Blood glucose levels were (top) 479 mg/dl and (bottom) 368 mg/dl

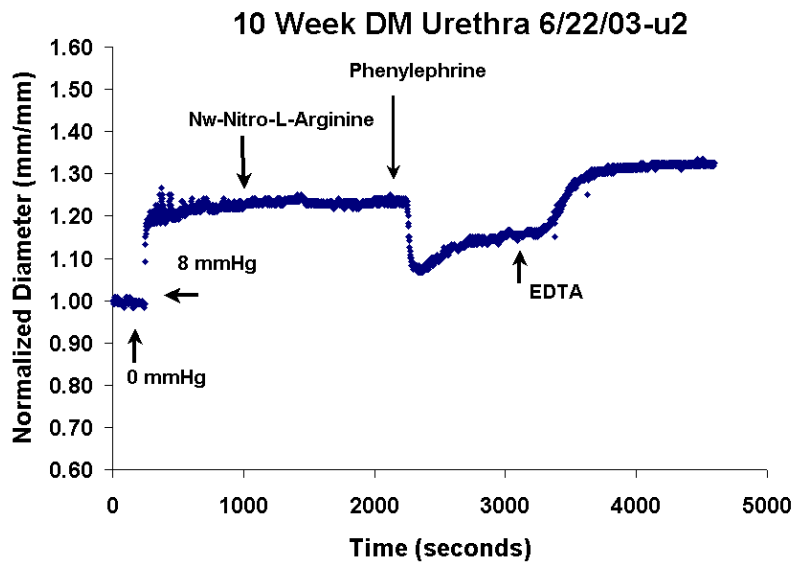
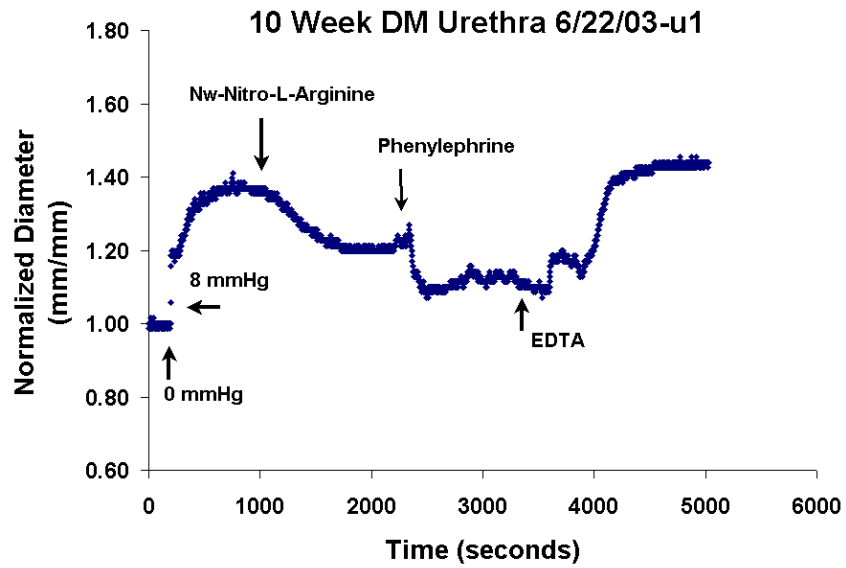


Figure A.75: Pharmacological data representing decrease and increase of the outer diameter of the middle portion of control urethras. Blood glucose levels were (top) 355 mg/dl and (bottom) 282 mg/dl

APPENDIX B. PROPOGATION OF ERROR ANALYSIS

The following error analysis to be performed is established from that of previous studies [106]. Before assessing the propogation of error in calculated quantities, the uncertainty in the directly measured parameters used in the calculations must first be determined or estimated.

The system will be set up with a normal rat urethra tied in to the ex vivo system. A mercury manometer will be used to measure each maximum and minimum pressure value for each pressure range used to calculate low (0-6mmHg), middle (6-12 mmHg), high (12-20 mmHg) pressure compliance values. This will be repeated several times. The resulting measurements will be averaged and a standard deviation will be computed.

Next, the laser micrometer will be used measure proximal, middle, and distal outer diameters of the urethra, separately. Measurements will be repeated at low, middle, and high pressure ranges. Values for maximum and minimum diameter values will be averaged and standard deviations will be computed.

In summary, the following uncertainties will be needed for to evaluate the propogation of error for compliance:

$\sigma_{P_{max}}$ = uncertainty value for *maximum* pressure

$\sigma_{P_{min}}$ = uncertainty value for *minimun* pressure

$\sigma_{D_{max}}$ = uncertainty value for *maximum* outer diameter

$\sigma_{D_{min}}$ = uncertainty value for *minimum* outer diameter

After determination of uncertainties, the next step will be to compute the propogation error for the compliance calculation. Below are the required equations:

Error analysis is based on **Equation B.1:**

Equation B.1

$$\sigma_{\lambda}^2 = \left(\frac{d\lambda}{d\alpha} \right)_{\beta,\gamma}^2 \sigma_{\alpha}^2 + \left(\frac{d\lambda}{d\beta} \right)_{\alpha,\gamma}^2 \sigma_{\beta}^2 + \left(\frac{d\lambda}{d\gamma} \right)_{\alpha,\beta}^2 \sigma_{\gamma}^2$$

where, λ is a computed quantity and α , β , γ are either a directly measured quantity or a previous calculated quantity, each with a known uncertainty, σ . The differentials for λ with respect to α , β , and γ are the average uncertainties, which are usually taken as 2 standard deviations for 95% confidence limits. Squared terms are appropriate for treatment of random errors.

Simple addition (Equation B.2) and multiplication (Equation B.3a and B.3b) will be used to assess the error in various calculated quantities.

If $\lambda = \alpha + \beta + \gamma$, then;

$$\frac{d\lambda}{d\alpha} = 1, \frac{d\lambda}{d\beta} = 1, \frac{d\lambda}{d\gamma} = 1$$

Incorporating these values into Equation A-1, the resulting equation is reduced to **Equation B.2**:

Equation B.2

$$\sigma_{\lambda}^2 = \sigma_{\alpha}^2 + \sigma_{\beta}^2 + \sigma_{\gamma}^2$$

This relation will be used to describe the propagation of error for the differences between maximum and minimum pressure measurements, as well as for respective diameter measurements.

If $\lambda = \alpha \beta \gamma$, then;

$$\frac{d\lambda}{d\alpha} = \beta\gamma, \frac{d\lambda}{d\beta} = \alpha\gamma, \frac{d\lambda}{d\gamma} = \alpha\beta$$

Incorporating these values into Equation A-1, the resulting is reduced to **Equation B.3a**:

Equation B.3a

$$\sigma_{\lambda}^2 = (\beta\gamma)^2 \sigma_{\alpha}^2 + (\alpha\gamma)^2 \sigma_{\beta}^2 + (\alpha\beta)^2 \sigma_{\gamma}^2$$

For further simplification, this equation may be divided through by $\lambda^2 = \alpha^2 \beta^2 \gamma^2$ yielding **Equation A-3b**:

Equation B.3b

$$\% \sigma_{\lambda}^2 = \% \sigma_{\alpha}^2 + \% \sigma_{\beta}^2 + \% \sigma_{\gamma}^2$$

This relation will be used to describe the propagation of error when using the pressure-diameter relation, compliance. For the compliance equation (Equation 2.2), the error will need to be calculated for the differences in pressure and diameter, separately. For pressure, $\Delta P = P_{\max} - P_{\min}$:

$$\sigma_P = \sqrt{(\sigma_{P_{\max}}^2 + \sigma_{P_{\min}}^2)}$$

For diameter, $\Delta D = D_{\max} - D_{\min}$:

$$\sigma_D = \sqrt{(\sigma_{D_{\max}}^2 + \sigma_{D_{\min}}^2)}$$

and to complete for the entire diameter relation, $\frac{(D_{Max} - D_{Min})}{D_{Min}}$:

$$\sigma_{Dfinal} = \sqrt{\left(\left(\frac{1}{\sigma_{Dmin}} \right)^2 \sigma_D^2 + \left(\frac{1}{\sigma_{Dmin}} \right)^2 \sigma_D^2 \right)}$$

The final calculation that will provide the propagation of error for the compliance calculation (σ_C), **Equation B.4**:

Equation B.4

$$\sigma_C = \sqrt{\left(\frac{1}{\sigma_P} \right)^2 \sigma_{Dfinal}^2}$$

BIBLIOGRAPHY

1. McLaughlin, Eileen, (2000) "Diabetes Mellitus." *North Memorial Health Encyclopedia*. Retrieved January 07, 2003, from <http://www.northmemorial.com/HealthEncyclopedia/>
2. Spanheimer, RG. Umpierrez, GE., Stumpf, V.(1988) Decreased collagen production in diabetic rats. *Diabetes*, 37, 371-376.
3. Dayhaw-Barker, P. (1995) Mechanisms of Pathogenesis in Diabetes Mellitus. *Optometry and Vision Science*, 72,417-24.
4. Pozzilli, P. and Di Mario, U. (2001) Autoimmune Diabetes Not Requiring Insulin at Diagnosis Latent Autoimmune Diabetes of the Adult. *Diabetes Care*, 24, 1460-67.
5. Boden, G.(2001) Pathogenesis of Type 2 Diabetes. *Endocrinology and Metabolism Clinics of North America*, 30, 801-13.
6. Elbadawi, A. (1996) Functional Anatomy of the Organs of Micturition. *Urologic Clinics of North America*, 23, 177-210.
7. Steers, WD. (1994) *Clinical Manual of Urology*. McGraw-Hill Co.: New York.
8. Brading, AF. (1999) Physiology of the Mammalian Urinary Outflow Tract. *Experimental Physiology*, 84, 215-221.
9. de Groat, W. C. and Booth, A. M. (1980) Physiology of the Urinary Bladder and Urethra. *Annals of Internal Medicine*, 92, 312-315.
10. de Groat, W. C., Fraser, M. O., Yoshiyama, M., Smerin, S., Tai, C., Chancellor, M. B., Yoshimura, N., Roppolo, J. R.(2001) Neural Control of the Urethra. *Scandinavian Journal Urology Nephrology Suppl*, 207, 35-43.
11. Appell, R. A. (2000) *Voiding Dysfunction: Diagnosis and Treatment*. Human Press: Totowa.

12. Moller, C. F. (1980) Diabetic Cystopathy: Epidemiology and Related Disorders. *Annals of Internal Medicine*, 92, 318-21.
13. Goldman, H. B. And Appell, R. A. (1999) Voiding Dysfunction in Women with Diabetes Mellitus. *Int. Urogynecol. J.*, 10,130-133.
14. Ellenberg, M.(1980) Development of Urinary Bladder Dysfunction in Diabetes Mellitus. *Annals of Internal Medicine*, 92, 321-323.
15. Mastri, A. R. (1980) Neuropathology of Diabetic Neurogenic Bladder. *Annals of Internal Medicine*, 92, 316-318.
16. Bradley, W. E. and Andersen, J. T. (1976) Abnormalities of Bladder Innervation in Diabetes Mellitus. *Urology*, 7, 442-8.
17. Peltonen, J. T., Kalliomaki, M. A., and Muona, P. K.(1997)Extracellular Matrix of Peripheral Nerves in Diabetes. *J. Peripher. Nerv. Syst.*, 2, 213-26.
18. Ueda,T., Yoshimura, N., Yoshida, O. (1997) Diabetic Cystopathy: Relationship to Autonomic Neuropathy Detected by Sympathetic Skin Response. *Journal of Urology*, 157, 580-587.
19. Kaplan, S. A., Te, A. E., Blavis, J. G. (1995) Urodynamic Findings in Patients with Diabetic Cystopathy. *Journal of Urology*, 152, 342-344.
20. Lincoln, J., Crockett, M., Haven, A. J., and Burnstock, G. (1984) Rat Bladder in the Early Stages of Streptozotocin Induced Diabetes: adrenergic and cholinergic innervation. *British Journal of Urology*, 26, 24-30.
21. Pinna, C., Zanardo, R., Cignarella, A., Bolego, C., Eberini, I., Nardi, F., Zancan, V., Puglisi, L. (2000) Diabetes Influences the Effect of 17beta-Estradiol on Mechanical Responses of Rat Urethra and Detrusor Strips.*Life Science*, 66, 617-627.
22. Kolta, M. G., Wallace, L. J., Gerald, M. C. (1985) Streptozotocin-induced Diabetes Affects Rat Urinary Bladder Response to Autonomic Agents. *Diabetes*, 34, 917-21.
23. Moss, H. E., Lincoln, J., Burnstock, G. (1987) Study of Bladder Dysfunction During Streptozotocin Induced Diabetes in the Rat Using an In Vitro Whole Bladder Preparation. *Journal of Urology*, 138,1279-1284.
24. Torimoto, K., Mitsuharu, Y., De Groat, W. C., Yoshimura, N., Chancellor, M. B., and Fraser, M. O. (2002, May) Dramatic effects of Diabetes Mellitus on In Vivo Urethral Function: Implications for Understanding the Pathogenesis of Diabetic Cystopathy. *American Urological Association Conference*, Orlando, Florida.

25. Andersson, P. O., Fahrenkrug, J., Malmagren, A., Uvelius, B. (1992) Effects of age and streptozotocin induced diabetes on contents and effects of substance P and vasoactive Intestinal polypeptide in the lower urinary tract of the rat. *Acta Physiology Scand.*, 144, 361-368.
26. Chun, A. L., Gill, H. S., Wein, A. J., Levin, R. M. (1989) Pharmacological comparison of Isolated Whole Urethra Model to Urethral strip Methodology. *Pharmacology*, 39, 192-199.
27. Labadie, R. F. Antaki, J. F., Williams, J. L. Katyal, S., Ligush, J., Watkins, S. C., Pham, S. M, and Borovetz, H. S. (1996) Pulsatile perfusion system for ex vivo investigation of biochemical pathways of vascular tissue. *Am. J. Physiol. Heart and Circ. Physiol.*, 39, H760-8.
28. Streng T., Santti R., Talo A (2002) Similarities and differences in female and rat voiding. *Neurourol Urodyn.*, 21,136-41.
28. Ligush,J., Labadie, R. F., Berceci, S. A., Ochoa, J. B., Borovetz, H. S. (1992) Evaluation of Endothelium Derived Nitric Oxide Mediated Vasodilator Utilizing Ex Vivo Perfusion of an Intact Vessel. *J. Surgical Research*, 52, 416-421.
30. Brant, A. M., Teodori, M. F., Kormos, R. L., and Borovetz, H. S. (1987) Effect of variations in pressure and flow on the geometry of isolated canine carotid arteries. *J. Appl. Physiol.*, 62,679-83.
31. Vorp, D. A., Severyn, D. A., Steed, D. L., Webster, M. W. (1996) A Device for the Application of Cyclic Twist and Extension on Perfused Vascular Segments. *Am. J. Physiol*, 270, H787-5.
32. Steers, WD. (1994) Rat: Overview and innervation. *Neurourology and Urodynamics*, 13,97-118.
33. Corcos, J. and Schick, E. (2000) *The Urinary Sphincter*. Marcel Dekker: New York.
34. Hayashi K. (1993) Experimental approaches on measuring the mechanical properties and constitutive laws of arterial walls. *J Biomech Eng.*, 115, 481-8.
35. Nishimatsu, H., Moriyama, N., Hamada, K., Ukai, Y., Yamazaki, S., Kameyama, S., Konno N., Ishida, Y., Ishii, Y., Murayama, T., Kitamura, T. (2000) Contractile responses to α_1 -adrenoceptor agonists in isolated human male and female urethra. *BJU International*, 84, 515-520.

36. Werkstrom, V., Ny, L., Persson, K., Andersson, K.E. (1997) Neurotransmitter release evoked by alpha-latrotoxin in the smooth muscle of the female pig urethra. *Naunyn Schmiedebergs Arch Pharmacol*, 356, 151-8.
37. Teramoto, N., McMurray, G., Brading, A.F. (1997) Effects of levromakalim and nucleoside diphosphates on glibenclamide-sensitive K⁺ channels in pig urethral myocytes. *Br J Pharmacol*, 120,1229-40.
38. Rakieten, N., Rakieten, M. L., Nadkarni, V. (1963) Studies on the diabetogenic action of streptozotocin (NSC-37917). *Cancer Chemother. Rep.*,29, 91-8.
39. Partin, K. and Peters, N. (2002) *Campbell's Urology* (8th edition).Saunders: Philadelphia.
40. Tancrede, G., Rousseau-Mignerot, S., and Nadeau, A. (1983) Long term changes in the diabetic state induced by different doses of streptozotocin in rats. *Br.J. exp. Path.*,64, 117-124.
41. Schafer, W. (2001) Some biomechanical aspects of continence function. *Scand. J. Urol. Nephrol. Suppl*, 207, 44-60, 2001
42. Colstrup, H. (1984) Rigidity of the resting female urethra. Part I. Static measurements. *J Urology*, 132, 78-81.
43. Thind P. and Lose G. (1992) Urethral stress relaxation phenomenon in healthy and stress incontinent women.*Br. J. Urology*, 69,75-8.
44. Yalla, S. V., Burros, H. M., Ivker, M. I. (1973) Physical properties of female urethral wall: experimental method for determining relative degree of urethral wall stiffness. *Urology*, 2, 269-75.
45. Mayo ME. And Hinman F. (1973) The effect of urethral lengthening. *Brit. J Urology*, 45, 621-30.
46. Kwon, H. Y., Wein, A. J., and Levin, R. M. (1995) Effect of anoxia on the urethral response to phenylephrine. *J. Urology*, 154, 1527-31.
47. Masiello, P., De Paoli, A. A., Bergamini, E. (1979) Influence of age on the sensitivity of the rat to streptozotocin. *Hormone Research*,11,202-17.
48. Bolzan, A. D. and Bianchi, M. S. (2002) Genotoxicity of streptozotocin. *Mutation Research*, 512, 121-34.
49. Ar'Rajab, A. and Ahren, B. (1993) Long term diabetogenic effects of streptozotocin in rats. *Pancreas*, 8, 50-7.

50. Yalla, S. V. and Burros, H. M. (1974) Conduit and compliance responses of female canine urethra. *Urology*, 3, 598-604.
51. Nordin, M. and Frankel, V. H. (1989) *Basic biomechanics of the musculoskeletal system*. Williams and Wilkins: Baltimore.
52. Bagi, P., Thind, P., Colstrup, J. K., Kristensen, J. K. (1993) The dynamic pressure response to rapid dilatation of the resting urethra in healthy women: an in vivo evaluation of visco-elastic properties. *Urological Research*, 21, 339-43.
53. Yin, F., Wassef, M., Esposito, D., Henrion, D., Glagov, S., and Tedgui, A. (1992) Compliance changes in physiological and pathological states. *J. Hypertension*, 10, S31-33.
54. Peiro C, Lafuente N, Matesanz N, Cercas E, Llergo JL, Vallejo S, Rodriguez-Manas L, Sanchez-Ferrer CF. (2001) High glucose induces cell death of cultured human aortic smooth muscle cells through the formation of hydrogen peroxide. *Br J Pharmacol.* ,133, 967-74.
55. Turner WH., Brading AF. (1997) "Smooth muscle of bladder in the normal and diseased state: Pathophysiology, diagnosis, and treatment." *Pharmacol. Ther.*, 75, 77-110.
56. Hickey, H. S., Phillips, J. I., Hukins, D. W. L. (1982) Arrangements of collagen fibrils and muscle fibers in the female urethra and their implications for the control of micturition. *Brit. J. Urology*, 54, 556-61.
57. Ofulue, A. F. and Thurlbeck, W. M. (1995) Effects of streptozotocin induced diabetes on postpneumonectomy lung growth and connective tissue levels. *Pediatr Pulmonol.*,19, 365-70.
58. Spanheimer, R. G., Umpierrez, G. E., and Stumpf, V. (1988) Decreased Collagen Production in Diabetic Rats. *Diabetes*, 37, 371-76.
59. Paul, R. G. and Bailey, A. J. (1996) Glycation of collagen: the basis of its central role in late complications of ageing and diabetes. *Int. J. Biochem. Cell. Biol.*, 28, 1297-1310.
60. Andreassen, T.T., Seyer-Hansen, K., Bailey, A. J. (1981) Thermal stability, mechanical properties and reducible cross links of rat tail tendon in experimental diabetes. *Biochim. Biophys. Acta* , 677, 313-17.
61. Sims, T. J. and Bailey, A. J. (1996) Quantitative analysis of collagen and elastin cross links using a single-column system. *J. Chromatog.*, 582, 49-55.

62. Berry, K. L., Cameron, J. D., O'Brien, R. C., and Meredith, I. T. (1999) Systemic arterial compliance is reduced in young patients with IDDM. *Am. J. Physiol.* 276, H1839-45, 1999
63. Crijns, F. R. L., WolffenButtel, B. H. R., De Mey, J. G. R., and Boudier, A. J. (1999) Mechanical properties of mesenteric arteries in diabetic rats: consequences of outward remodeling. *Am J Physiol.*, 267, H1672-77.
64. Romney, J. S., and Lewanczuk, R. Z. (2001) Vascular compliance is reduced in the early stages of type 1 diabetes. *Diabetes Care*, 24, 2102-6.
65. Mumtaz, F. H., Khan, M. A., Thompson, C. S., Morgan, R. J., and Mikhailidis, D. P. (2000) Nitric oxide in the lower urinary tract: physiological and pathological implications. *BJU International*, 85,567-78.
66. Mamas MA., Reynard J.M., Brading A.F. (2003) Nitric oxide and the lower urinary tract: current concepts, future prospects. *Urology*, 61, 1079-85.
67. Traub, O., Berk, B. C. (1998) Laminar shear stress: Mechanisms by which endothelial cells transduce an atheroprotective force. *Arterioscler Thromb Vasc Biol.*, 18, 677-685.
68. Ho, K. M., McMurray, G., Brading, A. F., Noble, J. G., Andersson, K. E. (2003) Human female urethral striated sphincter and its association with neuronal nitric oxide synthase. *J Urology*, 161, 2407-11
69. Szkudelski, T. (2001) The mechanism of alloxan and streptozotocin action in B cells of the rat pancreas. *Physiol. Res.*, 50, 536-46.
70. Pandolfi, A., Grilli, A., Cilli, C., Patruno, A., Giaccari, A., Di Silvestre, S., De Lutiis, M. A., Pellegrini, G., Capani, F., Consoli, A., Felaco, M. (2003) Phenotype modulation in cultures of vascular smooth muscle cells from diabetic rats: association with increased nitric oxide synthase expression and superoxide anion generation. *J. Cell Phys.*, 196,378-85.
71. Mumtaz, F. H., Thompson, C. S., Steif, C. G. (1999) Alterations in the formations of cyclic nucleotides and prostaglandins in the lower urinary tract of the diabetic rabbit. *Urol. Res.*, 27, 470-5.
72. Brading, A. F., Teramoto, N., Dass, N., McCoy, R. (2001) Morphological and physiological characteristics of urethral circular and longitudinal smooth muscle. *Scand J Urol. Nephrol Suppl.*, 207,12-18.
73. Takeda, H., Matsuzawa, A., Igawa, Y., Yamazaki, Y., Kaidoh, K., Akahane, S., Kojima, M., Miyata, H., Akahane, M., Nishizawa, O. (2003) Functional characterization of beta-adrenoceptor subtypes in the canine and rat lower urinary tract. *J Urol.*, 170, 654-8.

74. Griffith, R. K. (2003) *Burger's Medicinal Chemistry and Drug Discovery*. John Wiley and Sons: Virginia.
75. Brading, A. F., McCoy, R., Dass, N. (1999) Alpha 1- adrenoceptors in urethral function. *European Urology*, 36, 74-79.
76. Bishara, N. B., Dunlop, M. E., Murphy, T. V., Darby, I. A., Sharmini Rajanayagam, M. A., Hill, M. A. (2002) Matrix protein glycation impairs agonist-induced intracellular Ca²⁺ signaling in endothelial cells. *J Cell Physiol.*, 193, 80-92.
77. Yu, G., Zou, H., Prewitt, R. L., Hill, M. A. (1999) Impaired arteriolar mechanotransduction in experimental diabetes mellitus. *J Diabetes Complications*, 13, 235-42.
78. Ruffolo, R. R. (1991) *Alpha Adrenoceptors: Molecular Biology, Biochemistry, and Pharmacology*, 8, Karger: Basel.
79. Pieper, G. M. (1999) Enhanced, unaltered, and impaired nitric oxide mediated endothelium-dependent relaxation in experimental diabetes mellitus: importance of disease duration. *Diabetologia*, 42, 204-13.
80. Ischiropoulos, H. (1998) Biological tyrosine nitration: a pathophysiological function of nitric oxide and reactive oxygen species. *Arch. Biochem. Biophys.* , 356,1-11.
81. Etienne, P., Pares-Herbute, N., Mani-Ponset, L., Gabrion, J., Rabesandratana, H., Herbute, S., Monnier, L. (1998) Phenotype modulation in primary cultures of aortic smooth muscle cells from streptozotocin-diabetic rats. *Differentiation*, 63, 225-36.
82. Hickey, D. S, Phillips, J. I, Hukins, D. W. (1982) Arrangements of collagen fibrils and muscle fibres in the female urethra and their implications for the control of micturition. *Br J Urol.*, 54, 556-61.
83. Shimizu, M., Umeda, K., Sugihara, N., Yoshio, H., Ino, H., Takeda, R., Okada, Y., Nakanishi, I. (1993) Collagen remodelling in myocardia of patients with diabetes. *J Clin Pathol.*, 46, 32-6.
84. Dass, N., McMurray, G., Brading, A. F. (1999) Elastic fibers in the vesicourethral junction and urethra of the guinea pig: quantification with computerized image analysis. *J Anatomy*, 195, 447-53.
85. Rodrigues, B., Poucheret, P., Battell, M. L., McNeill, J. H. (1999) *Experimental Models of Diabetes*. CRC Press LLC.

86. Cameron, N. E., Eaton, S. E. M., Cotter, M. A., Tesfaye, S. (2001) Vascular factors and metabolic interactions in the pathogenesis of diabetic neuropathy. *Diabetologia*, 44, 1973-88.
87. Jankowski, R. J., Prantil, R. L., Fraser, M. O., Chancellor, M. B., de Groat, W. C., Huard, J. D., Vorp, D. A. (2004) Development of an Experimental System for the Study of Urethral Biomechanical Function. *Am J Physiol Renal Physiol.*, 286, F225-32.
88. Raghavan, M. L., Webster, M. L., Vorp, D. A. (1996) Ex vivo biomechanical behavior of abdominal aortic aneurysm: assessment using a new mathematical model. *Ann. Biomed. Eng.*, 5, 573-82.
89. Chan, O., Chan, S., Inouye, K., Vranic, M., Matthews, S. C. (2001) Molecular Regulation of the Hypothalamo-Pituitary-Adrenal Axis in Streptozotocin-Induced Diabetes: Effects of Insulin Treatment. *Endocrinology*, 142, 4872-4879.
90. Hunter, K. F., Moore, K. N. (2003) Diabetes-associated bladder dysfunction in the older adult (CE). *Geriatr Nurs.*, 3, 138-45.
91. Makker, G., Vorp, D. A., Lindenber, N., Fan, L., Wang, D. H. J., Qu, W., Stern, DM, Schmidt, A. M. (1998) Maintenance of Vascular Structural Integrity in Diabetic L. D. L. Receptor Null Mice Treated with Soluble Receptor for AGE (sRAGE)", 71st Meeting of the Amer. Heart Assoc., *Circulation*, 98:I-12.
92. Staubli, H. U., Schatzmann, L., Brunner, P., Rincon, L., Nolte, L. P. (1999) Mechanical tensile properties of the quadriceps tendon and patellar ligament in young adults. *Am J Sports Med.*, 27, 27-34.
93. Wagenseil, J. E., Wakatsuki, T., Okamoto, R. J., Zahalak, G. I., Elson, E. L. (2003) One dimensional viscoelastic behavior of fibroblast populated collagen matrices. *J Biomech Eng.*, 125, 719-25.
94. Muona, P., Peltonen, J. (1994) Connective tissue metabolism in diabetic peripheral nerves. *Ann Med.*, 26, 39-43.
95. Teppo, A. M., Tornroth, T., Honkanen, E., Gronhagen-Riska, C. (2003) Urinary amino-terminal propeptide of type III procollagen (PIIINP) as a marker of interstitial fibrosis in renal transplant recipients. *Transplantation*, 75, 2113-9.
96. Du, W. D., Zhang, Y. E., Zhai, W. R., Zhou, X.M. (1999) Dynamic changes of type I,III and IV collagen synthesis and distribution of collagen-producing cells in carbon tetrachloride-induced rat liver fibrosis. *World J Gastroenterol.*, 5, 397-403.

97. Nicoletti, A., Heudes, D., Hinglais, N., Appay, M. D., Philippe, M., Sassy-Prigent, C., Bariety, J., Michel, J. B. (1995) Left ventricular fibrosis in renovascular hypertensive rats. Effect of losartan and spironolactone. *Hypertension*, 26, 101-11.
98. de Groat , W.C. and Yoshimura, N. (2001) Pharmacology of the lower urinary tract. *Annu. Rev. Pharmac. Toxicol.*, 41, 691-721
99. Persson, K., Johansson K., Alm, P., Larsson, B., Andersson K.E. (1997) Morphological and functional evidence against a sensory and sympathetic origin of nitric oxide synthase-containing nerves in the rat lower urinary tract. *Neuroscience*, 77, 271-281
100. Cellek, S., Rodrigo J., Lobos, E., Fernandez, P., Serrano, J., Moncada, S. (1999) Selective nitrenergic neurodegeneration in diabetes mellitus – a nitric oxide dependent phenomenon. *Br. J. Pharm.*, 128, 1804-12
101. Mumtaz, F.H., Thompson, C.S., Khan, M.A., Mikhailidis, D.P., Morgan, R.J., Angelini, G.D., Jeremy, J.Y. (1999) Alterations in the formation of cyclic nucleotides and prostaglandins in the lower urinary tract of the diabetic rabbit. *Urol Res.*, 27, 470-5
102. Jankowski, R.J. (2003) Development of a muscle progenitor cell-based therapeutic approach for the treatment of stress urinary incontinence. Ph.D. thesis
103. Liao, D., Arnett, D.K., Tyroler, H.A., Riley, W.A., Chambless, L.E., Szklo, M., Heiss, G. (1999) Arterial stiffness and the development of hypertension. The ARIC study. *Hypertension*, 34, 201-206
104. Noma, T., Mizushige, K., Yao, L., Yu, Y., Kiyomoto, H., Hosomi, N., Kimura, S., Abe, Y., Ohmori, K., Matsuo, H. (1999) Alteration in aortic wall stiffness and accumulation of collagen during the prediabetic stage of type II diabetes mellitus in rats. *Jpn. Circ. J.*, 63, 988-993
105. Giezeman, M.J., VanBavel, E., Grimbergen, C.A., Spaan, J.A. (1994) Compliance of isolated porcine coronary small arteries and coronary pressure-flow relations. *Am. J. Physiol.*, 267, H1190-8
106. Brant, A.M. (1986) Hemodynamics and mass transfer aspects of arterial disease. Ph.D. thesis